Building Evaluation: The Decay Method as an Evaluation Tool for Analysing Thermal Performance

A thesis submitted in fulfilment of the requirements for the degree of Doctor of Philosophy

Andrew McKenzie Law

Bachelor of Engineering (Civil and Infrastructure), Honours First Class – RMIT University

School of Property Construction and Project Management

College of Design and Social Context

RMIT University

May, 2018

Declaration

I certify that except where due acknowledgement has been made, the work is that of the author alone; the work has not been submitted previously, in whole or in part, to qualify for any other academic award; the content of the thesis is the result of work which has been carried out since the official commencement date of the approved research program; any editorial work, paid or unpaid, carried out by a third party is acknowledged; and, ethics procedures and guidelines have been followed.

I acknowledge the support I have received for my research through the provision of an Australian Government Research Training Program Scholarship.

Andrew McKenzie Law

24th of May, 2018

Abstract

There is growing evidence of a significant gap between the designed thermal performance and the actual thermal performance of residential buildings. As heating and cooling energy accounts for approximately 40% of a building's total energy consumption, this poses a significant risk to carbon reduction policies and to achieving sustainable housing designs. The performance gap is primarily caused by incorrect assumptions across a range of variables in the predictive modelling, meaning there is a difference between what is designed and what is constructed. Differences in the thermal shell between model and reality can only be detected via in situ testing.

Evaluating the thermal shell as a whole is possible, but has its drawbacks. According to the literature reviewed, the most common in situ test that evaluates the building performance as a whole system is the co-heating test. However, the co-heating test is highly invasive, requiring between one and three weeks with an empty building. This severely limits its application in field, and means there is currently no sufficiently rapid or non-invasive tool for whole building evaluation of heat loss.

In response to the need for in situ testing that can be applied on a large scale, this thesis presents the 'decay method' as a means of evaluating the heat loss of a building in a non-invasive manner. The principle of the decay method lies in analysing the profile of overnight temperature decay. The use of overnight temperature decay allows the building to be used as normal at all other times, significantly reducing the impact on occupants. Four methods of analysing the temperature decay profile from the decay method have been developed for comparison:

- the calculated average method, using an application of Newtons Law of Cooling to calculate a decay constant for the building;
- the Excel Solver method, combining the Excel Solver add-in with the Law of Cooling to converge on a decay constant that provides the best match to the observed building temperature profile;
- the temperature Root Mean Square Error (RMSE) method, combining the experimental observations with a building simulation; and

- the measured heat pulse method, combining the temperature RMSE method with measured heat pulses included in both experimental and simulation processes.

Using a test cell building located on the CSIRO site in Highett, Melbourne, the four methods were compared against the co-heating test. The results of the case study showed that the Excel Solver method provided Heat Transfer Coefficient (HTC) estimates similar to the co-heating test, but with far larger uncertainty in the result. The measured heat pulse method provided similar estimates to the co-heating test with similar levels of uncertainty.

The case study proves it is possible to evaluate heat loss of the building as a whole, without requiring it to be subjected to a co-heating test. The success of the decay method shows that post-occupancy, in situ testing can be carried out without disrupting the occupants. Further work needs to be done to apply the decay method to multi-zone buildings and buildings of different construction types. Nonetheless, this represents a significant step forward in being able to determine the gap between design performance and actual performance, thereby improving the ability to minimise it.

Acknowledgements

I would like to acknowledge and thank a number of people who have been involved with this research. So many people have helped in so many ways, and this small smattering of words is entirely inadequate in expressing my gratitude to you all.

This PhD has been completed in conjunction with a Studentship agreement between RMIT University and CSIRO. CSIRO provided advice through Dr Peter Osman and Michal Ambrose, as well as equipment and access to testing facilities.

This thesis was edited by Rob Sheehan, Sharpwords.

Dr Ian Ridley and Dr James PC Wong for their support and guidance through the maze that is the PhD, keeping me on task and topic. I had no real idea what I was getting into when I started this, and after many emails, meetings and discussions I have made it this far with your help.

Dr Peter Osman for his original suggestion that doing a PhD was a good idea, as well as comments and feedback crucial for refining the thesis. The way you drove through the thesis and provided such in depth feedback in the timeframes you did is nothing short of amazing.

Michael Ambrose for seconding Peter's suggestion that this was a good move, for your help at CSIRO procuring the use of the test cells and assisting with a number of the experiments, and for making sure that researching buildings is a seriously fun thing to continue doing! Your enthusiasm was infectious, and I wouldn't be doing this if you hadn't passed it on.

Dr Kerry London for kick-starting my literature review and formalising what my thesis was, as well as being actively excited to listen to me talking about R-values during my milestone reviews. Your encouragement during the early part was invaluable.

Rob Sheehan for tightening the laces and providing a final spark of enthusiasm that helped get this across the line – it is infinitely better for your input.

Melanie van Ree for your tireless support, understanding and flexibility – I am forever grateful for all of the opportunities you've been able to put in front of me while I've worked

through this epic journey. Now we'll see what I can do when my brain isn't solving other problems!

The entire staff and student community at the School of Property Construction and Project Management for the help and support during this journey.

All of my family and friends – any time any of you have asked 'what is your PhD about?' it forced me to really push my own understanding of it and helped it gain clarity. It is one thing to research something; it's quite another to communicate it all, and each of these conversations was helpful to that end.

My parents, Heather and Keith, for their understanding and support throughout the program, especially when I needed to stop working to focus on writing. I would not have been able to finish the final year without your help, safe knowing that I had you to rely on.

Finally, Ashlee, for putting up with endless talk of heat loss gradients and spreadsheets. For being the sounding board while I thought out loud. For previewing all the graphs, even when they made no sense. For pushing when I needed it, and letting me go when I was on top of it. Your encouragement and endless faith in me has been extraordinary – many words have made it to page simply because you continually tell me I'm smart and I can do this.

This has been quite a journey, but I have (mostly) enjoyed every single second.

Table of Contents

Table of Figures

Table of Tables

Nomenclature

$\hat{y}$ –value predicted by model

µV – microVolt

^{0} – Degrees

^{0}C – Degrees Celsius

A – Area

hr –Hour

K –Kelvin

kW – kilowatt

m – metres

m^2 – metres squared

mm – millimetres

n – Volumetric air change rate per hour at atmospheric pressure

n_{50} – Volumetric air change rate per hour at 50 Pa

Pa – Pascal

Q_i – heat flux readings in W/m^2

Q_{input} – power input from heat source

Q_{solar} – power input from solar

R – Thermal resistance

R^2 – Coefficient of determination

r_{ext} – Surface resistance due to external air

r_{int} – Surface resistance due to internal air

s – second

U – Thermal conductivity

V – Volts

V_{ol} – Volume

W – Watt

y – Observed value

ΔT – Temperature difference

ΔTs_i – Temperature difference between internal and external surfaces

Abbreviation

ABCB – Australian Building Codes Board

ABS – Australian Bureau of Statistics

ACT – Australian Capital Territory

BESTEST – Building Energy Simulation Test

C1A – Configuration 1, Test A

C1B – Configuration 1, Test B

C2 – Configuration 2

C3 – Configuration 3

COAG – Council of Australian Governments

CSIRO – Commonwealth Scientific and Industrial Research Organisation

DEWHA – Department of the Environment, Water, Heritage and the Arts

HTC – Heat Transfer Coefficient

HLC – Heat Loss Coefficient

IPCC – International Panel on Climate Change

ISO – International Organization for Standardization

MEES – Minimum Energy Efficiency Standards

NatHERS – Nationwide House Energy Rating Scheme

NRMSE – Normalised Root Mean Square Error

SAP – Standard Assessment Procedure

RBEES – Residential Building Energy Efficiency Study

RMIT – Royal Melbourne Institute of Technology

RMSE – Root Mean Square Error

VBA – Visual Basic

ZCH – Zero Carbon Hub

Chapter 1 - Introduction

Reductions in building energy use is a major goal of governments worldwide, and a vital part of reaching the targets for reduced carbon emissions (Bernstein et al. 2007; Parkinson et al. 2010; European Union 2010). Heating and cooling loads form a major part of the energy use in residential buildings, accounting for 40% of total energy consumption (Morrissey *et al.* 2011; Yan *et al.* 2012; Pulselli *et al.* 2009). The International Panel on Climate Change (IPCC) directly identified the improvement of building efficiencies as a means of reducing the influences on climate change and mitigating the effects (Bernstein et al. 2007). Many governments have reacted to this by including energy efficiency legislation as part of the national building codes; examples include the Nationwide House Energy Rating Scheme (NatHERS) in Australia, the Energy Performance Coefficient in the Netherlands, and Minimum Energy Efficiency Standards (MEES) with requirements for Energy Performance Certificates in England and Wales. This is an important step, though the requirements of these standards are based on design data. There is growing evidence of a significant gap between the designed performance and the actual performance of the building (Asdrubali et al. 2014; Byrne et al. 2013; Roetzel et al. 2010). This undermines any carbon reduction policies a government may have, and being able to identify the size and extent of the gap should be considered a priority (ZCH 2014).

The performance gap is caused primarily by incorrect assumptions in the predictive modelling, either regarding the materials and construction resulting in an underperforming building envelope, or regarding the climate, behaviour of the occupants and other modelled effects, such as air mixing. This means there are differences between the design as modelled, and the building as constructed. Materials do not necessarily combine in the same way in-field as they did in the laboratory, and the imperfect nature of construction can unintentionally create building flaws that have not been accounted for in the simulation (Asdrubali et al. 2014). These are elements that can only be detected with in situ testing.

Evaluating the performance of the entire building envelope is possible; the most popular whole building test being the co-heating test, as set out by Johnston et al. (2013) to calculate the Heat Transfer Coefficient (HTC). No international standard exists. The reliability

of the results is sensitive to weather conditions; however, it is a very comprehensive test and one of the very few methods that evaluates the entire building system rather than individual elements in the fashion of heat flux tests. The issue with the co-heating test is that it is highly invasive, requiring between one and three weeks with an empty building. This severely limits its application in field (Stamp 2011). Ultimately, this means there is no way of readily identifying the quality of the building stock completed before energy efficiency measures were introduced, and no easy way of confirming those designed under these regulations perform to the designed standard.

1.1 Australian Context

Mandatory energy efficiency measures have been included for housing in Australia since 2003 (ABCB 2013). Since this initial inclusion, the standard has been lifted to a six-star rating as part of the NatHERS regulatory pathway under Section 3.12 of the National Construction Code (NCC). As these requirements form part of the NCC (and are adapted individually by each state or territory) they refer only to the physical thermal envelope and assumed internal heat loads of the building, and therefore, in terms of energy use, relate to the heating and cooling loads of the building.

Overall energy consumption in Australia is expected to rise 14% from 2010 levels by 2020 (Parkinson *et al.* 2010). This will result in increased pressure on existing energy networks, and potential increases in carbon emissions (depending on advances made in the renewable energy sector). As part of a wider response to this, the Prime Minister's Task Group in Energy Efficiency's recommendations regarding buildings were to consider "pathways towards Zero-Emissions buildings", and strengthen "the capacity to assess building energy use" (Parkinson *et al.* 2010). Additionally, the National Energy Productivity Plan (NEPP) has outlined actions such as, "Improve residential building energy ratings and disclosure", and " Improve compliance with building energy efficiency regulation" (COAG 2015). Disclosure measures already in place in the ACT have resulted in an increase in property value in line with increased energy performance (Reidy *et al.* 2008).

Building regulations apply only to new constructions or major renovations, and therefore have little impact on the current housing stock. Based on the 2016 Census, Australia had a stock of approximately 9.9 million dwellings (ABS 2018), up by 1.3 million from 8.6 million in 2011 (ABS 2013). An update to the NCC was issued in May of 2011 (ABCB 2011), meaning

approximately 13% of 2016 residential building stock was built to 'modern' Australian standards. There currently exists no post-construction testing as part of building certification and handover. By the year 2050 58% of residential buildings will have been constructed after 2019 (ASBEC & ClimateWorks 2018). As the NatHERS pathway for achieving compliance with the energy efficiency provisions in the NCC relies on simulating the building plan, the performance gap represents a significant risk to achieving the 40% improvement target in Australia's energy productivity set in the NEPP (COAG 2015).

1.2 An Alternative Evaluation Method

It is clear that there is a need for an effective way to carry out post-construction evaluation of houses. The presence of the performance gap is a clear threat to the integrity of energy efficiency schemes and reaching carbon emission targets. In markets with mandatory disclosure it represents additional quality assurance that the building performs in the way advertised. To be a truly effective tool, it is required to be minimally invasive, enabling it to be conducted in occupied dwellings.

This research proposes the decay method as an alternative to the co-heating test for estimating a building's HTC. The initial concept was inspired by a 'thermal step response test' used by CSIRO as a way to further examine the physical properties of homes taking part in the Residential Building Energy Efficiency Study (RBEES). Due to a large number of unknowns, however, it was decided the method would require further development to establish whether conclusions could be drawn.

The decay method has two parts: data collection and data analysis. This thesis presents a single data collection procedure, referred to as the 'decay test', and four different techniques to analyse this data.

The decay test records internal temperature and external weather conditions continually over the course of a two-week period. Each night, the test follows two phases: the pre-heating phase, and the decay phase. The pre-heating phase requires a calibrated heater to heat the building between midnight and 2.00am to create a temperature difference. At 2.00am the decay phase begins as the heater is turned off and the internal temperature drops. No mechanical heating should be used until after 6.00am when the decay phase ends.

Temperature data can be collected using temperature sensors located throughout the building. Conducting the testing and data collection overnight takes advantage of the times when the house is expected to be in 'free running' or 'unconditioned' mode where there is no active heating or cooling of the building, and influences from building occupants is minimal. This allows for the building to be occupied throughout the data collection process.

The four analysis methods are proposed in order of increasing complexity of the analysis technique. The thesis presents each in turn, discussing the process and analysing how effective each method is for estimating the buildings' HTC.

The four versions of the decay method analysis are:

- the calculated average method, conducting analysis on the observed temperature profile of the building to calculate a decay constant;
- the Excel Solver method, using the Excel Solver add-in to determine the decay constant that best describes the temperature profile;
- the temperature Root Mean Square Error (RMSE) method, combining the experimental observations with a building simulation; and
- the measured heat pulse method, combining the temperature RMSE method with measured heat pulses included in both experimental and simulation processes.

To gain an understanding of the performance of the thermal shell, the main focus of the analysis is on the decay phase. The pre-heat phase is analysed as part of the measured heat pulse method. The continual temperature monitoring of the building is used as part of the building simulations for the temperature RMSE and measured heat pulse methods to ensure any heat gains or losses observed during the other 18 hours of the day are accounted for in the model. This maintains a common history between the model and the building.

The goal of this research is to determine whether the decay method can predict the HTC of a building to within an acceptable level of accuracy under semi-controlled conditions.

1.3 Research Questions

In addressing the goal and developing the decay method, the following research questions have been identified:

- Can the decay method be used to estimate the Heat Transfer Coefficient of a building and provide the same values as the co-heating test?
- Can the estimates made by the decay method be made with similar levels of uncertainty as the co-heating test?

Additional sub-questions relating to the main research questions were also defined:

- What limitations are there on the usability and reliability of the decay method?
- What are the key elements of the decay method in relation to:
    - Minimum data collection
    - Required equipment
        - Minimum accuracy of equipment
    - Procedure/Required steps?

1.4 Research Methodology

The approach to evaluating the decay method's effectiveness is to compare the results of the four analysis techniques to the co-heating test. The success of the decay method relies on it being able to evaluate the heat loss of the building to similar standards but with its less invasive procedure. It should be shown that either the HTC can be estimated from the decay method results, or that there is a relationship between specific HTCs and decay rates.

The initial proof of concept for the decay method used the building simulation program EnergyPlus. This showed that the methods were theoretically valid and robust under a variety of conditions. The simulations showed direct correlations between straight line approximations of temperature decay profiles and HTCs, and that the RMSE could correctly identify a particular model from an array of models.

To demonstrate real world application of the decay method and comparison with the co-heating test, a small test cell building provided by CSIRO located at Highett has been used as a case study. The building is a building is a platform floored building with an enclosed and ventilated

subfloor, timber frame construction clad in compressed fibre cement sheet with a single door and single window. Initially, there existed no insulation in the wall cavity, but glass wool wall insulation batts were installed in three different configurations to allow for comparison of different buildings. External conditions were monitored by the Bureau of Meteorology weather station in Moorabbin and confirmed using an on site weather station operated by CSIRO. Blower door and heat flux tests were conducted for further understanding of the building, also providing another evaluation method for comparison.

1.5 The Decay Method Procedure

1.5.1 Data Collection

Air Temperature

Minimum data collection requires external air temperature and internal air temperature measurements. For this study, readings are taken every 60 seconds; however, additional research may show that readings can be taken less frequently.

The analysis of internal air temperature assumes the temperature record is representative of the entire air space. The case studies in this research use an array of 27 temperature sensors to calculate the average air temperature and a fan to mix the air. The use of a single sensor per zone is generally sufficient for the co-heating test (Johnston et al. 2013).

For buildings with multiple zones, it is suggested that the average internal temperature be calculated by weighting the temperature in each zone with respect to the volume of the zone, in the same fashion as the co-heating test (Stamp 2013). This is important as the temperature decay should be based on total air volume, not the temperature decay per zone.

Heat Energy

The measured heat pulse method also requires recording the amount of energy input to the building during the heat pulse phase. The minimum data requirement is simply aggregate energy used to heat the building during this period; however, finer detail and higher resolution data may provide additional insights during analysis. In this research, for ease of equipment set up and consistency, readings are taken every 60 seconds to match with the temperature data collection.

1.5.2 Calculated Average Method

1. Calculate Daily Decay Constants

Using an application of Newton's Law of Cooling, a decay constant is calculated for each night of the test. This evaluates the temperature decay as an exponent based on the internal temperature profile and the average external temperature observed during the decay phase.

For ease of use it is recommended that hours are used as the unit of time regardless of the data collection interval. This makes the final decay constant easier to understand and communicate, and the larger magnitude allows differences between buildings to be more easily identified.

The average difference between internal and external temperature is also calculated.

2. Calculate Average Decay Constant

The average of the Daily decay constants is calculated. This figure represents an estimate of the overall decay constant for the building. The higher the decay constant, the faster the building temperature approaches the external temperature.

1.5.3 Excel Solver Decay Method

1. Set up Cooling Model

Using an application of Newton's Law of Cooling, a mathematical model that estimates the temperature profile during the decay phase is set up. The model uses the observed initial temperature and adjusts for changes in the external temperature at each data collection interval.

2. Engage Excel Solver Add-In

The Excel Solver add-in is used to minimise the difference between the cooling model and the observed temperature of the building, using the Root Mean Square Error as the measure of closeness. The Solver achieves this by changing the value of the decay constant applied to the cooling model to find the value that gives the smallest RMSE. As with the calculated average method, higher decay constants indicate faster rates of heat loss.

1.5.4 Temperature RMSE Method

1. Create Building Models

Using a building simulation program, in this case EnergyPlus, a model is developed that is representative of the building's thermal shell. Based on this model, variations to the material properties are made to create an array, such that the extreme best case and extreme worse case scenarios for the quality of the building fabric are covered. In this research, 48 separate models have been used to cover the combinations of possible air leakage rates, wall insulation, ceiling material R-value, and thermal mass of the building. These have been based on in-field experiments conducted as part of the research.

2. Simulate Co-Heating tests

Co-heating test simulations are run on all the building models. Ideally the simulated HTCs will be evenly spaced across the simulated range; however, this is not always possible as small changes combine in different ways and some clustering may occur. This is not critical, as there should be a correlation between these specific models and the simulated decays.

3. Simulate Decay Test

Using the data collected on site, simulations using the external conditions and the initial 2.00am internal temperature are run, allowing the models to simulate temperature decays under those conditions.

4. Calculate RMSE

For each decay profile, the RMSE between the simulated data and the field data is calculated. The model or models with the smallest values indicate the best representations of the building's behaviour. The HTC of the building is estimated as the HTC of the model with the smallest RMSE. Where one or more models have the same RMSE, the HTC of the building is the average of the HTC from these models. The Normalised Root Mean Square Error (NRMSE) is also used to represent the results as a percentage difference between simulation and observation.

1.5.5 Measured Heat Pulse Method

The measured heat pulse method uses the basic techniques of the temperature RMSE method, but includes analysis of the energy used during the pre-heating phase.

1. Create Building Models

Create the computer model of the building as per the temperature RMSE method outlined in Section 1.5.4.

2. Simulated Co-Heating Tests

Simulate the co-heating tests on the building models as per the temperature RMSE method outlined in Section 1.5.4.

3. Simulate Decay Test

Using the data collected on site, the building model is set to match the internal temperature recorded during the decay period, and the energy required by the simulation to match this is recorded. The simulation then decays in the same fashion as the temperature RMSE method outlined in Section 1.5.4.

4. Calculate RMSE

The temperature RMSE is calculated as per the temperature RMSE method outlined in Section 1.5.4. The only different is that the NRMSE is recorded for use in the analysis.

5. Calculate Energy Differences

The difference between energy use during the pre-heat phase simulated by the model and observed on site is calculated. The smaller the difference the closer the match. This is represented as a percentage.

6. Determine the Predicted HTC

Using the ratio between percentage energy difference and NRMSE, the models kept are those that meet the criteria indicating a HTC estimate of +/-10% of the observation are. The rest are discarded. Part of the outcome of this research is identifying these criteria, which is detailed in Chapter 7. Further research is required into determining these criteria for different buildings. The HTC is reported as the average of the models that meet the criteria

specified in Chapter 7. The highest and lowest HTCs from the simulated models represent uncertainty in the HTC estimate.

1.6 Research Scope

The research conducted in the PhD study has certain restrictions on time and resources. To overcome this, the research focused around a case study evaluating the heat loss of a test cell building. This is appropriate both as part of the PhD and in the testing of a new building diagnostic tool – it limited the scale to something manageable by a single person, and enabled the commitment of enough technical resources to the research without exceeding the amount of resources available. It also reduced complexity to the simplest possible in-field scenario, providing the greatest chance to prove if the decay method could potentially be used to evaluate a residential building. The following sections provide greater detail on specific parts of the research scope that assisted in retaining focus on the research questions.

1.6.1 Heat Loss Evaluation

To prove the value of the decay method in the suite of available tools, it has been compared against the co-heating test which only evaluates heat loss under cool conditions. It may be possible to apply the decay method to evaluate heat gain in warmer conditions. This was not done as a part of this research, largely due to the lack of whole-building, cooling-load oriented evaluation tools which limits a like-for-like comparison. As previously mentioned, there were also issues surrounding long term monitoring of a residential building for the PhD program.

In addition to this, the project is not aimed at defining the building type or identifying features of the building, only at providing a means by which different buildings may be compared. There is no intention to calculate thermal mass or determine a 'type' of building (for example, brick veneer or double brick) from the test. This research focused on determining the HTC by a means other than the co-heating test.

1.6.2 Single Zone Building

The test cell is a simple single zone building. Multi-zone buildings may present more difficulties in data collection, and in creating the representative model for the RMSE method. To reduce the complexity in developing and analysing the decay method, tests on multi-zone buildings have not been attempted.

1.6.3 Relative Performance of the Test Cell

The test cell is not intended to be representative of a typical building, and no comparisons have been made between the heat loss of the test cell and the heat loss of a standard house. The purpose in using the test cell was to enable analysis of a building under real weather conditions, and test whether real data collection techniques were effective, rather than relying on simulations. Comparisons between the test cell configurations have been made as both co-heating and decay tests were conducted

1.6.4 Temperature Distribution

To create the best possible conditions to show the decay method can work in field, a fan was used to facilitate mixing of the air, and the empty building enabled sensors to be hung throughout the space. This provides the best possible assurance that the average temperature used in the analysis is a true representation of the air temperature within the test cell. This aligns with the co-heating test where the use of a fan to facilitate air mixing is well documented (Johnston et al. 2013). No analysis has been conducted without the fan, or with sensors simply located on the walls. This creates some uncertainty as to how accurate the test will be in an occupied house, but it eliminated another potential source of uncertainty in the analysis of the method under development.

1.6.5 Building Type

Due to the nature of the case study, the only building evaluated is the test cell. The test cell is a lightweight structure, and no analysis was undertaken of how this method may behave when applied to a building with a higher thermal capacitance.

1.6.6 Decay Constant and HTC Correlations

Application of the experimental decay methods requires confirmation that the correlation observed in the case studies exists in the wider building stock. Prediction of the HTC based on the case study results may not be accurate when applied to multi-zone buildings, or different building types.

1.6.7 Heat Pulse Ratio Calculation

To identify the accurate models, applying the measured heat pulse method in the industry requires knowledge of the ratio between energy and temperature variations. During the course of this research the ratios common across the three test cell configurations was determined; however, further research is required to show whether the same ratio applies to other buildings and building types.

1.7 Performance of the Decay Method

The performance of the decay method is promising. The calculated average method provided HTC estimates of the test cell to within 8% of the co-heating test estimates. The uncertainty in these estimates, however, is significantly greater than that of the co-heating test. The Excel Solver method estimated the HTC to within 2% of the co-heating test. The uncertainty associated is approximately double that of the co-heating test. Further work is required to quantify the relationship between the HTC and the decay constant in other buildings. Alternatively, using LORD to analyse the decay test data may provide an alternative for directly estimating the HTC. Further development of the experimental methods is desirable as they only use field data, and there is no need to create building simulations to complete the evaluation. The temperature RMSE method appears more robust in theory, and would allow direct comparison with the HTC; however, it has been shown to have problems eliminating inaccurate estimates and is prone to significantly underestimating the HTC. The measured heat pulse method, however, overcomes the problems in the temperature RMSE method by including the heat pulse which enables the assessor to remove inaccurate estimates and confidently estimate the HTC to within 10% of the observed HTC.

It is important to remember that the decay method adds to an existing suite of tools available to researchers and assessors. It has limitations and is not intended to provide evaluation of specific areas in the building or account for occupant behaviour. However, it does allow for in situ evaluations of the whole building envelope's performance.

Chapter 2 - Literature Review

The literature review will identify the current means for testing the thermal performance of homes. It discusses spot tests that can identify the performance of single building elements such as heat flux testing, and the ability for more invasive testing to gather indicators of thermal performance for the whole building. The literature review also discusses ways that building evaluation is carried out by researchers in this field, and how other evaluation methods have been tested.

Ultimately, the aim of this research is to evaluate the application of a new building diagnostic tool that can be used for quality assurance or compliance purposes. To that end, it is relevant to discuss the elements of the building fabric, thereby showing the complexities involved in evaluating buildings, and to discuss the benefits and limitations of various building evaluation methods as they may apply in an industry compliance context. In doing so, the literature review shows that building performance evaluation is an important element of building sustainably, and highlights the need and potential for low-impact, rapid assessment tools.

2.1 Research Focus

The research reviewed here has been selected to focus on the need to develop methods of post-construction assessment and quality assurance of buildings which verify whether they meet various energy efficiency regulations, and that those regulations are achieving their intended outcomes.

2.2 Research Context

Residential energy use accounts for 20% to 40% of total energy consumption across all sectors, depending on location (Pérez-Lombard, Ortiz & Pout 2008; Rehdanz 2007; Tommerup, Rose & Svendsen 2007; Yu et al. 2011). Heating and cooling accounts for approximately 40% of residential sector energy use (ABS 2009; Reardon et al. 2007; DEWHA 2008), again varying by location – in Tasmania it has been estimated as high as 50% (McLeod & Fay 2010). This forms the largest single portion of energy use in the home. It is widely recognised as holding great potential for reducing residential energy use, including by bodies such as the European Parliament (2010) and the Council of Australian Governments

(COAG 2015), both of which recognise how important improving thermal performance of buildings is to achieving energy reduction targets. The International Panel for Climate Change has also named reduction of building energy use as one of the keys to mitigating climate change (Mlecnik, Visscher & Van Hal 2010). Research groups such as the Zero Carbon Hub (ZCH) in the UK, and the National Renewable Energy Laboratory (NREL) in America, have been set up to facilitate research that pursues this goal. Responses have been made in the housing industry through implementing certain energy efficiency requirements in various building codes. Across Europe the Energy Performance Building Directive requires all European Union members to have performance based energy regulations (Guerra-Santin & Itard 2012). Other examples are seen around the world, including the National Construction Code (NCC) in Australia. These building regulations are an important part of reducing energy consumption. Leth-Petersen & Togeby (2001) and Beerepoot & Beerepoot (2007) found improvements in building performance due to energy regulations.

Despite efforts to implement design standards, there is a concerning trend of studies finding that actual energy use differs from predicted energy use (Asdrubali et al. 2014; Branco et al. 2004; Byrne et al. 2013; Roetzel et al. 2010). The gap between designed and built performance is an issue facing the building industry. That gap threatens to undermine energy efficiency and carbon reduction targets set by governments around the world.

2.3 The 'Performance Gap'

The performance gap is the observed phenomena that show a difference between the expected value of heat transfer or energy use for a material, or part, or whole of a building, and the actual value observed (Asdrubali et al. 2014; Byrne et al. 2013; Roetzel et al. 2010). The observation is that the constructed building uses more energy than the analysis of the design indicated (Johnston, Miles-Shenton & Farmer 2015). The Zero Carbon Hub (2014) states that a performance gap undermines a government's carbon reduction plan, and that identifying the origin, size and extent of that gap should be the priority.

Evidence of the performance gap has been shown by Bell et al. (2010), Lowe et al. (2007), Ridley et al. (2014), Thompson & Bootland (2011) and Wingfield et al. (2008). Additionally, it is reported to exist by Gupta & Dantsiou (2013), Ryan & Sanquist (2012) and De Wilde (2014). Notably, Bell et al. (2010), Ridley et al. (2014) and Wingfield et al. (2008) observed the performance gap under experimental conditions, and when buildings are in use by the

residents. This indicates there are multiple elements to the performance gap. As Wingfield et al. (2008) stated,

> …the root causes of the gap in performance are much more complex than a simple list of design flaws, construction faults and system inefficiencies and relate to the interrelationship of the various parts of the construction process from design conception right through to occupation.

Accurately predicting heat loss and energy use is vitally important for making well informed decisions regarding energy efficiency actions and policy changes (Byrne et al. 2013). The presence of the performance gap shows that the predictive methods used, whether calculations based on reported material properties or simulations of building performance, are underestimating the level of heat transfer, and/or the amount of energy being used. The major effect of this is in reporting of meeting energy efficiency standards (Byrne et al. 2013; Roetzel et al. 2010), and at least in the UK action has been taken to address this issue by implementing the Building Performance Evaluation competition in 2010 (Gupta & Dantsiou 2013). As these standards are generally based on buildings 'as-designed', limitations in the estimation methods can result in an inflated measure of the building's energy efficiency (Roetzel et al. 2010). This indicates that the ability to evaluate the buildings in situ performance is very important if we are to realise actual energy savings targets from the housing industry.

The performance gap is caused by two distinct areas: incorrect assumptions about the materials and construction, causing an underperforming thermal envelope, and incorrect additional assumptions about occupant behaviour and weather conditions.

2.3.1 Underperforming Thermal Envelope

The performance gap has been observed in both specific elements of the home, such as heat loss through a wall, and in whole house performance. In relation to the thermal envelope, this is the observation that parts or the whole of the building transfer more heat than was expected, based either on calculations from reported material specifications, or from simulating the building's thermal responses.

Studies such as Asdrubali et al. (2014) show how the in situ wall does not meet the expected standard based on the data reported by the material manufacturer. In this series of case

studies, five out of six walls were found to have greater than expected thermal transmittance based on the summation of manufacturer reported data. Asdrubali et al. presented four points as potential explanations:

1. The performance data declared by the producers of building materials are often overestimated for marketing reasons;
2. Thermal performance of building elements and materials are measured in controlled laboratory conditions;
3. The actual installation of the materials in real buildings is imperfect;
4. External conditions (for example, rain and wind) can influence measurements.

Doran (2008) also provides evidence of a specific element underperforming, finding that thermal resistance was "around 38% less than that expected on the basis of measured cavity width".

Bell et al. (2010), Ridley et al. (2013) and Guerra-Santin et al. (2013) all show examples of the entire thermal shell underperforming in a co-heating test compared to the designed heat loss. The estimations made by Ridley et al. (2013) and Guerra-Santin et al. (2013) were based on calculations inherent in the PassivHaus Planning Package, and Bell et al. (2010) by a calculation based on thermal properties. All these examples, however, were based on high efficiency homes, and the validity of the co-heating test in this setting is questioned by Guerra-Santin et al. (2013) on the basis that the building's sensitivity increases in solar radiation, similar to the overheating observed by Stamp (2013). Bell et al. (2010) did conclude that this discrepancy was due to a combination of underestimating the R-value of the walls and the effect of thermal bridging. This presents a combination of underperforming thermal shell and possible errors in the standard assumptions: the actual wall R-value was influenced by a significant amount of additional timber, and the thermal bridging assumption from the Standard Assessment Procedure (SAP) was deemed inappropriate (Bell et al. 2010). The gap disappeared when these two elements were accounted for, but forensic analysis was required. In addition to these exceptionally high efficiency buildings, a review of the Leeds Beckett co-heating database, conducted by Johnston, Miles-Shenton & Farmer (2015), showed fabric losses exceeded designed loss by a not negligible amount in 22 of 25 homes. It is not clear how the designed loss was determined, but the homes were built to "exceed the fabric requirements of Part L1A

2006". The comparison of predicted and measured HTC is shown in Figure 2.1. Note that since publication of Johnston, Miles-Shenton & Farmer's (2015) study, terminology has been changed from 'Heat Loss Coefficient (HLC)' to 'Heat Transfer Coefficient' (Jack et al. 2017).

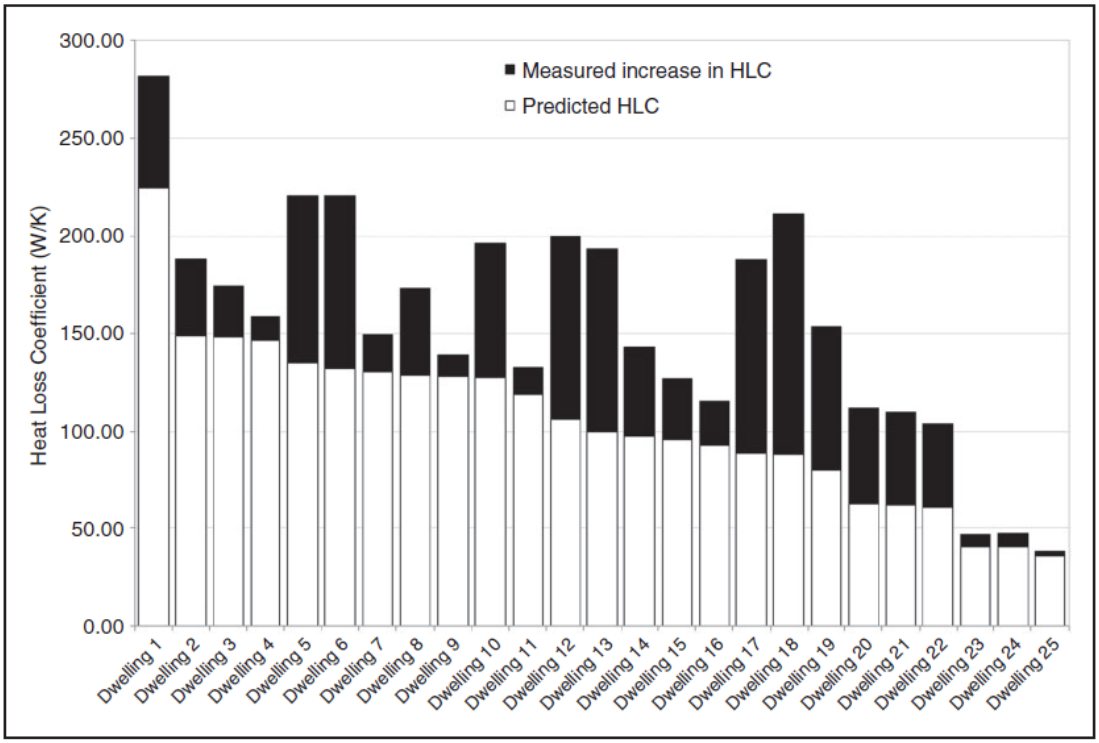

Figure 2.1 Performance gap, Johnston *et al.* (2015)

Tests conducted by Thompson & Bootland (2011) for the Good Homes Alliance also observed a 30% increase in measured heat loss over designed heat loss. Each of these examples demonstrates a thermal envelope performing well under the design specification, and indicates issues with design assumptions that surround the thermal envelope's physical properties. Again, this is highlighted by the Zero Carbon Hub (2014) with their recommendation for a review of conventions for calculating inputs relating to the building fabric. At present, it appears that performance of the thermal shell as a whole system is overestimated.

2.4 Influences on Energy Use

Many things contribute to a home's energy use (Balaras et al. 2005), and as Su (2008) states, "Ignoring one design factor could damage the energy efficiency of an entire building". The influences on energy use for residential buildings are broadly separated into four categories – the outside micro-climate, building envelope, inside climate, and occupant behaviour

(Buchberg 1969). The building envelope is what separates the inside from the outside (Sadineni, Madala & Boehm 2011). On its own, it dictates a base level of the internal conditions, largely driven by interactions between the building and its external weather conditions. Occupant behaviour sits on top of this, either accepting the base level provided or making some change, typically by turning on heating or cooling. This may change depending on which internal space they are using, and how the internal spaces interact with each other. The efficiency of the appliance also influences final energy use as it works to meet occupant demand. It may be argued that the occupant's perceived comfort level is the major factor in the end energy use; however, the building's physical characteristics dictate the amount of energy required to reach desired levels of comfort. Improving the house's thermal performance is generally accepted to mean making changes to the building envelope (McLeod & Fay 2010). However, this is not limited simply to the materials used in construction. It also includes passive design elements such as building orientation, size and layout. In fact, Pacheco *et al.* (2012) concluded that these passive design factors held the greatest influence of all facets of the building envelope.

As noted above, internal conditions are, at least in part, driven by interactions between the building and its environment. It must be noted that simply because a design action results in an energy saving in one location, that does not automatically translate to energy savings worldwide, or even year round (Pacheco, Ordóñez & Martɪnez 2012). Different climates require different energy saving strategies, depending on the balance between heating and cooling loads for the building. In Australia, Queensland's warmer climate dictates a different approach to building design than applies in Hobart. The balance for Sydney's more mild climate, or even Melbourne, again requires different solutions as the balance between keeping warm or cool is sought at different times of the year (Ambrose et al. 2013).

Even when physical and behavioural aspects are taken into account for a given home, the increase in building envelope efficiency presents new complications – phenomena such as the 'rebound effect' come in to play, reducing the overall effectiveness of energy saving action due to an increase in the occupants' capacity for energy demand (Greening, Greene & Difiglio 2000; Hsueh & Gerner 1993).

The rest of this chapter details how building elements, behaviour and climate influence the building's heating and cooling load of. It focuses more on typical building elements (such as

walls, windows and roofing) and their principles in terms of thermal performance. It does not account for more specialised and innovative technologies, such as a Trombe wall. The intention is to provide an understanding of the main elements required for a home to meet minimum design standards, not to demonstrate how to create a 'zero emissions' home.

2.4.1 Building Design

A number of studies have been conducted into what parts of the building envelope influence the building's energy use. Each element that goes into constructing the building envelope influences the way the building responds to its surroundings. These combine in different ways, enabling similar results to be achieved using different methods, or resulting in similar materials being quite effective depending on other design features.

As stated previously, the building envelope is the physical barrier that separates the inside from the outside (Sadineni, Madala & Boehm 2011). This includes walls, roof and anything inset into them, such as doors and windows. The building envelope's performance largely depends on good building design, including selecting and distributing materials, and building orientation and layout (Gasparella et al. 2011). The major elements of building design that influence how heat is transferred between the building's inside and outside are insulation, thermal mass, glazing, air leakage, orientation, size and shape, and shading (Sadineni, Madala & Boehm 2011; Tommerup, Rose & Svendsen 2007).

2.4.1.1 Orientation

The building's orientation relates to the 'passive solar building design'. Orientation has a large impact on the solar energy the building gains, as it determines the location of living spaces and glazing with respect to the sun. Effective orientation, alongside location on the site (to mitigate effects such as overshadowing from neighbouring homes) and landscaping changes, may reduce energy requirements by 20% (Spanos, Simons & Holmes 2005). Buildings with poor orientation require more energy due to reduced heating benefits in winter (increasing the heating load), a reduction of available daylight (increasing the lighting load), and increased heating in summer (increasing the cooling load) (Morrissey, Moore & Horne 2011). Orientation also impacts the effectiveness of the building's thermal mass.

2.4.1.2 Size and Shape

Over recent decades, a number of studies have been carried out into the effect of building size and shape. All conclude that a building's size and shape have a significant impact on

heating or cooling loads. Pacheco, Ordóñez & Martınez (2012) summarises that "building shape not only determines the total area of the facade and roof that receive solar radiation, but also the surface exposed to the outside, and thus to energy losses". Depecker et al. (2001) and Su (2008) both concluded that more compact buildings (that is, buildings with smaller external surface area to volume ratios) were better at retaining heat during cold winters. Depecker et al. (2001) also state there was little to no influence on heating and cooling loads for mild climates. However, a case study by Elasfouri, Maraqa & Tabbalat (1991) determined that in a very hot climate the radiation hitting the building surface could impact the cooling load by 25%. In Victoria, Morrissey, Moore & Horne's (2011) modelling study found smaller homes were better able to overcome other design shortcomings than larger homes.

All of this points to the importance of home size and shape, at least in climates where either heating or cooling dominates. In cool climes, there is benefit from reducing the thermal shell's surface area, thus reducing the area from which heat can be transferred to the cold air outside, and in hot climates reducing the area impacted by solar radiation may assist in reducing the cooling load. In a mild climate, where heating and cooling loads are more even, there appears to be no significant benefit from constructing compact homes.

2.4.1.3 Insulation

Thermal insulation assists the building in resisting or slowing the transfer of energy between internal air and external air (Doran 2008). Most structural and cladding materials used in constructing the home provide little insulation (Reardon et al. 2007). Insulation in addition to the structural materials is generally required, depending on climate. Improvements in building insulation is the most obvious way to improve the home's efficiency; Ballarini & Corrado (2012) describe it as being "considered the most effective way of increasing the thermal resistance of a building component, even under a dynamic driving force". Su (2008) found a 42% increase in electricity use per cubic metre for New Zealand homes without insulation compared with insulated homes.

There is a well proven inverse relationship between increased insulation and decreased energy use for heating (Ballarini & Corrado 2012; Kim & Moon 2009; Pan et al. 2012), however, any effects on required cooling energy appears tenuous. Pan et al. (2012) were unable to find improvements for the warm climate in Guangzhou. Kim & Moon (2009) found

no changes to cooling load in either cool or warm climates. Ballarini & Corrado (2012) concluded the lack of reduction in cooling load was due to greater influences from the "transparent envelope", namely the glazing, including shading influences. Questions regarding the robustness of Kim & Moon's (2009) results due to thermostat and behavioural aspects of their simulations not being presented, are assuaged given their findings are in agreement with Ballarini & Corrado's (2012) study. The Australian study by Ambrose et al. (2013) did not specifically evaluate insulation; however, there was no significant improvement in cooling loads for improvements in energy star rating, which also lends credence to the findings of Kim & Moon (2009), and Ballarini & Corrado (2012), Ambrose et al.'s (2013) study was done via long term monitoring rather than simulation.

In addition to other findings, Kim & Moon (2009) also evaluated a law of diminishing returns for increases in insulation levels in cool climates beyond approximately R5.28 for walls, R7.04 for ceiling, and R0.88 for windows.

Over time, the effectiveness of insulation can diminish. As insulation performance relies on trapped still air, reducing the volume of the material also means reducing the effective R-value (Ambrose et al. 2013). For example, as bulk insulation batts age they begin to flatten. Other forms of insulation, such as 'blow in' polystyrene balls or wool fibres which use smaller particles spread evenly across the ceiling or filling the wall cavity, can shift and so create thin sections that increase heat flow (Ambrose et al. 2013).

Insulation is the most straightforward, and generally most cost effective, way of improving a building's thermal performance; however, its effectiveness may be overstated in warm climates. It acts as a barrier to heat transfer both in and out of the home, and it is generally shown that improving insulation reduces energy use. As with all the elements that go into the thermal shell, the presence of insulation does not guarantee good thermal performance; however, lack of insulation all but guarantees poor thermal performance.

2.4.1.4 Thermal Mass

Where insulation will simply assist in resisting heat transfer, thermal mass helps the building regulate the temperature by absorbing and releasing heat gradually, both from internal and external energy sources. It can cover anything that absorbs heat, from building materials to furniture, either as part of the external building or inside (Zhou et al. 2008). The principle of

thermal mass, as it applies to passive building design, is effectively one of load shifting – that is, delaying the point during the day at which the internal air is heated (Geros et al. 1999; Shaviv, Yezioro & Capeluto 2001). The effect during winter is straightforward: heat is absorbed during the day when air temperature is warmer than the thermal mass, and heat is released at night as air temperature dips below the temperature of the thermal mass. As the thermal mass releases energy back into the air, it maintains the internal air temperature for longer and reduces the heating load. The action is the same during summer when heat is absorbed during the day and released at night; however, summer night time release should be coupled with ventilation, either natural (opening windows), mechanical (exhaust fans), or both (Geros et al. 1999). Adding ventilation allows the use of cooler night time air to cool the building instead of mechanical cooling, and the presence of the thermal mass has lowered the cooling load during the day. However, without ventilation reducing overnight temperature, the building may act as a large heat sink and the overall cooling load may remain the same, simply offset by a number of hours. The use of thermal mass has been found to be generally more effective in hot locations where there is a large difference between external daytime and night time air temperatures (Geros et al. 1999; Givoni 2011; Sadineni, Madala & Boehm 2011). The effectiveness of thermal mass during summer also relies heavily on shading – if left unshaded the building may gain more heat than can be dissipated overnight and the building will remain warmer the following day, increasing cooling loads. This is particularly important in areas prone to longer heat waves. The initial response of the thermal mass is beneficial, but once it reaches capacity it continues to radiate heat for a number of days. During winter, however, that same shading may reduce the effectiveness of the thermal mass as it is more effective when allowed to absorb radiant heat from the sun. As thermal mass is primarily a passive design feature, its effectiveness is largely impacted by passive solar design features such as shading, orientation and glazing.

2.4.1.5 Glazing

The effect of glazing on building thermal performance is influenced by a number of window unit characteristics, including thermal transmittance, solar transmittance, and air leakage due to the frame itself and the frame into the wall (Gasparella *et al.* 2011). As part of the thermal shell, glazing allows radiant energy from the sun to enter the building, providing heat and light. Generally, a single glazed window has a lower R-value than a wall section, and thus allows heat to be conducted more easily than non-transparent building elements.

Double glazing helps reduce the heat conducted across the window by providing a still air gap between two panes of glass. An otherwise well insulated building can be negatively affected by poor placement of glazing (Su 2008). Kim & Moon (2009) determined that the largest heat gains and losses in a hot climate, Florida in this case, were through windows. Heat gain was found to be greater than heat loss, therefore having a greater impact on the cooling load than the heating load. It was found that 46.5% of the building's energy gain was due to windows – 36.2% from solar radiation and 12.3% for heat conduction through the windows.

In addition to heat simply being transferred through the windows, the size and orientation of windows influence the building's natural light levels, but more importantly for a colder climate, they influence the ability to heat any internal thermal mass.

2.4.1.6 Air Leakage

Air leakage results in internal and external air being able to interact directly, bypassing insulative effects of the thermal shell. Liddament & Orme (1998) estimated that across all non-industrial building stock, air leakage accounts for 36% of heating energy loss. This figure does include a number of large, non-residential building types such as hospitals, schools and offices, and so should be used as an indication of the importance of air leakage in homes, not as a specific target for improvement. The key items that influence the natural leakage rate of a residential building are design, including building type and construction method, and workmanship (Pan 2010; Sinnott & Dyer 2012). Homes constructed from pre-build panels are generally the tightest, followed by typical timber frame constructions, where masonry constructions tend to have the highest levels of air leakage (Pan 2010). Dwellings occupied by low income households are also shown to have higher rates of leakage than so-called 'conventional' and energy efficient homes (Chan et al. 2005). The building's total air leakage rate is influenced by local weather conditions, particularly wind that hits and flows around the thermal shell. A home with a high leakage rate will have this exacerbated during high wind events as more air is pushed through the home (Nabinger & Persily 2011). Despite the fact that the total heat loss through air leakage can be related to local weather conditions, Pan (2010) found no seasonal variation in leakage rates, though it was noted this is inconsistent with other research.

Improvements to a home's air leakage rates can be made through various weather sealing retrofit actions, ultimately blocking gaps in the thermal shell, most notably around windows and doors. Nabinger & Persily (2011) found a 10% reduction in heating and cooling use after weather sealing, and found the home better equipped to resist heat lost during high wind events. Some actions are so effective and cheap to install that in Australia they were provided under government schemes at no cost to occupants. These include the VEET scheme in Victoria and RESI in New South Wales.

Despite air leakage being one of the faster, more direct evaluations a building can undergo, it appears that levels of air leakage are generally not well known. This can be reflected in the assumed rates input into building simulation software, such as AccuRate. In 2010, four years after building regulations regarding air leakage were implemented in the UK, Pan (2010) noted that there appeared to be a lack of empirical research to evaluate the air tightness of buildings built under the new regulations. Similarly, Ambrose et al. (2013), on a small dataset of 20 homes, found evidence to justify further research into air leakage rates as the measured rates differed significantly from the standard assumptions made within the building rating program, AccuRate.

2.4.2 Climate

The building's internal conditions are informed by how the thermal shell interacts with the climate. Similar buildings in different climates may perform wildly differently as different conditions create different heating and cooling load profiles. It is not guaranteed, for example, that a home designed for high efficiency in Melbourne performs with the same efficiency in Brisbane (Ambrose et al. 2013). It is for this reason that climate zones are considered when calculating the energy star rating of a building under NatHERS. The climate therefore plays a substantial role in determining how the building behaves, and in determining how the building should be designed to begin with. It is therefore also important to note that buildings in climates with large seasonal changes may perform very differently in different seasons. These elements are particularly relevant for southern parts of Australia where heating load is the dominant energy use, but large peak cooling loads are experienced during summer (Ambrose et al. 2013).

Buchberg (1969) wrote:

> …it can only be stated that quantitative generalizations regarding the influence of the urban microclimate on the thermal behaviour of a structure or on the resulting indoor climate are very difficult if not impossible to make.

Though Buchberg's (1969) study was conducted via simulations nearly five decades ago, the findings are still relevant as they show the variation that micro-climatic events cause in building performance. When validating AccuRate, Dewsbury (2011) showed a comparison between the 'Typical Meteorological Year' climate files included in the software and site-measured data. Dewsbury (2011) concluded:

> …trends in the figures show that the general daily pattern is similar, but that the maximum and minimum values are consistently different. This would cause a considerable difference between [AccuRate] simulations using either the default climate file or the measured air temperature data.

This is reinforced by Nabinger & Persily's (2011) paper showing local windspeeds affected building infiltration rates. The implication is twofold: first, climate has a significant impact on building energy use, and second, the micro-climate is a very significant factor as it directly affects the building. Krüger & Givoni (2008) came to a similar conclusion, showing that using the site-specific ambient temperature instead of the nearest meteorological data increased the average external temperature by 1.3 degrees. This nearly doubled the number of cooling degree days that the building in the micro-climate of its local street actually experienced when compared to what meteorological data would predict. Climate influences the building energy used, and the micro-climate the building is actually responding to can differ significantly from the climate in the general area.

With the threat of global warming coming more and more into focus, changes in the design climate for a building are becoming a very real possibility. In a study evaluating the effects of a changing climate, Wang, Chen & Ren (2010) detailed how differently rated homes would respond to this new climate. The research here is important for a number of reasons. First, it shows how a home's energy use will change under different climatic conditions. Second, it shows how changing climate will effect building energy use overall. Using absolute figures, higher efficiency homes were found to experience less change than lower

efficiency homes. It was also noted in a heating dominated climate the changes in energy used for space conditioning would largely balance, as the reduction in cooling load was balanced by the increased heating load. In cooling dominated climates, however, overall energy consumption rose. An additional paper by Wang, Chen & Ren (2011) also stated that for energy efficiency and carbon reduction schemes to be effective they should take into account the warming climate.

The building's internal climate is driven ultimately by the external microclimate of its surroundings, which is related to the climate of the wider geographic area. The building's energy use is a description of how the occupants wish to alter the internal climate, usually to increase their comfort levels. Understanding current climate behaviour is one of the most important elements in understanding the building's thermal behaviour.

2.4.3 Behaviour

While external conditions drive the building's internal climate through interactions with the thermal envelope, it is the reaction of the building occupant to internal conditions that result in energy use. Without the occupant intentionally turning on heating or cooling appliances to satisfy comfort requirements, there is no energy used by the building in this regard (Schweiker & Shukuya 2010).

Fabi et al. (2012) term all factors influencing occupant behaviour as 'drivers', and summarise them into five groups: physical environmental, contextual, psychological, physiological, and social. Physical environmental are basic responses to temperature and humidity. Contextual drivers are the elements of the thermal shell that are interacting the physical environmental driver, and 'indirectly' influencing the behaviour. Psychological drivers revolve around satisfying occupant needs and wants – the desire to be warmer for example – but also include elements such as finance or habit. Physiological drivers include age, health situation, clothing and other items regarding the occupant's physical wellbeing. Social drivers refer to interactions between different occupants in the home. All these drivers combine in such a way that even if the physical environmental and contextual drivers are the same (for example, identical constructions, side by side and experiencing the same weather conditions), differences in psychological, physiological and social drivers will alter energy consumption.

Different studies estimate the influence of differing behaviour at different levels, from 4.2% (Guerra-Santin, Itard & Visscher 2009) to 11.9% (Guerra-Santin & Itard 2010), and even up to 21% (Al-Mumin, Khattab & Sridhar 2003) though this depends on the initial heating and cooling loads of buildings in particular parts of the world. Additionally, one study showed that promoting energy-saving behaviour could reduce energy use by more than 10% (Ouyang & Hokao 2009). As people age, heating loads tend to increase as comfort level changes and the need to keep warmer grows (Liao & Chang 2002). This impact on behaviour due to an aging population is estimated by Brounen, Kok & Quigley (2012) to balance out any future technological advances, meaning the internal temperature will be more comfortable but the energy use will not be reduced. Beyond simply having different comfort levels, using technology and decisions regarding how to heat or cool the home influence the final level of energy used. Guerra-Santin & Itard (2010), analysing data from a self-reporting survey, found that duration of use has greater influence on energy than temperature setting. Bell et al. (2010), reviewing a series of high-efficiency homes, found the complexity of the air conditioning and ventilation systems installed meant residents were not confident enough in using the systems effectively, and consequently were unable to use the building in the most effective way. Choices about whether to open a window and create a cross breeze, utilising passive design features of the home, or simply turning on the air conditioning, have a big impact on energy consumed. It is also shown that owner-occupied homes spend less money on heating and cooling than rented properties (Rehdanz 2007).

Behavioural aspects of energy use manifest in a far more complicated way when improvements are made to a building, represented by the 'rebound effect'. The rebound effect refers to the phenomenon of an efficiency measure being less effective due to an increase in the effective supply (Greening, Greene & Difiglio 2000). In the context of energy efficiency, the effect is seen when a home becomes easier to heat, thus achieving the same level of comfort for a smaller financial cost or without the appliance running at full capacity. This provides the occupant with greater ability to increase their comfort level by using the heating or cooling at a greater intensity or for longer periods. Estimations of reductions in energy use were not found to always account for this. Hsueh & Gerner (1993) stated that, "In the face of lower per unit warmth, households may increase their demand for warmth, offsetting the reduction in fuel demand". The meta-analysis by Greening *et al.* (2000)

estimated the rebound effect for heating to be between 10% and 30%, and cooling up to 50%, for a 100% increase in efficiency; however, the data analysed did not include measurements regarding increases in conditioned space, or increases in comfort levels. The authors also stressed that the studies reviewed tended to define the limits of the rebound in different ways. Despite these drawbacks, this does indicate that the building fabric and appliances can only bring the energy consumption down so far – the rest relies on the occupant's behaviour. It is perhaps this effect that has been observed in the long term study conducted by Ambrose et al. (2013) that found little benefit during the summer months for an increase in the Energy Star rating.

2.4.4 Summary of Effects on Energy Use

Buildings are complex thermal systems with many individual elements coming together to create the final energy use. Influences from climate, building design (including materials), and occupant behaviour combine, depending on the composition, to form highly efficient or inefficient buildings. Improving thermal efficiency of buildings is widely recognised as one of the key elements in reducing energy use. This has benefits to the individual in reducing energy bills, and to society in reducing carbon emissions. It is important therefore to ensure that buildings are becoming more efficient. Due to the system's complexity, this is no easy task. The following section discusses ways in which a building's thermal performance is evaluated, the difficulties involved, and the areas in which improvements might be made.

2.5 Evaluation of Thermal Performance

Evaluating thermal performance relates to discovering how well or poorly a building resists changes in the local microclimate to maintain its internal temperature state. It has relevance to occupants' comfort level and informs the amount of energy that may be required to achieve it. This in turn informs the carbon emissions and financial costs of maintaining the comfort level. Generally, however, the evaluation rests wholly on determining how the building's physical properties are responding to specific conditions, removing the occupants' behaviour from the evaluation to enable comparison across a number of buildings.

There is a number of techniques used to evaluate building performance. These include:

- Using computer simulations and/or standard thermal properties of the construction materials to predict performance

- In situ testing of the response of the whole building, or specific building elements, to known inputs
- Analysing survey data to determine influences of overall home energy use
- Long term monitoring and field data collection of temperatures, and heating and cooling energy use.

It should be noted that these tools are used for a wide variety of studies with different aims, and there is a difference between post-construction evaluation and post-occupancy evaluation. Post-construction evaluations deal purely with the physical nature of the thermal shell as built. Post-occupancy evaluations may also include some element of post-construction evaluation, but will also show how the occupant's behaviour affects building performance. The most important thing to identify here is that a post-construction evaluation can determine whether the design has been executed, but a post-occupancy evaluation can determine how well that design actually works. An example of this includes the side-by-side study on two Welsh homes by Ridley et al. (2014), where post-construction evaluation determined the homes technically performed very well, which was backed up by a post-occupancy evaluation. However, the post-occupancy evaluation also found the homes were overheating in summer, likely due to over-specifying the glazing to account for worst-case cooling loads, and some behavioural aspects. These are elements that post-construction diagnostics would not have discovered. This is a very specific example, but it serves to highlight the difference between applications of some of the tools available. In situ testing would be considered as post-construction evaluations, and survey analysis and long term monitoring would be considered as post-occupancy evaluations.

Many studies use a combination of some or all of these approaches, such as Ridley et al. (2014), Baker & Van Dijk (2008) and Johnston et al. (2014), either in an attempt to show how a given factor is influencing building energy use, or demonstrating the validity of an evaluation tool. Demonstrating a tool's validity may be done by showing that a new method gives the same or better information than a current method with the same or better reliability, or that particular results of a post-construction test give an indication of post-occupancy performance.

Survey analysis is acknowledged as an important part of the suite of tools available for evaluating building performance. Survey analysis is more attuned to evaluating long term trends and behavioural impacts. As the focus of this study is on evaluating the thermal shell's performance, studies using survey analysis have not been reviewed.

2.6 Monitoring

The monitoring of actual heating and cooling energy consumption, together with building temperature and humidity over time, seems the most straightforward method of gathering real world performance data. This generally forms an evaluation based on a combination of building performance and occupant behaviour under real conditions, and is different to the performance of a building observed under controlled conditions.

Building monitoring usually involves setting up a number of instruments to take readings of temperature and relative humidity both externally and internally throughout the building, logging energy use and gathering additional information that might provide insights into what additional variables may be affecting the behaviour of the occupants or the building. It is generally used as a means of showing how energy efficiency measures, whether improvements in the thermal shell or building technologies or behavioural changes, can influence energy use. In this way it attempts to show what is effective in improving comfort or reducing energy use, and therefore worth including in future building designs or policy decisions. The CSIRO study by Ambrose et al. (2013) is an example of how monitoring was used to evaluate the effectiveness of a broad increase in energy efficiency standards, while Stazi, Mastrucci & Perna (2012) used monitoring to demonstrate specifically how solar walls might improve building performance. Many other studies have taken this approach, either using case studies for proof of concept, or large-scale research projects to show overall effectiveness. Examples include studies by Branco et al. (2004), Dewsbury, Fay & Nolan (2008), Gregory et al. (2008), Hens (2010), Krüger & Givoni (2008; 2004), Makaka, Meyer & McPherson (2008), Rezaie, Dincer & Esmailzadeh (2013), Ridley et al. (2014), Ridley et al. (2013) and Sugo et al. (2005; 2004).

In determining the performance of the building envelope, it is desirable to split energy consumption by end use. This makes it possible to determine the energy deliberately used to heat and cool a building, as well as energy dissipated in other appliances that would have

the end result of adding heat load to the building. This approach is the only way to determine exactly how behaviour influences building performance, and how much energy is actually used. The other methods of building evaluation can provide indicators, but are focused on the building fabric and unable to show the influence of behaviour.

The 'Monitoring energy and carbon performance in new homes' guidelines state that these types of long term studies attempt to measure energy consumption and related carbon emissions to determine how key features of new designs (increased insulation in walls and ceiling, improved airtightness through the entire structure) improve performance compared to a baseline set of houses (Energy Saving Trust (EST), 2008). For these types of studies it is suggested that 100 homes should be used to reduce the uncertainty of results to ±5% (Energy Saving Trust (EST), 2008); however, the Residential Building Energy Efficiency Study (RBEES) report also discussed sample sizes and determined a much larger sample of 240 homes was needed for statistical significance. This would be true for studies attempting to validate design changes on a population and evaluate different levels of energy efficiency in design. The same monitoring approach can be applied to case study buildings with meaningful results (Energy Saving Trust (EST), 2008).

Another example of the effectiveness of long term case study monitoring is the Camden Passive House (Ridley et al. 2013). Through extensive, high level monitoring this study identified a number of issues with the housing design, and showed that the performance standard was exceptionally high (65kWh/m^2), but not quite at the level of the designed Passive House criteria (46kWh/m^2). The overall approach shows how powerful high levels of data collection can be; identifying issues through summer that "would not have been found" had monitoring of the building not been in place. The major issue, however, remains that discovery and rectification of these issues required a high level of detailed monitoring and expert analysis. With greater numbers of highly efficient houses, it would be expected that these 'teething issues' would be solved. In terms of behavioural influences, however, it is likely that at least seasonal monitoring will always be necessary to identify key human factors, such as comfort levels and manually operated passive design features (such as opening windows to allow cross ventilation).

Though determining building performance through long term monitoring appears straightforward, it is not without shortcomings. It requires a large amount of time,

potentially years, large amounts of equipment, and volunteers willing to participate. The amount of equipment required is demonstrated in a case study conducted by Stecher & Allison (2012). In evaluating over the course of two years a US-located Passive House design, sub-metering of each electrical circuit was required, as well as consultation with an electrician to ensure each sub-metered section was on a separate circuit. Air temperature was taken in ten different locations in the occupied areas of the house, as well as additional sensors around and inside the cooling unit, and outside the house. Similar levels of equipment were required for the three case studies conducted by Ridley et al. (2013; 2014). As noted previously, the study by Ambrose et al. (2013) also required large amounts of equipment. In both cases, with the exception of the temperature sensors used by Ambrose *et al.*, the equipment was also connected to a wireless modem to allow for remote collection. These studies by Ambrose et al. (2013) and Ridley et al. (2013; 2014) are examples of the equipment arrays required to effectively monitor building performances over long periods. Due to the large amount of technical equipment required, performing large-scale monitoring can be very expensive. As technology improves, however, these costs are expected to reduce, and long term studies may become financially easier to implement. Eventually, with higher quality sensors and a large baseline dataset, patterns may emerge that mean year-long studies are not required to provide the same troubleshooting for high efficiency homes, as was required for the Camden Passive House (Ridley et al. 2013). However, any study attempting to account for seasonal variation is expected to require a year, if not multiple years, of monitoring to observe these effects.

Additionally, because of the requirement of having volunteer participants, studies monitoring energy use in homes are potentially likely only to draw people interested in their energy use. This may be a potential source of error in the study as the vast majority of volunteers questioned by Ambrose et al. (2013) agreed to some extent that they were “an energy conserving household”, though overcoming this difficulty may be near to impossible. In addition, gaining willing participants can be difficult. Possible disruptions to normal life due to installation of equipment, and potentially feelings about a lack of privacy, may reduce the number of people willing to participate in studies using high-volume data collection techniques.

Applying long term monitoring is probably the most comprehensive way to determine a building's energy use, and to draw conclusions about the effectiveness of any energy efficiency strategies implemented. It enables the researcher to gather data on nearly every aspect they feel is relevant, and to determine exactly how much energy is used, what the temperature really is, and so on, instead of relying on indicators, either via experimentation or surveying building features. Despite all the advantages, the shortcomings due to time, complexity and cost of equipment, and availability of volunteers, tend to result in long term monitoring being used more in case studies than large-scale evaluations. Some of the issues surrounding cost and disruption to residents may be side-stepped by using surveys and energy use data gathered from energy providers, but the only way of determining the actual temperature inside the building is to place sensors inside and monitor it over time. However, it may be that rather than running additional long term studies, once sufficient data is gathered it can be used to inform computer models that evaluate how changes to the building fabric or occupant behaviour influence temperature and energy use.

Long term monitoring studies should usually be considered post-occupancy studies. Their use as a compliance tool to ensure the thermal shell is performing as intended is severely limited due to the timescales on which they operate. However, the importance of conducting long term studies cannot be understated as they show how particular building elements, behaviours or diagnostic results translate into actual energy use.

2.7 Building Simulation

Building simulation involves developing a computer model of the building that is then subjected to virtual weather and conditioning profiles, resulting in a theoretical output of building behaviour. The major advantages of simulation are that they enable the analysis of "situations that are difficult to examine experimentally" (Hitchin, Delaforce & Martin 1993), and that similar buildings can be simulated under a multitude of different conditions relatively quickly. Simulation can indicate how alterations to the building envelope may affect energy consumption under imposed conditions, and can also be used to compare different evaluation methods. It is often used in addition to other techniques, such as long term monitoring or in situ testing. These real-world data collecting areas are often used to validate the simulation program and provide support for conclusions drawn from alternate scenarios being simulated.

Simulation software, while powerful, do have their limitations. Each relies on assumptions made within the basic algorithms, and about the treatment of real world cause and effect in the virtual realm. Lomas et al. (1997) used two small, highly understood buildings (a one room construction and a two room construction), and their known element values including actual performance readings under certain conditions, and ran the same simulation through 25 different combinations of software packages and users from around the world. They discovered variability between the simulated and real results, and between the results from different software packages. This highlighted the potential issues in relying on modelling utilising only plan data as a definitive way of assessing actual levels of housing performance.

Validating simulation models is complex and costly (Lomas et al. 1997), and not without problems. Hitchin, Delaforce & Martin (1993) described validation methods for making measurements in the building, and attempting to reproduce them in the model, as "weak" and providing "little information to the model builder or user of which components of a model are strong, and which are weak". In this way, Hitchin, Delaforce & Martin (1993) suggest that due to the inherent complexity of building thermal behaviour, simple validations of a building model cannot ensure that changes to the building model resulting in reduced energy use will translate in to real-world energy savings. In addition, Hitchin, Delaforce & Martin (1993) found that:

> …the widely-used 'perfect-mixing' assumption not only breaks down, but does so in a manner which has serious consequences when predicting transient thermal response: the actual air temperature response is much slower than that predicted.

Despite these shortcomings, either in validating the models or the assumptions the model makes, simulation tools are immensely powerful tools of evaluation, and are widely used for research and determining compliance with building standards.

2.7.1 Use of Simulation Software for Building Evaluation

The more prominent use of building simulation serves to evaluate building performance, rather than test an evaluation method. Simulation for building evaluation purposes is used in two ways: either to evaluate building design to determine if it meets minimum performance standards for compliance, such as NatHERS in Australia, or to use multiple variations to determine how changes to a building may affect performance. These may be

physical changes to the thermal shell, such as different materials or orientations, changes to the building's environment, or changes to occupant behaviour. Used in this way, simulation software demonstrates in a short amount of time, and at minimal cost, how effective different changes to a building can be.

It is important to realise that software used in rating homes under NatHERS are not intended to predict energy use for the home once occupied. The intention is to provide a consistent approach to evaluating design of the thermal envelope, and to do this certain assumptions must be made. It should come as no surprise that homes that are used differently use different levels of energy, but the purpose of the scheme is to evaluate the building. To do this with some measure of consistency for the entire building stock, some standard assumptions regarding comfort levels and behaviour patterns must be made. If done correctly, it would seem using standard assumptions would not be an issue. However, Ambrose et al. (2013) suggest some of these assumptions may not represent reality. This is reflected in the fact that no improvements were observed for summer, despite an improvement in the summer portion of the rating calculation. If this is the case, it is possible that the evaluation inflates the rating of some homes, and deflates the performance of others. Other studies, such as Ryan & Sanquist (2012), also suggest that assumptions surrounding occupant behaviour are potential sources of error in building simulation.

There are many examples of simulation software being used for studying the effects of building alterations, and in some respects this is the staple method for building research. When evaluating low-cost approaches to overcoming increases in Australia's energy efficiency standards, Morrissey, Moore & Horne (2011), and McLeod & Fay (2010), designed simulation experiments to showcase low cost influences on the star rating. Morrissey, Moore & Horne (2011) found that across 81 different designs, the standards were easier to reach in smaller homes, and that passive design features (such as optimising orientation) are effective and low cost measures that can assist in reaching these standards. McLeod & Fay (2010), focusing on a case study in Hobart, did not evaluate the effects of differing orientations, but they showed that house types other than standard brick veneer could achieve the same levels of performance for a reduced cost, though they speculate that "higher levels of thermal performance than the ones presented could be obtained if the floor plan was altered". In both cases, no real world validation was used, but Morrissey,

Moore & Horne (2011) highly recommended it for future research. Other examples of simulated experiments without real world validation include Depecker et al. (2001) determining the effect of building 'compactness' on energy use for cold and mild climates, Kim & Moon (2009) evaluating effects of insulation, also in cold and mild climates in the US, and Pan et al. (2012) also evaluating insulation, but in cool, mild and warm climates in China. All these projects used building simulations to provide evidence for how different factors change the building's thermal performance and energy use, but they were able to conduct this research much faster, and at far less cost than would have been the case if each simulation was set up as a real world experiment. This is the main advantage of simulation software – it allows conduction of a series of scientific experiments with full control over all variables. Each experiment is repeatable, with individual factors easily isolated. For Morrissey, Moore & Horne (2011) to conduct research on 81 different designs in the real world, creating an environment where all experienced exactly the same conditions, inputs and loads, is near impossible and highly costly.

Additional examples of simulated analysis of either building performance, or effects of building elements on performance include, Gasparella et al. (2011), Krüger & Givoni (2004), Persson, Roos & Wall (2006) and Wang, Chen & Ren (2010).

2.7.2 Combining Simulation with in situ Evaluation

Simulation may also be combined with in situ evaluations, generally for the purposes of validating the modelling software or technique so that it can be used confidently in future research. The processes are straightforward and almost always involve a small test cell. The values of in situ testing and monitoring are in providing information about the thermal characteristics of the materials, and how the building responds under certain stimulus. The thermal information is used by the model, and the conditions then simulated. This is broadly the basis for the BESTEST certification process (Lomas et al. 1997) which was in turn used by Henninger, Witte & Crawley (2004) for evaluating EnergyPlus, and how Hitchin, Delaforce & Martin (1993) evaluated the shortcomings of parts of the simulation calculation. The empirical validation of AccuRate by Dewsbury (2011) continued this in Australia, and Ambrose et al. (2013) might be said to have used a similar philosophy. However, Ambrose et al. (2013) was not concerned with replicating conditions in a test cell, but with whether efficient building elements rewarded by NatHERS, and represented by higher star ratings,

translate into real world performance on the large scale. Other examples include Blomsterberg et al. (1999), Carrillo, Dominguez & Cejudo (2009), Belleri, Lollini & Dutton (2014), and Raftery, Keane & O'Donnell (2011).

2.7.3 Summary

Simulation tools allow for conduct of a significant amount of research in a short time and at minimal cost. They are, with the notable exception of the PassivHaus design tool, the best way of evaluating building design, and therefore catching any design flaws early. They are exceptionally useful when evaluating how different buildings will respond to different stimuli, without requiring a huge number of physical buildings or large amounts of time to monitor them. Getting design right early is a major part of successfully constructing energy efficient housing. Being able to evaluate changes to the building in the design phase reduces the risk of having to retrofit additional energy saving technologies, and saves time and money over the lifetime of the building.

The issue with using simulation is that of the performance gap. Comparisons between designed performance and actual performance show that analysing building design using modelling software underestimates heating and cooling loads. This may undermine efforts to reduce energy use via energy efficiency regulations that rely on a simulation tool for compliance. This may also be a substantive issue for any mandatory disclosure program. Field testing is therefore a vital part of building evaluation. It would be expected that in situ testing can provide some level of quality assurance that the finished construction has all the characteristics of the design, and can provide some data with which to calibrate the model.

2.8 In situ Testing

In situ testing refers to the systematic approach of subjecting a building to certain conditions and measuring the response. A number of methods and signals can be used and processed. These methods test one or a number of building elements, either focusing on evaluation of the R-value or heat loss of the material or building, or the ventilation of the building. Some of these tests include:

- **Heat Flux**: In situ measurement of thermal resistance and transmittance, international standard ISO 9869:1994

- **Infra-Red Thermography**: Qualitative detection of thermal irregularities, international standard BS EN 13187:1999
- **Air Permeability (blower door test)**: detection of permeability/leakage levels of building enveloped (Pressurisation method), international standard BS EN 13829
- **Co-Heating Test**: Steady state response of thermal envelope – no international standard, however Leeds Metropolitan protocol is accepted as the de-facto UK standard.

These tests evaluate the thermal shell as built, and are considered 'post-construction tests'.

2.8.1 Heat Flux Tests

The use of a heat flux sensor allows for in situ determination of the R-value or R-value of building elements in a non-destructive manner (Desogus, Mura & Ricciu 2011; Rye & Scott 2010). The use of heat flux sensors has a long history. There are some references to early prototypes in use in the early 1920s, and much work conducted into improving accuracy and reduction in size and cost in the mid-1980s (Heard & Ward 1982; Trethowen 1986), the recommendations from which appear to have been incorporated into modern procedures.

The heat flux method is detailed in international standard ISO 9896, and measures the direct heat flux through the element and the temperature difference across it (Desogus, Mura & Ricciu 2011; ISO 2014; Rye & Scott 2010; Stamp 2011). This is done by directly attaching the sensors to the element being evaluated, and collecting data for a minimum of 72 hours before using one of the two analysis techniques detailed in the standard. The Average Method, or Progressive Mean Method, applies cumulative averaging of the heat flux and temperature difference to determine the conductance, providing that the criteria for the heat balance are met (Cucumo et al. 2006). The more complex method detailed in Section 7.2 of the standard can be applied if the element has a high thermal mass and the criteria for the Average Method are not met (ISO 2014). Alternative analysis procedures have been suggested and analysed. Cesaratto, De Carli & Marinetti (2011) evaluated the Average Method, an alternative Daily Method first presented by Bloem (1994), and the Black Box method. Cesaratto, De Carli & Marinetti (2011) found that when the external temperature had an overall trend across the monitoring period (the data used in the study showed a decrease), the Daily Method provided a more stable estimate of the U value than the Average method. Cucumo et al. (2006) demonstrated an analysis method utilising a

'finite differences calculation code'. In essence, this provided a trial-and-error calculation and percentage root mean square error (RMSE) calculation to determine the equivalent thermal conductance. The authors deemed this to be more applicable than the Average Method as it could be applied when thermal energy is stored within the wall during the test (Cucumo et al. 2006). However, since the latest release of the ISO standard is from 2014, it can be concluded that these alternatives require further evaluation before replacing the Average Method as the international standard.

Maintaining a temperature difference across the testing element is one of the most immediate influences on the accuracy of the heat flux test. Both Desogus, Mura & Ricciu (2011) and Doran (2008) quote 10 K as the minimum difference for maximum confidence in the accuracy of results. Stable conditions for the test period increase the reliability, as demonstrated by Cesaratto, De Carli & Marinetti (2011). Trends in external temperature are not the only climatic element that may influence the results of a heat flux analysis. Zhu et al. (2009) also note that solar radiation can influence readings, and measures to reduce this effect are included in the ISO analysis procedure. Doran (2008) also noted effects of sun, but additionally pointed out that wind can influence determination of thermal conductance. Wind passing over or through the wall, thereby passing over or through the insulation, removes heat from the materials. This increases observed conductance; however, Doran (2008) states that this is not an error in the experiment but reflects "genuine variation in the R-value". Peng & Wu (2008) went as far to suggest that measuring the heat flow rate at all was inherently difficult and presented an alternative that does not utilise the heat flux meter at all. In spite of this, there are repeated and continued examples of in situ determination of conductance by measuring the heat flux and using the averaging method since this publication: examples include Ridley et al. (2014), Ridley et al. (2013), Rye & Scott (2010) and Stamp (2011).

Heat flux sensors are generally applied in the field to enable evaluation of the effective R-Value of the building element as it stands, rather than using standard figures or laboratory test examples as indicators. This is an important factor in building evaluation as the effective R-value in situ may not always agree with the standard figures for a given element composition, or with the declared figures from laboratory tests or manufacture specifications (Doran 2008; Peng & Wu 2008). Doran (2008) quotes "moisture-related

phenomena, adventitious air movement or factors that may be influenced by workmanship or performance of machinery" as possible causes for these discrepancies. Rye & Scott (2010), and Baker (2011), are both examples of using heat flux sensors as an evaluation tool to determine in situ R-value of walls where standard calculation methods are expected to be somewhat unreliable. These studies both focused on 'traditional' construction, where wall composition is generally solid stone and masonry, and not entirely homogenous, but also covers some timber frame structures with different infill materials (Rye & Scott 2010). Both these studies indicated that figures used in R-value calculation for building evaluation purposes were underestimating thermal performance of the traditional building. A Greek study by Haralambopoulos & Paparsenos (1998) utilised heat flux measurements to evaluate the R-value of a building to be retrofitted where the building was sufficiently old and materials degraded to the point where no standard estimates could be made confidently. The research shows that for building evaluation, the main application of heat flux sensors is to provide a reliable estimate of the thermal properties of the construction, particularly where reported figures or standard calculations are reasonably expected to contain some error.

While this is generally accepted as a very reliable method of determining the thermal conductance, there are disadvantages to the method, particularly when attempting to evaluate occupied homes. In terms of practicality, Rye & Scott (2010) note that since the heat flux sensor must be stuck to the walls, walls with wallpaper were avoided over concerns the surface would be damaged. It is also necessary to set up wiring and datalogging equipment through the home, and occupants may object to this, making it difficult to implement on a large scale. Zhu et al. (2009) overcame both these issues somewhat by embedding their sensors into the wall's plaster layer, but this was facilitated by the homes being designed specifically as Zero Energy Houses and designated for research of this kind.

The heat flux sensor also only measures the conductance of the area in which the sensor is located. Areas that may provide thermal bridging, such as wall studs, or sections that have incomplete insulation coverage, will not provide an accurate representation of the overall wall structure. This can be overcome. Rye & Scott (2010), and Doran (2008), used thermographic imaging to ensure the temperature distribution across the wall was even,

and the sensor's location therefore representative of the whole. Cesaratto, De Carli & Marinetti (2011) also evaluated the effect that the presence of the sensor might have on readings, and this was found to be negligible with current equipment. Secondary to this, and the main issue with the heat flux tests for whole building evaluation, is that on its own it cannot provide a figure for whole house heat loss. The heat flux sensor only measures the flow perpendicular to the surface: it does not account for heat lost through conductance at corners, or by air leakage. However, generally it is not intended as a tool to predict whole house heat loss or energy use, but the results of testing individual elements can be used as an indicator of whether overall performance is likely to be good or poor.

2.8.2 Air Leakage Tests

Air Permeability tests, also grouped with tests of air leakage or tests for infiltration rates, are conducted in two ways: Tracer Gas Method and Pressurisation Method. The two methods measure different but related elements: either 'infiltration' by the tracer gas, or the 'tightness' of the building by the fan pressurisation (Sfakianaki et al. 2008), though they are not always presented as being truly interchangeable (Blomsterberg et al. 1999). The measurement of air leakage allows for calculation of heat lost through this action, but does not provide any indication of heat lost via transfers through non-permeable sections of the thermal shell. In addition to energy use, tests are also used to indicate indoor air quality (Sherman 1990).

2.8.2.1 Tracer Gas Method

The tracer gas method measures the decrease in concentration of specific gases, commonly CO_2 although others have been used. The tracer gas method relies on conserving total air mass within a zone. By measuring changes in concentration of the tracer gas, an air change can be inferred and calculated (Hitchin & Wilson 1967; Sherman 1990). There are many approaches to using a tracer gas. The tracer decay is most widely used but alternatives include the pulse technique, constant injection, long term integral and constant concentration (Hitchin & Wilson 1967; Sherman 1990). In all cases, the most important assumption is that the air is sufficiently mixed, and the most common mistakes in using tracer gas involve insufficiently mixed air (Hitchin & Wilson 1967; Sherman 1990). Each technique is also more appropriate for a different set of conditions; the decay and pulse

methods, for example, take less time to set up and run, where constant injection and concentration may provide greater accuracy but require more equipment.

2.8.2.2 Fan Pressurisation Method

The Pressurisation Method, commonly referred to as a blower door test, uses a large fan installed in a doorway (or window frame) to pressurise and depressurise the building (Kim, Jo & Jeong 2013; Sfakianaki et al. 2008). A large amount of the initial work on this method was conducted by Kronvall (1978). The pressure is changed such that a 50 Pa difference exists between the internal building and atmospheric pressure. Measurements of the required air volume being moved to maintain this pressure provides the Air Leakage at an air pressure difference of 50Pa between the interior and exterior environments, n_{50}. This can be represented in either m^3 or, if the building volume is known, Air Changes per Hour. Average infiltration is shown to increase linearly with leakage rates (Jokisalo et al. 2009), and so using the 'divide by 20' rule proposed by Kronvall (1978), the n_{50} reading can be translated into the average infiltration rate. This is a fairly crude estimate, and there are different estimates of what the denominator should be. A more complex analysis of the 'leakage-infiltration ratio' by Sherman (1987) estimated figures between 15 and 30 depending on the test conditions, and simulations by Jokisalo et al. (2009) showed the ratio as high as 39.

2.8.2.3 Comparison

These two methods have both been widely used to determine the air leakage, and by extension the heat loss, of buildings. Examples of blower door tests include Alfano et al. (2012), Bassett (1983), Chan, Joh & Sherman (2013), Chan et al. (2005), Jokisalo et al. (2009), Kalamees (2007), and Sinnott & Dyer (2012). The tracer gas alternative was selected by Belleri, Lollini & Dutton (2014), Malik (1978), Nabinger & Persily (2011), and Stymne, Boman & Kronvall (1994), while the study conducted by Sfakianaki et al. (2008) used both methods. Studies that combine energy use and air leakage measurements seem to have opted for the fan pressurisation method, such as those by Ridley et al. (2014), Ridley et al. (2013), and Stamp (2013).

The figure relevant to energy use – that is, the figure used by the infiltration losses calculation – is the infiltration rate, directly measured by using the tracer gas method. The air tightness measured by the fan pressurisation method is shown to be related to the

infiltration rate, though the 'divide by 20 rule' is also shown to have some significant variation. The tracer gas method is expected to provide a more accurate measurement of the infiltration, however is more likely to be affected by the climatic conditions during the test than the fan pressurisation method (Sfakianaki et al. 2008). Kim, Jo & Jeong (2013) suggested that the fan pressurisation method is more popular as, despite the high initial cost of equipment, the cost per test is comparatively lower than the tracer gas method over the lifetime of the equipment. It is also simpler to conduct.

Evaluating the infiltration rate is seen as an important part of determining performance; however, it cannot be considered a whole building test. It does provide part of the energy losses not evaluated by the heat flux test, and so theoretically combining the two could provide whole house heat loss. This still uses a sum of the parts approach, however, and the system in combination may not perform in the same way.

2.8.3 Infrared Thermography

Infrared (IR) Thermography uses a thermal imaging camera to detect infrared radiation emanating from a surface, and converts it to temperature (Barreira & Freitas 2007; Bauer et al. 2015; Titman 2001). It is non-destructive and generally used qualitatively as a method for detecting defects in building fabric (Balaras & Argiriou 2002; Barreira et al. 2013; Barreira & Freitas 2007; Bauer et al. 2015; Grinzato, Vavilov & Kauppinen 1998; Titman 2001). The main process is identifying areas of the building fabric that show anomalous temperature readings, either higher or lower than the mean. In doing so thermography can identify gaps in insulation, thermal bridges (ceiling rafters or wall frames, for example), areas of air leakage, areas of moisture, and deterioration of certain materials (plaster delaminating from the wall, for example) (Balaras & Argiriou 2002; Barreira et al. 2013; Barreira & Freitas 2007). Quantitatively, a thermography assessment attempts to show the severity of the flaw, and as measurements need to be taken precisely, further training and data analysis is required (Bauer et al. 2015).

Thermography testing approaches, according to Maladague (2001), can be broadly divided into two sections: Active and Passive. Passive thermography simply observes temperature variations across the surface, whereas active thermography also involves some external thermal stimulation and a longer monitoring period. Active thermography both observes

variation in temperature across the surface, and how changes to thermal stimulation affect the surface overall.

Thermography is used with considerable frequency for a number of research applications. These generally focus on detecting flaws when diagnosing a building, as Haralambopoulos & Paparsenos (1998), and Doran (2008), demonstrated as part of pre-renovation analysis. Reviews by Balaras & Argiriou (2002), Lo & Choi (2004), and Titman (2001), focus on discussing thermography in this fashion, and studies by Barreira et al. (2013), Barreira & Freitas (2007), and Bauer et al. (2015), utilise it to this end. Alternatively, Rye & Scott (2010) used thermography as a supplementary tool to ensure correct placement of heat flux sensors, ensuring they were not placed atop anomalous segments of the wall. Taylor et al. (2012) proposed its use during construction to detect defects early when correcting them is significantly easier. These approaches are all qualitative and provide supplementary information about overall building performance. In practice it is likely that they are applied once sub-par performance of the thermal shell has been identified in an attempt to provide explanation and recommend a course of action. When used in this fashion, thermography can be a fairly quick and straightforward analysis tool.

Quantitative analysis methods are more complex, but provide figures that can be applied to thermal performance. Grinzato, Vavilov & Kauppinen (1998) demonstrate apparently early forays into quantitative analysis, with a number of examples of how temperature differences are calculated but offer no satisfactory discussion on the relationship to overall thermal performance. The method demonstrated by Asdrubali, Baldinelli & Bianchi (2012) shows how the analysis techniques have advanced, estimating the additional heat being lost through the thermal bridging around the window, thus providing a means to adjust the total wall's heat loss estimate. This provides a direct link between thermography data and overall energy use. Budadin et al. (2003) also successfully demonstrated a method of determining the building's overall thermal properties, or at least the building element, using thermographic images to determine building behaviour and calculating the possible range of thermal properties that could provide the observed responses.

Generally, the major advantage of thermographic analysis is the ease of interpreting qualitative data. Areas of thermal bridging, for example, can be very quickly identified based on the thermographic image. However, quantifying thermographic analysis is more complex

because potential sources of error can create false readings if not accounted for; consequently, good understanding of the technology is required. Lo & Choi (2004) list 14 elements that can affect the reading; however, based on the review by Titman (2001) and highlighted by Bauer et al. (2015), wind and rain are the major considerations for qualitative analysis where absolute readings are less important. However, a quantitative analysis should also account for emissivity, colour, reflectivity, ambient temperature, and solar radiation – the thermal camera detects infrared radiation from the surface and all these elements can influence that reading.

Infrared thermography is a very useful, non-destructive method of analysing building performance. The main drawback is that in isolation it cannot provide information on how the entire thermal shell performs. It would be difficult, for example, to determine the performance of a well-constructed house that is poorly designed or orientated. Nevertheless, it is exceptionally powerful when used to qualitatively diagnose the cause and areas of heat loss, and can be used for quantitative studies, though this still has less application.

2.8.4 Co-Heating Test

The co-heating test, in its current form, follows an in situ testing methodology laid out by Johnston et al. (2013). There is no international standard for this procedure; however, work by Johnston et al. (2013) represents the current accepted standard. In addition to the basis of analysing building heat input and temperature difference, variations on analysis methods account for the influences of solar irradiance and wind. Examples of these adjustments include a simple window solar transmission analysis, the Siviour Method, multiple regression methods, and combinations of the above (Jack et al. 2017). Bauwens & Roels (2014) conducted a comprehensive review, describing the test as “a quasi-stationary test method based on linear regression analysis of aggregated building performance data, acquired during appropriate heating experiments”. Its history dates to the late 1970s, being initially proposed as a method for evaluating the efficiency of the heating system in the home, but discussion of the overall Heat Transfer Coefficient (then known as Heat Loss Coefficient) appears in Sonderegger’s (1979) second paper on the method. The test’s effectiveness was clearly apparent, with Ortega et al. (1981) describing it in their study just

two years later as “fairly well established as an experimental method for determining the total Heat Transfer Coefficient (HTC) in conventional residential buildings”.

The procedure as described by Johnston et al. (2013) involves elevating the internal temperature, typically with electric resistance heaters, and maintaining that temperature for one to three weeks. During this time, the energy input is measured, and the daily heat input in Watts is calculated. This is then compared with the daily mean temperature difference. The linear regression provides the HTC in W/K. Ortega et al. (1981) suggest that reducing some of the dynamic effects of any thermal mass requires a period of pre-heating. While this is not explicitly stated in the methodology set out by Johnston et al. (2013), the method does require that a steady, uniform internal temperature is reached before the co-heating test proper begins. It is expected that this observation would incorporate the saturation of the thermal mass, and therefore setting up the heat balance assumed in the analysis.

This procedure is well accepted as a comprehensive analysis of the whole building envelope, and its main advantage is just that: the analysis of the whole building. Other advantages are that it is relatively simple in concept, analysis and result presentation. The co-heating test, however, is subject to some error and influence from climatic conditions. The methodology itself recommends achieving a temperature difference of 10 K, and that testing should be carried out during winter months (Butler & Dengle 2013; Johnston et al. 2013). Even when following those prescriptions, one test carried out by Stamp (2013) experienced overheating and rendered it invalid. It must be noted, however, that this test was carried out on a house built to the Passivhaus standard, and the small amount of additional energy added by the towel rail being on had a large effect on the overall test. The low heat loss of the building in this case resulted in extra energy not being released and the building overheated. The issue with overheating due to solar radiation is not simply that the building has gained energy that has not been accounted for. Part of the design of a high-performance solar building is to utilise solar radiation to minimise additional heating. The energy gained due to solar radiation can be calculated and the test adjusted, though this does add uncertainty due to additional measurements and calculations (Jack et al. 2017; Stamp 2011). The more pressing issue is that it adds energy to the building’s thermal mass, and disturbs the energy balance the test relies on to reduce the dynamic effects of the thermal mass charge and discharge

cycle (Stamp 2011). Some simpler analysis techniques only include the solar radiation gained via the transparent shell (Bell et al. 2010). However, Bauwens & Roels (2014) suggest that the simple adjustments for solar gains require assumptions that can be difficult to justify. They suggest that a multiple linear regression model is a more suitable approach. Variations in analysis of solar gains has been shown to be the main cause for variation in results between different research teams performing co-heating tests on the same building (Jack et al. 2017). Conducting the test during periods of low solar radiation, typically winter months, reduces this effect and should increase the test's reliability.

Only being able to carry out the test in conditions where a 10 K difference can be maintained, and with limited impact of solar radiation, constrains its application. It can be conducted only in cooler climates and during certain times of the year. Additionally, it is required that opening and closing doors and windows, and using electricity beyond that required for the test itself, is kept to a minimum and ideally avoided entirely (Johnston et al. 2013). This means no-one can live in the house while the co-heating test is running, making it difficult to use as it either displaces residents for up to a month (after initial pre-heating and three weeks of testing has occurred) or, in a development context, removes the home from the sales process for up to four weeks (Butler & Dengle 2013; Thompson & Bootland 2011). There are multiple examples of the co-heating test in use; however, they tend to be limited to small sample sizes, likely due to test duration making it difficult to gain volunteers, as observed by Thompson & Bootland (2011). These examples include Bell et al. (2010), Guerra-Santin et al. (2013), Lowe et al. (2007), Ridley et al. (2014), Ridley et al. (2013), Rhee-Duverne & Baker (2015) and Wingfield et al. (2008). In a broader instance, Johnston, Miles-Shenton & Farmer (2015) evaluated 25 homes. The PASSYS project, precursor to PASLINK, also demonstrated use of the co-heating test in evaluating specific building components within highly calibrated test cells (Baker & Van Dijk 2008; Garcıa-Gáfaro et al. 2012). In this case it is simply labelled as 'steady state performance', however the general approach aligns with Johnston et al. (2013) and the graphical analysis with Siviour (1981). The methodology discussed by Baker & Van Dijk (2008) disaggregates the performance of a specific component from the overall performance of the test cell, making it unique to the other studies discussed.

The co-heating test remains one of the best methods of evaluating building performance as it accounts for whole house performance in situ. It is not without its problems as climate and test duration limit its application. It also only evaluates heat loss, thus making it effective only in cooler climates, and essentially meaningless in warm climates or in evaluating summer cooling requirements. There are alternative methods that utilise the co-heating philosophy but attempt to reduce the required duration. Examples include the PSTAR test (Subbarao et al. 1988), PRISM (Fels 1986), and QUB (Mangematin, Pandraud & Roux 2012) and PASLINK (Baker & Van Dijk 2008; Bloem 2010).

2.8.4.1 Solar Irradiance Adjustments

As mentioned above, co-heating test results are influenced by solar gains as this adds to the building's heat input. If this is not adjusted for, the HTC will be underestimated as some of the heating energy is ignored. The literature shows a range of different approaches, summarised as the 'Simple window transmission method', the 'Siviour method', multiple regression methods, and a combination of the Siviour with multiple regression (Jack et al. 2017; Johnston et al. 2013; Stamp 2011). All methods require gathering solar irradiance data. Stamp (2011) notes that it is best to orient the pyronanometer used for the solar irradiance measurements on a vertical plane, as using a horizontal plane tends to overestimate solar gains. All these methods seek to estimate how much additional energy the building has gained from the sun and add this to the energy measured from the mechanical heater used in the co-heating test. This forms the 'solar adjusted power' that should be used for the HTC calculation, and is likely to be a more accurate estimate of the HTC for the building.

2.8.4.1.1 Simple Window Transmission

The simple window transmission method calculates the total area of relevant glazing, and multiplies this by the amount of solar irradiation that would strike this surface (Bell et al. 2010). As most co-heating tests have been conducted in the Northern hemisphere, this is always reported as 'South-facing glazing'; however, for Australian or other southern hemisphere applications this should be adjusted to use North-facing glazing. This approach seems to be crude: it does not account for the performance of the glass, and there does not appear to be much adjustment for East/West orientation of the glass, or the sun's moving position. Implementation of this method also ignores that solar gains can occur through opaque surfaces as well as glazed surfaces.

2.8.4.1.2 Siviour Method

The Siviour method (Siviour 1981) is a graphical approach for calculating the HTC itself. It also includes an estimate of the solar aperture, this being the equivalent area of building fabric through which solar gains are received. It is already more sophisticated than the Simple method because it will adjust for different levels of glazing and will not require judgement about what to include or exclude as 'relevant glazing'.

The Siviour method graphs the daily power input divided by temperature difference on the Y-axis against the daily average solar irradiance, also divided by temperature difference, on the X-axis. The y-intercept is the HTC of the building, and the slope of the line is the solar aperture. The HTC calculated via this method intrinsically includes adjustments for solar gains. Figure 2.2 shows an example of a Siviour plot from Everett, Horton & Doggart (1985).

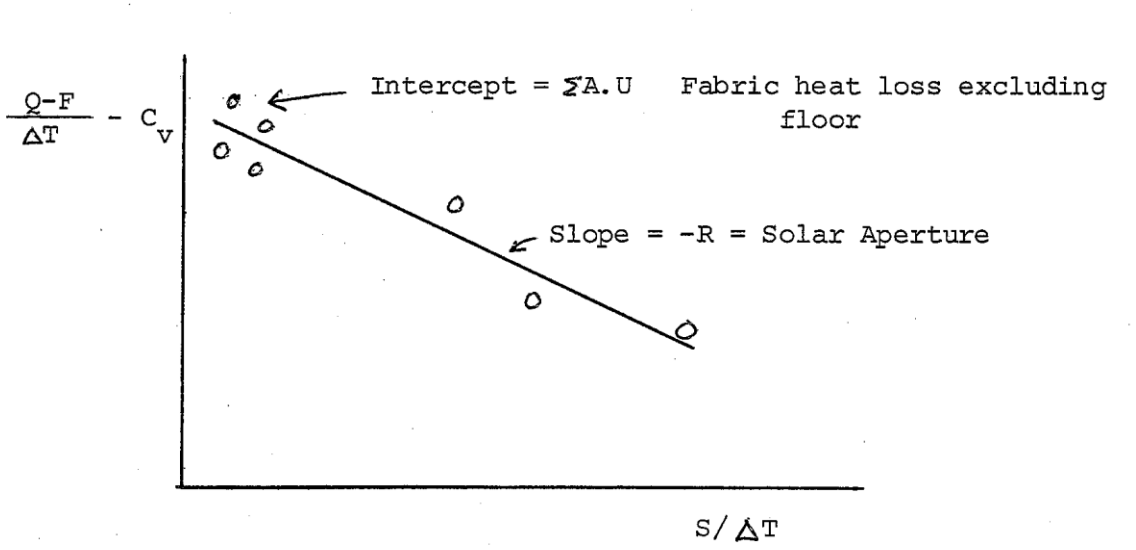

Figure 2.2 Thermal Calibration Plot (Everett, Horton & Doggart 1985)

2.8.4.1.3 Siviour plus Regression

It should be noted that while the Siviour method is widely used, the HTC it provides is not the final figure that is quoted. Often the solar aperture is estimated from the Siviour analysis to adjust the power input before the standard HTC linear regression analysis is conducted. In this process, raw power (power input from the mechanical heating source) is adjusted using Equation 1:

Equation 1 Solar adjusted power

$$Solar\ Adjusted\ Power = Raw\ Power + |Solar\ Aperture| \times Mean\ Solar\ Irradiance$$

2.8.4.1.4 Multiple Regression

Multiple regression analysis calculates the solar coefficient by using power as the dependant variable, and then at least temperature and solar irradiance as independent variables. The intercept constant is assumed to be zero, aligning with the linear regression of power to temperature difference. The solar coefficient is used in the same fashion as the solar aperture from the Siviour analysis, calculating solar gains and adjusting raw power into solar adjusted power. HTC is then calculated using the standard co-heating plot using solar adjusted power.

2.8.4.2 Windspeed Adjustments

Two methods have been identified to assist in accounting for the influence of wind on the HTC. Generally speaking, an increase in windspeed from particular directions will increase the heat loss during that period. It has generally been discovered that wind has less impact on the HTC results than solar gains; however, this is also likely to be highly specific to each building and analysis should be done to understand the possible influences for each test.

2.8.4.2.1 Removal of Data

The simplest approach is to remove days where the windspeed is higher than a specified level. Some figures used include 12 MPH (Judkoff et al. 2000) and 7.5 m/s (Butler & Dengle 2013). Rhee-Duverne & Baker (2015) used a figure as low as 1 m/s to identify wind-driven outliers. If utilising this approach, any calculations for solar gains should be conducted afterwards so only ‘clean’ data is included throughout the analysis.

2.8.4.2.2 Multiple Regression

An alternative is to include windspeed as an additional independent term in the multiple regression analysis, with the temperature difference and solar irradiance (Jack et al. 2017). If utilising this approach the HTC may be taken directly as the temperature coefficient, or the solar and wind coefficients can be used to adjust the power input and calculate the HTC via the co-heating plot. This approach essentially estimates the HTC with no wind, the same as the solar gains adjustments. This may be prone to error due to complexities of the interactions between variables, and the building’s specific shape (Jack et al. 2017). An alternative is to calculate HTC for a windspeed of 4 m/s, which aligns with typical windspeed for assessing U-values (Jack et al. 2017).

2.8.4.3 Infiltration Losses

It is possible to separate the infiltration losses from the fabric losses, though the separation is not always reported (Jack et al. 2017; Johnston et al. 2013). The application of either tracer gas methods or a blower door test are used to determine the infiltration rate. The infiltration heat loss is estimated by multiplying the infiltration rate, building volume and the specific heat capacity of air (Johnston et al. 2013). Conducting a blower door test provides a single value for the infiltration, where the tracer gas methods can be conducted while the co-heating test is running (Jack et al. 2017; Johnston et al. 2013) and values for each day may be calculated. Jack et al. (2017) noted no difference between blower door and tracer gas results, though more variation in tracer gas results was observed. They suggest that this could reflect actual changes in infiltration rates due to windspeed and internal-external pressure differences.

2.8.5 Co-Heating Test Alternatives

There is a number of alternative in situ tests that incorporate some part of the co-heating test. These include, but are not limited to:

- Primary and Secondary Terms Analysis and Renormalization (PSTAR) (Subbarao et al. 1988)
- Princeton Scorekeeping Method (PRISM) (Fels 1986)
- Quick measurements of energy efficiency of buildings (QUB) (Mangematin, Pandraud & Roux 2012).
- PASLINK dynamic tests (Bloem 2010)

2.8.5.1 PSTAR

The PSTAR, or 'Primary and Secondary Terms Analysis and Renormalization' method, utilised by Subbarao *et al.* (1988) represents the initial attempt at shortening the required timeframe for testing. It uses the following procedures to evaluate overall building performance (Judkoff et al. 2000):

- A shortened co-heating test, determining the HTC
- A cool down test, evaluating heat capacitance properties
- A floating temperature test to determine the response to solar energy absorption
- A blower door test or tracer gas test, determining the air leakage
- Measurements of weather variables, including solar radiation.

Additional measures include heat flux testing and thermographic imaging while the other diagnostics are being run (Subbarao et al. 1988). This data all serves to calculate the Building Loss Coefficient (BLC), which is effectively the HTC with corrections from the additional data gathered. Gathering additional data requires far more equipment but enables testing completion inside three days.

2.8.5.2 PRISM

PRISM uses a year's worth of monthly billing data, daily temperature readings and long term degree-days to determine the effective heat loss rate (Fels 1986). The theoretical basis is similar to the co-heating test in that it determines the rate of fuel used compared to an internal temperature set-point and the average daily temperature. By using actual consumption readings of the lived-in home it attempts to include behaviour as part of the performance analysis, as well as building fabric characteristics (Fels 1986; Rachlin, Fels & Socolow 1986; Stram & Fels 1986). This approach provides minimal disruption to the resident; however, it requires a full year of monitoring before an evaluation can be made. Using less time can cause significant variation and uncertainty (Rachlin, Fels & Socolow 1986). An additional advantage, however, is that the PRISM method was shown to have potential application in determining performance under both cooling and heating loads, which all previously discussed methods have been unable to accomplish (Stram & Fels 1986). The authors, indicated, however, that this analysis was carried out on a small dataset in a heating-dominated climate and further research would be required to fully validate this application.

Bauwens & Roels (2014) list PRISM as part of the co-heating test's evolution. Yet the length of time and type of data suggests it has more in common with a long term monitoring or survey study, though the analysis does aim to provide information about heat loss in the same way the co-heating test does.

2.8.5.3 QUB

QUB utilises a two-step approach, consisting of a heating phase and a cooling phase, to determine an overall HTC (Mangematin, Pandraud & Roux 2012). Adding the cooling phase to the heating phase, similar to the co-heating test, this approach enables estimation of the building's apparent heat capacity. This then allows for estimation of dynamic behaviour, and therefore does not require the length of time for the building to reach a steady-state. It is

suggested that the test can be conducted inside a day or two, but requires the building to be empty (Mangematin, Pandraud & Roux 2012). Again, this shows promise though as the authors point out, it has only been demonstrated on a relatively new building described as having fairly even heat loss through the thermal shell and is evenly heated by under-floor heating.

2.8.5.4 PASLINK

PASLINK refers to a network of research sites across Europe and an agreed testing methodology (Baker & Van Dijk 2008; Bloem 2010; Garcıa-Gáfaro et al. 2012; Strachan & Vandaele 2008). PASLINK is an evolution of the original PASSYS project (Baker & Van Dijk 2008; Garcıa-Gáfaro et al. 2012). The key change is a shift from steady-state experiments to dynamic experiments (Baker & Van Dijk 2008; Bloem 2010). To evaluate the building, usually a PASLINK test cell, a heater is used in a pseudo random sequence to 'excite the system' (Bloem 2010). In warmer climates a cooling system is used rather than a heating system (Baker & Van Dijk 2008). This represents a large difference in the application of PASLINK compared with the co-heating test as warm-weather performance can be directly measured. The test duration is eight days, though may be followed with six days of validation sequencing (Baker & Van Dijk 2008). The information gathered from this experiment is used to inform mathematical models that aim to estimate the 'resistances, capacitances and heat flow admittances' of the building (Baker & Van Dijk 2008). Tools such as CTSM, LORD or SIT in MATLAB have been developed to identify these thermal parameters (Bloem 2010; Garcıa-Gáfaro et al. 2012). The test cells are routinely re-tested to ensure consistency across the sites (Baker 2008). Strachan & Vandaele (2008) presented a collation of case studies performed on the PASLINK test cells across Europe. These case studies all evaluate the performance of a specific addition or alteration to the test cell. The results can be applied to models of full sized buildings.

The PASLINK network represents a hugely sophisticated collection of research facilities. The method used can be applied to a wide range of building components, both active and passive. At this stage the application of the PASLINK dynamic analysis is primarily on the PASLINK test cells. Rhee-Duverne & Baker (2015) however demonstrate application of LORD software for determining the HTC of a Victorian terrace house from a co-heating test, comparing dynamic and steady state analyses. Their determination was that the dynamic

analysis was better able to predict daily heat requirement. Though this conclusion was based on over a month's worth of data, it is possible that the dynamic analysis could have been completed from a shorter experiment. The dynamic analysis is more complex (Rhee-Duverne & Baker 2015), which may be why the steady state method is more widely used. Using LORD in this way however still relies on the co-heating test methodology to gather data.

2.9 Limitations of Post-Construction Evaluations

One of the biggest challenges in meeting energy efficiency targets in the housing industry is reducing the performance gap. To enable this, it must be possible to evaluate the building envelope's post-construction performance. For this purpose, not all methods are created equal. Each method of evaluation and testing is good when applied correctly, but not without limitations, particularly in determining the building's actual heating and cooling loads.

Implementing a long term monitoring study or survey analysis is exceptionally powerful in showing whole house energy use; however, it cannot be considered a post-construction evaluation tool due to the time required to gather sufficient data, and the possibility of occupant behaviour influencing analysis. Computer simulations or calculations do not evaluate the building as-constructed unless some sort of calibration is carried out, and this must be informed by in situ testing of some kind.

The only remaining option therefore is conducting in situ tests, and again these are not without fault. Using heat flux testing measures only the element it is placed on, and while a very effective tool it is less able to evaluate heat lost via joins or other thermal bridging. Using a thermal camera may help to discover these additional areas, but quantifying the heat being lost is difficult, even with specialist training. Heat lost via air leakage must also be added, and this is achieved through using a blower door test. The combination of all these elements, however, is the evaluation of individual elements, with the assumption that the sum of the parts will be the same as the whole, and still does not fully satisfy conduction losses at joints or thermal bridges.

Of the tests that do provide analysis of the entire building, the PRISM method requires 12 months of data for accuracy, making it unsuitable for determining the presence of the

performance gap. Overall, the co-heating test is the most effective technique; however, the test's three-week, empty building requirements severely limit its application. Similarly, while significantly shorter, both PSTAR and QUB methods are highly invasive, making them difficult to conduct while access to the home is required. The use of LORD demonstrated by Rhee-Duverne & Baker (2015) was also conducted on a vacant terrace house, suggesting similar issues.

Consequently, there is potential for a new tool that can quantitatively determine building heat loss which can be applied quickly and with minimal disruption to day-to-day building operation.

2.9.1 Heat Loss Bias

In addition to issues surrounding the ability of the tests to evaluate the entire building in field, post-construction tests are also geared only to determine heat loss. This is likely due to the development of these tests in cool and cold climates: much of the co-heating test work has been conducted in the UK. Little evidence was found in the literature of applying these tests in milder climates where the building also experiences a significant cooling load. This is, particularly for Australia, a large shortcoming. The tests are geared to evaluating the building's ability to retain heat, and there is no guarantee that buildings with low HTCs do not overheat in the warmer months, or have lower cooling loads than buildings with high HTCs. It is also possible that the elements that would assist these buildings to either prevent heat gain or facilitate dissipation may require action from occupants – for example, engaging movable shading or opening windows for cross ventilation. The tests of the building fabric do not account for these behaviour actions. Further research is required to establish whether there is a relationship between HTC and summer cooling loads.

The PASLINK methodology is the obvious exception: it specifies to use a cooling system when conducting experiments in warmer conditions. This directly evaluates warm weather performance, rather than inferring it based on heat loss testing. The limitation of the PASLINK methodology, however, is that all examples evaluate a specific component installed within the test cell. While simulations have been conducted to show the application of the component to other buildings, the methodology does not appear to be applied in determining post-construction performance of a full-sized home. As discussed previously, LORD (developed for PASLINK (Gutschker 2004)]), has been used on a full sized house (Rhee-

Duverne & Baker 2015) but used the co-heating test methodology for data collection, thus still determining heat loss performance.

2.10 Testing Evaluation Tools

Having established the requirement for a new building evaluation tool, an inspection is required of the ways in which previous research has analysed tools. Previously, this has been done with the aid of computer simulation to show proof of concept, the use of fully climate controlled laboratory facilities or semi-controlled test cell facilities to show real world applications, and comparisons with other established tests to prove validity.

2.10.1 Test Facilities

When analysing the application of a building evaluation tool, tests are either carried out on a residential home, or using a test facility, either in a laboratory or using a test cell. Researchers use both approaches extensively. Each has different advantages. In short, the advantage of using a real home is complete demonstration of the tool as it can be applied in the field, while the test facility allows for a much higher level of control over test conditions (Baker & Van Dijk 2008; Cattarin et al. 2016; Dewsbury 2011).

2.10.1.1 Occupied Buildings

Analysis of a method as it applies to a real building is a direct evaluation of the test's overall application, beyond analysis of the theory alone. It provides insight into the difficulties that will arise when testing in other homes, such as site access and disrupting occupant routines. It can be difficult, however, to differentiate all the factors that influence results due to the complex nature of the building system (Cattarin et al. 2016). Subbarao et al. (1988) demonstrated the application of the PSTAR method on a residential home, though this study did not compare the PSTAR results with other benchmarks. Butler & Dengle (2013) used two residential homes to demonstrate different influences on the co-heating test, and its comparison with the design parameters. This showed the application of the co-heating test in the real world, and was applied to two different homes, one control and one with various alterations. It showed the test's repeatability, and the influences of real world conditions (such as sun and wind) on test reliability. Window shading use enabled analysis of how high solar gains would influence the test. Stamp (2011) also applied the co-heating test to two high efficiency buildings to evaluate test uncertainty.

These studies are valuable as they show the application of the tests in field, which both provides information regarding their feasibility, and evaluates performance of the tests.

However, they are not the initial application; the examples provided are of tests that have undergone much theoretical development and experimentation in controlled environments.

2.10.1.2 Test Cells and Laboratories

Applying test methods in field is the culmination of much work in designing and adjusting methods on the basis of controlled testing, either in laboratory settings or outdoor test cell buildings. These test facilities provide a means to simulate real world performance on a real building under fully known or controlled stimulus (Achenbach 1981; Baker & Van Dijk 2008; Cattarin et al. 2016; Dewsbury, Nolan & Fay 2007b; Lomas et al. 1997). Using test cell buildings is exceptionally popular since they give the researcher full access and control over all elements. The preference is for the test cell to be specifically designed for the study, such as those used by Dewsbury, Nolan & Fay (2007b), Hitchin, Delaforce & Martin (1993), Lundin, Andersson & Östin (2004) and Sugo et al. (2004): this enables incorporation of specific design requirements. For example, Lundin, Andersson & Östin (2004) included ways to alter airflow into the test cell. Dewsbury, Nolan & Fay (2007b) designed the timber frame to ,among other things, allow windows to be retrofitted for future studies. However, it is not always feasible to build a new test facility from scratch, and cells are re-used when they are available and still fit the requirements, such as the PASLINK buildings used by Baker & Van Dijk (2008) and Cesaratto, De Carli & Marinetti (2011). These studies all investigated elements which require significant knowledge of the building as part of the validation process, or they would be negatively impacted by increased complexity. The experiments discussed by Baker & Van Dijk (2008) require a number of days, and the test cell allows this without disrupting building residents. These studies all investigated new building evaluation procedures, or quantified different influences. Other examples of using test cells to investigate building evaluation tools include Cucumo et al. (2006), Letherman & Palin (1982), and Loutzenhiser et al. (2009).

2.10.2 Validation

The approaches to validating testing procedures are logical and follow general principles of a controlled experiment. Results of the new test procedure are compared to results of a previously known method. The control method can range from theoretical values based on an assessment calculation method or a simulated model, results of a long term monitoring project, or a different post-construction test (Mangematin, Pandraud & Roux 2012).

2.10.2.1 Simulation tools for Validation

Simulated models are often used as the first step in showing an analysis technique or approach works on a theoretical level and warrants additional research. It can show that conclusions can be drawn when certain data is available.

In some cases, comparison with the real world is unnecessary. Wang & Chen (2002) used computer simulations to demonstrate a different procedure for calculating conduction transfer functions and thermal response factors of multilayer walls. There was no need for external, real world validation as the study's aim was to provide the simulation mechanic with a faster and more reliable method of arriving at the same answer. Ballarini & Corrado (2012) implemented a similar approach, using EnergyPlus to show how the principle of superposition can be used to determine the level of influence of the forces driving the cooling load of a building. This type of analysis is impossible to do in the real world, as the simulation allows alteration of physics and application of adiabatic building elements which are effectively impossible to apply to an in situ case study of a real building. Karlsson, Karlsson & Roos (2001) developed a new method of evaluating window performance in computer models, and were able to show how it fared against previous models. These examples show a wider application to simulation than using it only for predicting the building's response.

There are weaknesses in using simulation as the validation tool, mostly due to problems with the simulation program (Hitchin, Delaforce & Martin 1993). A clear example is that of the 'perfect mixing' assumption that Hitchin, Delaforce & Martin (1993) showed as incorrect when compared with experimental data from a well-mixed room.

2.10.2.2 Experimental Validation

Comparisons with other post-construction tools generally show how the tool improves upon either the application or the accuracy of previous tools. The benchmark tool to be compared against is generally well understood, if not the standard procedure for the particular test. Cucumo et al. (2006) utilised the average method of heat flux testing as the benchmark for proposing a different analysis of heat flux data. The aim was to increase the application of heat flux meters for in situ evaluation of R-values. However, Ficco et al. (2015) used alternative tests to evaluate parameters affecting heat flux tests. Judkoff et al. (2000) used co-heating tests as their benchmark in evaluating performance of the STEM test for

evaluating HTC. Cesaratto, De Carli & Marinetti (2011) provided an alternative, using a series of trials to show what effects the presence of the heat flux meter itself might have on the results. Repeating heat flux tests under different conditions, and noting the variation, indicated that differences in emissivity might have a small effect, and that using the heat flux meter surface temperature would also improve accuracy.

These are not tests designed to evaluate the building's energy use. They are all designed to estimate, in some way or format, the overall R-value of the building. With previous work linking how R-values influence building performance, there is no need to conduct long term monitoring tests to validate each new tool evaluating the building R-value. It is far easier to use previously developed tools as benchmarks for comparison.

2.11 Literature Summary

The literature review has shown the presence of the performance gap and the impact on energy use it has, and may continue to have, if left unchecked. To effectively determine the extent of the performance gap, and then to reduce its impact, requires in situ evaluation of buildings, post-construction. To provide further background to why this is required, the literature review includes a discussion of elements that influence building energy use. Each is important, and making a mistake with one can reduce the efficiency of an otherwise high-performing building. This highlights the importance of detecting flaws in situ.

The review then outlined current evaluation tools and methods. It showed how building monitoring and computer simulation may be applied in building research, giving understanding of both real and theoretical behaviour. It highlighted how the elements of thermography, blower door testing and heat flux meters may be used to form conclusions about certain building segments, while highly invasive co-heating test achieves the most reliable measure of whole building performance. Each method is effective. Each has limitations. There exists no single test that provides whole building feedback without being hugely invasive. This indicates the need for alternative methods or tools for building evaluation which concern whole building performance and which can be used with minimum disruption to the occupant.

Finally, the review highlighted various approaches to validating building evaluation tools. It indicated that a combination of test cell buildings, simulation software and currently used evaluation tools form the general set of techniques used by researchers.

For future research purposes it is also important to note that the review also identified a bias of evaluation techniques applied to full size buildings to be concerned largely with heat loss. This is unsurprising since most of the research concerning these techniques has been carried out in cooler climates where the larger portion of energy use is for heating. However, the lack of applying tools to measure the heat gain of a building represents another gap in the knowledge and should be remembered for future research opportunities.

Chapter 3 - Methodology

This chapter discusses the theoretical approach for evaluating the decay method. It discusses the logic and reasoning for using the co-heating test as the main point of comparison and validation, using a test cell case study instead of a residential home, and using data logging equipment to facilitate all field experiments. An introduction is provided to the test cell and its location. The chapter also discusses the purpose and value of computer simulation, as well as the choice of EnergyPlus as the simulation program and the main statistical measures used in the analysis.

3.1 Validation of the Decay Method

The most comprehensive way to prove that the decay method works would be to conduct experiments on a large number of buildings with known differences in heating and cooling energy use, and analyse whether the decay method detects these differences. This is an advanced research method, requiring time, resources and volunteers. Given that the method was unproven and still required analysis to identify best practices, the logistics of this approach were deemed unreasonably costly and complex. In consequence, a set of smaller scale experiments was deemed more appropriate.

As comparison with long term energy use across a number of houses is understood to be unviable, comparison with current known tests is a suitable alternative. Showing that the decay method results correlate with known thermal shell testing indicates that the decay method can be used to evaluate thermal performance in the same way these tests are used currently. Of the tests reviewed, the co-heating test was identified as the most appropriate comparison point as it provides information about the thermal shell as a whole, though heat flux testing and blower door testing were also conducted as they provide useful information and comparisons. These tests all measure building performance in terms of heat loss, and provide performance benchmarks that allow for comparison between different buildings. There is additional advantage as the popularity of the co-heating test observed in the literature means generally it is well understood, and there is much information already available regarding its limitations.

The research carried out was therefore aimed at showing how effective the decay method is by using the co-heating test as the measure of thermal performance. The test was to show whether the decay method offered a means for predicting the HTC of a building to a sufficiently accurate level.

3.2 Research Methodologies

3.2.1 Empirical Research Methodology

Empirical research methodology involves collecting data, or empirical observations, to answer the research questions (Dewsbury 2011; Moody 2002). It is closely aligned with the 'Scientific Method', making systematic measurements of observed phenomena. There is no need to deviate from the proven approaches of the building research field in devising ways to conduct experiments. All literature reviewed that discusses a way to measure performance of a building in a quantitative manner, such that a minimum standard may be set for compliance, conducts experiments based on gathering and analysing empirical evidence. The co-heating test itself uses the empirical research approach, with readings of temperature and energy taken at regular intervals. The simplest approach for directly comparing the decay method with the co-heating test, and indeed with other research in this field, is to utilise the same research methodology. This approach reduced the need to source new equipment that may be unproven in this area, and eliminated potential confusion and misinterpretation of results due to differences in methodologies and analysis techniques.

3.2.2 Case Study

As previously noted, it was expected to be difficult to gain access to a large number of buildings in which to conduct experiments, particularly as a number of experiments were to be carried out over the course of the PhD research, and this would require buildings to be available for months at a time.

Quite often, however, in demonstrating an evaluation technique, a case study is conducted showing the application of the concept in the real world. Examples of this include Aktacir, Büyükalaca & Yılmaz (2010), Asdrubali, Baldinelli & Bianchi (2012), Guerra-Santin et al. (2013), Haralambopoulos & Paparsenos (1998), Ridley et al. (2014) Subbarao et al. (1988), and many more. The advantage of the case study is that because it focuses on one building, the analysis can be detailed and the building very well understood. The case study does

leave the conclusions open to the criticism of being a single data point, but in building research it has generally been used to show that a theoretical principle translates into the real world and warrants further research. Alternatively, if the principle encounters difficulty in real world application then the case study is a relatively low-cost way of revealing these issues before large scale application is attempted.

The case study is also an appropriate choice for work carried out in the PhD context as it makes good use of the limited pool of resources available. The case study makes it possible for a solo researcher to set up the necessary equipment and run the experiments in a timely fashion. It is also useful for the researcher to see first-hand any difficulties experienced in field, to learn about the experimental techniques, and to use the equipment. These may not be directly related to the research aim, but they are nevertheless useful additions to the PhD process overall.

3.3 Data Collection

The data collected was aimed at a quantitative analysis, and is itself quantitative in nature. From the literature review conducted, it was determined that the many measurements to be carried out are generally required to be taken at regular intervals, potentially at a very high frequency, and would be somewhat precise. All examples from the literature use some sort of data logging equipment to facilitate an automatic collection of the various data sets. This allows for experiments to be set and left running continuously without the presence of the researcher, which expands the experimental windows of opportunity, such as overnight or weekends. This was particularly useful for carrying out research using the co-heating test as the building should not be accessed during the test, and the equipment can simply be left running. It also allowed for experiments to be run while other research or analysis was conducted.

3.3.1 Selection of Equipment

Equipment was selected as a balance between products demonstrated in the literature to be useful in this field, and those which were easily available through RMIT University and CSIRO. Using the same, or similar, equipment from the same manufacturers as used by the experts in the field increases confidence in the integrity of the data. It was also useful to use equipment well known to researchers at RMIT University and CSIRO as it provided easy access to expert advice in the face of any issues. Detailed descriptions of the equipment can

be found in Chapter 4. In addition to on site equipment, weather data was gathered from the Bureau of Meteorology weather stations located at Moorabbin Airport, 5.5 km south-east from the test cell location, and Tullamarine Airport, 35 km to the north-west.

3.3.2 Calibration of Equipment

The equipment used was generally brand new, and pre-calibrated by the manufacturer. HOBO sensors were newly purchased from Onset by RMIT University at the time of installation. Though the sensors were already calibrated by Onset, a comparison of a subset was conducted in a small insulated box. No particular patterns were observed outside reported variation of the sensors. Hukseflux heat flux sensors were also newly purchased and specifically calibrated by the manufacturer. The calibration figures reported by the manufacturer were programmed to the CR3000 datalogger when the sensors were installed.

The K-type thermocouples were not independently calibrated beyond programming of the datalogger. This is an oversight in the experimental set up and uncertainty associated with the temperature readings from these sensors is unknown.

The CR3000 datalogger includes a self-calibration procedure based on monitoring internal voltage. The data reported by the logger was checked for validity each time the unit was reinitialised after data was downloaded. This was usually within a two week period, and follows guidelines included in the CR3000 manual for setting up the datalogger and programming. The unit was not checked for imperfections between the analogue terminals.

The watt-meter readings were confirmed by calculating the expected readings when the electric blow heater, known to be 2 kW, was in use. The pulses, recorded on 30 second intervals, count 16 or 17 watt-hours, which equated to 1920 W or 2040 W. The watt-meter only sends the pulse when the full 1 Wh is used, and over time this averaged to the expected 2000W.

External weather data from the Bureau of Meteorology is collected in accordance with World Meteorological Organization standards. Data available for use from the Bureau also follows a quality assurance procedure incorporated in the same standards. Details of the weather station operated by CSIRO are unavailable, and thus the CSIRO data is used only as a qualitative guide to confirm consistency between the local conditions and the conditions at the weather station 5.5 km south-east of the test site.

3.3.3 Limitations and Risks

The lack of calibration of the K-type thermocouple represents the most serious limitation on the dataset's quality. This is compounded by the lack of external calibration of the CR3000 datalogger.

The CR3000 has the capacity to measure pulse frequencies up to 250 kHz. The Elster AC100 Wattmeter used in this study sends a square wave, each pulse lasting 100 ms, for every 1 Wh of energy used. Based on the equipment monitored in this research, the frequency of the pulses recorded is less than 1 Hz and well within operating standards for the CR3000 datalogger.

The basic resolution of the analog inputs used for collecting the heat flux meter and thermocouple data is 33.4 µV. The sensitivity of the heat flux meter output is 60 µV, and the expected range of operation is between -10 and 70 mV. The size of the signal from the heat flux meter is three orders of magnitude higher than the sensitivity range of the datalogger, and these readings should not therefore be influenced by any uncertainty inherent in the CR3000 circuitry.

Uncertainty in the K-type thermocouple cannot be estimated accurately. This data is only used for the calculations of the material R-value, meaning the accuracy of the R-value estimates cannot be quantified. To mitigate this, calculated R-values are compared with theoretical R-values based on manufacturer specifications where available, or standard conductivities if specific data is unavailable. This mitigates the risk of large inaccuracies in the estimates by ensuring the readings are in a range that is sensible given the building materials. The R-values calculated in the heat flux analysis are used for an initial theoretical estimate of the test cell HTC, and to inform the base models for the EnergyPlus simulations. No conclusions are drawn based on the theoretical HTC as to the effectiveness of the decay method. The risk of inaccurate R-value estimates in the building models is a concern; however, part of the analysis of the EnergyPlus simulations includes altering the model's R-values and comparing performance of an array of models to observed performance of the test cell, so eliminating the risk of drawing inaccurate conclusions based on this data set.

3.4 Test Cell

As previously mentioned, while using a residential building is perhaps the most direct approach, it was not a viable option for this research. Evaluating the decay method required full access to the building for months at a time and disruption to the occupant was expected to result in no-one volunteering their home. However, 'test cells' or laboratory experiments that can simulate real world conditions are often used in building research. Dewsbury, Nolan & Fay (2007b) grouped test cells into two different categories: standard, and PASSYS (now PASLINK). Standard test cells are exposed to the elements on all sides, allowing for greater research capacity into overall building performance (Dewsbury, Nolan & Fay 2007b).

Two good examples of standard test cell facilities in Australia are the set of four at University of Newcastle (Page et al. 2011) and set of three at University of Tasmania in Launceston (Dewsbury, Nolan & Fay 2007b). The University of Newcastle test cells were built to research influences of thermal mass in the Newcastle climate, and are therefore concrete slab on ground with brick wall constructions (Sugo et al. 2004). The Tasmanian thermal performance test cells were purpose built for Dewsbury's (2011) validation of AccuRate. Both sets are representative of construction practices in their respective regions at the time of building. Dewsbury (2011) elected to mimic the size of the Newcastle test cells to enable future comparisons between the sites. One key difference, however, is the Tasmanian test cells are defined by the internal dimensions, where the Newcastle test cells by the external dimensions. Dewsbury's (2011) approach allows for the internal volume to be consistent across all buildings. This is critical for comparisons between observed and simulated results as the dimensions in AccuRate represent the internal air volumes. Dewsbury, Nolan & Fay (2007b) took great care to document and publish the construction processes. This is partly to allow future facilities to be built to the same specification (similar to the PASLINK network in Europe), and partly to maintain construction quality. This provided the best assurance that all elements of the test cells could be matched in AccuRate, thus enabling the validation of the software.

Two test cell buildings were available for use in this research, both located at the CSIRO site in Highett, Melbourne. The buildings were left over from previous durability studies conducted by CSIRO, and were identical in size, orientation, construction, and material, except for the application of single sided foil under the roof tiles of the southern building.

The size and construction of the test cells provided potential for easy customisation of thermal characteristics, primarily via adding insulation to the wall cavities. In effect, this offered what can be thought of as a number of different buildings that should have different heat losses, and that could be measured by the co-heating and heat flux tests. The test cells therefore provided the means to compare the four decay method analyses with the co-heating test across multiple buildings.

3.4.1 Description of the Test Cell

The buildings were located on an open space in the south-eastern corner of the site. The internal space measured 4515 mm (NW/SE Walls) by 4510 mm (NE/SW Walls) by 2370 mm high. They are similar height but smaller floor area than the Launceston and Newcastle test cells.

The buildings were a timber frame construction, clad on the outside in 7.5 mm 'Cemintel' fibre cement sheeting, and three of the internal wall surfaces lined with 10 mm 'Gyprock' plasterboard. The ceiling and internal surface of the south-western wall were lined with pine board. The building had an enclosed perimeter, platform floor consisting of a single layer of chipboard. The sub-floor was open to the ground and accessable through the trapdoor in the centre of the room. The roof was concrete tile, and in Test Cell 2 it was lined with single sided reflective foil. Both buildings had a single entry point on the south-eastern side, and a single window on the north-western wall. None of the walls, or the ceiling cavity, were initially insulated; however, glass wool wall batts were installed in Test Cell 2. The exact R-value of the invidiual batts was unknown; however, the batts were approximately 100 mm thick when uncompressed, and had expanded somewhat over time after CSIRO installed and removed them from other test walls. The depth of the batts suggested they should be in the range of R1.9 to R2.0, based on the glass wool product specifications (Knauff 2014). The sub-floor space was vented, but vents could be closed with the aluminum sliders provided. Electricity to the test cells was via one of the nearby laboratory spaces on the south-western edge of the field.

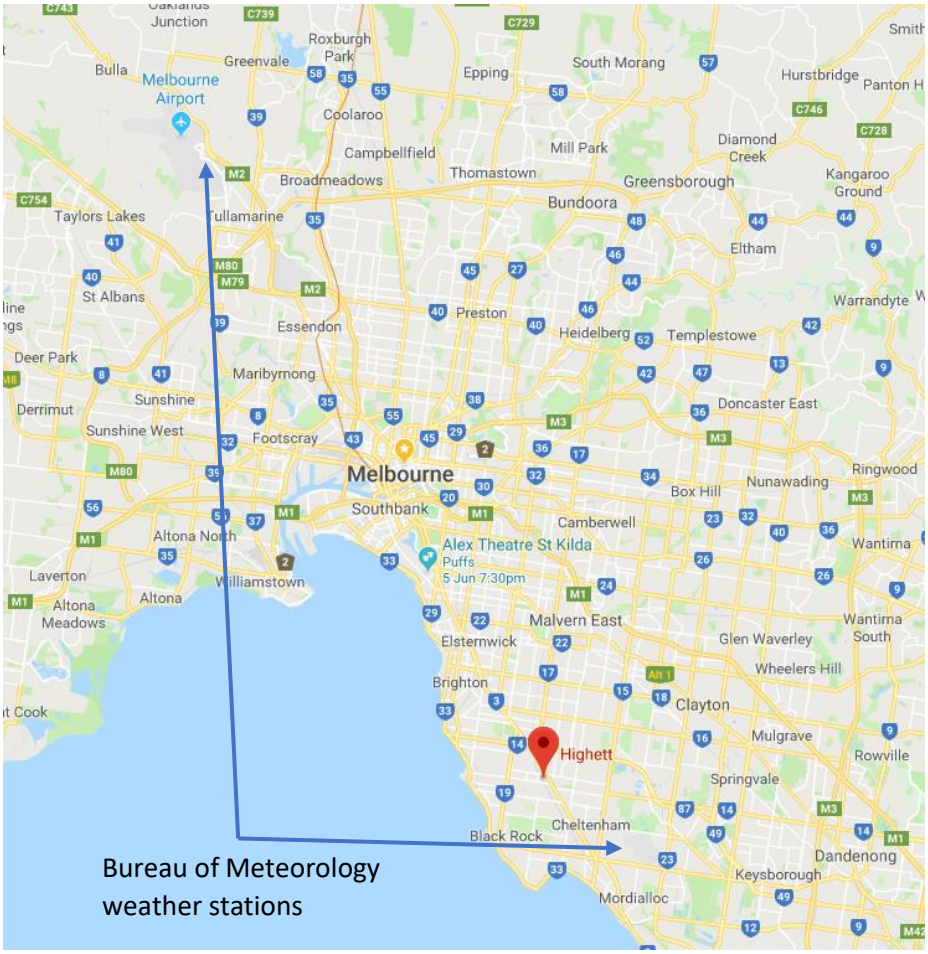

Figure 3.1 Location of Highett relative to Melbourne and weather stations

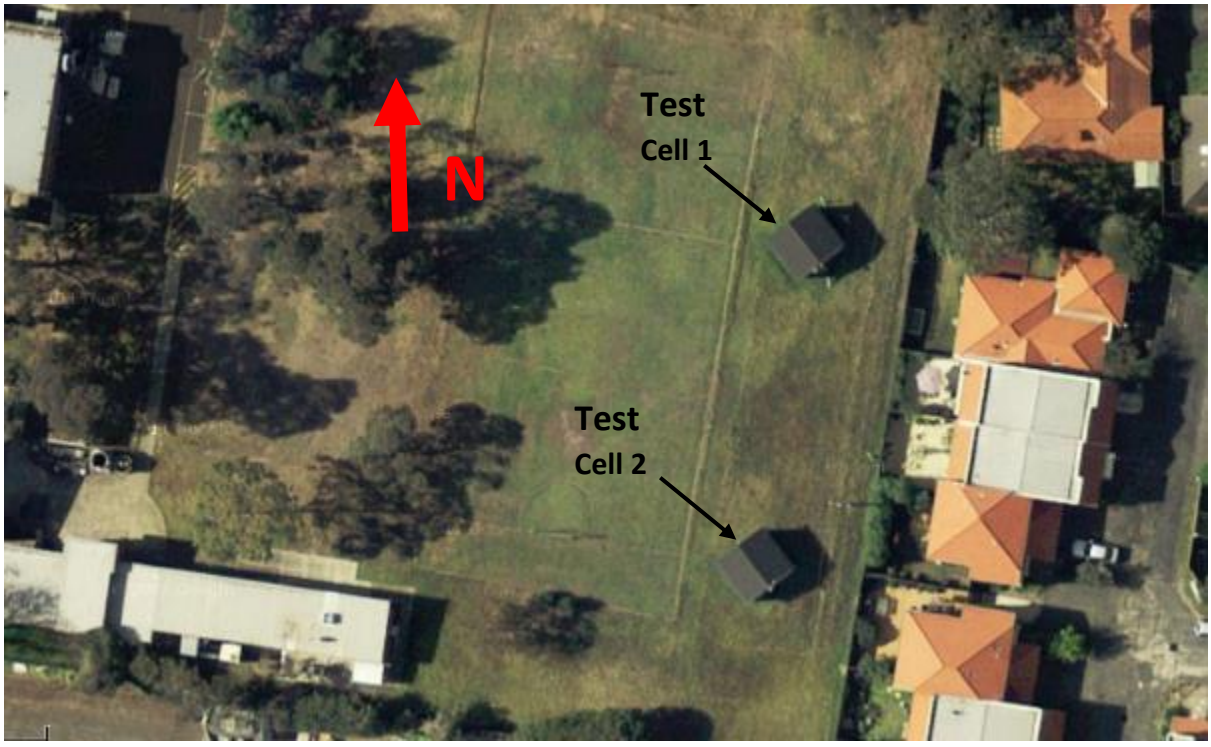

Figure 3.2 Satellite view of test cells at the southern end of CSIRO site at Highett

Figure 3.3 Test Cell 2, Exterior

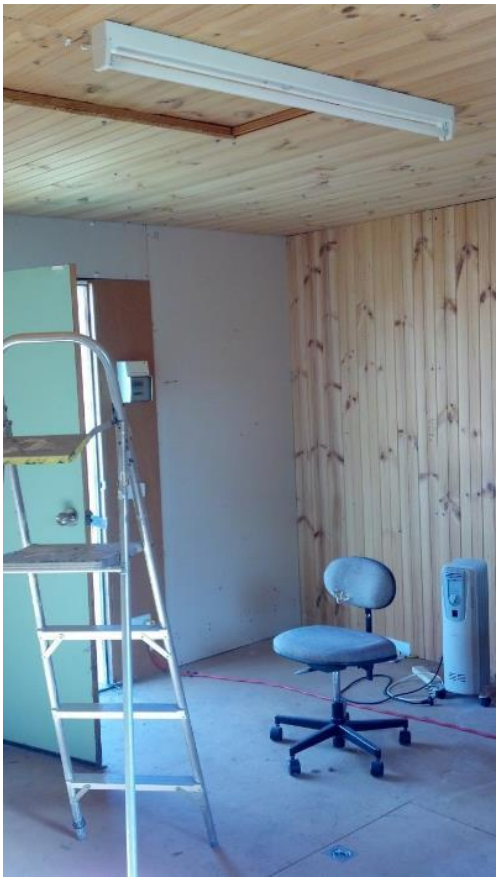

Figure 3.4 Test Cell 2, Interior

3.4.2 Limitations

3.4.2.1 Pre-Existing Structure

Using these test cells and the additional available insulation was valuable to the study; however, it is noted that using pre-existing buildings may have limitations. Built by CSIRO scientists for other research projects, with different research goals, the buildings plans and specifications are no longer available.

The most ideal solution would be to construct new test cells to the same specifications as documented by Dewsbury, Nolan & Fay (2007b), extending the Australian test cell network. This would have provided complete understanding of the building, including any features that may have caused uncertainty in any evaluation results. It would also have provided opportunities to conduct further research on the decay method and co-heating test in different Australian climates with comparable buildings. At worst, it would have eliminated all unknowns regarding the material properties. Despite the advantages of using a purpose built facility, the realities were that even at the cheapest level this would be expensive, requiring land, materials and labour, including the provision of electricity. Dewsbury, Nolan & Fay (2007b) is a key example of the work required to construct test cells from scratch. Given the expectation that building from scratch would be expensive, it was not feasible to do so when the Highett test cells were offered for free. The drawback, however, was the presence of unknown materials in the building and unknown quality of the construction: some of the uncertainty in the building evaluations and simulations may be due to limitations in the test cell's thermal shell rather than problems with the evaluation methods.

3.4.2.2 Multi-Zone Buildings

A multi-zone building is required to fully understand how the decay method can be used, and how it compares to other evaluation methods, particularly the co-heating test. Using a residential building could provide direct insight into applying the decay method, whereas using the test cell does not fully address real-world applicability.

There are two main issues with attempting to use a multi-zone dwelling for initial evaluation of the decay method. Additional zones increase the complexity of the building's thermal system as they would introduce heat flow between internal sections of the building that must be balanced and accounted for. A single zone building reduces the complexity of the system, and if the decay method could not be shown to have merit under these conditions

there would be no need to attempt it under more arduous conditions. To effectively evaluate the decay method, the other tests must also be carried out to provide the benchmark. As discussed previously, current methods are time consuming and invasive, and gaining access to a residential building for the required amount of time to carry out this research was likely to be unreasonably difficult for providing the first evaluation of an unproven method.

Using the test cell reduced the complexity of the thermal system being observed, and did not require a volunteer to donate a home for months at a time during the PhD study.

3.5 Computer Simulation

Simulation software is widely used in building research and a large variety of software exists. The major advantage that simulation software provides for the researcher is the ability to quickly evaluate a huge number of buildings, or variations of a building. The basis of using computer simulation in this research was that it is a very good way to estimate how a building may react under different stimulus, and essentially this is what the decay method analyses: the response of the building overnight under varying initial temperature conditions. An example from the literature is that of Morrissey, Moore & Horne (2011) – a study in which the authors simulated how changes in orientation effected building heating and cooling loads. Much time and effort in conducting field experiments was saved using a computer simulation program to assist in the initial determination of the potential steps in the decay method set up and analysis. This allowed for increased quality and direction of the field experiments, and as time was saved, increased the number of experiments that could be run.

Furthermore, once the field experiments were completed, the data could be fed back into the computer simulation to assist in answering any additional questions about any anomalous readings in the field. The computer simulation allows for full control over various physical elements, such as removing the influence of the sun or wind, or disabling heat flow through certain areas of the building.

3.5.1 Choice of Simulation Software

The choice of simulation software was made on the basis of suitability for the study, access to knowledge and training, and cost.

The critical elements required were:

- A robust, proven, thermal simulation engine, having passed the Building Energy Simulation Test (BESTEST). Software that has passed this test is recognised for its quality and accuracy by the International Energy Agency.
- To be fully capable of simulating the testing conditions of at least the co-heating test. This required the ability to fully customise thermostat settings, and create and modify weather inputs. If the co-heating test could be simulated, it was expected that the software would handle any other combinations of thermostat settings and weather conditions.
- The ability to output data at regular intervals, in a spreadsheet format or similar, regarding internal temperature, power input, and external conditions.
- Fast access to troubleshooting and training.
- Low cost.

Additional desirable elements included:

- Ability to bulk process multiple simulations.
- Ability to automate complex analysis of results (linked to the format of data output).
- Flexibility in disabling and enabling certain elements of building physics, such as removing the effects of sun or wind.
- Ability to create an Energy Rating Certificate to compare test results with NatHERS star rating standards.

Three Australian-based, NatHERS approved software, AccuRate, BERS Pro and FirstRate 5, and EnergyPlus, operated by the United States Department of Energy, were identified as possible software. Table 3.1 and Table 3.2 show a comparison of the software against the criteria laid out above.

Table 3.1 Critical requirements of simulation software

Simulation software	Ownership/ Operator	BESTEST accredited	Customisable thermostat settings	Customisable weather	Data output format	Access to training	Cost to researcher*
EnergyPlus	Funded by U.S. Department of Energy, managed by the National Renewable Energy Laboratory (NREL)	Yes	Yes – full control to 1-minute time step for each day of year.	Yes – fully via in-built weather file builder to 1-min time step	.csv	Yes	Free
AccuRate	CSIRO/ Energy Inspection (reseller)	Engine only	Yes – limited to hourly settings for standard day, applied across the entire year	Yes – fully manual creation, 1 hour time step	.txt	Yes	Free
FirstRate 5	Sustainability Victoria	Engine only	Possible, if access to scratch file granted	Possible, if access to database granted	Energy Rating certificate – additional data requires access to database	Yes	Free
BERSPro	Energy Inspection – acquired from Solar Logic in 2015	Engine only	Yes – limited to hourly settings for standard day, applied across the entire year	Yes – fully manual creation, 1 hour time step	.txt	Yes	Free Trial

*Note: Costs to researcher specific to this PhD study.

Table 3.2 Desired additional features of simulation software

Simulation software	Capable of bulk simulation	Data output can be analysed automatically	Flexibility for customising building physics	Creation of Energy Rating Certificate
EnergyPlus	Yes	Yes – fully	Yes – fully	No
AccuRate	Multiple simulations via additional program, AccuBatch	Yes – fully	Possible, if additional information provided on the structure of the SCRATCH file	Yes
FirstRate 5	Yes	Yes – fully	No – Scratch files are encrypted	Yes
BERSPro	Yes	Yes – fully	Possible, if additional information provided on the structure of the scratch file	Yes

FirstRate 5, BERSPro and AccuRate all use the same Chenath engine to drive the underlying calculations, and each has its own front-end graphical user interface. Due to the studentship arrangement with CSIRO, both FirstRate 5 and BERSPro were discounted. Only the use of AccuRate, and the version of the Chenath engine provided with the AccuRate software, was explored.

The scratch file generated by AccuRate containing the direct inputs required by Chenath is open to be edited directly by users outside of the AccuRate program. To run this file, the engine must be called directly from the command line or run through the CSIRO's batch simulation software, AccuBatch. Technically, this does allow for full customisation within the limitations of what Chenath accepts as inputs. The main limitation is that thermostat settings in the scratch file are based on a single 24 hour profile, repeated for each day of the year.

EnergyPlus is itself a backend program, and all inputs and outputs are based on .csv files, making it exceptionally customisable. All the equations that inform the EnergyPlus thermal

engine are available in the Engineering Reference (NREL 2015). EnergyPlus is available as a free download, as are all updates. Senior supervisor of this PhD study, Dr Ian Ridley, is a long time user of EnergyPlus; thus there was great access to training and help with troubleshooting the models. Through implementing a program developed by Phillip Biddulph at University College London, bulk processing of EnergyPlus simulations was possible. The .csv file output also enabled automated analysis using macros written in Excel. EnergyPlus comes with a weather file builder in the box, and this is flexible enough to build weather files with one minute readings if this is available without gaps in the data source. The thermostat settings are also customisable for each minute of each day, for every day of the year. This allows for on site temperature data to be input directly for specific time periods and mimicked exactly by the building model. The only shortcoming was that EnergyPlus does not automatically generate Energy Rating Certificates. It is technically possible to manually generate them if the base assumptions made in the Chenath engine were matched. This was not seen as critical to the research and not pursued.

Both AccuRate and EnergyPlus are highly respected software packages with varying strengths. The main advantages of customising weather and temperature inputs for EnergyPlus up to a 60-second frequency and defining unique profiles for each day, made it the best choice for this research project. Based on this assessment, EnergyPlus was selected as the building simulation software for this research.

3.6 Uncertainty Analysis

There is some variation in the literature regarding the approach for analysing uncertainty in co-heating tests. This study uses three approaches to estimating uncertainty. Each of the experiments uses a number of measurement devices, each with a reported level of uncertainty. Using the Differential Sensitivity Analysis (Lomas & Eppel 1992), the change in result due to uncertainty in each instrument can be estimated, allowing for the calculation of total uncertainty of the analysis. This approach was used by Jack et al. (2017) analysing the reliability of the co-heating test, and has been used in this research for the co-heating tests and the experimental decay method tests conducted on the test cell.

There is no uncertainty due to instrument accuracy in the EnergyPlus outputs; the temperature of the simulation, for example, is exactly what is reported. The uncertainty reported in the simulations is therefore taken as the statistical uncertainty of the analysis

method. This follows an alternative approach taken by Stamp (2011) where the overall uncertainty is related to the standard deviation in daily readings, to a 95% confidence level. This can be applied to the co-heating simulations and the calculated average decay method as both generate a daily result.

The RMSE decay method compares the overall data sets from the simulations with the observed data. The method generates a range of HTC estimates, and makes an estimate of the HTC based on the average. The uncertainty reported in the HTC estimate from the RMSE decay method is based on the overall range of HTCs that meet the criteria for inclusion.

A detailed uncertainty analysis is undertaken for each experiment and discussed in the relevant chapters.

3.7 Statistical Measures

During analysis of the decay method and co-heating tests, some statistical tools were used to assist in determining reliability of the results. These tools are the coefficient of determination (R^2) standard deviation, root mean square error (RMSE), Excel Data Analysis Tool and the Excel Solver add-in.

3.7.1 Coefficient of Determination

The decay method and the co-heating test both fit curves to data to evaluate the building, and it was appropriate therefore to test how well the curves fit the data. Analysing the fit allowed for flagging of potential problem areas in the overall method, and provided information as to the validity of the final result.

The coefficient of determination, or R^2 statistic, showed this information in a simple and easy to understand fashion. It must be noted that R^2 provides evidence of correlation rather than causation and so must be used with some degree of caution. This can be calculated manually, or by using built-in features of Microsoft Excel.

The points at which the R^2 figure is used all analyse two variables. Adjusted R^2 was used where more than two variables were assessed as part of multiple regression analysis. Predictive R^2 was not required as the analysis is carried out entirely on data collected during the test.

3.7.2 Standard Deviation

Standard deviation measures the spread of results from the mean. It shows the size of variation between the values of a data set. In this study it has been used to determine the uncertainty of the simulated co-heating tests by measuring the dispersion of daily results.

This research applies the Population Standard Deviation function in Excel as the data analysed is considered as the whole of the data set, not a sample.

3.7.3 Root Mean Square Error (RMSE)

The root mean square error is a means of evaluating the quality of a model. It calculates the relative difference between the predicted result and the observed result. Alternative uses include comparing the relative closeness of two datasets. The closer to zero, the more closely the two datasets match on average. The units of the RMSE calculation are the same as the units of the datasets. The RMSE is calculated using Equation 2:

Equation 2 Root Mean Square Error

$$RMSE = \sqrt{\frac{\sum_{t=1}^{n}(\hat{y}_t - y_t)^2}{n}}$$

Where:

n = number of records

t = record number

$\hat{y}$ = predicted value

y = observed value

A variation of the RMSE, the normalised RMSE (NRMSE) is calculated simply by dividing the RMSE by the range of the observed data. This provides the RMSE as a percentage.

3.7.4 Excel Data Analysis Toolpack

The desktop edition of Microsoft Excel 2016 includes the Analysis toolpack, which provides a number of statistical analysis tools and outputs. This research uses the regression analysis functionality of the Analysis toolpack to conduct the multiple-regression analysis in Section 5.3.3. The regression analysis tool uses the 'least squares' method to fit the model to the observed variables. This is the same functionality as the 'LINEST' worksheet function.

The output of the analysis includes the adjusted R^2, F-test for overall significance, p- and T-tests for significance of the variables, 95% confidence intervals for the model and the individual variables, and generation of the residuals of the model. Where multiple regression analysis is used, these figures are reported and discussed.

3.7.5 Excel Solver add-in

The Solver add-in for Microsoft Excel is a powerful tool used to solve equations subject to changing specific inputs. It contains three main targets: minimising the objective, maximising the objective, or solving for a specific objective value. This is done by changing one or many 'variable cells', subject to any constraints required (such as limiting the range of a variable).

There are three Solver engines available: Simplex LP, GRG Nonlinear and Evolutionary. Simplex LP is designed for linear problems, GRG Nonlinear for smooth, nonlinear problems and Evolutionary for non-smooth, nonlinear problems. In this research the Solver add-in is used to determine which value for the decay constant results in the minimal NRMSE value for the cooling model in Section 6.5. The set of equations driving this result do not include logic functions and are therefore 'smooth'. As the functions are based on a 'sum of squares' technique they are non-linear. Therefore, the GRG Nonlinear engine is the appropriate choice.

The GRG Nonlinear Solving Method uses the Generalized Reduced Gradient (GRG2) code, which was developed by Leon Lasdon, University of Texas at Austin, and Alan Waren, Cleveland State University, and enhanced by Frontline Systems, Inc. (Frontline 2018).

3.8 Summary

The aim of this research was to evaluate the effectiveness of a new building diagnostic tool, namely the decay method. From the literature review, there are two ways to prove the effectiveness of a new diagnostic test. One is to correlate test results with particular levels of energy use for the building during normal use. The second is to correlate test results with results from other proven diagnostic tests.

In this study the most appropriate course of action, given the highly experimental nature of this research, was to evaluate the decay method against a number of currently accepted tools. Given the popularity of the co-heating test observed in the literature review, this was

the main test identified for comparison. It also had the advantage of being a relatively well understood whole-building test that can be replicated. As an additional comparison, the theoretical heat loss was included, utilising heat flux meters to measure in situ U values and a blower door test to evaluate the leakage rate.

As the co-heating test was the main point of comparison, the use of a residential home was likely to be difficult to attain, especially given the likelihood of repeat testing over a number of months and years. The use of a multi-zone house also increases the complexity of the thermal system, which would potentially make analysis of the decay method difficult. Using a test cell was a more appropriate choice, and two such buildings were available at the CSIRO site located at Highett.

As the testing is entirely based on measurement of building response, the empirical research methodology was the most obvious choice, and used the Highett test cell as a case study. To facilitate data collection, sensors programmed to take readings at regular intervals were used, either as multiple stand-alone units or all writing back to a central datalogger.

EnergyPlus was used to create building models and run simulated experiments to conduct initial analysis of the method, and then utilised additional data from the field experiments to explore the method further, as well as its use in the two RMSE decay methods. This provided insight into any uncertainty seen in the field experiments, and allowed for comparisons of the decay method and co-heating test results on a wider range of building types than simply the test cell.

All the matters discussed in this chapter facilitated a demonstration of whether or not the decay method relates to the co-heating test, and whether or not there is potential for it to be used as an equivalent measure.

Chapter 4 - Experiments and Data Collection

This chapter details the data that was collected to evaluate the buildings, and the equipment used to facilitate data collection and field experimentation. It shows how each piece of equipment fits into the overall experimentation methodology to allow each of the tests to be carried out.

4.1 Overview

Ultimately the test cells provide the real world case studies to which the testing methodology was applied. However, to fully understand the results and draw meaningful conclusions, a wide array of data is required and a number of currently understood tests needed to be carried out. This provides a benchmark against which a new evaluation method can be compared, allowing for a conclusion regarding how effective the new test is in terms of its accuracy, improvements in speed, and reduced invasiveness.

During field experimentation, the exact procedures used to collect data were reviewed and refined in response to the analysis conducted. This was also true of the experimentation methods deployed.

4.2 Field Experimentation/Tests

The focus of this research was on using the test cell building as a set of case studies for benchmarking via use of the co-heating, heat flux and blower door tests, and comparing these results with the decay method. This gave a practical, real-world proof of concept, taking on board a number of in-field realities the computer simulations could not provide.

Applying a new testing method is crucial to demonstrating its real world functionality compared to other testing methods, and to discovering potential flaws that computer simulations do not reveal.

This chapter presents the in-field testing carried out on the test cells during the course of the study. It details the layout of the test buildings and the testing apparatus, as well as the experiments carried out. This includes details of the specific equipment used and complications that arose during the experiments that may have impacted the results. Finally, comparisons of the results of the experiments are discussed.

The approach taken for the field experiment side of this research was intended as a demonstration of potential only, and not a definitive, wide-ranging analysis of the decay method.

4.2.1 Experimental Method

Two methods for determining the HTC are to be compared with the results of the decay method. These are the co-heating test and the heat flux test combined with the blower door test. The co-heating test is designed to test the overall response of the building's thermal shell, where the heat flux test takes spot readings of individual elements and combines them with the rate of air leakage determined by the blower door test. These methods are currently well understood and used to make judgements of the building's in situ performance. These two tests should give the same figure for the HTC.

The Figure 4.1 illustrates the relationship between the building evaluation methods being tested.

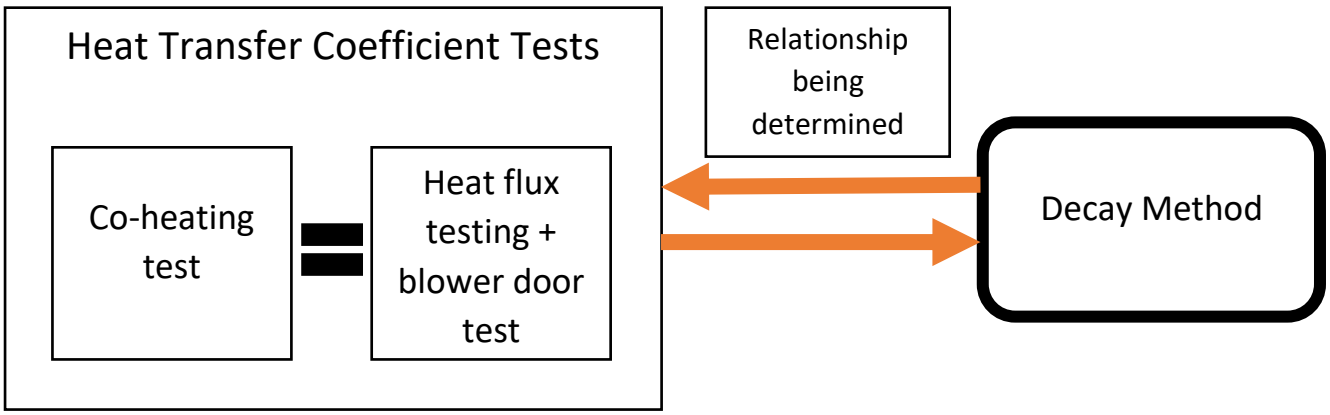

Figure 4.1 Theoretical experimental relationships

4.2.2 Experiments

4.2.2.1 Co-Heating test

The co-heating test requires setting up a steady-state thermal condition inside the building, and monitoring the energy required to maintain that state compared to the changing outside temperature. The suggested internal state is to create an internal temperature of 25 degrees centigrade, at a time of year where the external temperature will be cooler. The heat transfer through the thermal shell will therefore be from inside to outside. When this is averaged over a sufficient period, it is accepted as being equal to the rate of heat added to the building via a mechanical heat source.

This is expressed by Equation 3:

Equation 3 Building heat balance

$$Q_{input} + Q_{solar} = \left[\sum\{U \times A\} + \frac{1}{3}nV_{ol}\right]\Delta T$$

Where:

Q_{input} = power supplied by the heater, W

Q_{solar} = solar gain, W

U = U value of thermal shell element (i.e. wall), $Wm^{-2}K^{-1}$

A = Area of thermal shell element, m^2

n = ventilation rate at atmospheric pressure, ACH

V_{ol} = Volume of the building, m^3

ΔT = difference between average internal and external air temperature, K

The result of the test is calculating the HTC represented by Equation 4:

Equation 4 Heat Transfer Coefficient

$$HTC = \left[\sum\{U \times A\} + \frac{1}{3}nV_{ol}\right]$$

This is determined through measuring Q and ΔT, and rearranging Equation 3.

The experiment procedure is set up so that the building is closed (that is, doors and windows are shut, but no attempts at additional weather sealing are to be made) and heated until the steady state is reached. The building should be held in this state for two to three weeks. The temperature difference between inside and outside (degrees Kelvin, K) and heat input rate (Watts, W) is averaged over a 24-hour period. The 24-hour period for this research is from 6.00am-6.00am so that the full solar cycle is included in the same averaging calculation. This is so that the analysis period mimics the natural cycle of the building responding to the surrounding climate. On completing the test, the daily (24 hour) average temperature difference is parameterised against the average heating rate give the HTC in W/K. This is a measure of the rate of heat lost by the building for every degree Kelvin of difference across the thermal shell. The average heating rate is adjusted for solar gains and wind speed using multiple regression analysis. Solar gains and wind speed is also the 24-hour average. Co-heating tests conducted on the buildings had to be interrupted fortnightly to allow for data to be collected.

4.2.2.2 Heat Flux Testing

Heat flux testing provides the means to calculate the actual R-value and U-value of the entire building element (for example, wall or floor). It requires a heat-flux meter affixed to the element, usually on the inside surface, and temperatures measured on the inside and outside surfaces. Over the experimental period, Equation 5 is used:

Equation 5 Average method for calculating material U-value

$$U_t = \frac{1}{\frac{\sum_0^{i=t} \Delta Ts_i}{\sum_0^{i=t} Q_i} + r_{int} + r_{ext}}$$

Where:

U = U-value

ΔTs_i = internal surface temperature – external surface temperature in degrees Kelvin, K

Q_i = heat flux readings in W/m^2

r_{int} = Surface resistance due to internal air, assumed 0.13 W/m^2K

r_{ext} = Surface resistance due to external air, assumed 0.04 W/m^2K

When the U-value is plotted against time variations it should dampen and approach an asymptote. After a week the U-value should stabilise to within 5% of the final value from four weeks of testing (Rye, 2010).

Note that these calculations used static R-values for surface air resistance. In reality, the surface resistance of the material changes with temperature and air flow. Using assumed static values simplifies the calculation. This approach was used by Baker (2011) and Rye & Scott (2010) in their respective studies of in situ U-values. The values used are taken from ISO 6946:2007.

The different combinations of collection for the heat flux meters have been used. Set up 1 consisted of heat flux meters on the internal surfaces of the building, and a five second resolution. Set up 2 shifted the resolution to 30 seconds due to memory constraints of the data loggers, and kept placement of the meters on the internal surfaces. Set up 3 placed a heat flux meter on the inside, and a second meter on the outside of two walls, with a collection resolution of 30 seconds. Set up 4 placed heat flux sensors on both sides of the internal lining and external cladding (four sensors in total) in two different wall sections. In each case all heat flux sensors were accompanied by a thermocouple measuring surface temperature.

The first three combinations were applied to Test Cell 1 during the long term monitoring in the second year of this research. Set up 4 was applied to Test Cell 2 during the co-heating and decay tests. The co-heating test creates good conditions for the heat-flux testing to be conducted; however, the test is valid under any conditions.

4.2.2.3 Blower door test

The blower door test is used to measure the air change rate in, or infiltration rate of, the building. This is achieved by closing all doors, windows and other openings into the building shell, and creating a pressure difference between the internal space and the atmosphere, then monitoring the air movement required to maintain the difference. Two tests are conducted: one raising the pressure inside the building, and a second reducing the pressure until the air change at a difference of 50 Pa is measured or can be extrapolated. The average of the two tests is calculated and accepted as the air change rate.

The blower door kit used for this research is the Retrotec 3101 Hi-Power kit. The testing utilises the software 'FanTestic Lite' to carry the test out in accordance with Australian Standard ASTM E779-10. The software automates the process of powering the fan to incrementally change the pressure difference and take the required readings.

The results at 50 Pa are divided by 20 to give the infiltration rate, n (Kronvall, as cited by Stamp, 2010). This is used in the heat loss equation presented in the co-heating test Section 4.2.2.1. Infiltration heat loss (in W/K) may be then be calculated using Equation 6:

Equation 6 Infiltration heat losses

$$Q_{infiltration} = \frac{1}{3} n V_{ol}$$

Where:

V_{ol} = building volume in m^3

n = infiltration rate at atmospheric pressure, ACH

1/3 = specific heat capacity of air

4.3 Experimental Set-up

4.3.1 Data Sets

To effectively evaluate the building, a combination of experiments was carried out. Each test had unique data requirements, though some overlapped. Data was collected includes:

- Air temperature
- Building surface temperature
- Material heat flux
- Energy use
- Air leakage rate
- Local weather data
- Thermographic imaging.

Data was collected using two Campbell Scientific data loggers, a number of HOBO temperature and humidity loggers, a blower door kit, and the CSIRO run on site weather station.

Figure 4.2 Initial setup for experimentation period 1

4.3.1.1 Campbells Scientific Dataloggers

For this study, RMIT University provided two different Campbell Scientific data loggers: models CR3000 and CR850.

The dataloggers take readings in the form of voltage and then, based on the internal system baseline voltage and the collection program, the logger converts the readings into the desired value (for example, temperature) and records it in the on board memory. Both dataloggers can be programmed for read and collection frequencies of one second. For most experiments in this study, a read frequency of five seconds was used, and a write frequency of 30s. The loggers were programmed to write the average of the read values for each 30s interval.

The CR3000 has the capacity for 28 single-ended inputs, or 14 differential inputs and 4 pulse counters. It has a reported accuracy of ±0.04% of the reading, and a resolution of 0.33 µV (CR3000 Micrologger, 2014).

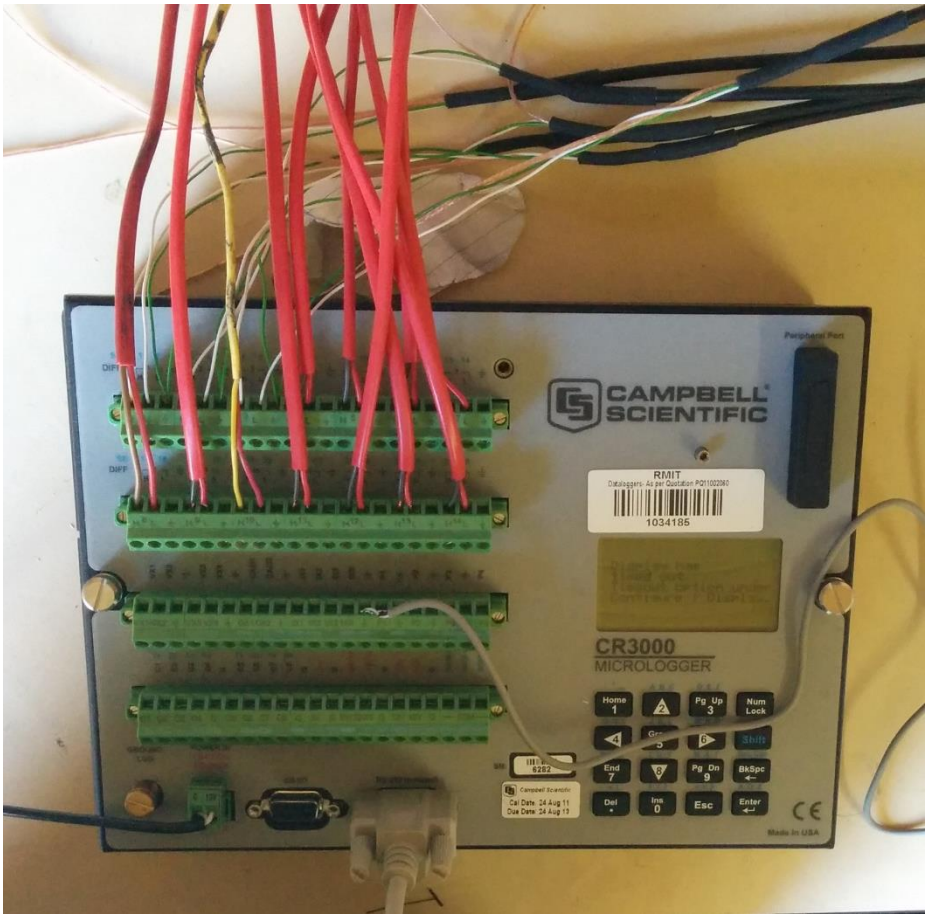

Figure 4.3 CR3000 Micrologger

The CR850 has the capacity for six single ended inputs (three differential) and one pulse counter. It has a reported accuracy of ±0.06% of the reading, and a resolution of 0.33 µV (CR850, 2014).

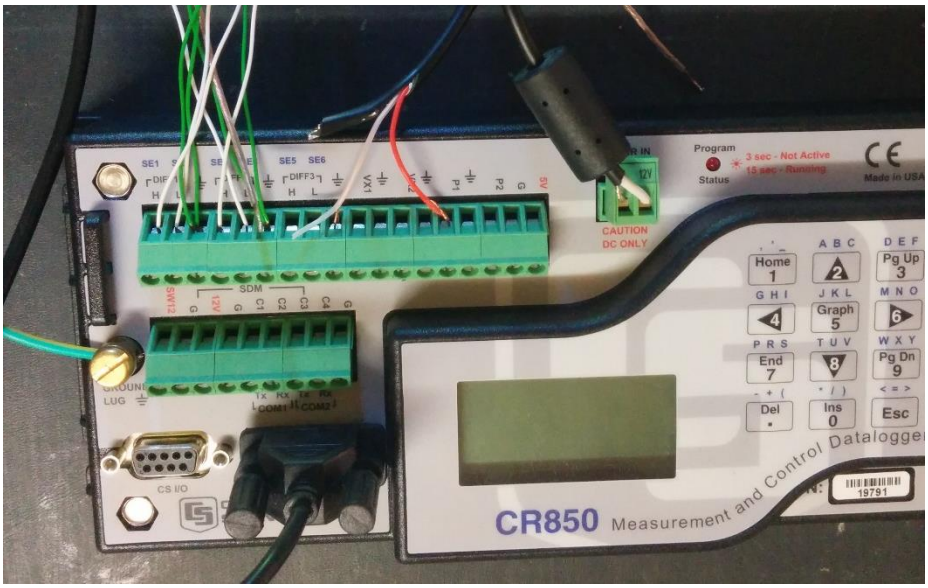

Figure 4.4 CR850 Datalogger

Both dataloggers are compliant with IEC 61326:2002 standards. The Campbell Scientific dataloggers were used to collect data referring to the building surface temperature, material heat flux and the energy use. These data sets were used as part of the heat flux tests, identifying the R-value of the building element, the energy portion of the co-heating test, and the measured heat pulse decay method. The power required to run the dataloggers was included in all power readings as they form part of the heat gain inside the test cell.

4.3.1.2 Internal Air Temperature

Internal temperature was collected by HOBO temperature and humidity dataloggers provided by RMIT University.

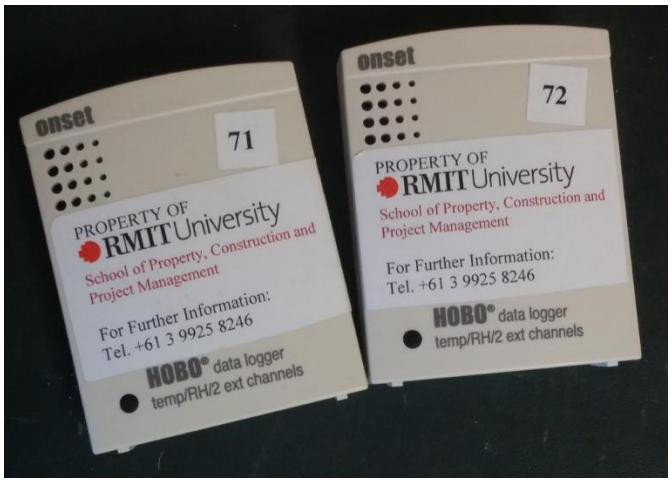

Figure 4.5 HOBO temperature and humidity dataloggers

The maximum recording frequency of the HOBO loggers is 60 seconds. 27 loggers were spaced evenly across Test Cell 2 in a 3x3x3 grid to determine the average internal temperature. Three sensors were placed in the attic space, and three in the sub-floor space. Additional sensors, where available, were placed at floor and ceiling height, and in the corners of the room.

Figure 4.6 HOBO sensor located in attic space

Figure 4.7 HOBO sensors located throughout Test Cell 2

At a collection rate of 60s, the HOBO loggers have a capacity to store approximately 15 days' data. They were programmed to not overwrite data once the memory bank was filled. The loggers record air temperature to a resolution of three decimal places, and have a reported accuracy of ±0.35^{o}C (Onset 2014).

The temperature data collected by these loggers is arguably the most vital piece of information being collected. Temperature data was used in the co-heating test to calculate the temperature difference across the thermal shell, and in all variations of the decay method to map thermal behaviour of the test cell.

4.3.1.3 Building Surface Temperature

K-type thermocouples were used to collect building surface temperature data, which required differential inputs on the Campbell dataloggers. The measuring tip of the thermocouple is a connection between two wires of dissimilar metals. The temperature difference between the measuring tip and the reference end of the wires creates a voltage. The datalogger then interprets the voltage and calculates the corresponding temperature.

When using these thermocouples outside, it was important to ensure they were shielded from rain as the oxidation the wire tip undergoes alters the voltage across the length of the

thermocouple, giving incorrect readings. This was done by creating plastic covers that shielded from the rain above, but were still open to allow air to pass through. This retained the integrity of the measurement by not creating an anomalous air pocket, but also ensured the sensor was shielded from rain and solar radiation. This is in accordance with data collection procedure outlined in ISO 9869-1:2014. This ensures the temperature recorded by the external sensors is the surface temperature of the building, and not a potentially higher value due to solar radiation detected at the sensor tip.

The surface temperatures were used to calculate the temperature difference across the building element in conjunction with the heat flux measurement to calculate the R-value of the element. This was more accurate than using the air temperature as it allowed for measurement of the temperature at the point the heat flux readings are taken, removing errors due to stratification of the air. It also removed the need to include assumptions about the R-value of the air films at each surface, which may change with temperature and air movement.

4.3.1.4 Material Heat Flux

Hukseflux heat flux plates were used to measure the heat flux through the building materials. The flux plate is coated with a thin layer of thermal paste to assist in heat transfer between the surface and the plate. This allows for a more accurate reading of the thermal flow through the material.

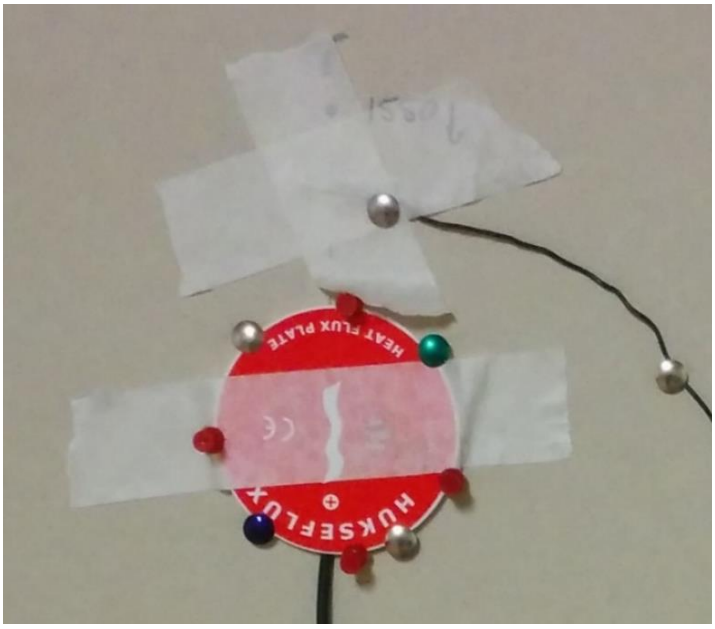

Figure 4.8 Hukseflux heat flux sensor with K-type thermocouple

Each sensor is individually calibrated and needed to be programmed separately into the datalogger. The plate has a sensitivity of 50 µV/Wm^2. It has a reported accuracy of ±5% for 12 hour totals (Hukseflux 2014).

The heat flux sensors located on the external walls were covered with a plastic case similar to the thermocouple covers. This shielded the sensors from rain and provided shading to ensure readings were not impacted by direct solar radiation on the sensor. As noted above, heat flux plates were used to calculate the R-value of the building element.

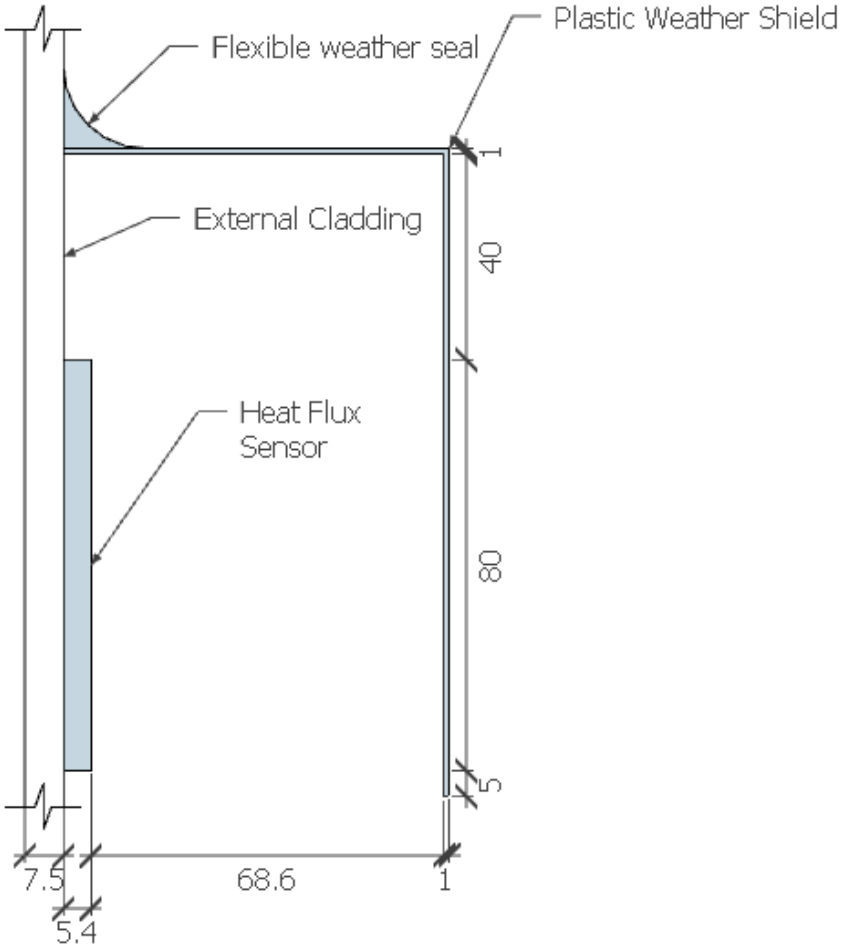

Figure 4.9 Heat flux sensor and weather shield

Note: Dimensions in mm

4.3.1.5 Energy Use

Energy used to heat the building is measured through an Elster A100C Wattmeter. This unit is connected in series with a 2 kW blow heater, with a pulse output wired to the Campbell Scientific datalogger. The Elster is rated at accuracy Class 1. Each pulse output to the datalogger is equal to 1 Wh (Elster 2014).

Figure 4.10 Elster A100C Wattmeter

The energy used by the heater was recorded as part of the co-heating test and the measured heat pulse decay method. In the case of the co-heating test it was used to calculate the average Watts required to maintain the average temperature difference. The measured heat pulse used the total from the pre-heat phase of the decay tests for comparison with the simulated building model.

4.3.1.6 Air Infiltration Rate

Air infiltration rate was determined by using the Retrotec blower door kit. The 6101 Hi-Power model (previously labelled 3101) was used to test both test cells. This model utilised a cloth door fitted on an adjustable frame to seal the door.

Figure 4.11 Fan and soft door during blower door test

The blower door test was conducted as a stand-alone procedure. The test kit was connected to the laptop running the test software 'FanTestic Lite'. Using air pressure sensors involved in the testing kit, the software automatically adjusts the fan speed to raise or lower pressure inside the building, taking measurements of air flow at an accuracy of ±5% (Retrotec 2014).

Air infiltration formed part of the theoretical prediction of building heat loss. Using the infiltration rate, heat lost due to warm air inside being replaced by cold air from outside was calculated. This was combined with the building's overall R-value to estimate heat loss in the same format as the co-heating test. As infiltration is an important part of building behaviour, it was also used to inform the building models.

4.3.1.7 Local Weather Data

Weather Data used for analysing the field experimentation and creating the custom weather file for the EnergyPlus simulations was gathered by the Bureau of Meteorology (BoM) weather station at Moorabbin Airport. This site is 5.5 km south-east of the test cell location. In addition, a weather station operated by CSIRO on the northern end of the Highett site was used for comparison. Both weather stations provided dry bulb air temperature, humidity, windspeed and direction, and rainfall data. The CSIRO weather station collected local solar radiation data, whereas the BoM solar data was gathered from the station at Melbourne Airport (Tullamarine), 35 km north-west of the test cell location.

Both Moorabbin and Tullamarine BoM weather stations made observations on a 60-second frequency. The CSIRO weather station recorded observations every 15 minutes. Information regarding the accuracy of equipment and weather station set up by CSIRO was not available. The BoM automatic weather stations are calibrated in accordance with quality assurance standards published by the World Meteorological Organization.

The HOBO and CR3000 dataloggers were recording at 60- and 30-second frequencies, and the EnergyPlus simulations were also set to calculate based on 60-second timesteps. As the BoM weather data matches these recordings more closely, and has published information regarding the equipment and quality control processes, the BoM dataset was used for all external weather observations. The literature review noted that there is some risk in using weather data collected off site. The CSIRO dataset was used to confirm that the Tullamarine

solar data was still sensible at the Highett location, and that the Moorabbin observations were likewise applicable for analysis of the test cell.

This was important for all co-heating and decay method tests, but not used for heat flux analysis as this required surface temperatures. The use of default weather files for the EnergyPlus simulations would also have created difficulties when comparing observed test results with simulated test results, and so BoM data was used to create the EnergyPlus weather file.

There are occasions when the BoM deemed a data point did not pass quality requirements. Consequently, some gaps, between 1 and 15 minutes, existed in the dataset. Where this occurred, data was linearly interpolated to fill the gap. Linear interpolation carries some risks at maximum or minimum temperatures (Miller 1990), however was effectively used by Liley (2017) in developing some aspects of Reference Meteorological Year weather files for NatHERS. The application of linear interpolation in these cases was on gaps of up to three hours. The gaps in the data used for this study are much shorter, and the risk of inaccuracies should therefore be lower than those in the above cases.

4.3.2 Additional Equipment

To heat the building, a 2 kW blow heater was installed in the building, with a HeaterMate digital thermostat and a digital timer. To help mix the air and provide an even temperature throughout the test cell, a stand-alone fan was also used.

4.3.2.1 Blow Heater and Fan

The 2kW blow heater used to heat the building was set to maximum capacity whenever it was switched on. This helped simplify the experiment, and gave the best possible chance for the heater to maintain the internal temperature during winter. The fan ran constantly, providing mixing for the entire data collection period. Fan power was added to all power readings. It was also not connected to the timer and thermostat as it was required to run independent of the heater cycle.

4.3.2.2 HeaterMate Thermostat

The HeaterMate plug-in thermostat has a control range of between 5 ^{0}C and 30 ^{0}C. It takes measurements every 10 seconds and has an accuracy of ±1 ^{0}C. In heating operation, once the set temperature is reached, the thermostat switches the controlled unit off until it registers a temperature drop of 1 ^{0}C. It was observed that the HeaterMate thermostat was

recording temperatures between 1^0C and 2^0C higher than the HOBO sensors, and was set at 27^0C to allow for the test cell to reach 25^0C. Temperature measured by the HeaterMate was not recorded.

Use of a digital thermostat was required for the co-heating test, specifically to maintain the most even internal temperature possible. Dewsbury, Nolan & Fay (2007a) note that the thermostat in the heater is likely to not be consistent and prone to influence from the heater rather than responding to air temperature.

4.3.2.3 Timer

To run the decay test, a digital plug in timer was used to switch the heater on and off as required. The timer was set to match the times of the HOBO and Campbell Scientific dataloggers.

Figure 4.12 HeaterMate and digital timer

The timer was used only for decay method testing. It was needed so that the heater was switched off to provide the decay period, and removed the need for manually operating the heater for this test. It also allowed the heat pulse to be applied in a specific time period before the decay phase began. The co-heating test required the heater to respond to temperature rather than timing, and so it was removed for the co-heating test set up.

4.3.3 Experimental Layout

The final layout for the test cell experiments is shown in Figure 4.13.

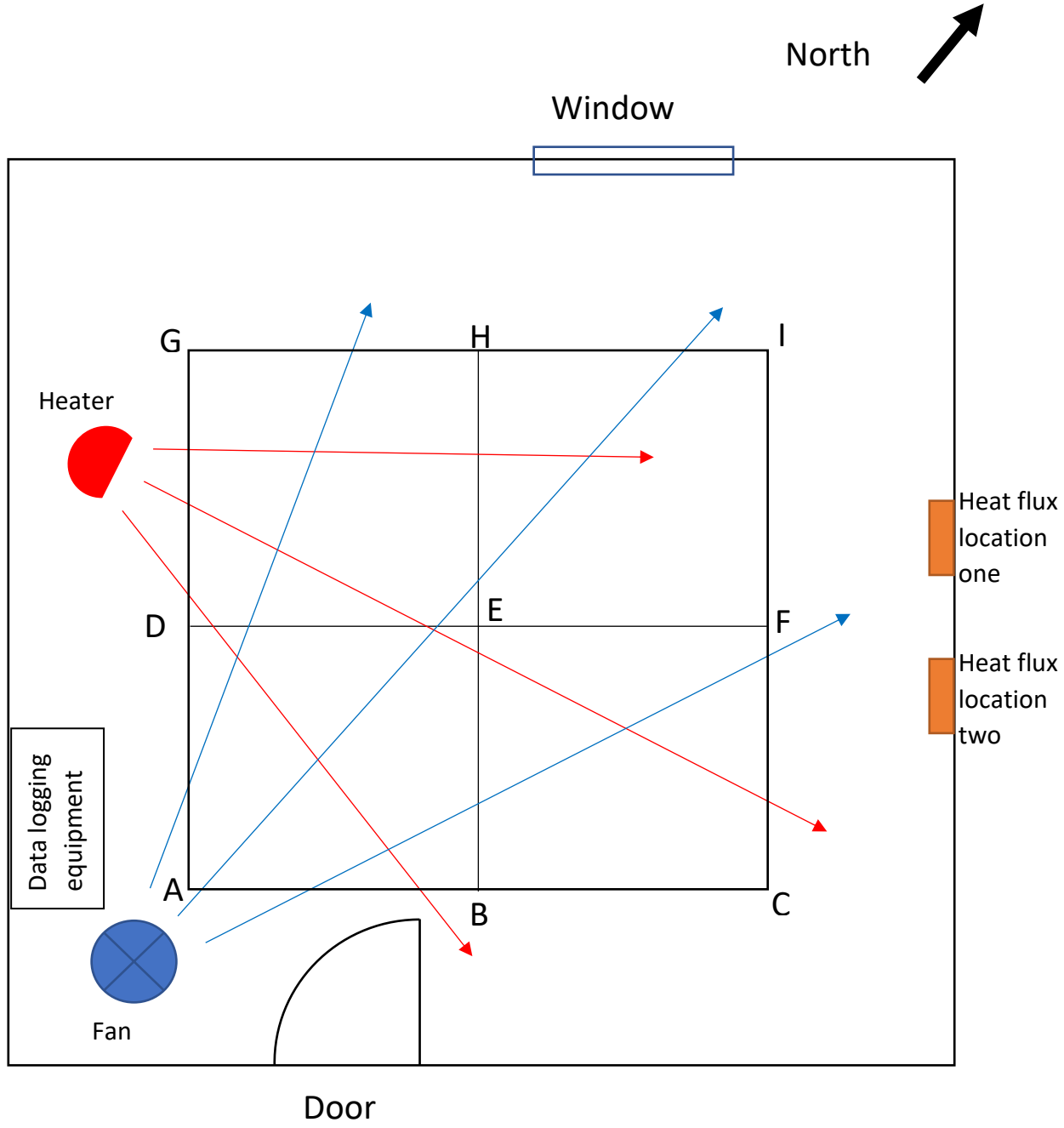

Figure 4.13 Test Cell experiment layout

*Not to scale.

**Distance from the walls to the outer ring of sensors is approximately 1255mm. Distance between all adjacent sensors is also 1255mm.

4.3.3.1 Temperature Sensors

Table 4.1 lists HOBO temperature sensor locations. They were arranged in a three-dimensional array to provide even coverage of the entire test cell. This went some way towards mitigating any effects of stratification, and reduced uncertainty from placing a single sensor at an arbitrary location within the room. The sensors heights are similar to those used by Dewsbury, Nolan & Fay (2007a). This array provided insight about the quality of air mixing, and an average temperature calculated from the array gave a more accurate representation of the test cell's overall air temperature.

Table 4.1 HOBO temperature sensor location

Vertical Position	Location
Floor	A,C,E,G,I
600mm	A-I
1200mm	A-I
1800mm	A-I
Ceiling	A,C,E,G,I

Limitations on the number of sensors available required some level of compromise. It was deemed that the central cube of 27 sensors (600mm to 1800mm, A-I) was the most important section to maintain a full dataset across all tests. The layout of these sensors broadly follows set out used by Dewsbury, Fay & Nolan (2008).

Ceiling and sub-floor sensors were located above and below point E as this was where the openings were to these areas in the structure. Access was limited, and sensors were placed within reach from all points, but away from floor and ceiling surfaces. This gave a reading more representative of air temperature of the space than the surface temperature of either floor or ceiling.

4.3.3.2 Heater and Fan

The heater and the fan were located on the floor, in a similar fashion to that of the co-heating test. Raising the height of the heater was expected to exacerbate any stratification that would have occurred.

The heater's diagonal direction was designed to heat the air of the test cell as evenly as possible, and minimise direct heating of the wall surfaces. Aiming it diagonally across the room gave the heated air the furthest distance to be blown before impacting a surface directly. It was decided that directing airflow towards the door may increase some of the leakage losses, as this would direct air towards a known gap in the thermal shell. Directing towards the window was also undesirable as direct heating of the internal window shade would potentially compromise the structure's integrity. Finally, directing the heater towards the datalogger is also likely to have influenced the system reference temperature. The exact positioning of the heater was such that it did not directly blow warm air onto the nearest of the HOBO sensors, and did not blow air onto the heat flux sensors. The location selected in the western corner provided a balance between these elements.

Positioning of the fan in the southern corner created a cross-breeze with the intention of being able to mix air thoroughly. Positioning the fan directly opposite the heater may have caused a singular heat-column in the centre of the room as the conflicting airflows met. The southern corner was selected instead of the northern corner as it was closer to the power socket.

4.3.3.3 Heat Flux Meters

The heat flux meters were located near to the centre of the north-eastern wall, approximately halfway up the wall. The wall construction at this location was representative of the majority of the building: the internal surface of the south-western wall was clad in the same timber as the ceiling was constructed from. It was also away from corners, the door and the window which may have influenced heat transfer through the structure. Sensors were placed on both sides of the internal lining and external cladding, and positioned between the wall studs to avoid measuring heat flux through the timber frame's thermal bridge. Thermocouples were placed immediately above each heat flux sensor. Figure 4.14 shows the layout of the heat flux sensors through the cross section of the wall.

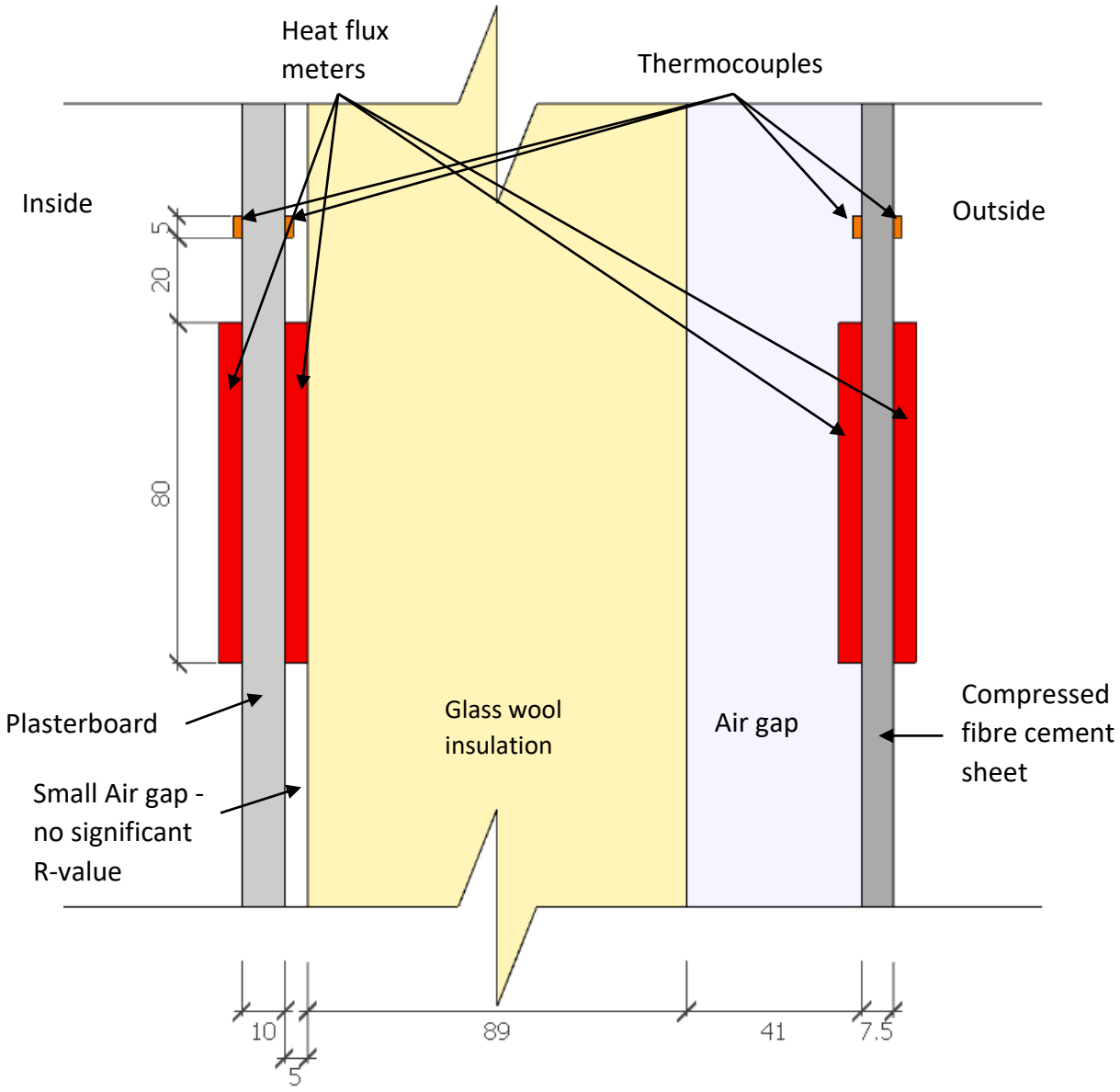

Figure 4.14 Cross sectional layout of heat flux Sensors

Note: Dimensions in mm

The heater location was based on requirements for the co-heating and decay tests. The heat flux testing was seen as an important but secondary test, and the integrity of the co-heating tests and decay method tests was of greater importance. Ideally the heat flux meters should be behind the heat source, however this would place them on the wooden internal lining of the South-Western wall, or near the corner or window on the North-Western wall. Some compromise therefore had to be made with the heat flux meters on the North-Eastern wall. Heat flux location 1 was out of the blow heater's direct line, and was taken as the main

collection point as the heat flux sensor should not be influenced by the heater. Heat flux location 2 may be impacted more, and was a back-up should sensor 1 fail for any reason.

4.3.3.4 Datalogging Equipment

The datalogging equipment location included the Campbell Scientific datalogger, the Elster Wattmeter and the HeaterMate thermostat controlling the heater.

These items were located on a desk in the room's southern corner. This kept them close to the required power socket and out of the heater's direct line, which may have otherwise influenced thermostat readings and created inconsistencies when controlling the heater.

4.4 Simulation Set-up

Simulation software was used extensively throughout this research. It was used as an early development tool, observing the ways in which we can analyse buildings and informing decisions about the first field tests of the experimental decay method. It was the main analysis tool for RMSE decay methods. Simulation software also allowed for elements of the benchmarking experiments to be analysed in ways which would otherwise have been difficult within the scope of this PhD project. For this thesis, the International Energy Agency's accredited building simulation tool EnergyPlus was used.

4.4.1 Development Tool

As this study's in situ experimental focus was limited to three case studies, the major benefit of utilising modelling software was the speed at which a number of scenarios could be simulated and analysed. The thermal system that is the building envelope is very complex, with potential for a wide array of variables. The time required, and the cost of the equipment necessary, to conduct these same sets of experiments in the real world was beyond the available capacity of a PhD project.

By using building models it was possible to conduct a large number of preliminary 'proof of concept' studies, and identify key areas that would impact real world experiments. This showed where potential issues were with data collection processes, highlighted the resolution and required accuracy for satisfactory results, and headed off any dead end exploration before any lengthy data collection was devoted to it. This approach was applied both in the initial theoretical research phase, and in reviewing and analysing the results of

the field experiments. In this way, the approach assisted in informing the review and refine process through the study's latter stages.

4.4.2 Analysis Tool

The benefits of using simulation to provide evidence and analysis of the decay method pre-experiment phase are the same as the benefits of using it as an analysis tool as part of the RMSE decay and analysing the observations made during benchmarking experiments.

The ability to turn off elements of the real world in a simulation (for example, eliminating solar radiation or wind from the simulation) enabled some sensitivity analysis and exploration into why there may be differences between a theoretical calculation and observed experimental result. This was particularly useful in exploring differences between heat loss calculations from the co-heating test compared with results from heat flux and blower door tests.

Using simulations also enabled a comparison of a wider range of buildings than were physically available for this research. A total of 144 building models were simulated for both co-heating and decay method evaluations. The results of the simulations differ slightly from observed tests, but are useful for showing reliability in applying the methods to a wider building set than just the test cell.

Simulation was integral to the process of the RMSE decay methods. This is for the same reasons as the pre-experiment phase: the speed at which multiple experiments could be simulated. The aim was to eliminate the invasiveness of the co-heating test as an evaluation technique, and so the need to estimate the HTC in a different fashion was critical. By simulating both the decay experiment and a co-heating test on multiple versions of the same building, the simulation program allowed estimation of the HTC without actually conducting the co-heating test in the real building.

4.4.3 Summary of Simulation Use

Throughout this research the simulation process was used to identify:

- The number and type of key data sets required for meaningful results
- Required frequency and resolution of data collection
- Sources of error and uncertainty
- Theoretical evidence for validity of the decay method
- Links between theoretical decay method results with those of simulated co-heating tests
- How different building constructions, weather conditions and initial internal conditions may affect results of any test
- Provide estimates of the HTC via the RMSE decay methods.

4.4.4 Energy Plus

The use of EnergyPlus for the simulation portions of this research was due to a number of factors. Currently in its eighth iteration (v8.1.0 to v8.6.0 were used), it was originally internationally accredited after version 1 passed the Building Energy Simulation Test (BESTest). It is an open source tool – the full version is available as a free download from the U.S. Department of Energy website. The program's open source nature makes it exceptionally customisable. Outside the basic engine, all inputs and initial conditions are customisable and recorded, and all the parameters necessary to run the simulation are available, including weather, materials, internal temperature, additional heating or cooling, convection coefficients, and the length of time the simulation should run for.

Senior project supervisor Ian Ridley has used EnergyPlus in a number of research programs, and the availability of a highly experienced user has been invaluable for managing the learning curve and rectifying issues in the models.

In addition, the capability of batch processing, a piece of script developed by Phillip Biddulph at University College London, enabled rapid creation of multiple building models. These two elements combined made it possible to create and run, in minutes, hundreds of variations on the same building model.

Once complete, the results were output as csv files and opened in Excel for analysis. By using Excel macros these hundreds of models could be imported into Excel and analysed in

seconds. Once the desired aspect of a building to inspect was been settled upon, these automation and customisation elements of EnergyPlus allowed vigorous testing and comparison of the decay technique under many different circumstances.

4.4.5 Creating the Building Models

A series of EnergyPlus models was created for all the simulation portions of this research. A 'base' model was developed based on in situ measurements of building dimensions, thermal properties and air change rates. The base model is the starting point for simulations based on the best available information regarding the thermal shell of the test cell. From this base an array of models with variations on the thermal shell properties were created.

The intention of these models is to create a model similar in design and specification to the real test cell, and that behaves in the same fashion when placed under the same conditions. Variations on this base model provided further opportunities to analyse relationships between the co-heating test HTC and the decay method outputs across a range of buildings with slightly altered characteristics, and variations that are not easily altered in-field. The intention is not necessarily to create perfect replicas of the test cell given there are known issues with simulated models generally. Calibrating to exact matches is considered time consuming, and potentially an impossible feat. This does not mean no care is taken to align inputs to the model with test cell site details, dimensions and thermal properties. However, this approach did acknowledge that despite attempting to minimise variations in the input data, there will be differences between reality and the building model.

4.4.5.1 Base Model

EnergyPlus uses a wire-frame computer model, and the 3D representation of the building uses zero-thickness surfaces. The thickness of the surface is taken into account by the creating the construction that is applied to the surface, not the length and width of the surfaces entered into the software. The heat conduction calculation is one-dimensional and perpendicular to the surface, and therefore only calculates heat conduction through areas of the building that directly connect air spaces together. The dimensions entered into the model are the internal dimensions as this represents the areas through which the one-dimensional heat transfer occurs. These dimensions were measured on site as plans for the test cell could not be sourced.

The building is modelled as three zones: sub-floor, roofspace and test cell zone. The focus of the research is the testing zone. To assist in calibrating the thermal response of this zone with the field observations, the Sub-floor and Roofspace zones were conditioned to the temperatures observed in the field experiments. The subsequent improvements in alignment between the model and the field observations is shown in Law, Wong & Ridley (2016). The test cell zone is intermittently conditioned to match either the Co-heating or Decay test requirements.

Thermal properties for the floor, wall and ceiling materials were determined via heat flux testing. This process and calculations are detailed in Chapter 5. The R-value of the insulation was not directly measured. It was derived from other heat flux testing conducted. Properties of the external wall cladding were taken from the manufacturer's specifications sheet. AccuRate default values were used for the door and window. The window is taken as Default Window ALM-001-02 A. This window is designed to represent a single-glazed, aluminium sliding window, but without information regarding the actual window used: this follows guidelines for Australian building assessors under NatHERS. The thermal properties for the roof tiles were taken as default values for concrete tiles in EnergyPlus. The walls around the sub-floor are constructed from the same material as the wall external cladding and the same manufacturer specifications were used. The floor of the sub-floor zone is unsealed earth; however, EnergyPlus requires a floor to be set for each zone simulated. To best simulate this connection, a thin layer of soil was set as the floor construction with the ground boundary condition. The air change rate of the test cell was determined from blower door tests. These calculations are discussed in detail in Chapter 5. Shading from the fence, trees and neighbouring buildings was estimated from observing Google Maps for location, and Google Street View for height. In addition to the electric blow heater, the fan and the Campbell Scientific datalogger had a power draw of 33 W. These ran continuously, and so were included as 'Additional Equipment' in the model, providing a constant 33 W to the building. This includes during the decay tests.

Six base models were created, two for each test cell configuration so the temperature settings for each of the co-heating and decay tests can be matched. This is particularly important for the roof space and sub-floor zones as the temperature in these zones varied throughout the experimentation period. Temperature variations were largely driven by the

different weather conditions and the differing temperature readings during the experiments.

4.4.5.2 Model Arrays

To increase the simulated data set's size, creating a wider range of results for comparison, a series of models was created based on the base model for each configuration. These models have a combination of changes to the thermal properties of the building materials and air change rates. The overall combination of these changes resulted in 144 models for each of three configurations. Combinations of these alterations was conducted in two sections: first, changes to wall insulation and air infiltration rates; and second, changes to ceiling properties and thermal mass of the internal lining.

The first set of changes is expected to account for any errors and uncertainties based on testing the R-value and air infiltration of the test cell. This is based on the principle that two elements determine the building's heat loss: fabric losses, and infiltration losses. Combinations of these changes may increase, decrease or have no overall influence on the building's heat loss if the size of the change in each term is balanced.

The second set is to test the simulated response beyond the experimental uncertainties. This set makes changes to the building model that are not based on the field observations to test the accuracy of the decay method if major errors are made in creating the building model (for example, overestimating the R-value of an element) and provides information regarding how steady state behaviour for two buildings can be the same, and yet the dynamic response can be different.

The changes to the insulation and air change rates are:

- Three levels of insulation
    - R1.5
    - R1.91 – as tested in situ
    - R2.5.
- Four levels of air change rates
    - 0.5222 ACH – Lowest expected ACH from goal seeking on HTC from base model.
    - 0.86625 ACH – 30% lower ACH than in situ

- 1.2375 ACH – As tested in situ
- 1.60875 ACH – 30% greater ACH than in situ.

Note that air change rates are volumetric changes per hour under atmospheric pressure.

These changes were intended to cover the first line of possible differences between the model and the test cell. In particular this covers possible variation on the air change rate, as the 1.2375 ACH figure is based on the n/20 rule of thumb, n being ACH at 50 Pa. This was based on a two-storey residential building and may not apply to a small building of the test cell's size but is the default figure used by Johnston et al. (2013). The full range of combinations of these elements results in 12 different models – that is, the base model (R1.92 and 1.2375 ACH) with 11 variations.

The second level of changes to the ceiling R-value and the thermal mass of the lining are:

- Increase R-value of ceiling material to R0.5.
- Double density of plasterboard lining to increase thermal mass.

Doubling the density of the plasterboard lining was chosen over applying a thermal mass element to the zone as it may also influence how heat is transferred through the layers of the construction, rather than just artificially adding thermal mass to the space.

The combination of these changes added three variations to the base model. The full array of combinations of these changes creates 48 different building models. Across the three configurations of the test cell this creates 144 models for comparison, each of which is subjected to a co-heating test and a decay test.

4.4.5.3 Thermostat Settings and Temperature Gradient

The thermostat settings for the building model were set to the same temperature as the test cell's observed temperatures, which are taken as the average of the 27-sensor array of HOBO temperature sensors. During the experiments, the building model thermostat was engaged for the same time periods as the test cell thermostat, and the simulations carried out on a 60 second time step. The thermostat value was therefore set for every 60 second timestep, to match the temperature recorded in the test cell.

Observations of the temperature readings during the experiments showed that despite the fan mixing the air there was some stratification, and higher sensors recorded higher

temperatures; lower sensors recorded lower temperatures. The test cell's air temperature was taken as the average of all temperature readings, and so the thermostat of the building model is set to this average. The thermostat height in the model was set at 1.2m as this best represented the height where air temperature matched average temperature. A temperature gradient based on the variation in readings and the five different heights was calculated and applied to the building model. This changed at various hours of the day, and so a gradient for each hour of the day was calculated and applied. The three configurations also had differing gradients, and so the gradient was modified for each model representing the different configurations.

Initial simulations did not set the temperature in the roof space or sub-floor zones, and observed a large difference in energy required to maintain the temperature recorded in the 'living' zone of the test cell. Temperatures for the roof space and sub-floor were recorded during the experiments on the same frequency, and so to assist minimising the differences in behaviour between the test cell and the simulations, temperature readings for the sub-floor and roof-spaces have been set to match the recorded temperatures at every timestep.

4.4.5.4 Thermal Bridging

The test cell is constructed from a timber-stud frame. This timber, along with the door and window frames, creates thermal bridging between the internal and external surfaces in the walls. If this were to be accounted for literally, each piece of timber would be required to be entered into the software as a separate wall. Instead, a general reduction of the R-value of the insulation layer of the construction is applied to account for the increased heat transfer through the frame elements. This is partly why an array of building simulations is used, and most importantly why the reduced R-value variation of R1.5 was included. This reduced R-value version of the model is intended to account for a worst-case scenario of reduced effectiveness of the insulation due to age, thermal bridging, and any gaps where the insulation does not fit perfectly within the frame. Framing factors are included in the theoretical HTC estimates found in Appendix B.

The framing elements have not been adjusted in the floor or the ceiling as there is no insulation or trapped air providing any form of insulation in these constructions, and thus the frame does not act as a thermal bridge.

4.4.5.5 Timing Drift

The clock on the digital timer did not maintain the same time as that of the data logging equipment. This is due to the timer being isolated, whereas both the Campbell Scientific datalogger and the HOBO temperature sensors were updated automatically at the end of each experiment when they were connected to the computer for data transfer. This manifests in the decay periods not beginning exactly at 2.00am each night, and is usually at 1:58am. The major difference is in Configuration 1 where the decay period begins at 1:27am. The simulations have been adjusted to reflect this behaviour.

4.4.6 Weather

The weather file used in all simulations was created based on observations from the Bureau of Meteorology weather stations. Solar radiation readings were from the Melbourne Airport (Tullamarine) weather station; all other readings were collected at Moorabbin Airport. The resulting weather file was created on a 60-second timestep as this was considered to be the most comprehensive representation of external conditions, and was aligned with the simulation time step. The weather file was created using the in-built 'Weather' utility provided with EnergyPlus.

4.5 Plan Summary

In the first stages of research, building modelling using EnergyPlus was carried out to develop the theoretical base for the decay method. During this time the test cells at Highett had temperature sensors and heat flux meters collecting data. blower door tests and heat-flux tests were conducted to inform creation of the EnergyPlus model for the rest of the simulations. Co-heating tests and decay tests were also carried out on the test cell. Differences between the heat flux and the co-heating tests were then analysed via building simulations. Analysis of the experimental decay methods was then compared with the HTC from the co-heating tests conducted on each configuration. Finally building models that generated different decay test profiles were analysed with the goal of showing how the decay coefficient related to the HTC. First, this increased the number of data points for the experimental methods, and second, was the basis of the RMSE analysis. The success of the experimental methods is based on the ability to identify both a clear difference in the decay analysis of each case study, and the relationship between the decay coefficient and the HTC. The RMSE tests already provide the link between the decay experiments and the co-heating experiment by simulating them on the same computer model. However, the success of

these variants is determined by how reliably they predict the HTC from the co-heating test conducted in the field.

Chapter 5 - Evaluation of Benchmarking Results and Analysis

5.1 Overview

This chapter details results and analysis of the heat flux, blower door and co-heating tests carried out both in-field and with the EnergyPlus simulation program, primarily from the second period of experimentation within the research period. These evaluation methods are generally understood and provide benchmarks against which the decay method can be compared. It also discusses the outcomes of the initial field experimentation that influenced refinements of the experimental set up, having identified some basic limitations and potential sources of error and uncertainty.

5.1.1 Experiment Timetable

There are two ways of determining the building's HTC – either summing the conductivity of the thermal shell area and the air leakage determined via heat flux testing and blower door testing, or performing the co-heating test. These two methods will be compared against the decay method to determine a level of aptitude and accuracy for the decay method.

To determine the sensitivity of the decay method, experiments on Test Cell 2 have been conducted with three different levels of insulation, laid out in Table 5.1. This allows for discussion of the sensitivities of the current methods, as well as providing the baseline for the decay method to be evaluated against. The results are grouped by experiment and any possible influences discussed before the experiments are compared to each other.

Table 5.1 Test cell insulation configurations

Configuration Number	Description	Co-heating test period, 2015	Decay test period, 2015
1, Test A	Estimated R2.0 glass wool insulation in all four walls. No insulation in subfloor or ceiling.	23 April to 7 May	8 May to 20 May
1, Test B	Estimated R2.0 glass wool insulation in all four walls. No insulation in subfloor or ceiling.	3 June to 17 June	18 June to 1 July
2	Estimated R2.0 glass wool insulation in south-east, north-east and north-west walls, and western half of the south-west wall. No insulation in subfloor or ceiling.	2 July to 16 July	17 July to 31 July
3	Estimated R2.0 glass wool insulation in south-east, north-east and north-west walls. No insulation in subfloor, ceiling or south-west wall.	1 August to 14 August	15 August to 28 August

The heat flux experiment was left to record data during the entire period. Heat flux experiments are, however, more reliable in steady state internal conditions, which the co-heating test provides. The heat flux data collected during the co-heating tests has been analysed and is treated as four separate tests for comparison. The heat flux data collected during decay testing has not been analysed as part of this research.

5.1.2 Weather Data

Figure 5.1 Location of weather station within the CSIRO site at Highett

Three sets of external measurements were collected during the co-heating tests: one by a thermocouple at the test cell attached to the Campbell datalogger, a second set by the CSIRO weather station at the northern end of the site, approximately 500 m away, as shown in Figure 5.1, and the third set from the Bureau of Meteorology (BoM) weather station at Moorabbin Airport, 5.5 km south-west of the CSIRO site. The thermocouple, attached to the Campbell datalogger, takes readings only of the air temperature every 60 seconds. The CSIRO weather station takes dry-bulb air temperature, relative humidity, wind, rain and

solar radiation readings, but only every 15 minutes. Data from the Bureau of Meteorology weather station at Moorabbin Airport was collected at 60 second intervals, and includes air temperature, humidity, wind, and rain observations. 60-second solar data for the Melbourne area collected by the Bureau of Meteorology is only available from the Melbourne Airport weather station, situated 35 km to the north-west.

5.1.2.1 Temperature

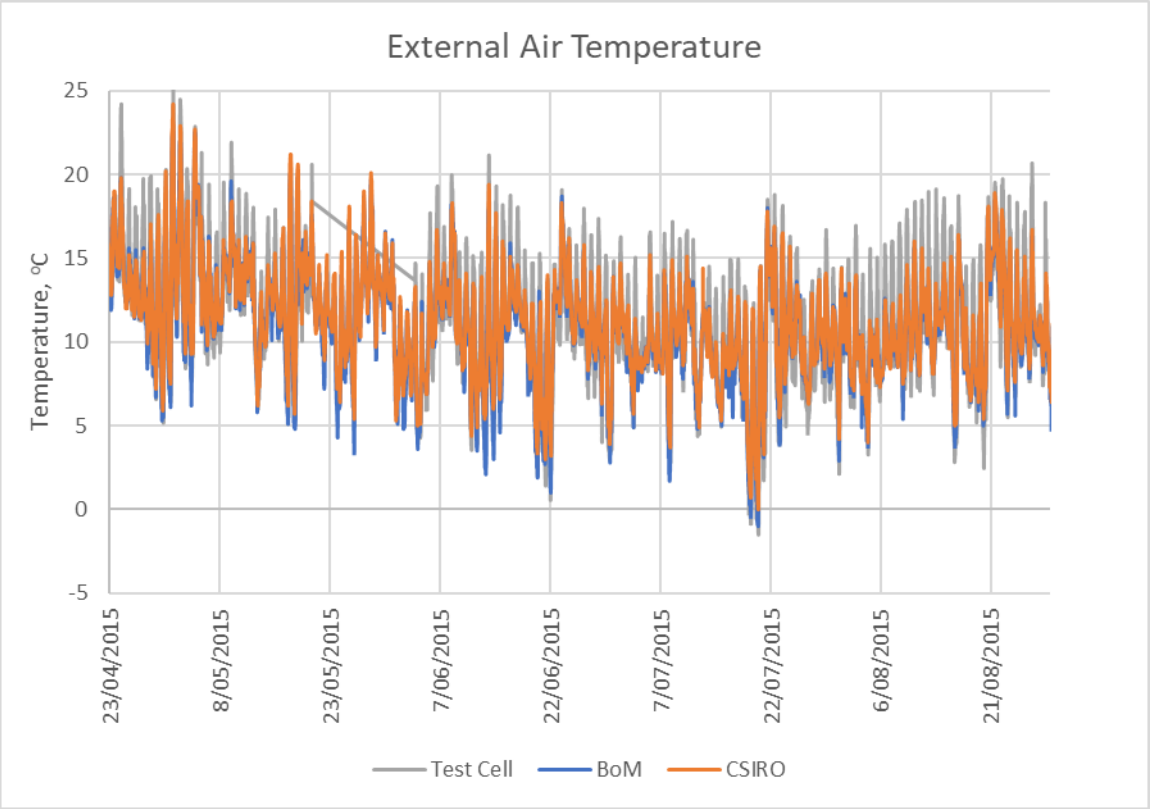

Figure 5.2 Comparison of external temperature data sources

The external air temperatures for the experimentation period are compared in Figure 5.2. The BoM data generally shows lower temperatures than those recorded by the CSIRO weather station, though overall trends are similar. This suggests the test cells may not be under as much stress as the BoM data indicates, and the analyses could be slightly overestimating the thermal shell's efficiency. The test cell data (Campbell Scientific with thermocouple) has much larger fluctuation in temperature which is likely to be partially due to lack of calibration during the equipment set up. As specific details of the CSIRO weather station are unavailable, the BoM dataset is considered more reliable. The similarities between CSIRO data and BoM data indicate that the BoM data is still applicable to the Highett site despite being collected from 5.5 km away.

5.1.2.2 Solar Radiation

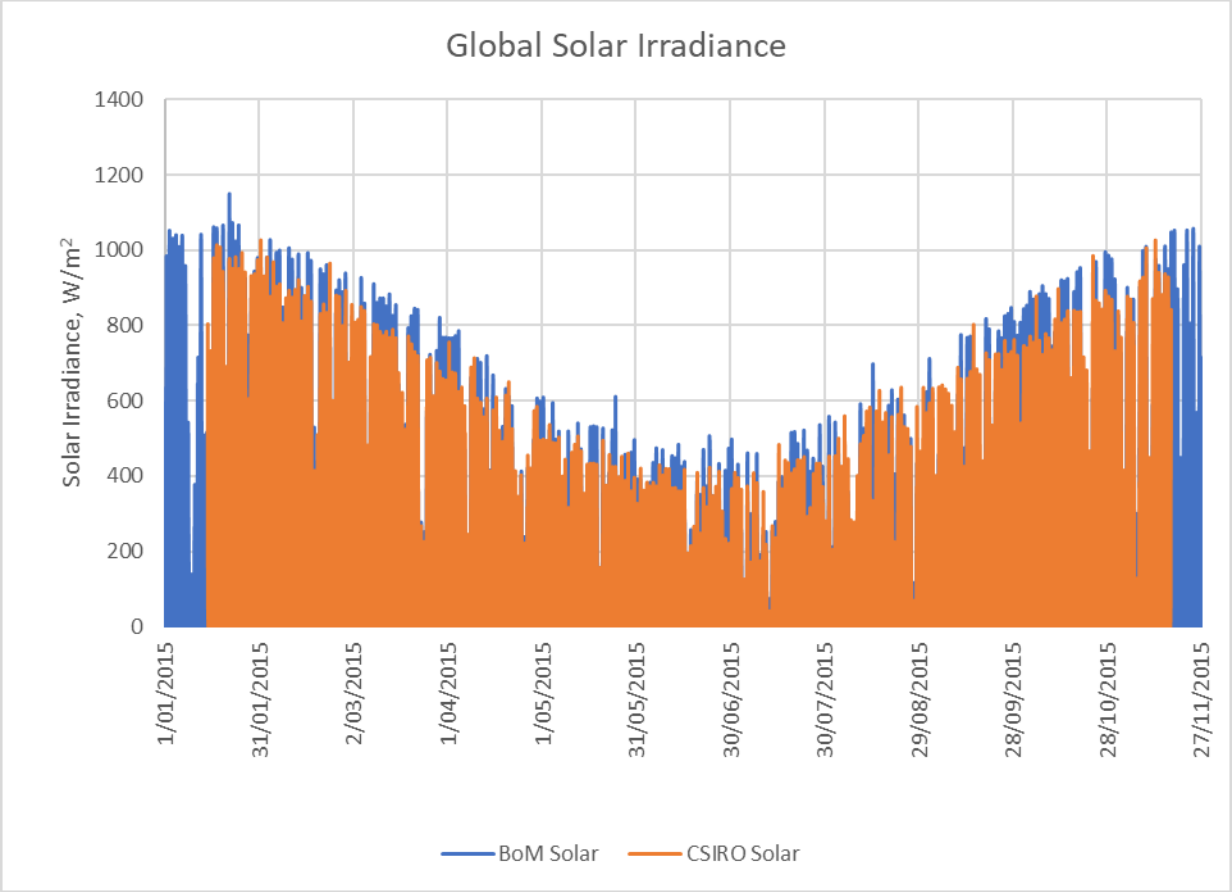

Figure 5.3 Solar radiation data comparison

The BoM solar radiation data shown in Figure 5.3 is generally higher than the CSIRO data; however, it follows a similar trend. The BoM data is provided with quality flags against each reading, and includes the azimuth for each reading. Using BoM data instead of CSIRO data will increase the values of the HTC from the co-heating test as the solar gains term in the heat balance equation will be larger. This increase will only be marginal as the average power input from the heater is much larger than the daily average solar radiation. Average power from the heater across each day approaches 1800-2000 W where the average solar radiation is approximately 50-100 W.

CSIRO's reputation indicates its data should be of good quality; however, there is no information available regarding the pyronanometer. Aside from the distance between the locations causing different readings due to cloud patterns, the CSIRO readings may simply be lower based on differences in equipment age and maintenance procedures in each organisation. As this information is available from the BoM regarding their data sets, and there is no significant difference in the pattern of solar radiation readings, the BoM data is

used for all analysis in this research. In addition to data quality, BoM data is recorded at 1-minute intervals which matches the rest of the data sets. This also makes it possible to build 1-minute weather files for EnergyPlus without interpolating between the 15-minute intervals of the CSIRO data.

5.2 Heat Flux and blower door Testing

The heat flux and blower door testing followed the methodology set out in chapter 4. The heat flux tests are required to provide information about the thermal properties of the building materials as they are in situ, rather than theoretical expectations. This is important as it is one of the ways buildings may be tested for in situ performance, and provides information that increases the building model's accuracy. The blower door test provides information about the building's level of air leakage, or sealing. This relates to estimating heat losses due to air flow that heat flux testing is unable to provide. The combination of the experiments provides the building's overall heat loss, which should be similar to the result of the co-heating test.

The heat flux test was carried out on the ceiling, floor, and north-eastern wall, with sensors placed to attempt to determine the R-value of the internal gyprock lining, the external fibre cement sheet cladding, and the overall wall unit. Heat flux testing on the walls was run continuously throughout the periods listed in Table 5.1, collecting readings during all co-heating and decay tests. The stable internal temperatures attained during the co-heating test create the best possible in situ conditions, and these results are presented as four separate tests. Due to limitations of the equipment, the ceiling and floor experiments were carried out at a different stage, in less ideal conditions, but the minimum conditions specified by ISO 9867-1:2014 were achieved during six consecutive weeks of data collection.

As the presence of insulation in Test Cell 2 showed a marked difference in the blower door test compared with Test Cell 1, additional blower door tests were conducted for configurations 2 and 3. The combination of heat flux and blower door tests provides a simple, theoretical marker for the HTC. The values determined by these tests are also used to assist in calibrating the EnergyPlus models.

The heat flux analysis is grouped in periods of 24 hours, beginning and ending at 6.00am. This is to mimic the natural variation due to solar radiation on the surface, and to ensure each period represents a full cycle of heat absorption during the day, and overnight release.

In accordance with ISO 9867-1:2014, Section 7.1, for elements with specific heat greater than 20 kJ/(m^2K), the test is ended when the following conditions are met:

1. Duration of the test exceeds 72 hours.
2. The R-Value obtained at the end of the test does not deviate by more than ±5% from the value obtained 24 hours before.
3. The R-Value obtained by analysing the data from the first time period on the n^{th} day does not deviate by more than ±5% from the values obtained from the data for the last time period of the same duration. The n^{th} day is defined by INT$(2 \times D_T/3)$ where D_T is the duration of the test in days and INT is the integer part.

Heat flux testing is conducted on the entire wall segment, as well as the internal lining and external cladding surfaces as individual elements. This section presents R-values for these elements and the ceiling and floor.

5.2.1 Walls

5.2.1.1 Datasheet Estimate

The wall being tested is the north-eastern wall. Wall construction is externally clad with fibre cement sheet, 'Cemintel Texture Base', and clad internally with Gyprock plasterboard. The cavity is insulated with glass wool wall batts, and there is an air gap between the external cladding and the glass wool. The wall measured is similar to the south-eastern and north-western walls. The only difference between north-eastern wall and the south-western wall is that the south-western wall is clad internally with pine. Based on the datasheets available for the wall materials, theoretical estimates of the R-value can be made using reported conductivity and material thickness.

Table 5.2 Theoretical estimate of wall R-value

Material	Manufacturer	Conductivity (W/mK)	Thickness (mm)	R-value (m^2K/W)
Cemintel Texture Base Sheet	CSR	0.2776	7.5	0.03
Air layer	N/A		40	0.15*
Glass wool	Knauff Insulation	0.45	90	2.0
Gyprock plasterboard	CSR	0.1429	10	0.07
Total				2.25

*Air layer R-value taken from EnergyPlus Ashrae Materials Database

Table 5.2 shows that the wall's total R-value is estimated as R2.25, based on the summation of materials. This provides a baseline against which to compare the experimental results, and provide some assurance that the results are feasible given the unknown uncertainty in the experiment. This estimate does not include resistance provided by the air film at the internal and external surfaces as this is not detected by the heat flux test. Adjustments for thermal bridging due to the frame are also not included. Thermal bridging factor and resistance of air films is included in the total estimated heat loss in Section 5.2.5 and shown in Appendix B.

5.2.1.2 Whole Wall

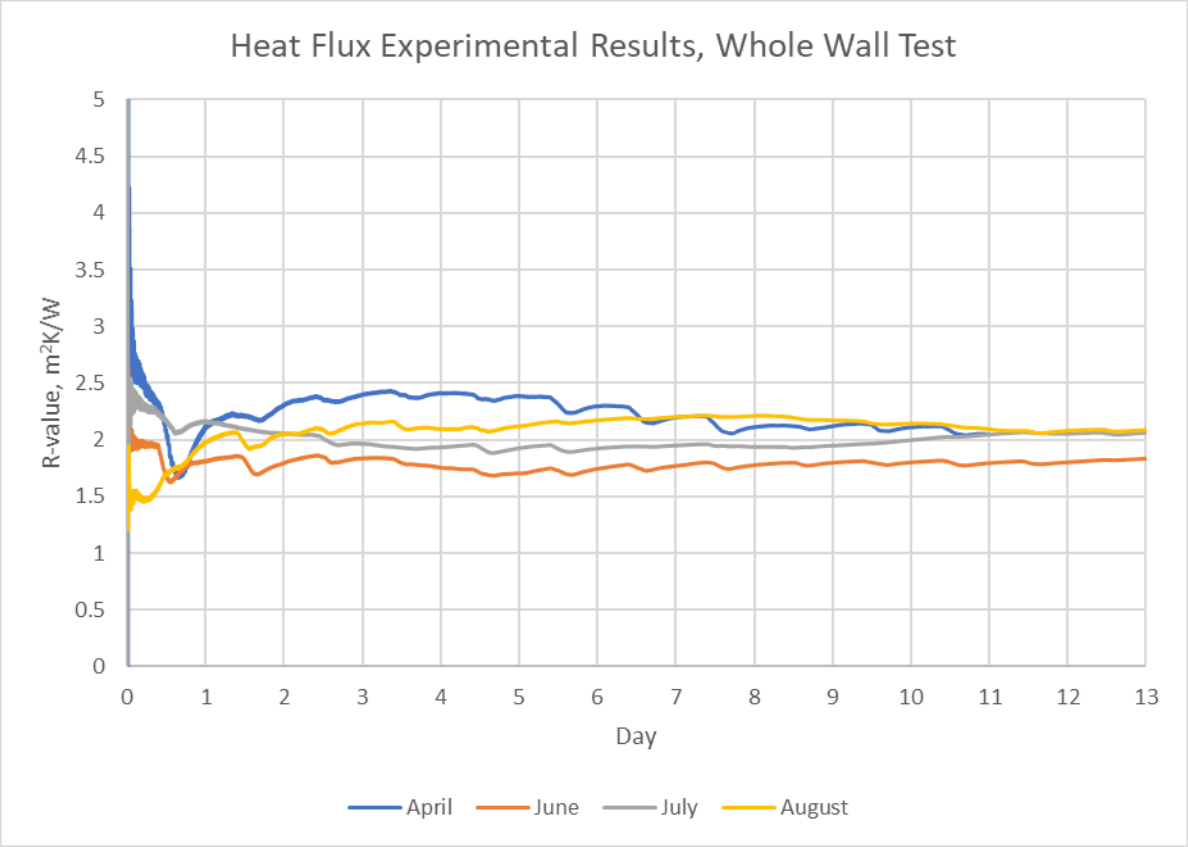

Figure 5.4 Heat flux Experimental Results, whole wall

Figure 5.4 displays the results of all heat flux tests conducted on the test cell's north-east wall. The graph displays the R-value calculated at each 30 second interval by the cumulative averaging function described in Section 4.2.2.2. As described above, the values at the end of each 24 hour period are used to determine whether the test can be ended and the R-value estimate meets the minimum standards set by the code. April and July show large variations initially. This is caused simply by a misalignment between the heat flux detected and the temperature difference across the wall. After a few minutes, the averaging takes effect and the readings settle to within an expected range. This is a good example of how heat flux testing can take time to complete to get reliable results.

Each of the tests could have been ended after 72 hours as technically they had satisfied the conditions set out in ISO 9867. Each test was within 5% of the previous 24 hours, and was within 5% of the estimate at the start of the n^{th} day, which was day 2 at that point. Had the test been ended at 72 hours, however, four different R-values would have been estimated, as shown in Table 5.3.

Table 5.3 R-values at 72 hours for North-East Wall

Test period	R-Value, m^2K/W
April	2.47
June	1.86
July	1.99
August	2.14

The differences in the estimates at this stage indicate the full data set should be considered, and the test should not be ended as soon as any individual test is deemed valid. Figure 5.4 also shows that in the first 10 days there are still sharp variations during the day, but in the June, July and August tests this is significantly dampened after 11 days.

At the end of the 11th day, the April, July and August tests had converged on estimates between R2.03 and R2.10, a variation of 3.3%. The June test shows a much lower R-value of R1.85. These values at the end of the collection period are the figures that should be included. Table 5.4 shows the R-value at the end of each 24 hour period.

Table 5.4 R-Values during heat flux testing for north-east wall

Day number (n)	R-Value, m^2K/W			
	April	June	July	August
1	2.39	1.92	2.01	1.97
2	2.42	1.86	1.99	2.05
3	2.47	1.88	1.93	2.14
4	2.47	1.80	1.91	2.09
5	2.43	1.74	1.9	2.12
6	2.33	1.78	1.9	2.17
7	2.24	1.8	1.93	2.2
8	2.14	1.8	1.92	2.21
9	2.15	1.82	1.93	2.17
10	2.14	1.82	1.98	2.14
11	2.08	1.81	2.03	2.10
12	n/a	1.82	2.04	2.08
13	n/a	1.85	2.05	2.09

As in Figure 5.4, Table 5.4 shows initial disagreement between the tests before three of the four converge between R-values of 2.05 and 2.09 m^2K/W. Between the highest and lowest values, August and June, the R-value varies by 11.4%. However, observing the overall list shows that the values collected during the first week of the April test are significantly higher than those collected during June, July and August – up to 0.38 m^2K/W higher than the nearest estimate on day 4. No changes were made to the wall or equipment between these tests. This difference again is likely to be caused largely by differences in the initial conditions of each of the tests, before the averaging process minimises the overall influence from any single record, or set of records.

5.2.1.3 Weather

Since the equipment set up is essentially the same, acknowledging potential for drift in the sensors over time, possible reasons for lower estimates in June may be variations in temperature, solar radiation, or wind speed and direction, between the tests. Table 5.5 shows the average temperature difference across the wall during each test. As the internal temperature is essentially the same, this variation is mostly caused by seasonal variation in the temperature as the seasons change.

Table 5.5 Average temperature differences during heat flux testing

Test Period	Temperature Difference, K
April	5.47
June	8.63
July	11.06
August	10.02

While the temperature difference in April is the smallest, there is no obvious relationship here between the temperature difference and the R-value. This alone does not provide any indication as to why the June estimate is lower than the rest.

As external temperature drops, it is expected that solar radiation also reduces as the season changes to winter. While the temperature sensor was shielded from the sun, the northern

facing wall may have experienced some changes in heat flux that are not related purely to surface temperature recorded. Figure.5.5 shows the average solar radiation for each test.

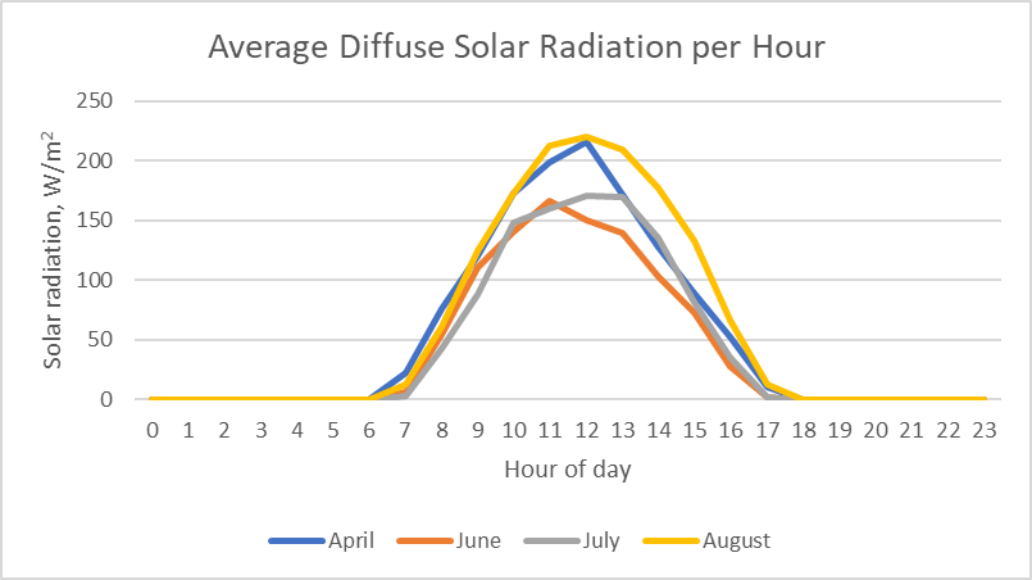

Figure.5.5 Average daily solar radiation per hour

If solar radiation was the key, it would be expected that June readings would be lower than the rest. While this is true, radiation in July is similar and yet the R-value estimate only differs from April (with the highest recorded solar radiation) by 0.03 m^2K/W, and August by 0.04 m^2K/W.

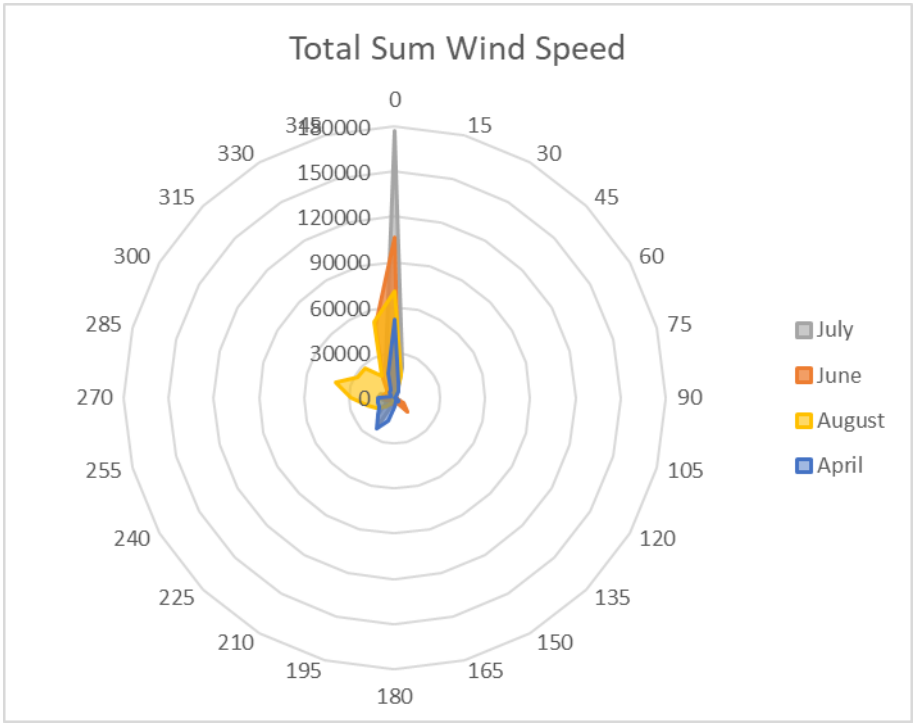

Figure 5.6 Average wind run during heat flux testing

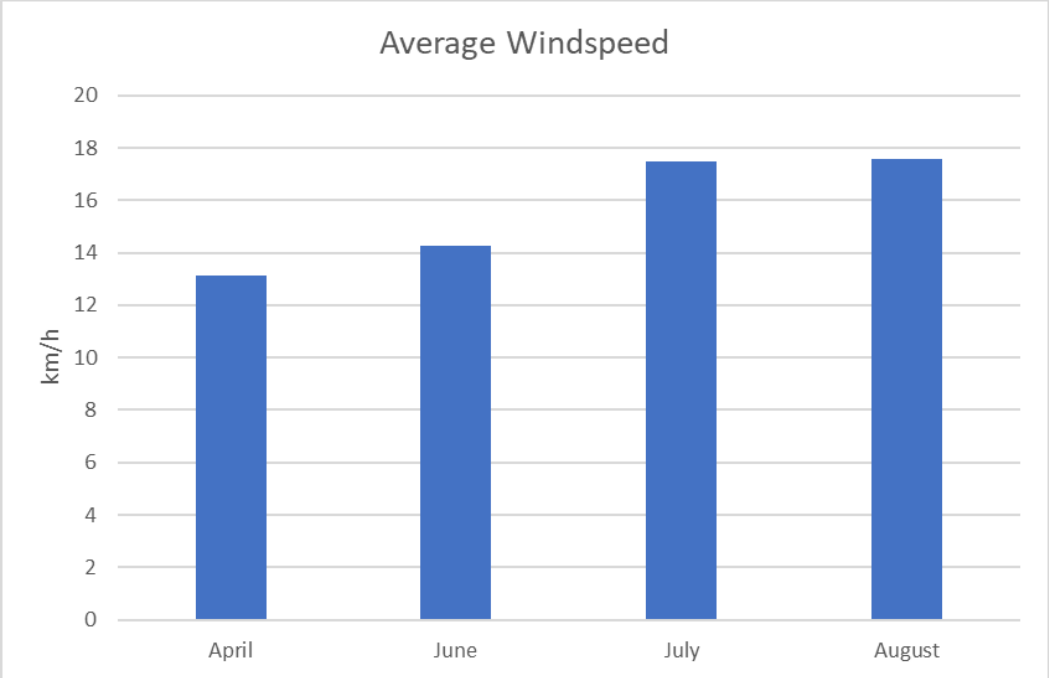

Figure 5.7 Average wind speed during heat flux testing

Figure 5.6 and Figure 5.7 shows how windy conditions were during each test overall, the wind direction, and average wind speed. Figure 5.6 is generated as a sum of wind speed during the test period, grouped by direction to the nearest 15^0 intervals, zero being north. April appears on average to be the least windy month, and July the most windy. The wind speed in July was on average higher than all other months, and almost exclusively from the north. Overall wind speed and direction in June cannot be considered special by comparison – it is neither significantly higher or lower, nor is it from a completely different direction. Observing individual readings, however, shows that while the average for June is lower than the overall average, there was a significantly higher number of strong wind gusts during the June test than any of the others. Figure 5.8 displays the number of records taken by the Bureau of Meteorology that are above 40 km/h for each test.

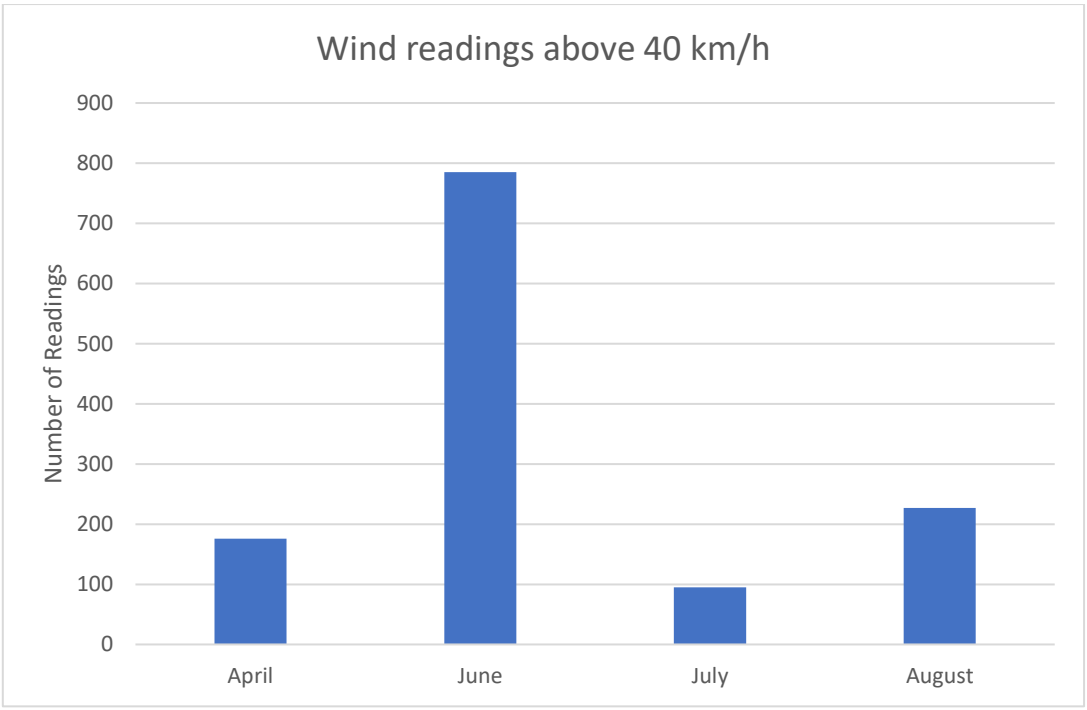

Figure 5.8 Number of wind readings above 40 km/h during heat flux testing

The June test had over three times as many readings of wind speed above 40 km/h than August, and over four times as many as April. Figure 5.9 shows the direction of these strong wind gusts.

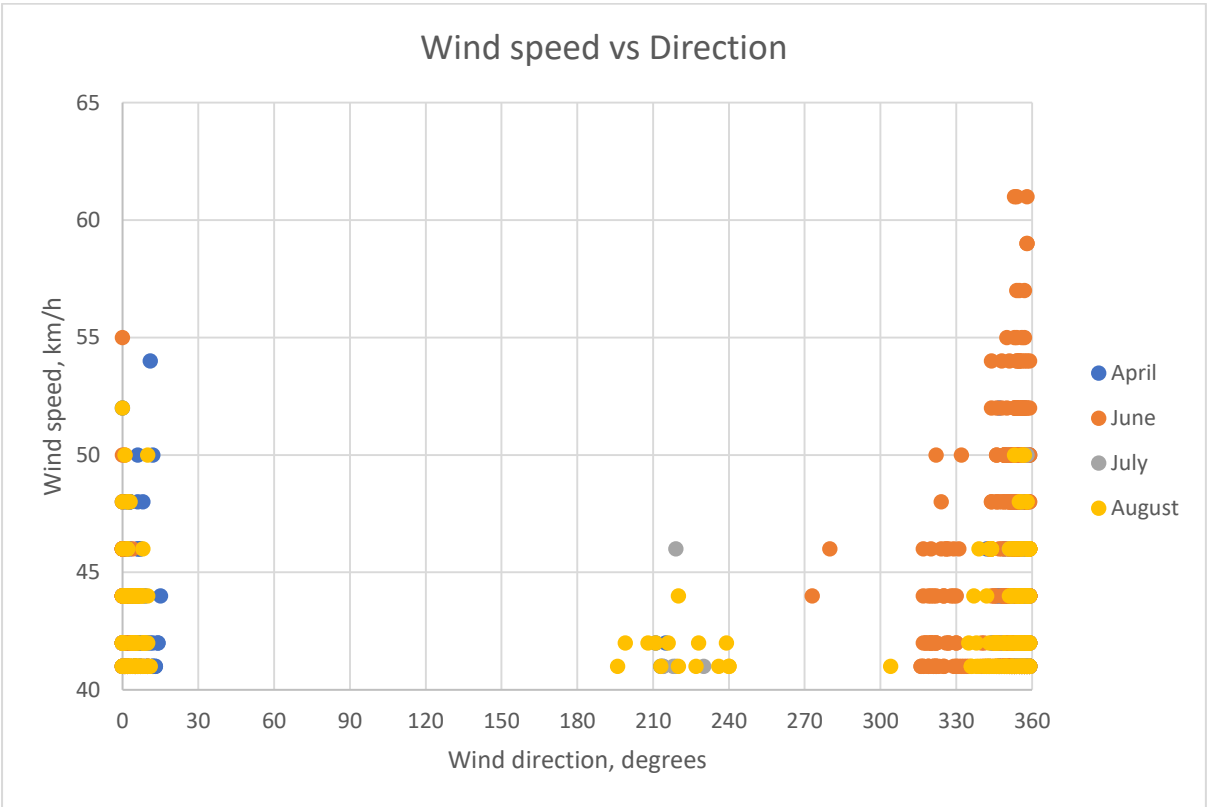

Figure 5.9 Windspeed vs direction for readings above 40 km/h during heat flux testing

The strong wind gusts tended to come from the north, between 45^0 and 315^0, directly hitting the wall being tested. The larger number of strong winds impacting the wall being tested by the heat flux sensors is likely to be the cause of the discrepancy between June and the other three tests. For this reason, the R-value estimate for June will not be included in estimating the R-value of the wall. The R-value estimated from the other three tests was averaged to provide a final estimate of 2.07 m^2K/W before resistance due to surface air films are added.

5.2.1.4 Interior Lining

Placement of thermocouples on each side of the internal lining and external cladding allows for the calculation of the R-value for the internal Gyprock lining. The analysis is conducted in the same way as the whole wall, using 24 hour periods and the thermocouple located on the 'external' surface of the cladding; that is, the surface facing into the wall cavity. As the intention of this analysis is to determine the R-value of the single material element, the R-value due to the surface air films has not been included.

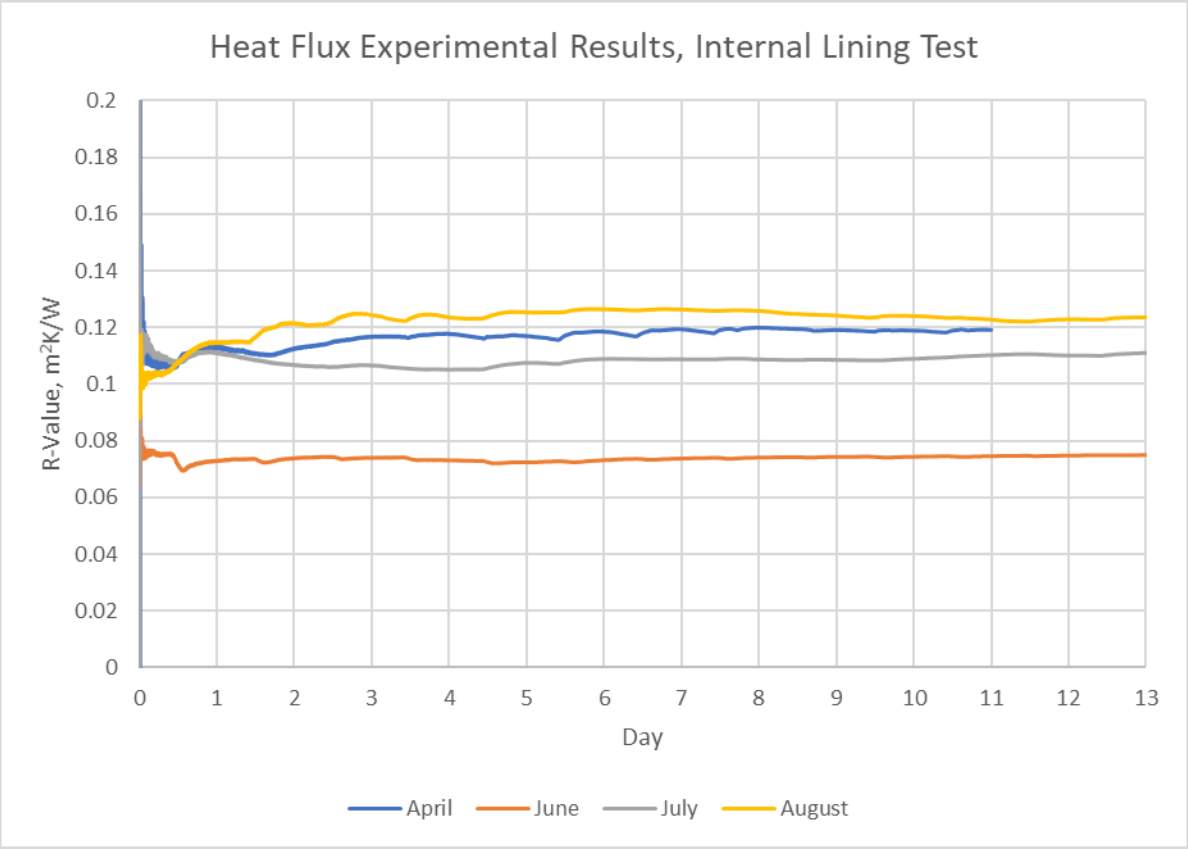

Figure 5.10 Heat flux experimental results, internal lining

Figure 5.10 shows the estimated R-value over time for the internal Gyprock lining. Similar to the 'whole wall' calculations, April and July had large variations in the first hour of the test, but this has settled by the end of the first 24 hours. Individually, each test satisfied the minimum standards after 72 hours, and the values do not vary significantly from this point in any of the four tests. Again, the R-value estimated in June is clearly lower than the other three. Table 5.6 shows the R-value estimated at the end of each 24 hour period for the internal lining.

Table 5.6 R-Values during heat flux testing for internal lining

Day number (n)	R-Value, m^2K/W			
	April	June	July	August
1	0.12	0.07	0.11	0.11
2	0.11	0.07	0.10	0.12
3	0.12	0.07	0.10	0.12
4	0.12	0.07	0.10	0.12
5	0.12	0.07	0.11	0.13
6	0.12	0.07	0.11	0.13
7	0.12	0.07	0.11	0.13
8	0.12	0.07	0.11	0.13
9	0.12	0.07	0.11	0.12
10	0.12	0.07	0.11	0.12
11	0.12	0.07	0.11	0.12
12	n/a	0.07	0.11	0.12
13	n/a	0.08	0.11	0.12

There is no difference in the value estimated after 72 hours and the end of the test in April and August, and a 0.01 m^2K/W increase in June and July. It is not surprising that the June result is lower than the other three as the internal lining calculation uses the same data from the internal surface as the whole wall calculation. Even though the wind does not directly impact the interior surface, it is probable it is still influencing the overall heat flux

through the wall. Taking the average of the other three tests gives an R-value of 0.12 m^2K/W, rounded to two decimal places.

5.2.1.5 Exterior Cladding

At no point during any of the tests was there a valid result for the external cladding. The results fluctuate and did not converge at the conclusion of each test. The surface temperatures of the external cladding are largely driven by external conditions, where the internal lining temperatures dictated by the stable internal temperature. The surface temperatures of the external cladding are therefore naturally prone to large fluctuations across each 24 hour period. The difference in temperature between internal and external faces of the exterior cladding is small and does not align with the direction of heat transfer detected by the heat flux meter. Calibration shortcomings discussed in Section 3.3.3 are the likely cause. In the absence of field data, the thermal properties from the manufacturer will be used to estimate the R-value of the external cladding.

5.2.1.6 Wall Summary

Based on heat flux testing results on the whole wall and the cladding surfaces, the R-value of the glass wool insulation can be calculated. As the external cladding test did not give a valid result, the manufacturer specified R-value will be used. The R-values for each layer are shown below in Table 5.7.

Table 5.7 Specified material properties vs in situ properties

Material	Specification R-value (m^2K/W)	Estimated in situ R-value (m^2K/W)
Cemintel Texture Base Sheet	0.03	0.03
Air layer	0.15	0
Glass wool	2.0	1.91
Gyprock plasterboard	0.07	0.12
Total	2.25	2.06

After accounting for internal lining and external cladding surfaces, there is only 1.91 m^2K/W remaining for the glass wool insulation and the air layer. This is 11% lower than predicted for these two layers, and 4.5% lower than predicted just for the glass wool layer. It is not surprising that a single element does not perform exactly to specification once installed, particularly a second-hand item. It is likely that after insulation is installed the remaining air gap is not large enough to influence the R-value of the wall construction, as well as some degradation of insulation over time. These batts were not brand new and having been installed and removed from previous constructions some loss of performance is not unfathomable. For these reasons, the air layer is assumed to have an R-value of 0, and the glass wool insulation an R-value of 1.91 m^2K/W. These figures will be used for the individual layers when building the EnergyPlus model.

5.2.2 Floor

Due to limitations on the data logger's memory, heat flux experimentation of the floor was carried out in consecutive 12 to 15 day periods, depending on site access at the time. This testing was done during November-December 2014, before the co-heating and decay tests listed in Table 5.1. There are gaps in the dataset where collection was interrupted so data could be collected and memory reset on the 12th and 25th days. These periods are considered to be one continuous test as the programmed inputs to the building were unchanged, unlike during the co-heating and decay test periods. The test follows the same pattern as that of the wall, using 24 hour periods from 6.00am to allow a full solar cycle to be included in a single period.

As with the internal lining, the surface air films have not been included in the calculation at this step. However, they will be accounted for when calculating the expected heat loss of the test cell in Section 5.2.5. Figure 5.11 shows the R-value estimate as the test progressed.

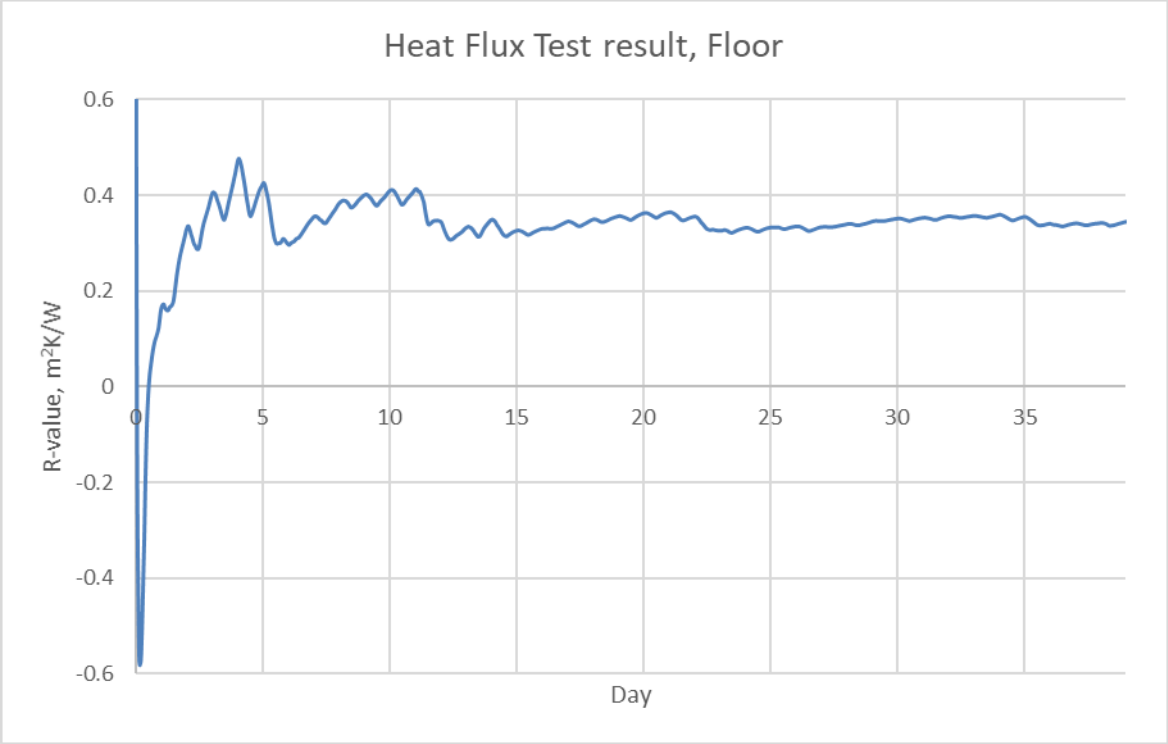

Figure 5.11 R-value calculation for floor

As shown in Figure 5.11, the R-value is highly variable, and it was not until the end of the 16th day of testing that the ISO conditions are satisfied, yielding an R-value of 0.33 m^2K/W. Given that the magnitude of the changes over time is small compared to the overall wall, it is possible that some of this variation could be attributed to uncertainty in the thermocouple readings. There is still some variation after the test first satisfied the conditions, so the entire 39 day range is used to estimate the R-value at 0.34 m^2K/W. Table 5.8 shows the R-values at the end of each day of testing.

Table 5.8 R-values for heat flux testing of the floor

Day	R-value, m^2K/W
1	0.16
2	0.33
3	0.40
4	0.47
5	0.42
6	0.30
7	0.35
8	0.38
9	0.40
10	0.41
11	0.41
12	0.35
13	0.33
14	0.35
15	0.33
16	0.33
17	0.35
18	0.35
19	0.36
20	0.36
21	0.36
22	0.36
23	0.33
24	0.33
25	0.33
26	0.34
27	0.33
28	0.34
29	0.35
30	0.35
31	0.35
32	0.36
33	0.36
34	0.36
35	0.36
36	0.34
37	0.34
38	0.34
39	0.34

5.2.3 Ceiling

The ceiling material was tested at the same time as the floor. Note that the experiment only tested the R-value of the ceiling material itself. It did not estimate the additional R-value that may be added due to the enclosed airspace above. The R-value for this airspace will be accounted for, however, when estimating the test cell's overall heat loss.

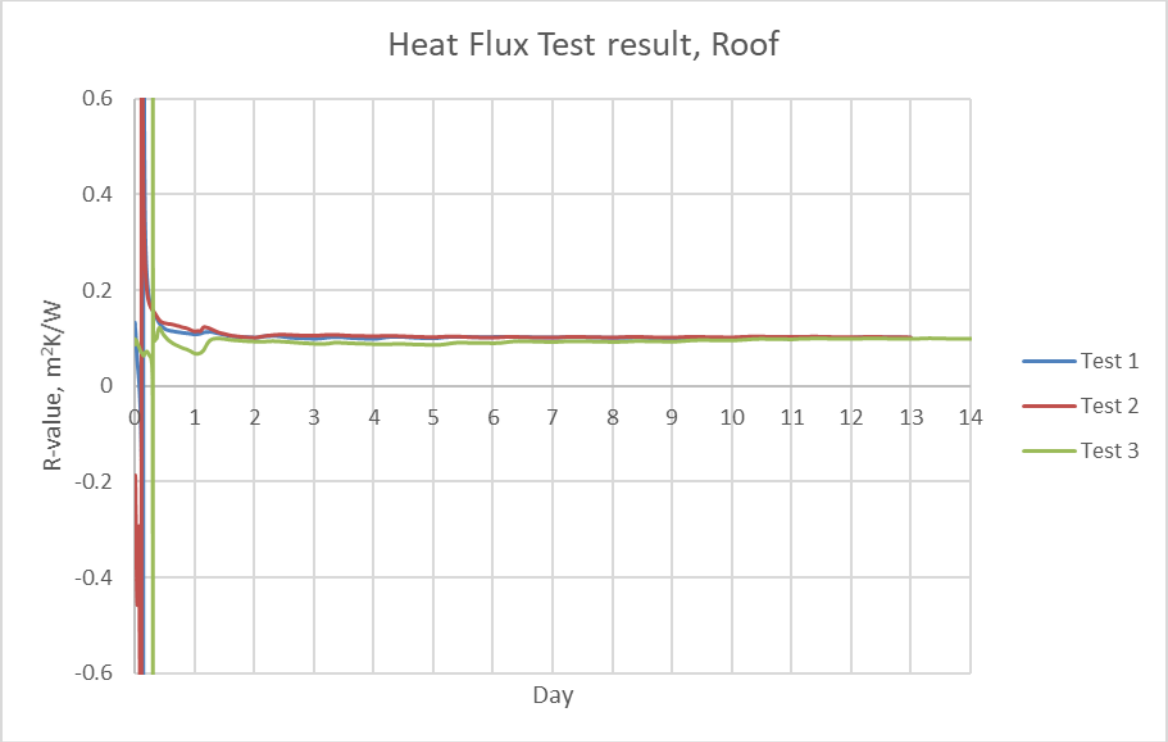

Figure 5.12 R-value calculation for ceiling

The ceiling R-value is much more stable, and satisfied the minimum conditions set by the ISO standard after the 5th day, with an estimated R-value of 0.10 m^2K/W. As the experiment was completed quickly, days 13-25 and 26-39 were also treated as stand-alone tests for comparison.

The second period satisfied minimum conditions after five days with an R-value of 0.10 m^2K/W, and the third period after six days with an R-value of 0.09 m^2K/W. The average of these three sections gives an R-value of 0.10 m^2K/W. Table 5.9 shows the R-values for the first 12 days of each period.

Table 5.9 R-values heat flux tests of the ceiling

Day	Test 1, m^2K/W	Test 2, m^2K/W	Test 3, m^2K/W
1	0.11	0.11	0.07
2	0.10	0.10	0.09
3	0.10	0.11	0.09
4	0.10	0.10	0.09
5	0.10	0.10	0.09
6	0.10	0.10	0.09
7	0.10	0.10	0.09
8	0.10	0.10	0.09
9	0.10	0.10	0.09
10	0.10	0.10	0.10
11	0.10	0.10	0.10
12	0.10	0.10	0.10

5.2.4 Blower door test

As discussed previously, the blower door test provides information about the building's air leakage. This is related to the heat lost via warm air leaving the building and cold air being introduced in its place. This is added to the heat flux calculations to estimate overall building heat loss. blower door testing was carried out under the supervision of Dr Ian Ridley (RMIT) and Michael Ambrose (CSIRO).

The infiltration rate is tested by closing all doors, windows and other openings and using a fan to draw air into, or suck air from the building, thus creating a pressure difference between the internal space and the atmosphere. The air movement required to maintain the pressure difference is monitored. The recorded result is the volume of air required to be moved per hour to maintain a pressure difference of 50 Pa. The test is conducted twice, once as a pressurisation test and once as a depressurisation test. This is to account for elements such as door seals or flaps that have high leakage if blown open from the inside during pressurisation, but remain well sealed if they are being sucked shut while the building is depressurised. The average of the two tests is taken as the building's air flow rate. For this study the test procedure was automated via software provided with the blower door kit, FanTestic Lite.

The initial value of air flow rate from the test is recorded in m^3/hr at 50 Pa. The form that is generally used, however, undergoes a 'rule of thumb' calculation and is divided by 20 to estimate the infiltration at atmospheric pressure. In this study the figure has also been normalised by the volume of the test cell to provide values as 'Air Changes per Hour', or ACH. This represents how often the building completely changes the air every hour.

5.2.4.1 Configuration 1

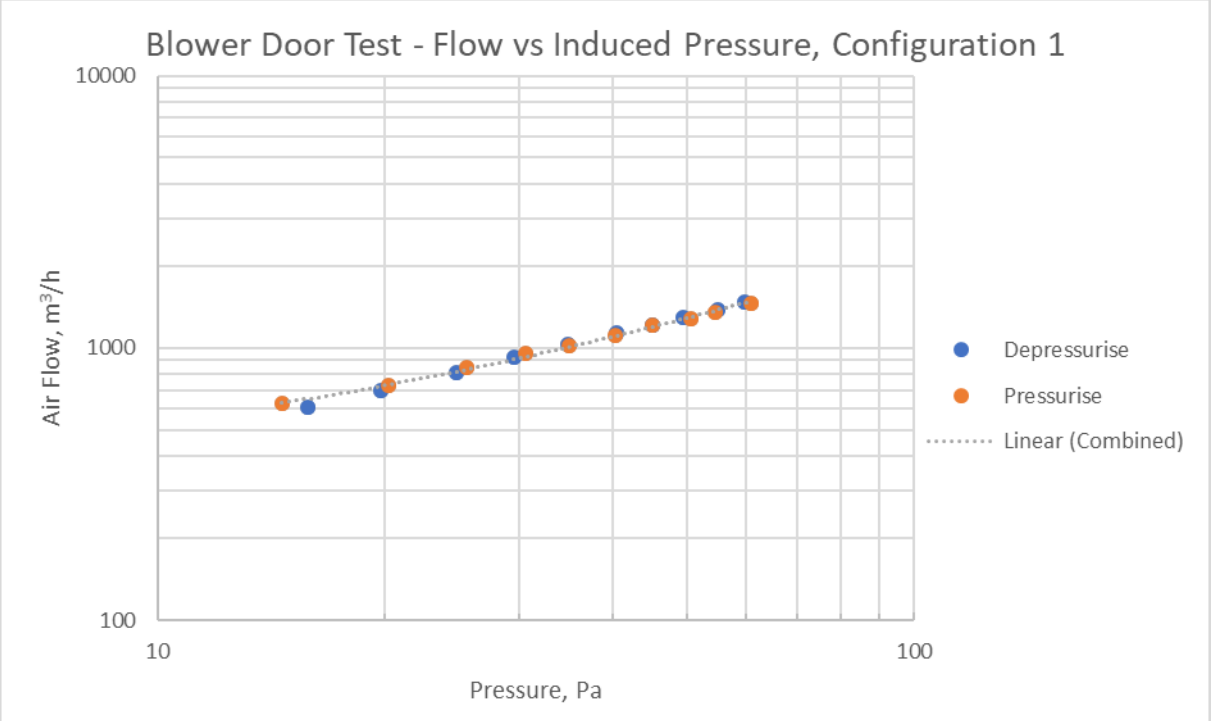

Figure 5.13 Blower door test, Configuration 1, Test Cell 2

Figure 5.13 shows that:

- Depressurisation test resulted in an air change rate of 25.05 air changes per hour at 50 Pa, ±1.2%.
- Pressurisation test resulted in an air change rate of 24.45 air changes per hour at 50 Pa, ±1.5%.
- The combined result, as presented in the software generated report, is 24.75 air changes per hour at 50 Pa, ±1.7%.
- Using the simple rule of ACH at 50 Pa divided by 20 equals the infiltration rate, the infiltration rate is equal to 1.2375 ACH.

5.2.4.2 Configuration 2

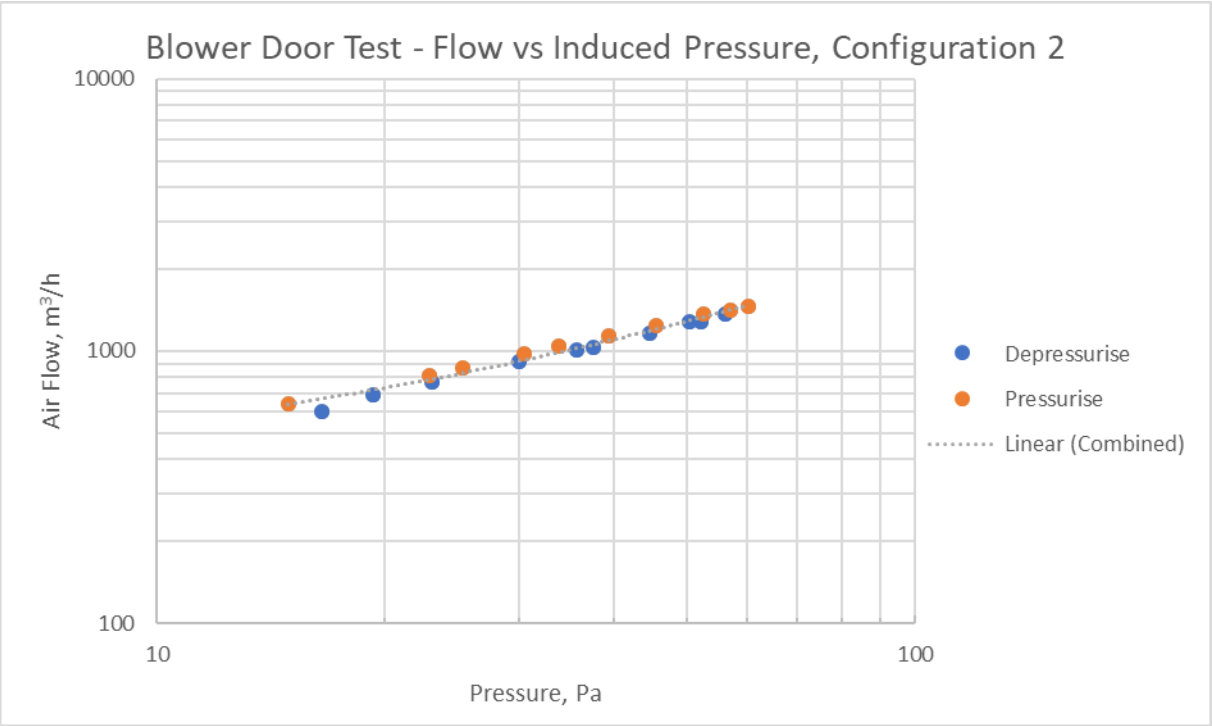

Figure 5.14 Blower door test, Configuration 2, Test Cell 2

Figure 5.14 shows that:

- The pressurisation test resulted in an air change rate of 27.07 air changes per hour at 50Pa, ±0.5%.
- The depressurisation test resulted in an air change rate of 26.74 air changes per hour at 50Pa, ±1.3%.
- The combined result, as presented in the FanTestic generated report, is 26.9 air changes per hour at 50Pa, ±0.9%.
- Using the simple rule of ACH at 50Pa divided by 20 equals the infiltration rate, the infiltration rate is equal to 1.345 ACH.

5.2.4.3 Configuration 3

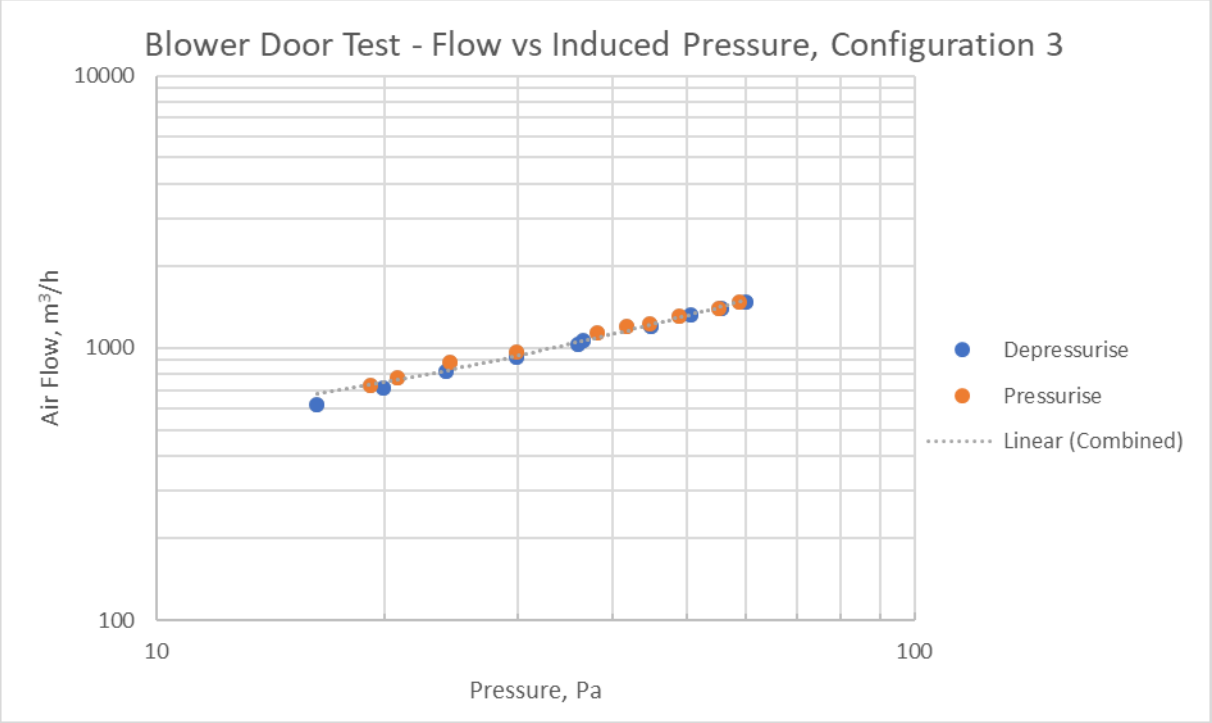

Figure 5.15 Blower door test, Configuration 3, Test Cell 2

Figure 5.15 shows that:

- The pressurisation test resulted in an air change rate of 27.51 air changes per hour at 50 Pa, ±1.3%.
- The depressurisation test resulted in an air change rate of 27.11 air changes per hour at 50 Pa, ±1.1%.
- The combined result, as presented in the FanTestic generated report, is 27.15 air changes per hour at 50 Pa, ±1.2%.
- Using the simple rule of ACH at 50 Pa divided by 20 equals the infiltration rate, the infiltration rate is equal to 1.3575 ACH.

5.2.4.4 Leakage Heat Losses

The heat loss due to air leakage is calculated using Equation 6, repeated below.

Equation 6 Infiltration heat losses

$$Q_{infiltration} = \frac{1}{3} n V_{ol}$$

The volume of the test cell zone tested is 48.26 m^3. Table 5.10 shows the heat loss for each configuration. It is noted again that the 'divide by 20' rule is a guideline, and may not be overly reliable in all situations or in all buildings.

Table 5.10 Estimations of leakage heat loss

Configuration	ACH @ 50 Pa, m^3/h	Infiltration rate, Air Changes per Hour	Heat loss, W/K
1	24.75	1.2375	19.91
2	26.9	1.345	21.64
3	27.15	1.3575	21.84

Table 5.10 shows the difference infiltration heat loss between the three configurations is minimal. For this test cell, the infiltration rate is inversely correlated with the presence of insulation. Configuration 3 has the least insulation, and the highest infiltration rate.

5.2.5 Total Estimated Heat Loss

By combining the heat flux and blower door tests, estimates of the overall building heat losses can be made, providing additional comparison points for analysing the decay method's effectiveness. The characteristics of individual elements are also valuable as they inform improvements in the accuracy of the EnergyPlus building model.

The test cell's heat loss is calculated as the sum of each individual component U-value (heat transmission coefficient) multiplied by its area, the infiltration heat loss coefficient derived from the blower door test and, ideally, an estimate of the heat loss due to thermal bridges.

All the walls are assumed to have the R-value determined by the heat flux test carried out on the north-eastern wall, except for the south-western wall which has a different internal lining material. To determine the R-value of the south-western wall, the R-value of the

internal lining is taken from the overall, and the R-value of the ceiling added, as it is the same pine board.

To better estimate heat loss through the floor and ceiling, the sub-floor and attic airspaces must be taken into account as they provide protection to the floor and ceiling surfaces against the external conditions. Using the National Construction Code, Volume 1, Section J 'Elemental Method'(ABCB 2016), an additional allowance to the R value of the air films can be made that reduces heat loss across the ceiling and floor surfaces. Instead of using 0.04m^2K/W for the underside of the floor, the enclosed air above ground can be increased to 0.57m^2K/W. The film on the upper side of the ceiling below concrete tiles can be increased to 0.24m^2K/W. These have been included in the tables below for estimating total test cell heat loss.

Factors for thermal bridging from SAP (2012) have been included for the walls as the timber frame provides a thermal bridge between the internal and external surfaces, bypassing the glass wool and air layer (in configurations 2 and 3). The floor and ceiling constructions are only a single layer of material. Consequently, it does not appear appropriate to include thermal bridging for these elements as there is no internal air gap or insulation layer that would be bypassed by the structural timber elements.

Standard factors have been included for the window and the door. These were collected from AccuRate materials and windows library. The door was a lightweight hollow-core construction rather than a standard solid core external door. The 'Timber (hollow)' construction provided with the software has been used. The window is assumed to be similar to default window ALM-001-01, a single glazed, aluminium-framed window, as was present in the test cell. The window has a measured system U-value of 6.7 W/m^2K.

The U-value is simply the reciprocal of the R-value. In practice, the R-value of the element includes the resistance of the film of air at each surface. As surface temperatures have been used to calculate the R-values, the resistance due to air has not been accounted for. There are concerns in the literature over the accuracy of heat flux using ambient air temperatures, due to effects such as stratification, and so the standard values for the internal and external air films are used. These assume the air is static, differs for horizontal and vertical heat flow, and is not being affected by convection currents or air temperature. The R-values for each

building component in each configuration, and how this translates into the test cell's heat loss, can be found in Appendix B. Table 5.11 summarises the total fabric and ventilation heat losses.

Table 5.11 Total heat loss estimates - heat flux and blower door testing

Configuration	Fabric losses (W/K)	Blower door (W/K)	Total heat loss (W/K)
1	97.00	19.91	116.91
2	104.30	21.64	125.94
3	111.62	21.84	133.46

As discussed previously, the only change between the three configurations is the removal of insulation from the south-western wall. This causes some additional leakage losses as the insulation plugs some of the gaps between the lining and the stud frame. The differences between the overall heat loss of each configuration are relatively small – less than 10 W/k, or around 6-7% for each configuration. Total uncertainty in heat loss cannot be estimated as uncertainty in surface temperature readings is not known.

These three estimates are the first benchmark of the heat loss estimate. The data gathered for R-value of individual materials and the ventilation losses will be used in creating the EnergyPlus models of the test cell. These heat flux and blower door estimates will be compared with the HTC from the co-heating test conducted in field, as well as the simulated co-heating test from EnergyPlus.

The limitation of this calculation is that it accounts for each element individually, and only considers heat loss through the building fabric perpendicular to the plane of the building surface. The heat flux and blower door tests effectively assess heat loss due to the specific element measured, but this may not reflect the overall complexity of building thermal behaviour.

5.3 Co-Heating Test

While the combination of heat flux testing and blower door testing gives a theoretical value for the building's total HTC, the co-heating test is designed to measure it directly. Four co-heating tests were completed on Test Cell 2; two for Configuration 1 and one each for Configurations 2 and 3.

As the co-heating test is the most effective experimental means for accurately determining whole-house HTC, the results of these tests are the main comparison point for evaluating the effectiveness of the decay method. It is important to gauge the co-heating test's sensitivity, and understand how local climate is impacting results. These influences are likely to have similar impacts on decay method results.

5.3.1 Calculation of Heat Transfer Coefficient

Each test consists of averaging results over consecutive 24 hour periods, starting and finishing at 6.00am. This places the averaging period on a similar cycle to the sun, allowing for any solar energy stored in the building material to be properly accounted for, and minimising any noise due to energy being carried into the following day.

Each of the tests uses the average from 27 HOBO temperature sensors spaced evenly throughout the building's interior as the internal temperature point, and is compared against the external temperature collected by a thermocouple placed at the test cell's south-eastern wall.

The HTC is the parametrisation of the temperature difference to the heating power injected into the building, averaged over a series of consecutive 24 hour periods. The thermostat controlling the 2 kW blower heater was set to 27 ^{0}C; differences in location and calibration between the thermostat and HOBO temperature sensors meant the average temperature in the building was between approximately 23.5 ^{0}C and 25 ^{0}C. The building always remained warmer than the external air.

Adjustments should be made to the power input into the building to account for solar energy gained through the building fabric and for variations in the HTC due to wind. For this experiment a Siviour analysis and multiple regression has been used in different combinations to adjust for these impacts. First, three Siviour analyses have been conducted on each co-heating test, the first not excluding any data on the basis of wind conditions, the

second removing all days with an average windspeed above 27 km/h, and the third removing all days with windspeed above 19.2 km/h. These match the two limits from the literature of 7.5 m/s set by Butler & Dengle (2013), and 12 MPH from Judkoff et al. (2000). The solar aperture from these is used to calculate the 'solar adjusted power', and then a multiple regression test is conducted to account for the specific wind.

In addition to the Siviour plus regression analysis, a pure multiple regression analysis is conducted to calculate the solar and wind coefficients, which are then used to adjust the power measurements. These analyses will present the heat loss where the windspeed is 0m/s.

5.3.1.1 Heater Capacity

During the co-heating test on Configuration 3, the heater behaviour changed on the third and fourth days. Weather conditions created a situation where the internal thermostat was below the set temperature for an extended period of time, and the heater therefore ran at full capacity regardless of the temperature difference. As the experiment tests the response of the power input against the temperature difference, these two days of data collection may underestimate the HTC and have therefore been excluded.

5.3.1.2 Overheating

The second half of Test A for Configuration 1 experienced three days of overheating. This is shown by the temperature not being dictated by the thermostat turning the heater on and off. When the heater is the driving force of the internal temperature, the measurements cycle up and down by approximately 1^0. This is an in-built function of the HeaterMate thermostat, requiring the air temperature to drop below the set temperature by 1^0 after the set temperature has been reached before it engages the heater again. The heater driven behaviour can be seen throughout the test. On the three days of overheating, the temperature does not oscillate in this fashion. This is shown in the red circles on Figure 5.16.

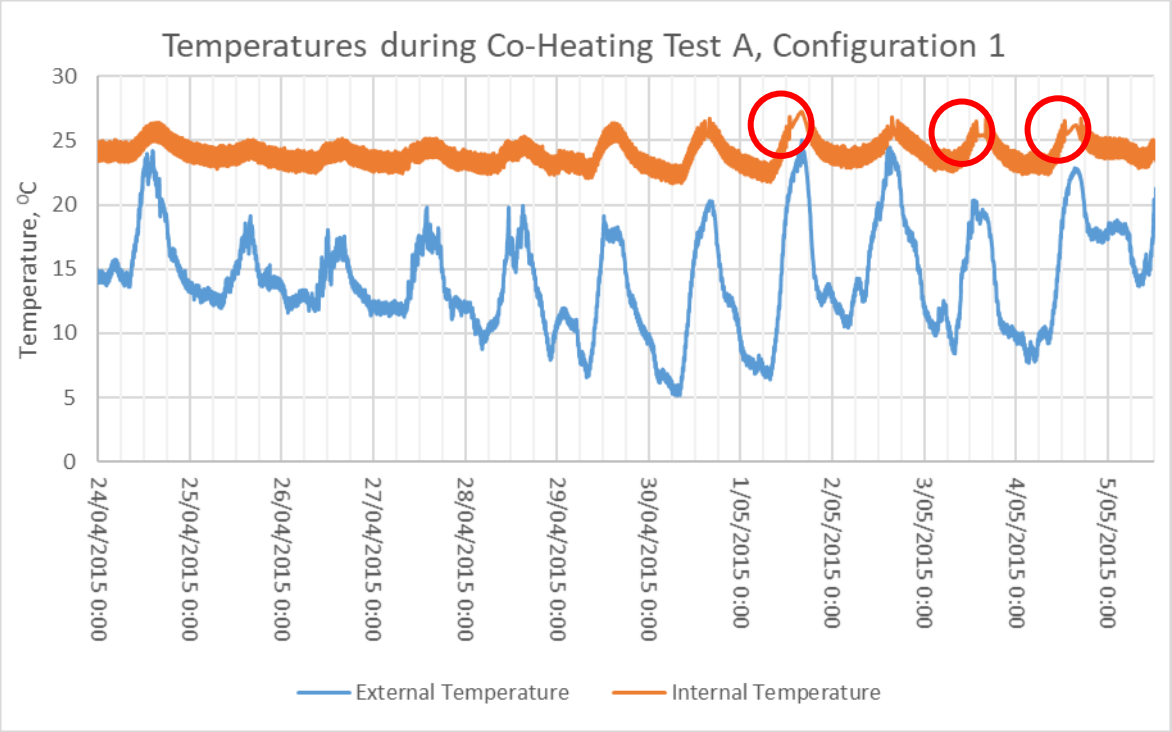

Figure 5.16 Temperature during co-heating test A of Configuration 1

The temperature was not necessarily outside the usual range for the test period; however, this may cause some issues when analysing the data as the temperature and recorded power are not necessarily linked for these days. It is also not clear whether the overheating on 1 May had an effect on the readings from 2 May. As two tests were run on the test cell in this configuration, this data set will still be analysed as a point of comparison.

5.3.2 Siviour Analysis

5.3.2.1 Siviour Plot 1

The first Siviour plot, shown in Figure 5.17, uses all data from the tests.

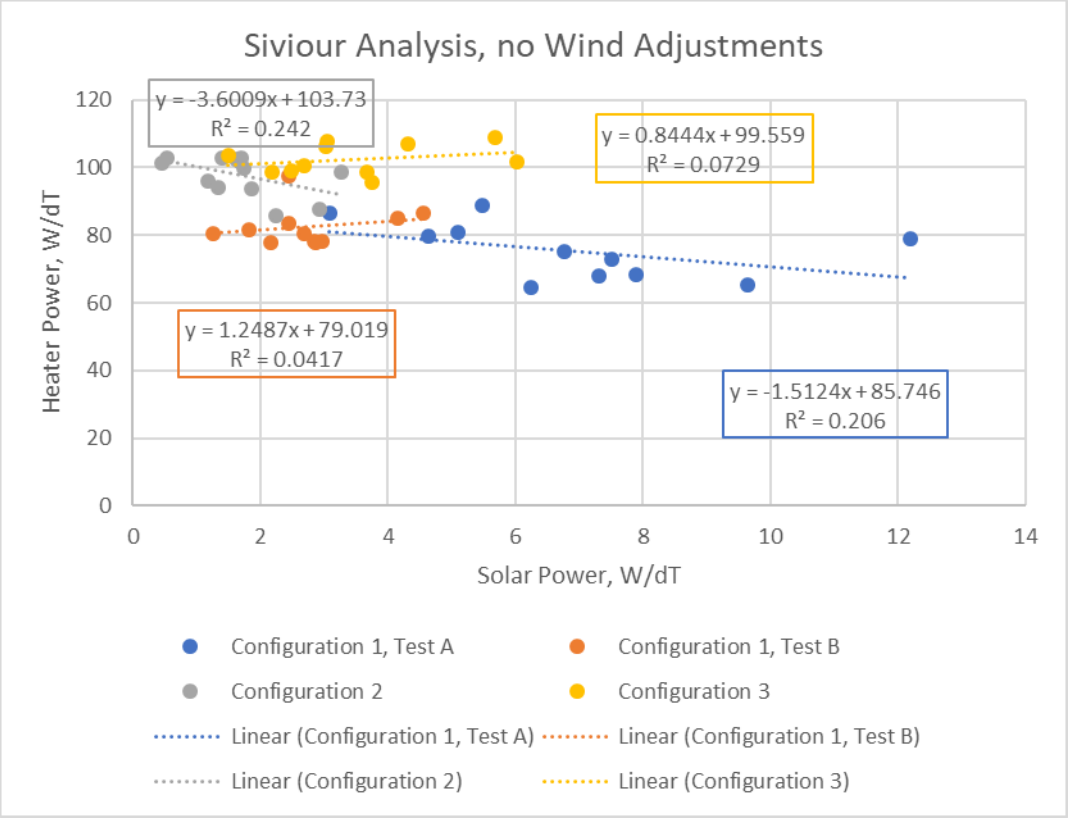

Figure 5.17 Siviour plot for co-heating tests, no wind adjustments

It is immediately apparent that the plots for Configurations 1 (Test B) and 3 do not match the expected pattern of a Siviour analysis. The positive gradient of the fitted curves indicates that as the solar radiation readings increase, the electrical power input also increases. The HTC based on this plot will underestimate the real heat losses. The plot for Configurations 1 (Test A) and 2 follow the expected pattern of a negative x-coefficient. Additionally, it is expected that Configuration 3 should have a higher HTC than Configuration 2 as it has less insulation. The HTCs from these Siviour plots estimates Configuration 2 at 103.73 W/K, nearly 4 W/K higher than Configuration 3 at 99.56 W/K. Cleaning the data based on the wind estimates should begin to address these issues.

5.3.2.2 Siviour Plot 2

The second Siviour plot, shown in Figure 5.18 removes the days where the average windspeed exceeds 27 km/h.

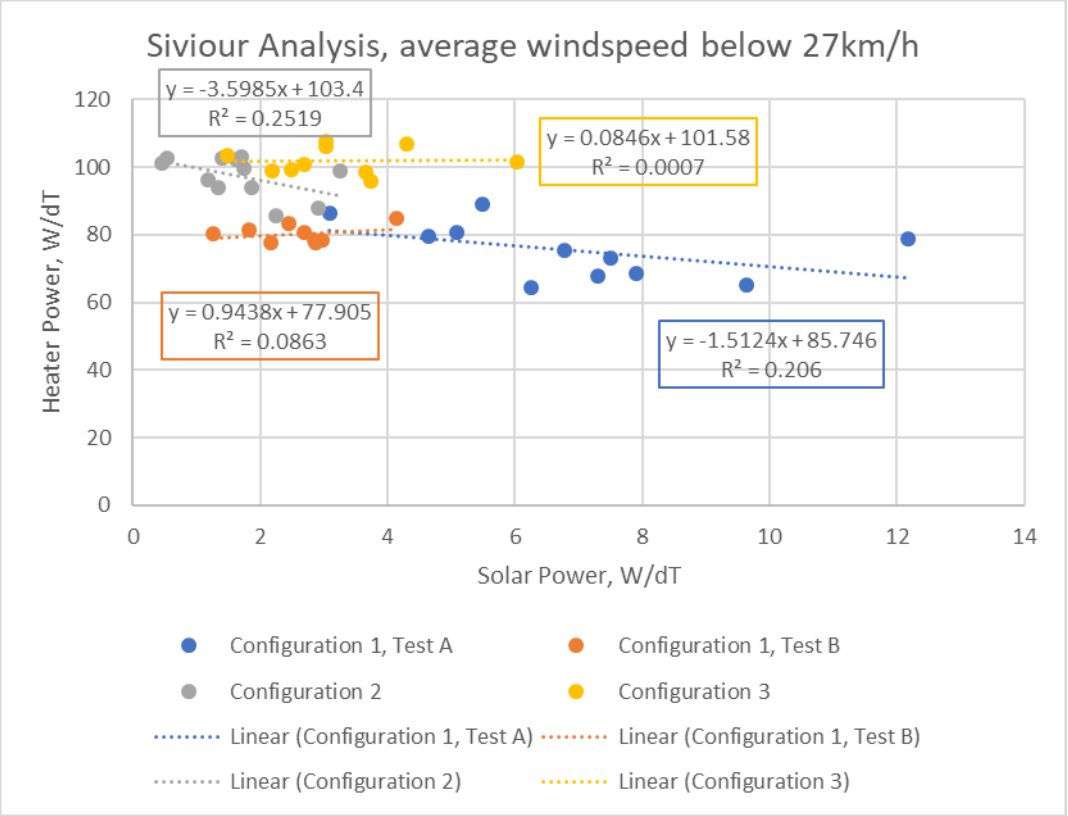

Figure 5.18 Siviour plot, average windspeed below 27km/h

The removal of data where windspeed exceeded 27 km/h has made some difference, but has not corrected the issues with Configuration 1 Test B, or Configuration 3. There is no change to the Configuration 1 tests as no day recorded an average windspeed above 27 km/h.

5.3.2.3 Siviour Plot 3

The third Siviour plot, shown in Figure 5.19 removes data where the average windspeed exceeds 19.2 km/h.

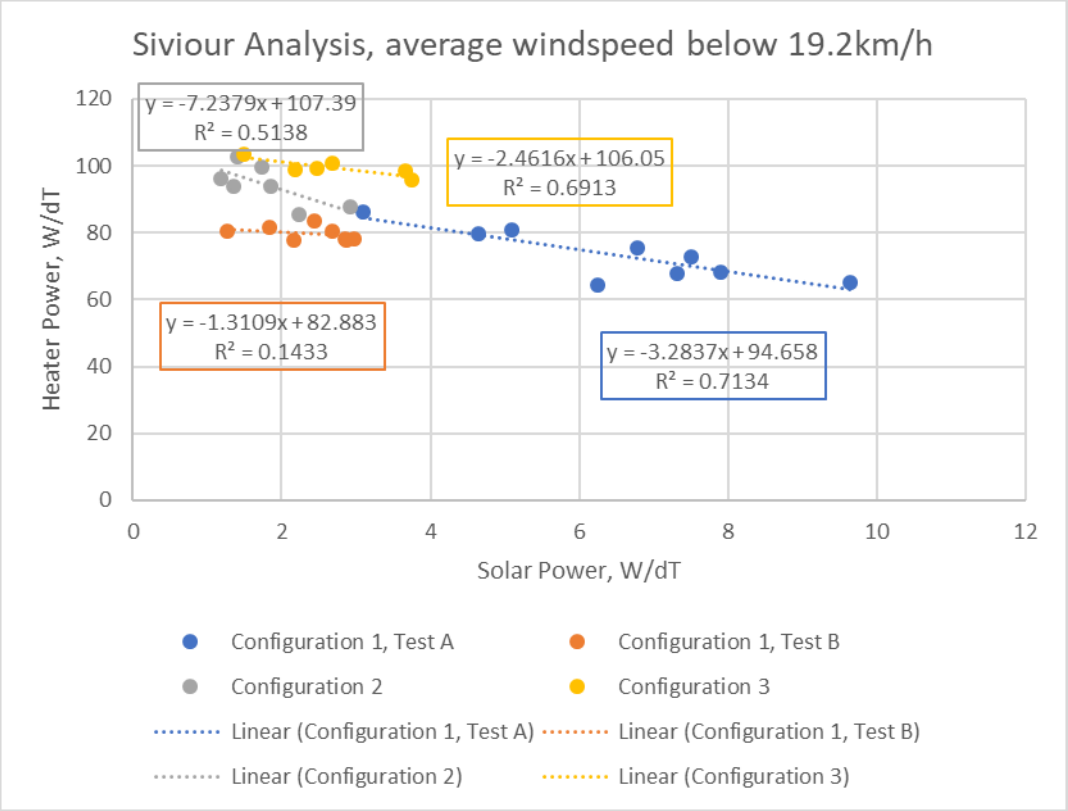

Figure 5.19 Siviour plot, windspeed below 19.2km/h

This final level of data cleaning provides expected patterns of results for all configurations. The HTCs predicted for Configuration 1 vary significantly; Test B estimates the HTC nearly 14 W/K higher than Test A. The HTC for Configuration 2 has increased to 107.39 W/K. Configuration 3 has the expected pattern; however, the HTC is lower than Configuration 2 which is against expectations. Removing the days with windspeeds exceeding 19.2 km/h removes nearly half the dataset for each test. It leaves only six to nine days of data on which to conduct the analysis, consequently reducing confidence in the results. Table 5.12 shows estimates of the solar aperture calculated from the three Siviour plots.

Table 5.12 Solar aperture from Siviour analysis

Configuration	Solar aperture, m^2		
	All data	Average windspeed <27 km/h	Average windspeed <19.2 km/h
1, Test A	1.5124	1.5124	3.2837
1, Test B	n/a*	n/a*	1.3109
2	3.6001	3.5985	7.2379
3	n/a*	n/a*	2.4616

*Note: n/a values represent invalid Siviour plots, i.e. positive x-coefficients.

From Table 5.12 it is possible to calculate the solar adjusted power for all configurations using the data where average windspeed does not exceed 19.2 km/h. The solar aperture for Configuration 2 is significantly higher than for the other configurations. This may be explained by lower solar radiation recorded during this test period compared to the other three, though this would not explain why there is a difference between the two Configuration 1 tests. Test B experienced lower solar radiation than Test A, but also had a lower solar aperture. Even after cleaning the data to exclude higher wind days, there is still a difference in wind conditions between tests, and wind may still cause some of the variation observed.

5.3.2.4 Solar Adjusted Power

For each test, solar aperture calculated is multiplied by the average daily solar radiation to give the power provided by solar gains in W. This is added to the average electrical power recorded to provide 'solar adjusted power', which is then regressed against the temperature difference to estimate the HTC.

Figure 5.20 shows the HTC using the initial uncorrected data, and Figure 5.21 shows the HTC using the solar corrected figures. Only the data where average windspeed is less than 19.2 km/h has been used for these plots.

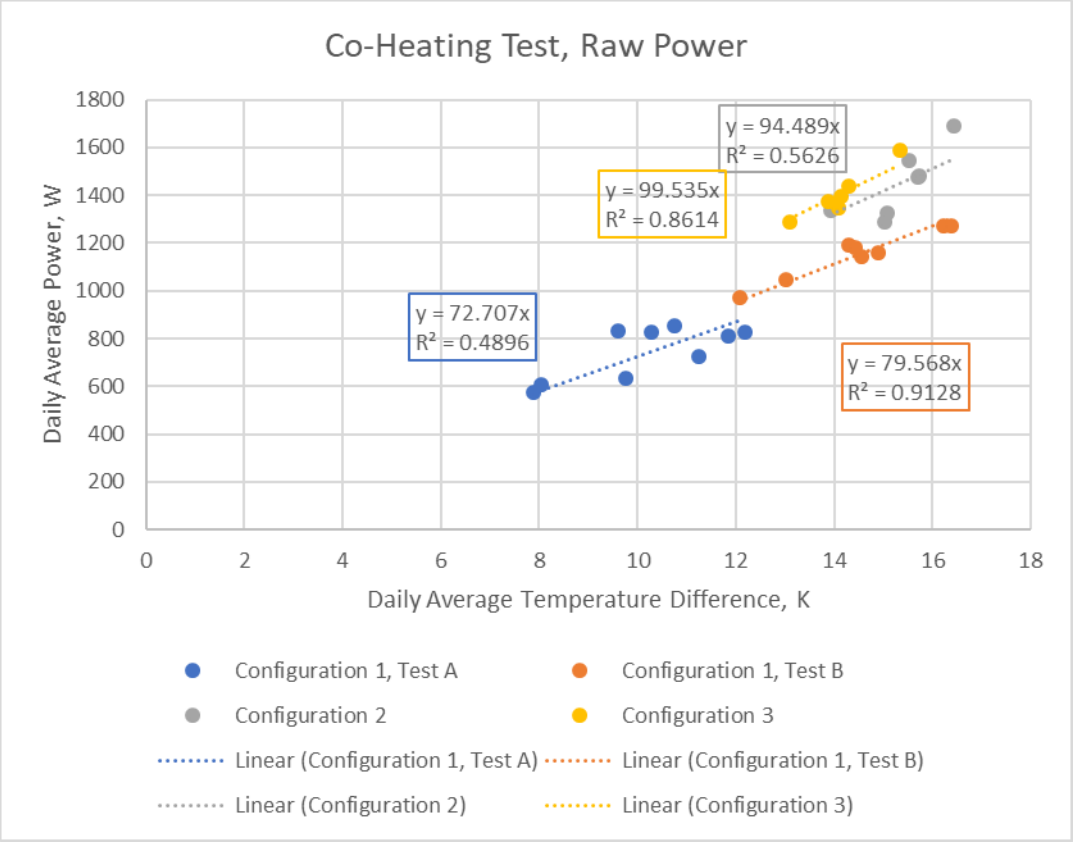

Figure 5.20 Co-heating test results, raw power

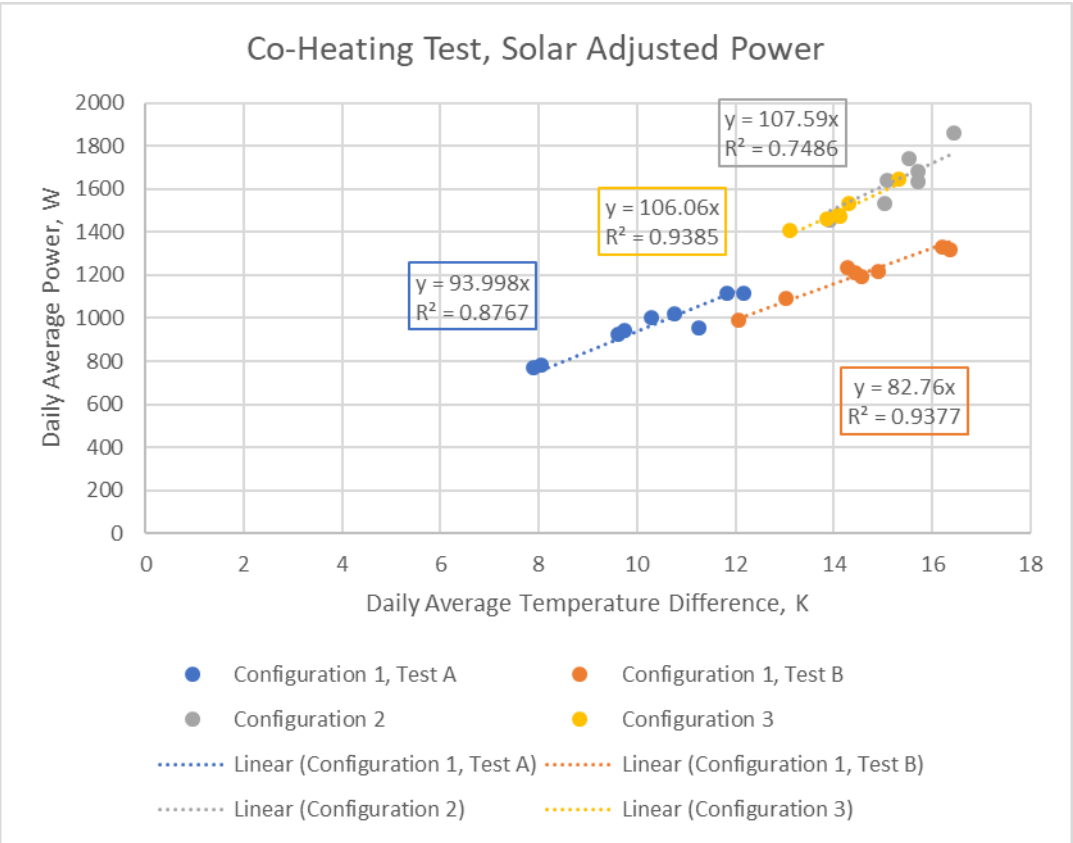

Figure 5.21 Co-heating test results, solar adjusted power

The results change entirely once solar gains were accounted for using Siviour analysis. All tests in Figure 5.21 report a higher HTC than in Figure 5.20, which is expected given the heat balance equation now has the additional solar heat input added to it. Once solar gains are accounted for, Configuration 3 still estimates a lower HTC than Configuration 2 which is surprising given the lower level of insulation. There is a huge difference between the two Configuration 1 tests; Test A estimates the HTC to be more than 13% higher than Test A. While the data has been cleaned for wind the wind effects have not been explicitly included in the HTC figure at this stage of the analysis.

5.3.2.5 Wind Regression Analysis

To account for the wind effects, the dependant variable, solar adjusted power, is regressed against the temperature difference and average wind speed as the independent variables. The coefficient was set to 0 so that the regression curve passes through the origin, aligning with the assumptions of the heat balance equation. HTC is estimated at windspeed of 0 m/s, and is shown in Figure 5.22.

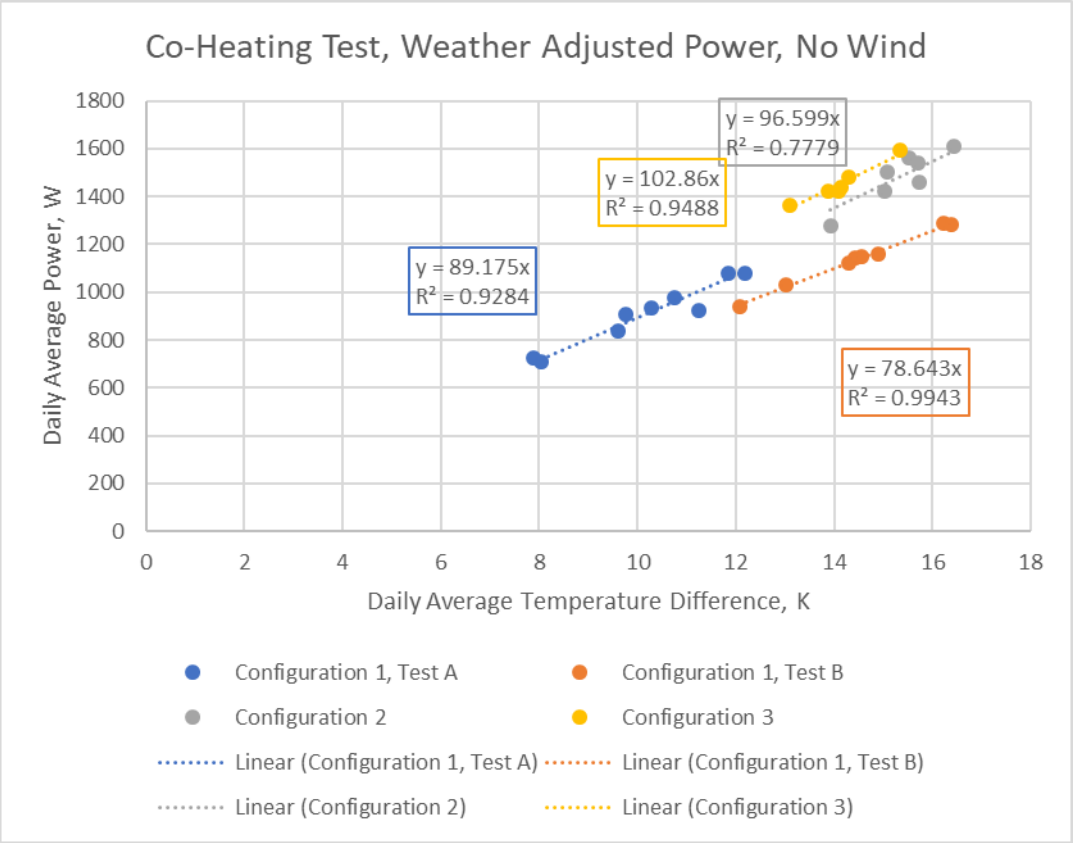

Figure 5.22 Co-heating test results, weather adjusted power for windspeed of 0km/h

The results once again vary dramatically depending on which windspeed assumption is made. Figure 5.22 shows a 6.2 W/K increase from Configuration 2 to Configuration 3, which is a reasonable estimate given the theoretical increase from heat flux testing was 8.2 W/K. Configuration 1, however, still shows large differences between Test A and Test B. The variation for Configuration 1 can be reduced by assuming average windspeed is 14.4 km/h (4 m/s), as suggested by Jack et al. (2017). However, this also reduces the estimate for Configuration 3 by so much that it is lower than Configuration 2 again. The HTC estimates from the Siviour analyses is summarised in Table 5.13.

Table 5.13 Summary of HTC estimates based on Siviour analysis

Configuration	HTC estimate, W/K			
	Raw data	Wind cleaned data, Siviour plot	Solar adjusted power	Weather adjusted power
1, Test A	72.71	94.66	94.00	89.18
1, Test B	79.57*	82.88	82.76	78.64
2	94.49	107.39	107.59	96.60
3	99.54*	106.05	106.06	102.86

*These tests had positive x-coefficients

The final estimate in Table 5.13 should account for solar gains and wind influences, which theoretically makes it a more reliable figure than the figure taken from the raw data. The data for Configuration 1 Test A casts some doubt over the analysis as it is significantly different from the Test B estimate. The cause of this variation may be the period of overheating in the second half of Test A. To apply a consistent method across the tests to gain a valid estimate of the solar aperture via the Siviour plot, all days where windspeed was above 19.2 km/h were removed. Wind speeds above 19.2 km/h, or 12mph, was considered 'windy' by Judkoff et al. (2000). In doing so, this reduced to six the number of included days for Configuration 3. As a result, the p-value for wind coefficient in the final multiple regression analysis is not considered statistically significant at 0.356. Likewise, Configuration 2 only included seven results, with a p-value for the wind coefficient of 0.137. Configuration 1 Test B was the only test with a statistically significant coefficient for the wind variable.

5.3.3 Multiple Regression

For the multiple regression analysis, the Data Analysis pack for MS Excel 2016 was used. The regression is set up such that measured power is the dependant variable, and the temperature difference, solar radiation and windspeed are the three independent variables. The constant has been set to zero in alignment with analysis used by Jack et al. (2017) as this uses the same assumption as the heat balance equation. The coefficients for solar radiation and windspeed have then been used to adjust the power measurements, and the usual linear regression for the co-heating test is then carried out to estimate the HTC. The regression statistics are displayed in Table 5.14.

Table 5.14 Multiple regression statistics for co-heating tests

Test	*Variable*	*Adjusted R Square*	*n*	*F*	*Sig. F*	*Coefficient*	*Standard Error*	*t Stat*	*p-value*
Configuration 1, Test A		0.872685	11	1437.3	3.988E-10				
	Temperature					81.345	4.050	20.085	3.94E-08
	Solar					-2.499	0.547	-4.565	0.001838
	Wind					7.937	1.493	5.317	0.000713
Configuration 1, Test B		0.874838	11	20522.25	3.647E-14				
	Temperature					81.313	1.187	68.477	2.3E-12
	Solar					-2.128	0.473	-4.494	0.002019
	Wind					6.419	0.425	15.105	3.65E-07
Configuration 2		0.89877	13	3248.326	5.694E-14				
	Temperature					93.678	3.684	25.431	2.03E-10
	Solar					-3.235	1.326	-2.440	0.034878
	Wind					8.057	2.161	3.728	0.00392
Configuration 3		0.874749	11	13303.8	1.662E-13				
	Temperature					97.907	1.451	67.487	2.59E-12
	Solar					-3.428	0.695	-4.932	0.001147
	Wind					13.443	1.860	7.229	8.99E-05

Each regression model displays a good fit to the data, explaining at least 87% of the observed variation in daily electrical power input to the building. Overall, each model is considered statistically significant with F-test p-values < 0.001. Individually, each variable is also statistically significant in each model with p-values 0.05 in all cases, and p>0.01 for all but the solar variable for Configuration 2.

Using the coefficients for solar and wind from the multiple regression analysis, the measured power can be adjusted for each day, giving ‘weather adjusted power’. Figure 5.23

displays the co-heating test plot using the weather adjusted power figures for all configurations.

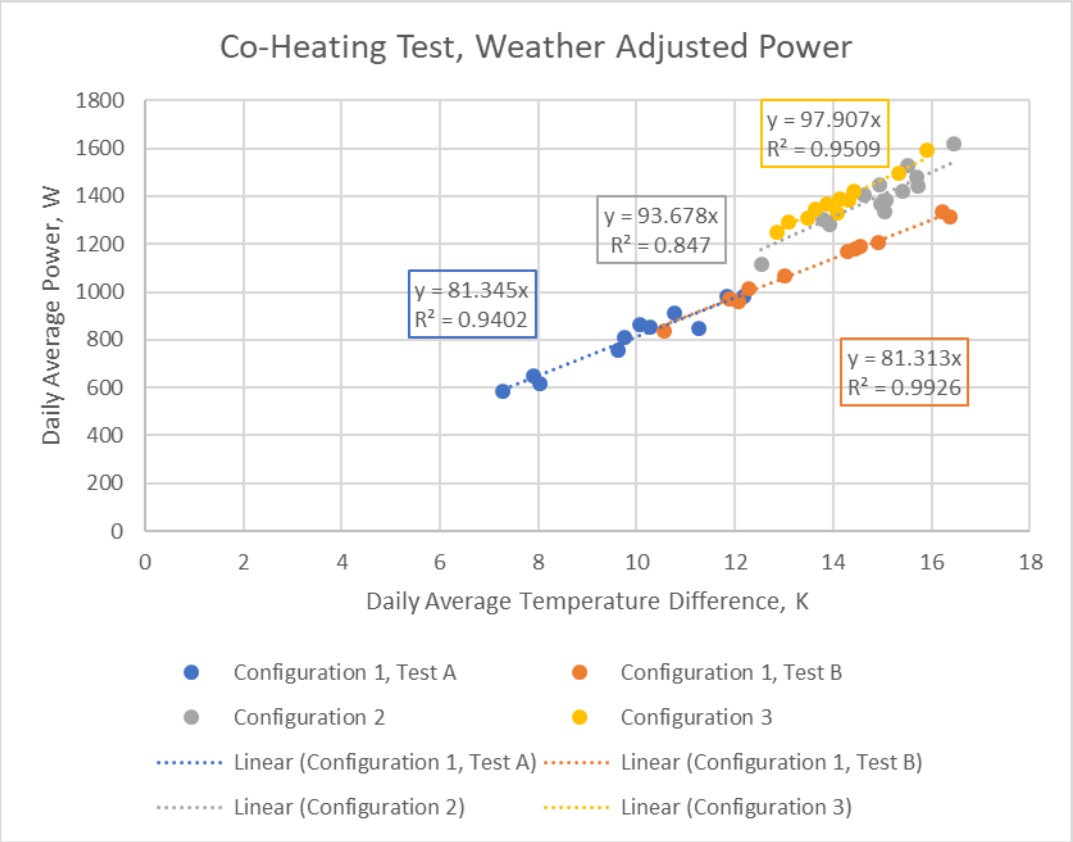

Figure 5.23 Co-heating test results, weather adjusted power from multiple regression analysis

The difference is striking between the spread of raw results observed in Figure 5.20, and the results in Figure 5.23, having adjusted for solar gains and windspeed via multiple regression. Both tests for Configuration 1 estimate the HTC at approximately 81.3 W/K, and both have good measures of fit with R^2 figures of 0.94 for Test A and 0.99 for Test B. There is a jump of over 12 W/K to Configuration 2 with the initial removal of wall insulation, and a smaller increase of just over 4 W/K associated with the additional wall insulation removed in Configuration 3. The literature review conducted indicated that any single weakness could compromise an entire building, and that is reflected in these results. The initial 'hole' in insulation created in Configuration 2 results in a comparatively large increase in heat loss, where the additional removal, despite being the same area of insulation, does not influence the heat loss as significantly as a weakness in the building fabric already exists.

5.3.4 Summary

Three approaches have been taken to estimate HTC for each test cell configuration. First, raw data making no adjustments for solar gains or wind was expected to be the least reliable. Second, the Siviour analysis plus regression, which is widely used in the industry, and third a multiple regression analysis. Table 5.15 summarises the HTC estimate for each configuration from the three analyses.

Table 5.15 Summary of HTC estimates

Configuration	HTC, W/K		
	Raw data	Siviour plus regression	Multiple regression
1, Test A	72.71	89.18	81.35
1, Test B	79.57*	78.64	81.31
2	94.49	96.60	93.68
3	99.54*	102.86	97.91

The weather conditions varied between each test, mostly clearly shown by the raw data analysis in Table 5.15 for Configuration 1 tests. When no adjustments are made to account for differing conditions, there is a difference of more than 9% between the two tests. However, when the conditions are adjusted for in the multiple regression analysis, estimates match almost exactly. With the exception of Configuration 1 Test A, this is also the case in the Siviour analysis, though Siviour analysis was conducted on the smaller dataset and did not show statistical significance for the wind term of the regression analysis. This reduces confidence in the Siviour estimate.

Taking these elements into account, if Configuration 1 Test A is excluded on the basis of overheating, then the Siviour and multiple regression analyses show good agreement: the variation between the two approaches is 5.1%.

Based on using all available data to generate a statistically significant model, HTC estimates from the multiple regression analyses will be used as the true HTCs for the test cell. The HTC for Configuration 1 will be taken as the average of the two tests.

5.4 Uncertainty Analysis of Co-Heating Test

The overall uncertainty of each co-heating test was estimated using Differential Sensitivity Analysis (Lomas & Eppel 1992). This involves identifying the uncertainty in each measurement and analysing the impact this uncertainty has on the overall result. Each value is recorded, and then the total uncertainty is calculated as the sum of the squares of the individual uncertainties. Table 5.16 shows the uncertainty in each measurement, the resulting variation in the HTC estimate, and the total uncertainty in each test.

Table 5.16 Uncertainty analysis of co-heating tests

Variable	Uncertainty in measurement	Variation in HTC due to uncertainty (+ or -)							
		Configuration 1, Test A		Configuration 1, Test B		Configuration 2		Configuration 3	
		+	-	+	-	+	-	+	-
Power	+/- 1%	1.0%	-1.0%	1.0%	-1.0%	1.0%	-1.0%	1.0%	-1.0%
Temperature difference	+/- 0.65 K	-4.5%	4.8%	-4.0%	4.3%	-3.6%	3.9%	-4.1%	4.4%
Solar radiation	+/- 3%	0.0%	0.0%	0.0%	0.0%	0.0%	0.0%	0.0%	0.0%
Windspeed	+/- 1 km/h or +/- 10% if windspeed >10 km/h	-0.1%	0.0%	-0.2%	0.0%	0.0%	0.0%	-0.1%	0.1%
Total		4.9%	-4.6%	4.4%	-4.1%	4.0%	-3.7%	4.5%	-4.2%

Note: Negative percentages indicate a decrease in HTC.

Table 5.16 shows that the largest influence in these tests is due to the uncertainty in the temperature difference, followed by power. Uncertainty in solar radiation and windspeed had little overall impact. The total uncertainty in all cases is less than 5%. Figure 5.24 shows HTCs for each configuration with the associated error bars from the uncertainty analysis.

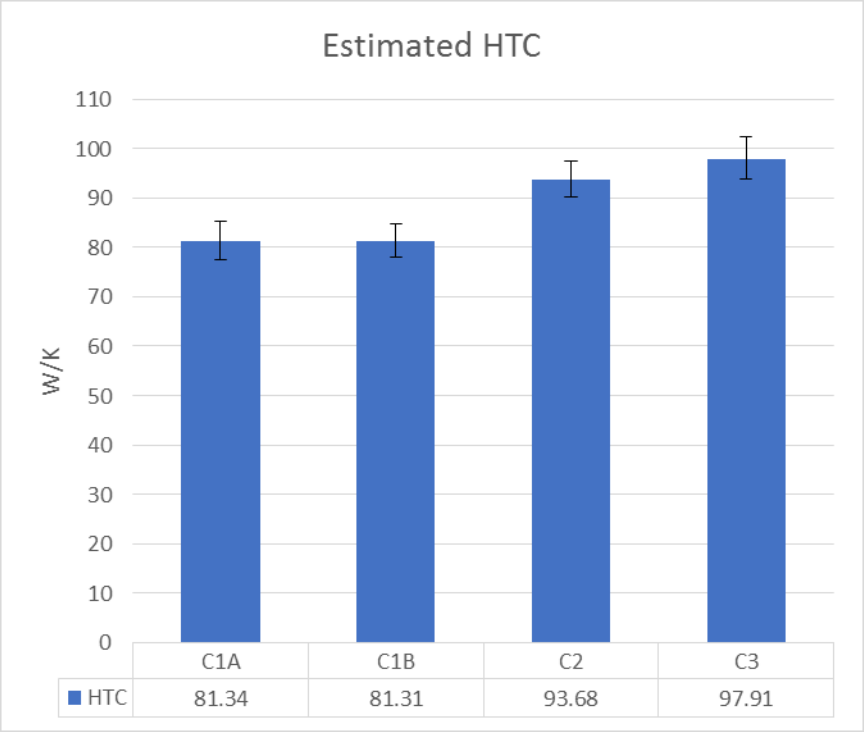

Figure 5.24 HTC Estimates including error bars

Based on the uncertainty analysis, there is a clear difference between the two Configuration 1 tests and the Configuration 2 and 3 tests. The upper estimates for Configuration 1 Test A and Test B are below the lower estimates for configurations 2 and 3. Configurations 2 and 3 however do overlap. This indicates that the Configuration 2 and Configuration 3 HTC estimates cannot definitively conclude the two configurations perform differently. This demonstrates a limitation on the sensitivity of the co-heating test and the ability to determine the difference between two buildings with similar performance characteristics.

The final estimate of the HTCs including uncertainty is displayed in Table 5.17. The larger Configuration 1 Test A uncertainties have been used as the overall uncertainty for the Configuration 1 HTC estimate.

Table 5.17 Estimated HTC from field co-heating tests

Configuration	HTC, W/K
1	81.33 +4.00/-3.74
2	93.68 +3.73/-3.49
3	97.91 +4.43/-4.10

5.5 Comparison of Co-Heating and Heat Flux Field Testing

The three different configurations are expected to return three different results. Table 5.18 shows the comparison between the expected (theoretical) HTC, based on the heat flux and blower door tests, and the HTC determined by the co-heating test.

Table 5.18 Comparison between theoretical and measured HTCs

Configuration	Theoretical HTC, W/K	Measured HTC, W/K
1	116.91	81.33
2	125.94	93.68
3	133.46	97.91

Table 5.18 clearly shows a significant difference between the theoretical heat loss from the heat flux plus blower door tests, and the co-heating test. The theoretical estimate is between 35 W/K and 39 W/K greater than measured heat loss, a variation of between 37% and 47%. This may be due to a number of factors. The uncertainty in the heat flux analysis may have resulted in underestimating the wall's R-value, and using the blower door analysis rather than a CO_2 decay analysis has overestimated in situ ventilation losses. Heat loss through the floor and ceiling may also have been reduced as standard values were used for the R-values of the attic and sub-floor spaces .

The variation between the configurations is different, but the theoretical estimates do predict some of the changes observed in the measured results. The change from configuration 1 to 2 is not as large as the change from 2 to 3. The difference between Configurations 2 and 3 from the theoretical estimate is larger as it does not adjust for the diminished impact of the second 5.8 m^2 of insulation removed. The only adjustment is in the leakage losses and this is a minimal change between configuration 2 and 3.

Measured HTCs will be used as the benchmark to test the decay method against, as these are in situ as built measures of performance. Theoretical estimates will be used as a base point for creating the EnergyPlus models, which will then be adjusted to goal seek for the measured values.

5.6 Simulated Co-Heating Tests

Simulations were used in two main parts: first, as a proof of concept before any experimentation had taken place to determine what experiments might provide meaningful information; and second, to assist in answering questions arising during analysis of experimental results. As part of the benchmarking analysis, the co-heating tests were simulated on the building models described in Section 4.4.5. This uses the co-heating test as a calibration tool for the models and confirms that observed HTC is included in the array of models. The building models were set up to use observed internal temperature, and the weather file created from the Bureau of Meteorology, to simulate the co-heating tests as conducted in field on each configuration. The simulation results were then analysed using the multiple regression analysis described in Section 5.3.3 so they can be directly compared with field results. This approach accounts for the solar gains and the wind conditions observed during the test period.

5.6.1 Simulation Results

Simulation results are grouped by configuration to show how changes to the thermal shell have influenced the HTC estimate. The uncertainty for the simulations has been taken as the 95% confidence interval of the daily variation in HTC, an approach used by Stamp (2011). This has been selected over an analysis based on altering data inputs as simulations do not have the same uncertainty due to the measurement instruments. The uncertainty presented in this fashion more closely represents the uncertainty inherent in the co-heating analysis, rather than the entire co-heating experiments.

5.6.1.1 Configuration 1

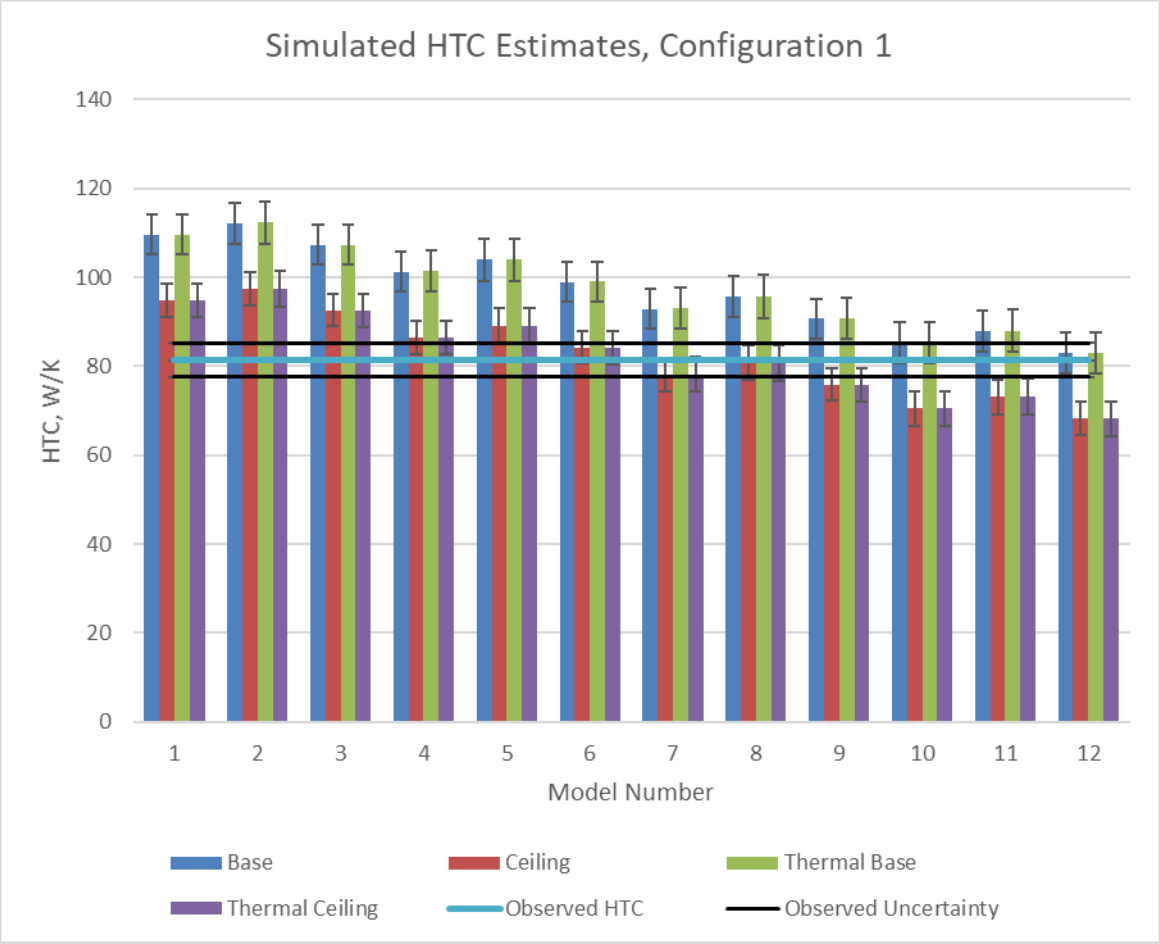

Figure 5.25 Simulated HTC estimates, Configuration 1

Figure 5.25 shows several simulations match closely with the observed co-heating test HTC, with a good spread above and below. There is a clear difference between the models with and without increased ceiling insulation, but no variation between the models with and without increased thermal mass.

Base Model 4 is qualitatively the best representation of the test cell based on the material data and the infiltration rate entered. This model overestimates the HTC by 24.5%. The best estimate of the HTC from the Base set is Model 12 however, which has R2.5 insulation in the walls instead of the estimated R1.91, and an infiltration rate of 0.52 ACH. The nearest matching estimate overall is from Ceiling Model 8 (R-Value 1.5, infiltration 0.866 ACH). This indicates the building performs better than expected based on initial estimates of thermal shell characteristics. This supports the observed difference, reported in Section 5.5, between co-heating test HTC and the heat flux test HTC.

5.6.1.2 Configuration 2

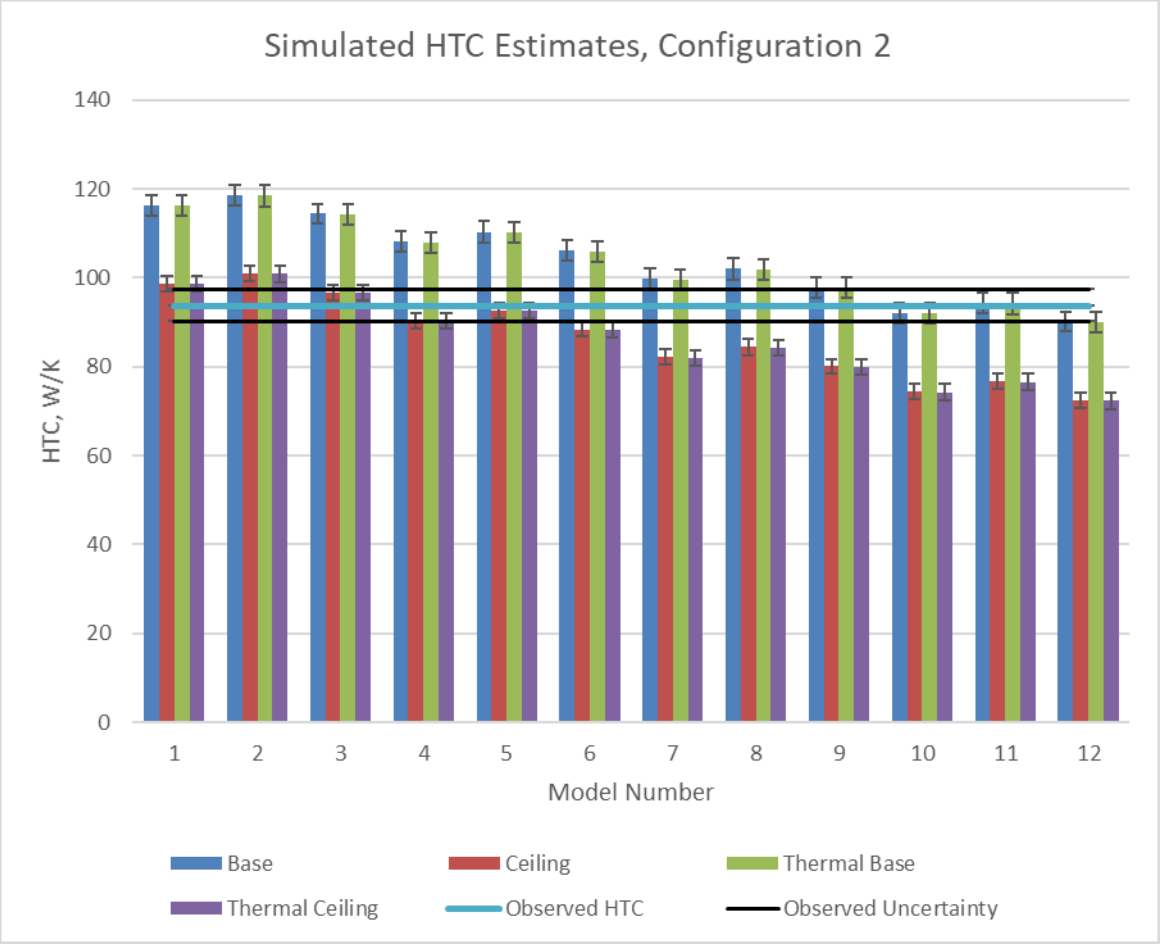

Figure 5.26 Simulated HTC estimates, Configuration 2

As in Configuration 1, Figure 5.26 shows many of the models have HTCs similar to that estimated for the test cell. The best estimate from the base model set is Model 11, which has wall insulation of R1.5 and an infiltration rate of 0.52 ACH. The nearest estimate is from Thermal Base Model 11, though the difference between this and the base model is only 0.1 W/K. The best qualitative representation of the test cell, Base Model 4, overestimates the HTC by 15.3%.

5.6.1.3 Configuration 3

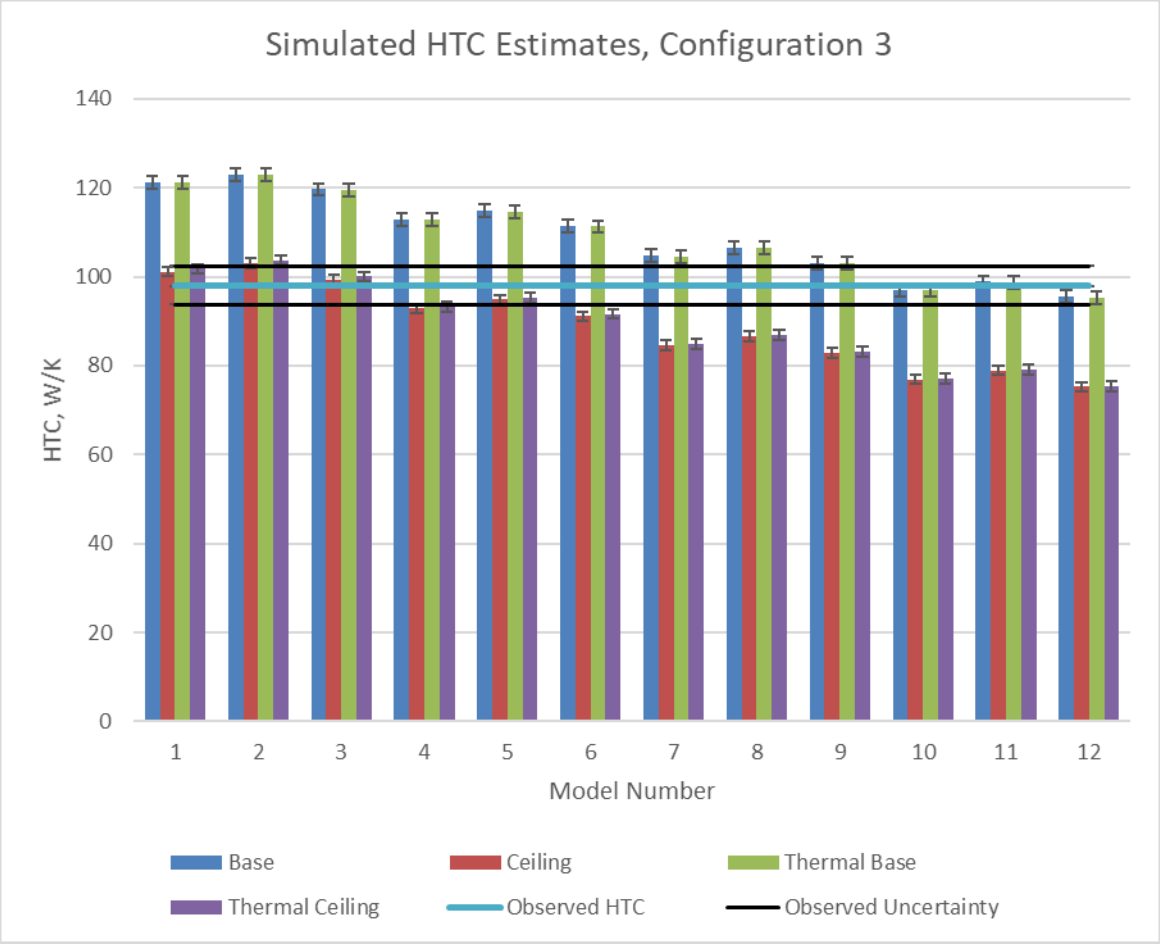

Figure 5.27 Simulated HTC estimates, Configuration 3

Figure 5.27 demonstrates the same patterns within Configuration 3 as were observed for Configurations 1 and 2. The best estimate from the base model set is Model 10 (R-value 1.91, infiltration 0.52 ACH). The best estimate overall is Thermal Base Model 11 (R-value 1.5, infiltration 0.52 ACH). The best qualitative representation of the test cell, Base Model 4, once again overestimates the HTC by 15.4%.

5.6.2 Discussion of Simulated Results

All three configurations show large differences between the sets with and without ceiling insulation, but almost no difference between sets with and without increased thermal mass. The steady-state nature of the co-heating test is designed to minimise the influence of thermal mass by eliminating the charge and discharge of energy throughout the day. These buildings are expected to show differences in dynamic behaviour, but the steady-state behaviour ultimately assesses the overall U-value of the building, regardless of whether it is a heavy or lightweight construction.

All four model sets (Base, Ceiling, Thermal Base and Thermal Ceiling) gave at least two models inside the uncertainty range from the field co-heating tests. These demonstrate how varied the characteristics of a building can be, and yet still have the same HTC, as well as showing that the simulated dataset covers a good range of building performances compared with the field testing.

The initial building model, Base Model 4, in each configuration overestimates the heat loss by more than 15%. This is in line with observations reported in Section 5.5 that the heat loss determined by heat flux and blower door testing was much higher than heat loss determined by the co-heating test. As information from this analysis informed the initial model, it is not surprising that heat loss is overestimated. Reducing theoretical losses by increasing R-values or reducing infiltration rates improves alignment between the simulated co-heating test and the field co-heating test. This indicates there is some part, or parts, of the building fabric that is being underestimated.

The purpose of the simulation analysis with respect to the overall research aim is to show how the decay method will identify the performance of different buildings. These simulations provide a combination of models that have the same HTC for different thermal shells, and different HTCs. This provides a valuable resource for analysing how the decay method will identify the buildings with different HTCs as well as what differences are observed when two differing models have the same HTC. The observation that the thermal mass makes little difference to the HTC is particularly important as it is expected that this will change the building's dynamic behaviour, providing good comparison between the analysis of the decay method and the co-heating test.

5.7 Conclusion of Benchmarking Tests

It has been demonstrated that even a simple box structure can be sufficiently complex such that a number of different values for heat loss can be provided, depending on the evaluation method used.

The analysis shows that the whole house heat loss, determined by the co-heating test, is not necessarily the same as the summation of the heat loss elements (that is, the infiltration losses and material losses), and that whole house evaluation should be the aim. The simulation also demonstrates that technically different buildings may result in the same heat loss. It is expected there may be variations in results for the co-heating test should it be repeated as the external conditions may influence the results, as seen in Configuration 1 Test A and Test B. While the co-heating test results are expected to provide the building's true heat loss, the small variation in HTC between configurations 2 and 3 is less than the test's uncertainty. This indicates that alternative evaluation techniques may also struggle to define the difference between the two configurations.

The experimental and analysis process to determine heat loss via the co-heating test in this building also proved to be far simpler than that of the heat-flux and blower door method, though as discussed in earlier chapters, significantly more invasive to apply to residential buildings.

Chapter 6 - Experimental Decay Methods

This chapter discusses the procedure for conducting the experimental decay methods and analysing results. It also presents a comparison between the methods and the co-heating test with regard to applying the test and the information gleaned from either one. The decay method should theoretically provide information about the building that can be related to the heat loss determined by the co-heating test.

In practice these versions of the decay method use only data collected in situ to assess the building performance; however, simulations have been used to assist in developing and confirming the relationship between decay constant and HTC.

6.1 Decay Method Concept

The decay method is based on the expectation that buildings with less efficient thermal shells will lose heat faster than buildings with more efficient thermal shells. The method aims to identify the rate at which the building loses heat. The external temperature, however, will also influence the rate of heat loss; thus, the internal/external temperature difference of the building should also be taken into account. This allows for comparison of buildings across different climatic conditions.

6.1.1 Initial Methodology and Early Analysis

The initial approach for the decay method followed three main steps, and based on simulation results concluded that the temperature decay curve could be approximated as a straight line, the slope of which indicates the rate of temperature change over the decay period. The same model exposed to different conditions shows different rates of decay, so the average external temperature is used to normalise the nightly rate and determine an overall decay constant for the building.

The initial decay method procedure follows three main steps: gather data, calculate nightly temperature decay rate, and calculate overall decay value. These are discussed below.

1. Gather data

Internal and external temperature data is gathered for a period of between 7 and 14 nights.

2. Calculate nightly decay profile and temperature difference

The internal temperature decay is calculated for the period between 2.00am and 6.00am by conducting a single linear regression of temperature with respect to time. The gradient of this line is recorded as the temperature decay rate. Figure 6.1 shows an example of the internal temperature and the straight line estimate.

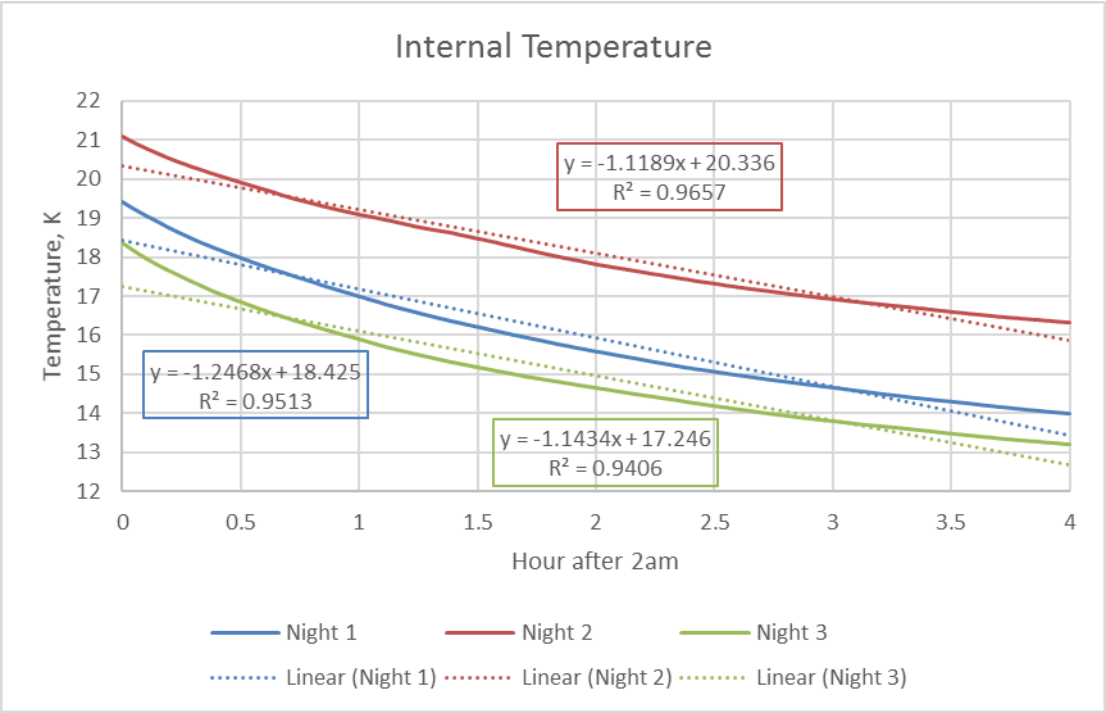

Figure 6.1 Internal temperature decay example

Figure 6.1 shows that in these sample data sets the linear regression of the temperature decay has a high R^2. As these R^2 figures are well above 0.9, this was initially considered to be an acceptable representation of the decay profile, despite the visual indication that the pattern of decay is not being preserved by the straight-line estimate. Average temperature difference is also recorded.

3. Normalise Decay against Temperature Difference

The temperature decay rate is graphed against the temperature difference for each night. Figure 6.2 shows this final graph.

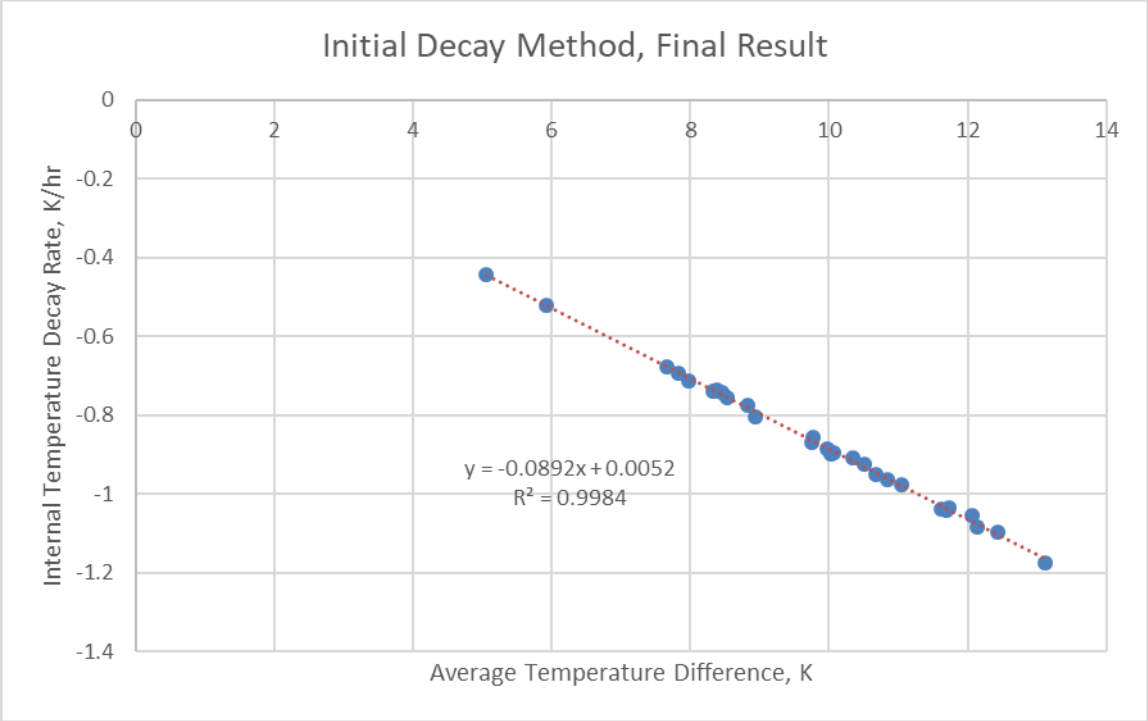

Figure 6.2 Decay method, initial concept, final analysis graph

Figure 6.2 shows an exceptional correlation between the gradient calculated from Step 2 with the average temperature difference during each decay period. The resulting coefficient of the single linear regression of temperature decay rate and temperature difference can be called the building decay value.

6.1.2 Concept Simulations

Proof of concept simulations carried out in EnergyPlus have two main points of focus:

- Showing the robustness of the decay method.
- Providing evidence of correlation to the co-heating test.

The very first simulations simply demonstrated how varying the internal and external conditions made very little impact on the results of a single building model. The second set of simulations showed how different HTCs relate to a difference in the decay method result. This provides evidence for a link between the two tests such that the decay method might be used as an alternative approach for defining the building's HTC.

6.1.2.1 Varied Initial Temperature

The first simulations of the decay method used a static initial temperature condition for all days. The variation in external conditions was the only influence providing different internal decay profiles. Simulating the method with different initial conditions internally did not

change the final result of the method. Figure 6.3 displays the comparison between the two sets of initial conditions.

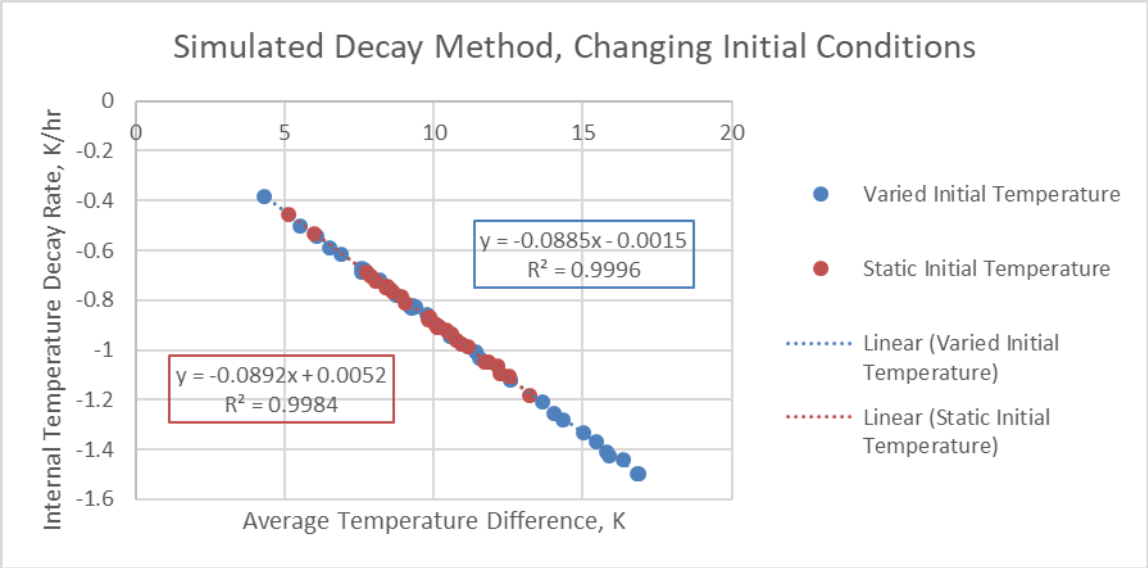

Figure 6.3 Comparison of decay method results under different initial internal conditions

6.1.2.2 Simulated Co-Heating Test Comparisons

Comparing the HTCs from the co-heating test and the building decay value of different buildings showed a strong relationship, indicating links between the two tests. Figure 6.4 displays the linear relationship between the building decay value and the HTC for the same model.

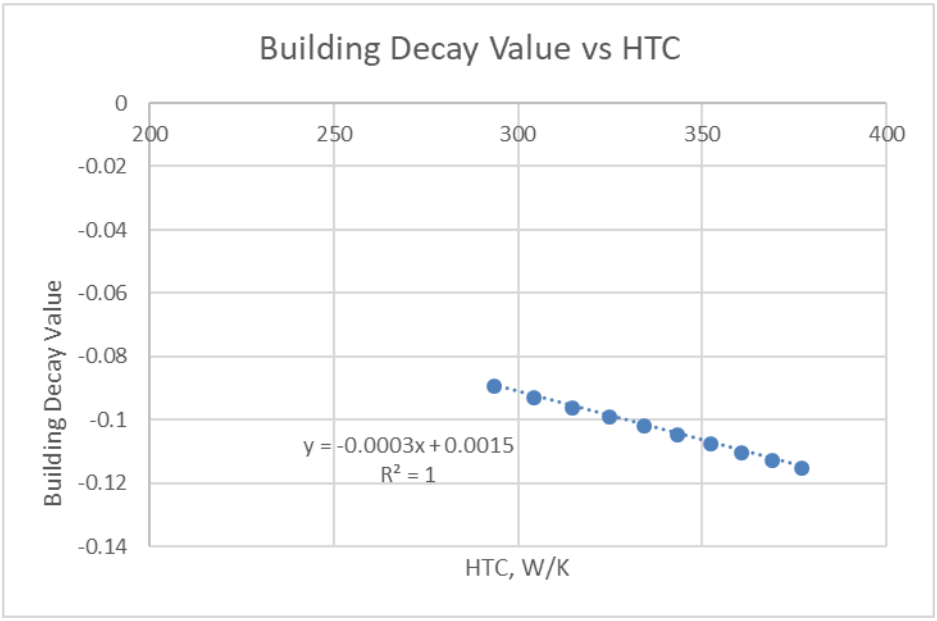

Figure 6.4 Initial simulated relationship between HTC and building decay value

This shows that theoretically there should be a direct correlation between the building decay value and the HTC.

6.1.2.3 Validity of Straight Line estimate

While this initial approach is useful in suggesting that there is a relationship between the rate at which a building loses temperature and the HTC, estimating the decay curve as a straight line overly simplifies the behaviour, ignores a large portion of the dataset, and may be unable to detect some subtle variations between buildings. Analysis of field data indicates the straight line estimate differed from the curve far more than expected based on the initial simulations, and is much better estimated as an exponential or a power curve. The straight line analysis is still useful in indicating there is a relationship; however, it is too crude to be applied with acceptable confidence and accuracy.

6.2 Exponential Decay Constant

As the theory for the decay method is based on the Law of Cooling, analysis of the building based on the law of cooling equation was revisited. The Law of Cooling is a simple model of energy flow that combines conduction, convection and radiative energy transfers into a single expression (Vollmer 2009). The equation underpinning the Law of Cooling is an exponential function that includes internal and external temperature as well as a decay constant. This makes it a much better choice than the straight line estimates as the external conditions are taken into account in the equation, and it estimates the decay as an exponent rather than a straight line. This allows greater agency in the analysis as more of the data is able to be used. The Law of Cooling is defined as Equation 7

Equation 7 Law of Cooling equation

$$T(t) = T_a + (T_o - T_a)e^{-kt}$$

Where:

T(t) = Internal temperature at time 't'

T_a= Ambient (external) temperature

T_o = Initial internal temperature

k = Decay constant

t = Time since decay began, in hours

There may be a limitation on the use of the Law of Cooling as there is no disaggregation of the heat transfer terms. Vollmer (2009) notes that the limitations of the Law of Cooling is relates to the ratio of convective to radiative heat transfer. If radiation is more dominant

than convection, there may be some deviation from the law at temperature differences below 30 K. While Vollmer (2009) suggests that using the law to predict cooling at room temperature works surprisingly well, its wider application may be nicely summarised in a statement from O'Connell (1999): 'Newton's law of cooling is one of those empirical statements about natural phenomena that should not work, but does.'

An alternative approach would be simply to fit an exponential curve. The disadvantage of this is that there appears to be a relationship between the decay constant and the coefficient which changes depending on the external conditions. Removing this variation by setting the coefficient to some known figure based on the initial conditions did not provide a curve with a good match to the data. Calculating the relationship between the coefficient and the decay value did provide a means to better fit the curves to the data; however, different buildings had different coefficients and different decay constants making it difficult to compare buildings based on these figures alone, even when these elements were regressed against external conditions.

Two methods have been identified based on the Law of Cooling Equation. The first rearranges the equation to calculate the decay constant for each night of the experiment and takes the average. The second uses Excel's Solver add-in to adjust the decay constant in a mathematical model of the internal temperature to identify a solution with the best match overall.

6.2.1.1 Calculating Average Decay Constant

The calculation of the average decay constant uses the observed temperatures, and rearranges and solves the Cooling equation for the decay constant, k.

Equation 8 Rearranged Law of Cooling equation to solve for k

$$k = \frac{1}{t} ln \left(\frac{T_t - T_a}{T_o - T_a} \right)$$

Where:

T_t= Internal temperature at time 't'

T_a= Ambient (external) temperature

T_o = Initial internal temperature

k = Decay constant

t = Time since decay began, in hours

As this calculation is determining the overall decay across a four hour period, t=4. This makes T(t) the final temperature of the decay experiment. The ambient temperature is assumed to be the average external temperature for the decay period each night. After the k-value is computed for each night, the average k-value is taken as the decay constant.

The decay constant is then plugged back in to the Law of Cooling equation, and a theoretical decay curve is calculated for each night. This is tested against the observations using RMSE to give an indication about the confidence that this decay constant is a good estimate for the building.

6.2.1.2 Excel Solver Decay Constant

Using the Microsoft Excel's Solver add-in, we can determine a value of k which best predicts the test cell's internal temperature across all nights of the decay test. This is done by modelling the internal temperature using the Law of Cooling equation and testing the difference between the measured temperatures and that predicted by this model. RMSE was used as the main test of good matching, and r^2 was also calculated. The Solver function was used to find the minimum value for the RMSE by changing the k-value.

The Law of Cooling calculates the internal temperature from a single starting temperature and assumes a constant external temperature, and is not necessarily designed to deal with a varying temperature over the decay curve's four hour timeframe. To determine how this influences the prediction, four different applications of the equation were used to determine which had the capacity for the smallest RMSE. These models change which value is used for internal and external temperatures, and the time value used at each point in the decay curve. Each model predicts a temperature for each minute of the decay period, aligning with the field data. The four models are summarised below:

1. T_O = T at time 0, T_a= External temperature at time 0
2. T_O = T at time 0, T_a= Average external temperature
3. T_O = T at time 0, T_a= External temperature at time t-(1/60)
4. T_O = T at time t-(1/60)*, T_a= External temperature at time t-(1/60)

*As t is in hours, 1/60 is the 1 minute time step. The units for t have been defined as hours as calculating for t in minutes made the final figures very small and difficult to interpret and communicate effectively.

The first two models set some initial conditions for internal and external temperatures, and have the internal temperature at each time point estimated based on the decay constant multiplied by the amount of time that has passed. The third model is similar, but only sets the initial internal temperature and uses the measured external temperature at each time point. The first three models all calculate internal temperature for t=0 to t=4. The fourth model is different and calculates a separate decay at each time point, where T_a and T_0 are the external temperature and the calculated internal temperature at the previous timestep. Models 3 and 4 should allow the equation to adjust to changing external conditions, and determine whether or not these are more or less accurate in predicting internal temperature each night.

6.2.1.3 Determining the Decay start point

The decay period has, to this point, been defined as the four hours immediately after the heater is turned off. This assumes that as soon as the heater is turned off there is no further heat energy applied to the building. Analysis of the change in temperature between each time point indicates however that this is not entirely true. Figure 6.5 shows how the temperature changes between each minute for the first hour from the point at which the heater is turned off.

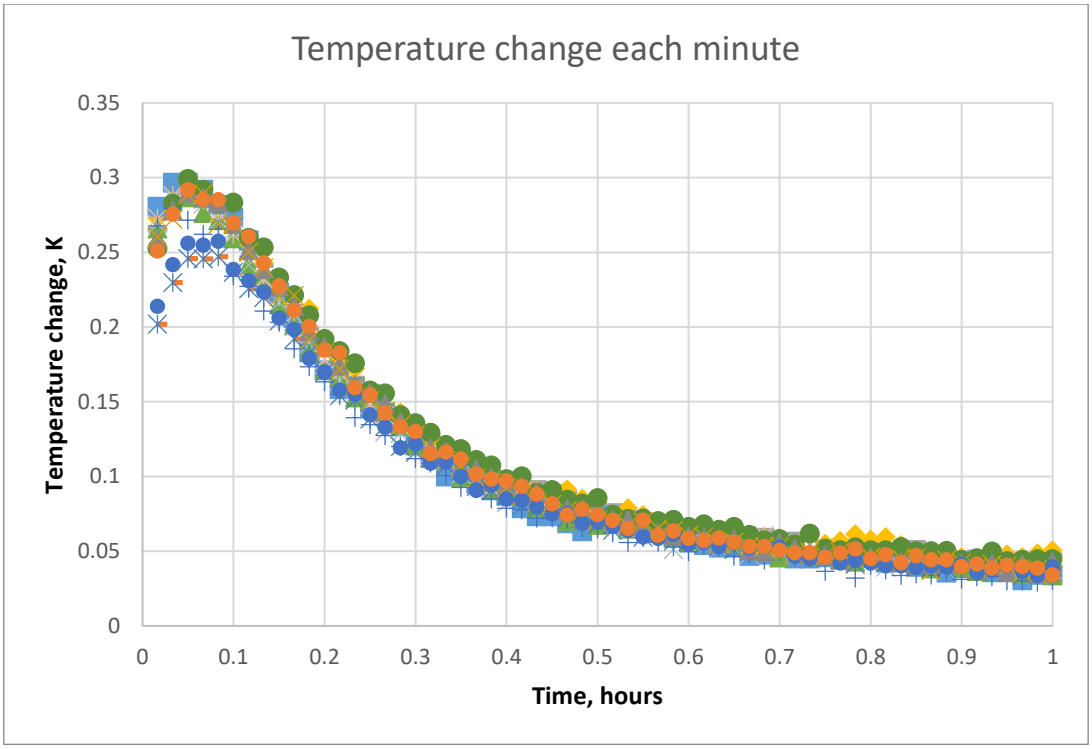

Figure 6.5 Example change in temperature over time during decay phase

The expectation is that as the temperature drops, the temperature difference decreases which slows the rate at which the internal temperature drops: that is, as time increases the temperature difference decreases, and the absolute change in temperature between each time point should also decrease. This is true, but only after the first five minutes. Before this, temperature change actually accelerates. This suggests heat is still being applied to the building at a relatively significant rate, despite the heater being off from T(0). If no heat were added, the rate of temperature change would decrease from the outset. The heater of course is still warm, and is still radiating some heat despite being switched off. Though it is not expected that all the heat is necessarily dissipated in this amount of time, after five minutes it appears it has dissipated sufficiently to allow the temperature to decay freely. Excluding the first five minutes of the decay from the models reduced the variation between the models and the observed temperature from between 7-9% to 5-7%. The heat radiated by the heater after it has been switched off is difficult to match in the EnergyPlus simulations as the heat rate is no longer specifically defined by the electricity monitoring.

In addition to addressing the heating rate after the blow heater is turned off, an analysis of what the decay constant would be at different points in time shows that retaining the same

decay period across buildings is crucial when applying the method. Figure 6.6 shows the change in the k-value calculated at different points in time over the decay period.

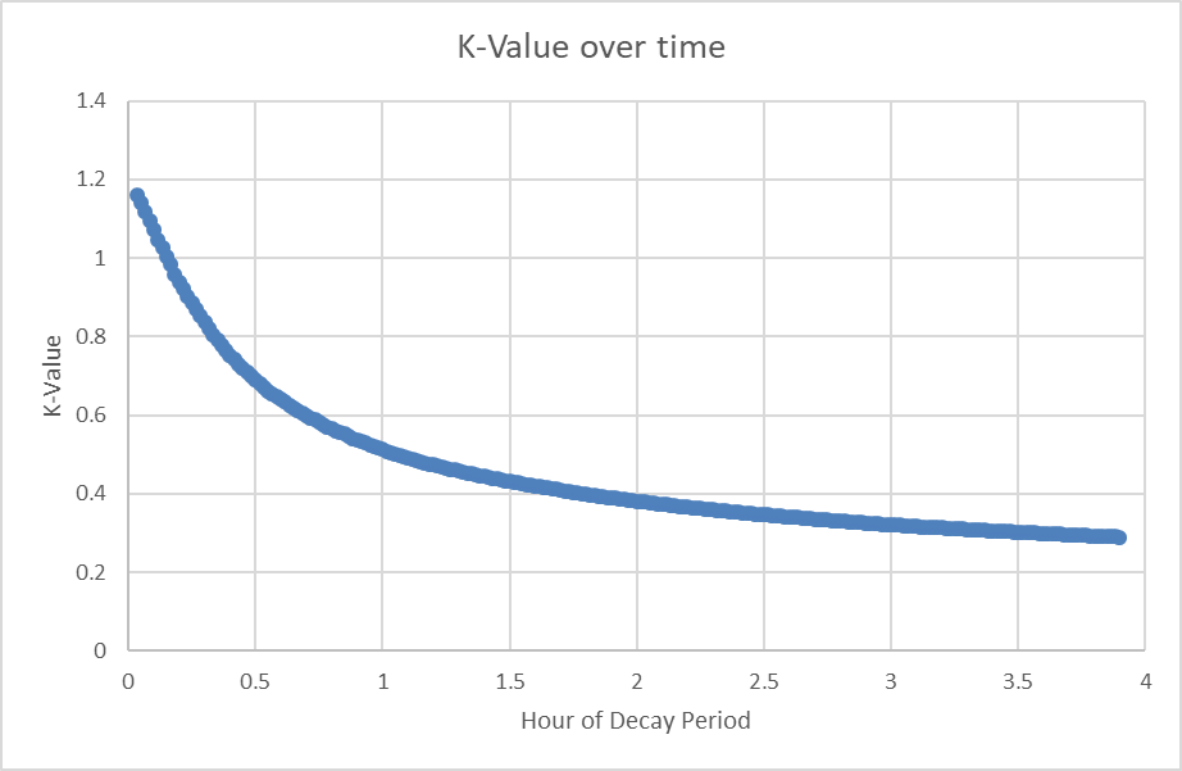

Figure 6.6 Calculated k-Value over time during decay test

Analysing different portions of the decay curve yields different results, regardless of which analysis technique is used. Figure 6.6 clearly shows that if the decay period is only defined as the first hour after the heating is switched off, then the k-value calculated is vastly different to the one calculated at four hours. Similarly, if the portion of the temperature decay that is analysed begins one hour after the heater is switched off, the k-value is again different. This is also true when using the Solver add-in to fit the best k-value to the data, as shortening the decay period increases the k-value, and choosing a later starting point reduces the k-value. It is important, therefore ,to analyse the same period of time, relative to when the heating is switched off, across all buildings.

The key points from this are that the analysis should use the earliest possible data in the decay curve, and decay for the same length of time in each experiment. For the case study, the earliest possible data is five minutes after the heating is turned off, and 3 hours 55 minutes is used as the length of time for the decay.

6.3 Field Experiments

Field Experiments of the decay method were carried out using Test Cell 2, in the same configurations as the co-heating tests. The same equipment set up detailed in Section 4.3 was also used.

To ensure a positive temperature difference, and therefore a drop in internal temperature over this period, the 2 kW blow heater was programmed using the digital timer to turn on at midnight and off at 2.00am. The thermostat remained set at 27 ^{0}C, though this is to simplify shifting between decay and co-heating test periods; achieving the set temperature is not critical for the decay test.

The internal temperature is taken as the average of the 27 HOBO temperature sensors placed throughout the building, and the external temperature is from the Bureau of Meteorology data from the Moorabbin Airport site. For each night in each test the temperature always dropped, providing valid decay data.

6.4 Calculated Average Method

6.4.1 Field Experiment Results

Using the method described in Section 6.2 the k-values for each curve have been calculated for each of the configurations using data collected in field. Table 6.1 shows the k-value for each night and the average across all nights for each configuration. The normalised RMSE is also displayed to show how well the average k-value explains the building behaviour.

Table 6.1 Calculated average decay constant results

	Configuration 1, Test A	Configuration 1, Test B	Configuration 2	Configuration 3
Night 1	0.300	0.281	0.311	0.285
Night 2	0.331	0.272	0.313	0.311
Night 3	0.285	0.243	0.279	0.366
Night 4	0.340	0.264	0.265	0.323
Night 5	0.317	0.334	0.474	0.300
Night 6	0.324	0.484	0.291	0.378
Night 7	0.391	0.347	0.468	0.611
Night 8	0.304	0.280	0.546	0.477
Night 9	0.357	0.261	0.399	0.316
Night 10	0.262	0.296	0.404	0.360
Night 11	0.272	0.306	0.346	0.354
Night 12	0.270	0.302	0.315	0.334
Night 13	0.242	0.255	0.429	0.313
Night 14	0.458	0.325	0.378	0.425
Average Decay Constant	0.318	0.304	0.373	0.368
Standard Deviation	0.055	0.058	0.081	0.084
RMSE	1.222	1.352	1.369	1.325
NRMSE	9.75%	9.16%	8.46%	9.37%

Table 6.1 displays the expected similarity between Configuration 1 Test A and Test B, but the average decay constant for Configuration 3 is lower than Configuration 2 which is against expectations. As the uncertainty in the HTC from the co-heating test indicated, these buildings are fairly similar and the small differences in performance may not be detected. The overlap between the decay constants for Configuration 2 and Configuration 3 may indicate a limitation on this version of the decay method, though the co-heating tests showed similar limitations when analysing these test cells.

All the decay constants estimated provided an NRMSE of less than 10%. This shows that across all nights of the tests these constants give good predictions of the building temperature profile.

Figure 6.7 shows the HTC for each configuration from Section 5.3.4 against the decay constant from Table 6.1.

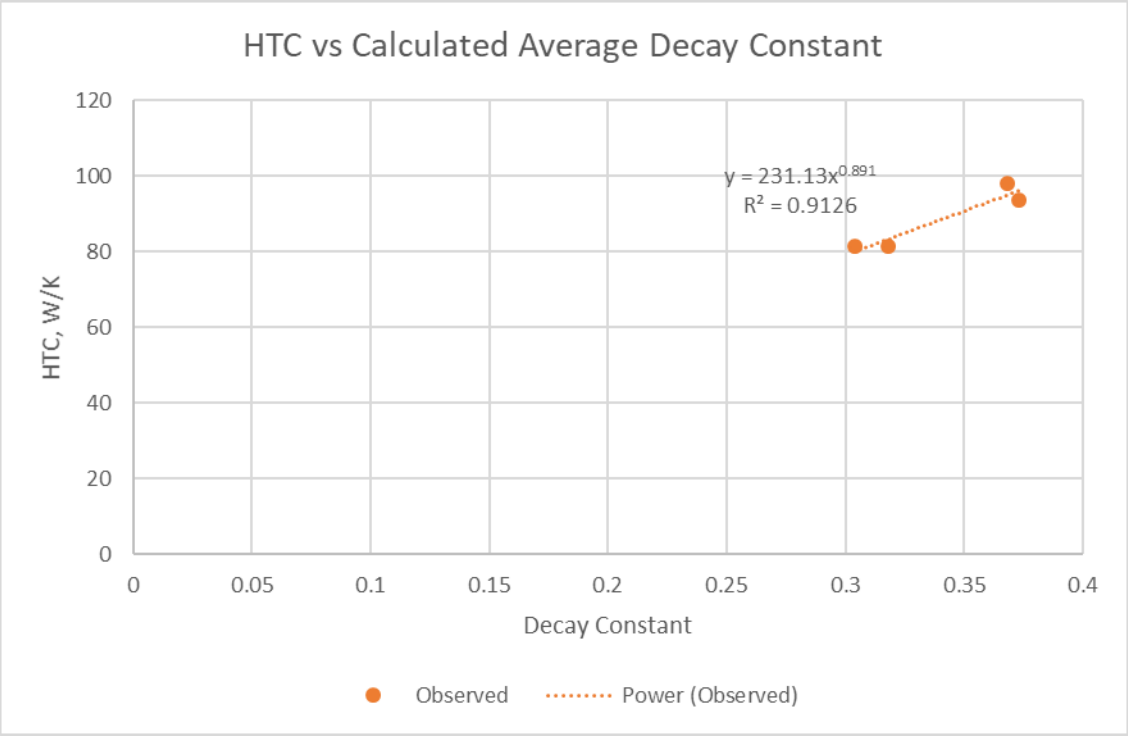

Figure 6.7 HTC vs decay constant, average decay constant calculated from field data

Figure 6.7 shows good correlation between the decay constant and the HTC for each of the four configurations ($R^2 > 0.9$). This relationship is modelled as a Power function as this fits the data very well and satisfies the logical notion of passing through the origin without

artificially supressing any constant. It is expected that if the decay constant is zero, then the building does not lose heat, and therefore should have a HTC of 0 W/K.

6.4.1.1 Uncertainty Analysis

The uncertainty analysis for the Experimental decay method assesses the influence of maximum or minimum temperature differences based on the uncertainty in internal and external temperatures. This follows the same approach as the Differential Sensitivity Analysis used in Section 5.4. Table 6.2 displays the actual and percentage changes in the decay constant due to the uncertainty in internal and external temperature readings.

Table 6.2 Uncertainty in calculated average decay constant

Configuration	Decay constant	Change in decay constant		% change in decay constant	
		ΔT +0.65 K	ΔT -0.65 K	ΔT +0.65 K	ΔT -0.65 K
1, Test A	0.318	-0.035	0.049	-11.01%	15.41%
1, Test B	0.304	-0.030	0.040	-9.87%	13.16%
2	0.373	-0.044	0.066	-11.80%	17.69%
3	0.368	-0.044	0.080	-11.96%	21.74%

Note: Negative values indicate a decrease in decay constant.

Changes in temperature readings cause significant variation in estimates of the decay constant. Reducing the temperature difference represents the largest risk; Table 6.2 shows an increase in the decay constant of up to 21.74% for Configuration 3. As the differences between the decay constants are small, the large influence of the uncertainty in temperature readings demonstrates a significant limitation of this analysis technique. Figure 6.8 displays the decay constants with the uncertainty represented by the error bars.

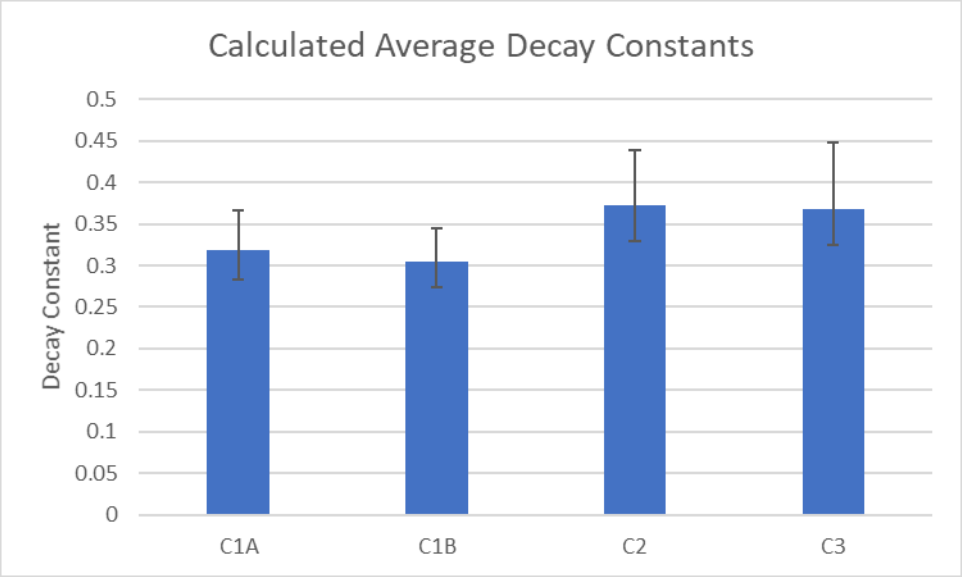

Figure 6.8 Calculated average decay constant

It is clear from Figure 6.8 that the uncertainty bars overlap, which reduces confidence that this method of analysing the decay constants is sophisticated enough to overcome the uncertainty in the measurements.

6.4.2 Simulated Decay experiments

To further test the application of the average decay constant, the array of models described in Section 4.4.5 have been analysed using this method. The models have been adjusted so that the simulation temperature has been controlled to match the observed temperatures until five minutes after the heater was turned off in the field experiments. As discussed in Section 6.2, this is to align the start times for the decay curve analysis as the blow heater was still radiating enough heat to the air to influence the decay rate. Figure 6.9 shows how the simulated results differ from the field experiments

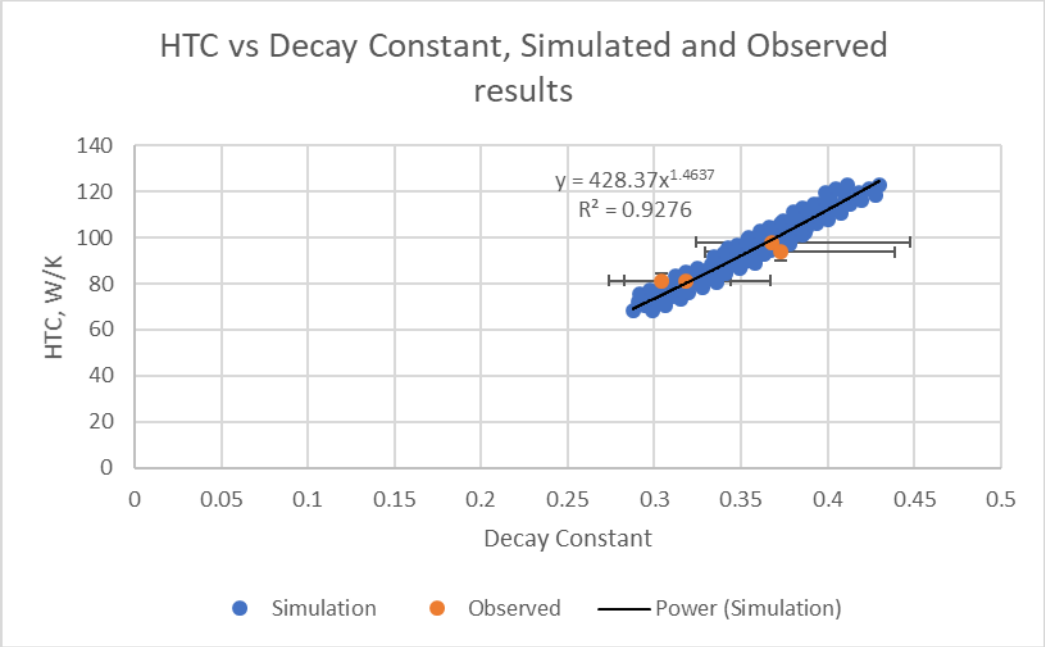

Figure 6.9 HTC vs average decay constant, field and simulated results

Figure 6.9 shows there is a good match observed and simulated data. There is good correlation in the simulated datasets between the decay constant and the HTC. There is a range of HTCs for each decay constant, which is not surprising given the complexity of heat transfer through a building and the relative simplicity of the decay test. It is also not surprising as the test cell's thermal mass is explicitly altered in the simulations, and this does not have any effect on the steady-state HTC, but does influence the dynamic response represented by the decay constant.

6.4.3 Predicting the HTC from Calculated Average Decay Constants

Using the simulated data as the basis for the model, regression analysis provides the function for predicting HTC from the decay constant as Equation 9

Equation 9 HTC estimate using calculated average decay constant

$$HTC = 428.37k^{1.4637}$$

Applying this function back to the simulated data shows a variation of between +8.06% and – 6.64% between the simulated HTC and the HTC estimated from this function.

If this function is applied to the decay constants calculated from the observed test cell data, it is shown that the variation underestimates the HTC by a maximum of 7.79%, and overestimates by up to 7.96%.

If the uncertainty in the decay constant calculation is accounted for, however, the uncertainty in the HTC predicted from the function increases dramatically. Table 6.3 shows the upper and lower estimates of the HTC based on the upper and lower bounds of the decay constant.

Table 6.3 HTC estimates from calculated average decay constant

	Estimates from field co-heating test		Estimates from decay constant	
Configuration	HTC	HTC range	HTC (% difference)	HTC range
1, Test A	81.34	77.60 – 85.34	80.08 (-1.55%)	67.51 – 98.77
1, Test B	81.31	77.97 – 84.88	74.97 (-7.79%)	64.40 – 89.84
2	93.68	89.99 – 97.41	101.14 (7.96%)	84.17 – 128.38
3	97.91	93.81 – 102.34	99.16 (1.28%)	82.30 – 132.25

The difference on a single HTC estimate for any of the configurations is within 10% of the estimated value from the co-heating test. However, Table 6.3 shows that if the uncertainty in the decay constant is accounted for, then the uncertainty in the HTC estimate could be a range up to 50 W/K. This could underestimate the HTC by up to 20.8%, or overestimate it by up to 37.0%.

This large uncertainty range is linked to the decay constant calculation relying on just two data points: the internal temperature at the start of the decay period, and the internal temperature at the end, four hours later. The change of +/-0.65 K can dramatically change temperature differences at the end of the decay period. Uncertainties in this range are not uncommon – note that the uncertainty on the Bureau of Meteorology air temperatures is +/-0.3 degrees and is calibrated to the current international standard. This makes the method fragile under standard conditions, particularly in low performance houses where temperature differences at the end of the decay period are expected to be closer to zero.

6.5 Excel Solver Method

As explained in Section 6.2, the Excel Solver method for determining the decay constant uses a model of the internal temperature defined by the Law of Cooling equation and estimates the internal temperature at each minute of the decay test based on a given k-value. This is compared with observed temperatures, and both the R^2 and RMSE are calculated to determine goodness of fit and closeness of match for the entire decay data set. The Solver function is then engaged to find the minimum possible RMSE by changing the k-value. The value that gives the smallest RMSE is recorded as the decay constant. As noted in Section 6.2, this provides greater use of the entire data set and provides a decay constant that better describes the test cell's entire behaviour rather than only observing initial and final conditions.

6.5.1 Implementation of the Law of Cooling

Four versions of the Cooling model were tested to determine how the Law of Cooling equation may be adjusted for variable ambient temperature. These were explained in Section 6.2, and are summarised in Table 6.4.

Table 6.4 List of cooling models for determining decay constant

Model	Internal temperature, T_0	External temperature, T_a	Model ID
1	Initial	Initial	II
2	Initial	Average	IA
3	Initial	Updated each minute	IM
4	Updated each minute	Updated each minute	MM

It was found that all the models were capable of producing a HTC estimate within 10% of the observed Co-Heating result. Model MM however provided the best estimate of the temperature decay profile, and has therefore been used to calculate the decay coefficients. Analysis of the models can be found in Appendix B.

6.5.2 The MM Model

The MM model may be considered as a chain of decay curves using Equation 7 as described below:

$$T(0) = Observed\ Temperature$$

$$T(1) = T_{a(1)} + \left(T(0) - T_{a(1)}\right)e^{-kt}$$

$$T(2) = T_{a(2)} + \left(T(1) - T_{a(2)}\right)e^{-kt}$$

$$T(n) = T_{a(n)} + \left(T(n-1) - T_{a(n)}\right)e^{-kt}$$

Note that the time term 't' is constant and set to the value of the timestep in hours. In this research the decay was measured in one minute time steps, so this is set to 1/60.

As noted above, once this chain is set up to estimate the internal temperature for each timestep in the decay test, the Solver function is engaged to find the value of k that minimises the difference between the model and observed temperatures.

6.5.3 Estimating the Decay Constant

Following the steps above, the MM model was used to calculate the decay constant for each configuration. Figure 6.10 shows the initial results.

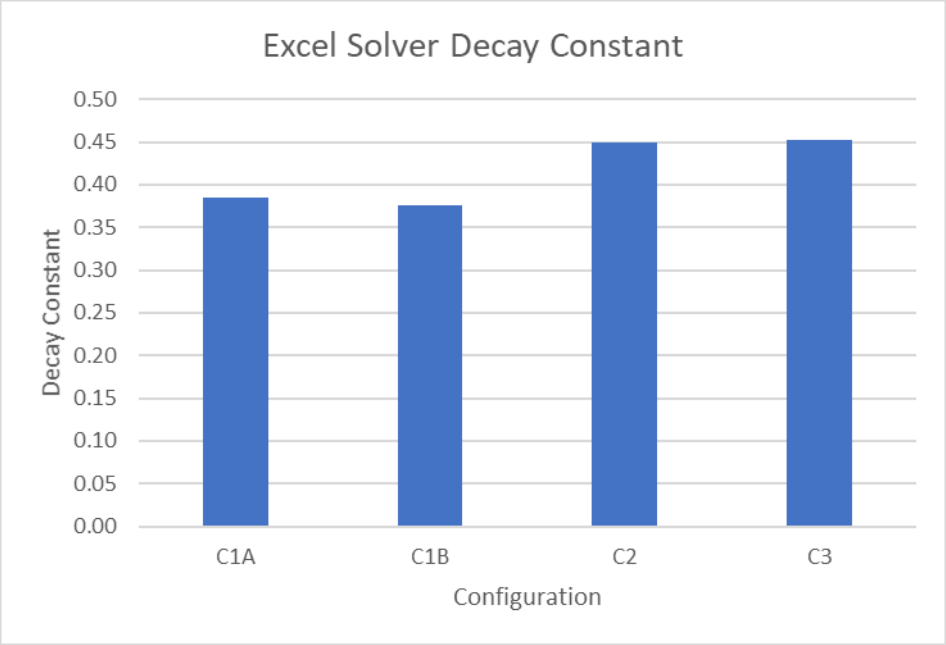

Figure 6.10 Decay constants determined by Excel Solver analysis

Figure 6.10 shows again there is not much difference between configurations 2 and 3. Configuration 3 has higher a decay constant than Configuration 2, which matches the

expectation that the thermal shell of Configuration 2 is better insulated than Configuration 3, but the difference between these configurations is less than the difference between the two Configuration 1 tests that are supposed to be the same. This is not surprising given that the uncertainty analysis conducted on the co-heating test results indicated there may not be a detectable difference between the two configurations.

The NRMSE for each configuration was below 8.5%, which is a smaller difference than the calculated average decay method. This is expected as this approach to analysing the decay profiles should allow for greater flexibility and adjustment to the specifics of the experiment conditions rather than the limited data inputs for the calculated average method. Figure 6.11 shows the relationship between the Excel Solver decay constant and the HTC for each configuration.

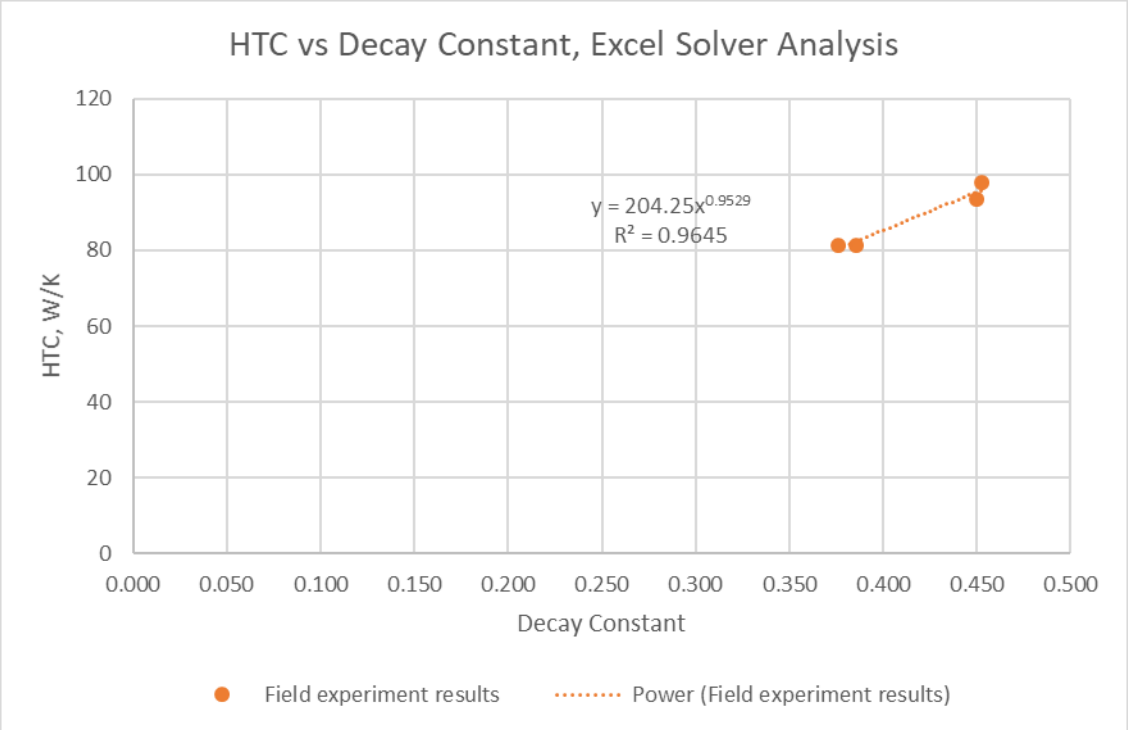

Figure 6.11 HTC vs Excel Solver decay constant

There is a high correlation between the decay constant and the HTC, Figure 6.11 showing an R^2 value of 0.96, though based only on the case study data set no definite conclusions can be drawn.

6.5.3.1 Uncertainty Analysis

Uncertainty analysis was conducted in the same fashion described in Section 6.4.1. Table 6.5 displays the results.

Table 6.5 Uncertainty analysis results for Excel Solver decay method

Configuration	Decay Constant	Change in decay constant		% change in decay constant	
		ΔT +0.65 K	ΔT -0.65 K	ΔT +0.65 K	ΔT -0.65 K
1, Test A	0.385	-0.034	0.041	-8.26%	10.04%
1, Test B	0.376	-0.032	0.038	-7.69%	9.28%
2	0.450	-0.042	0.052	-10.17%	12.56%
3	0.453	-0.043	0.053	-10.40%	12.90%

The maximum uncertainty in the decay constant due to the uncertainty in temperature readings is +12.90%, -10.40%. This is a smaller variation than observed in the calculated average analysis, which indicates that the Excel Solver analysis is more robust. Figure 6.12 shows how the uncertainty relates to the HTC.

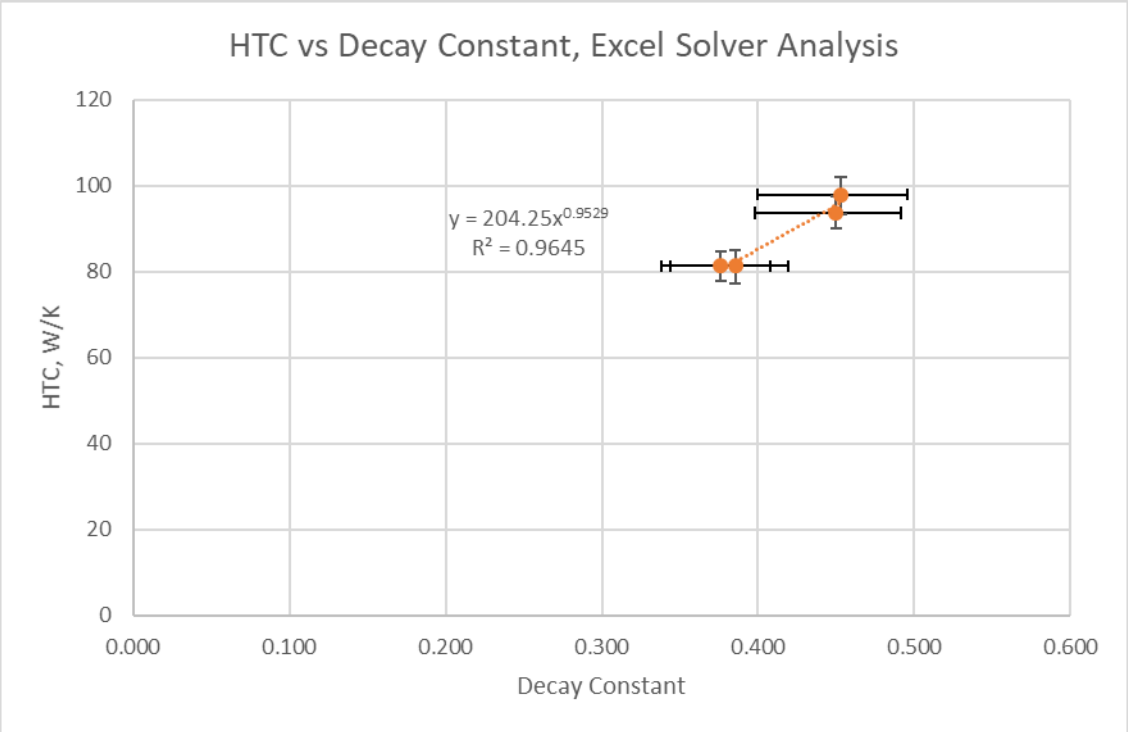

Figure 6.12 Uncertainty analysis of HTC vs decay constant from Excel Solver analysis

As with the calculated average, the error bars for each configuration in Figure 6.12 overlap. This shows again that the uncertainty in temperature measurements limits conclusions that can be drawn from this decay analysis about building performance.

6.5.4 Simulated Decay Experiments

To expand on the field data, the simulated decay curves have been analysed using the Excel Solver method. This uses the same EnergyPlus outputs described in Section 6.4.2, but applies the Excel Solver analysis method. Figure 6.13 shows how the HTC estimates and the decay constants for the simulations compare against the field data.

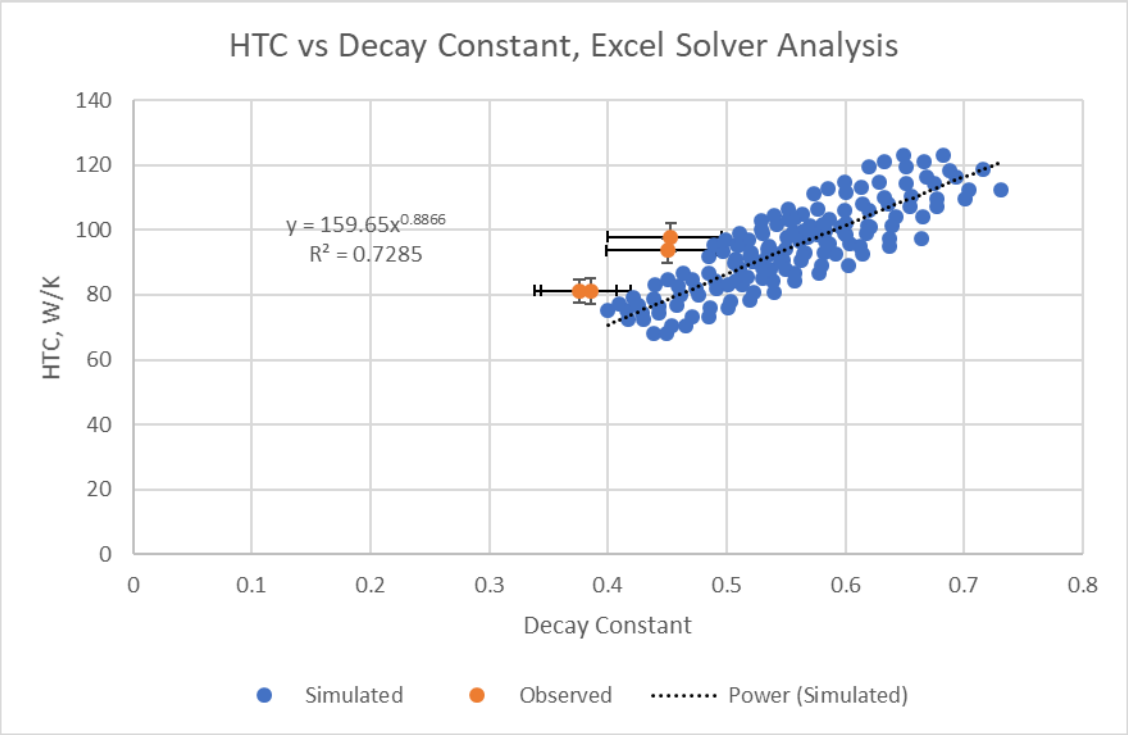

Figure 6.13 HTC vs Excel Solver decay constant for simulated decay curves

Figure 6.13 immediately shows that the simulated correlation between the decay constant and the HTC is not as strong as the calculated average simulation analysis. In this case the R^2 value is 0.73, compared with 0.928.

The error bars from the observed data overlaps with the edge of the simulated cluster, however does not cross the trend line as the calculated average method did. This suggests that using simulated data to predict the observed HTC will not produce better initial estimates than the calculated average method.

6.5.5 Predicting the HTC from Excel Solver Decay Constants

Using the same approach described in Section 6.4.3, a regression analysis of the simulated dataset shows the function for predicting HTC from the decay constant in Equation 10:

Equation 10 HTC estimated using Excel Solver decay constant, simulated correlation

$$HTC = 159.65k^{0.8866}$$

This equation is markedly different from the calculated average HTC function, but this is entirely due to differences in size of the decay constant. The Excel Solver method calculates larger decay constants, and so the correlation between these and the HTC is different from the correlation determined in Section 6.4.3.

Table 6.6 shows the estimated HTCs of each configuration using this function, and the range associated with the uncertainty in the decay constant.

Table 6.6 HTC estimates and uncertainties from Excel Solver decay analysis using simulation correlation

Configuration	Estimates from field co-heating test		Estimates from Excel Solver decay constant	
	HTC	HTC Range	HTC (% difference)	HTC Range
1, Test A	81.34	77.60 – 85.34	68.55 (-15.73%)	63.17 – 75.02
1, Test B	81.31	77.97 – 84.88	67.07 (-17.52%)	62.04 – 73.07
2	93.68	89.99 – 97.41	78.64 (-16.05%)	72.13 – 86.59
3	97.91	93.81 – 102.34	79.10 (-19.21%)	72.44 – 87.26

The HTC predictions shown in Table 6.6 all underestimate HTC by more than 15%. The HTC range is much smaller; the maximum variation is 14.82 W/K. This makes the Excel Solver analysis more precise, but less accurate.

This is due to the decay constants calculated for the simulated data not representing the simulated decay curves as accurately as the observed decay constants represent the observed decay curves. The NRMSE for the observed data ranges from 7.7% to 8.6%, whereas the simulated data ranges from 11.1% to 14.5%. This is also the likely explanation

for the reduced correlation between simulated decay constants and HTC estimates from simulated co-heating tests.

If the correlation between the decay constants and HTC estimates based on field data is used instead, the predictions of HTC are understandably more accurate. This changes the HTC estimate as shown in Equation 11:

Equation 11 HTC estimated using Excel Solver decay constant, field test correlation

$$HTC = 204.25k^{0.9529}$$

Table 6.7 shows the HTC estimates if this function is used instead.

Table 6.7 HTC estimates and uncertainties from Excel Solver decay analysis using field data correlation

Configuration	Estimates from field co-heating test		Estimates from Excel Solver decay constant	
	HTC	HTC Range	HTC (% difference)	HTC Range
1, Test A	81.34	77.60 – 85.34	82.32 (1.20%)	75.40 – 90.70
1, Test B	81.31	77.97 – 84.88	80.42 (-1.10%)	73.96 – 88.18
2	93.68	89.99 – 97.41	95.42 (1.86%)	86.96 – 105.83
3	97.91	93.81 – 102.34	96.02 -1.92%)	87.36 – 106.71

The range created from the uncertainty displayed in Table 6.7 is slightly larger than that in Table 6.6, and is greater than the uncertainty from the co-heating test, but the HTC estimate is within 2% of the estimate from the co-heating test. The uncertainty in the decay constant estimate means the difference between the three configurations cannot be absolutely stated, but it could be said it is likely that Configuration 1 Test A and Test B have lower heat losses than configurations 2 and 3.

The function is based only on the four case study data points. Further research is required to apply the decay constant to other buildings and building types (for example, heavy thermal mass structures) to determine whether this function is adequate, or if different building types will require different estimates.

6.6 Comparison with Co-Heating Test

6.6.1 Implementation of the Tests

Collecting data to evaluate the building via the decay method was initially designed to be less invasive than the co-heating test, only requiring internal and external temperature data to be collected. The analysis showed that the timing of the decay curve is important. Changing the interval between when the heater was disengaged and the 'start' of the decay curve changed the building's decay constant. The case study was conducted on a building which had no internal heat gains from people or appliances during the decay period, though it was seen that the heat radiating from the heater in the minutes after it was turned off impacted the calculation of the decay constant. It is expected there will be some impact on the decay method due to internal heat gains from occupants and appliances (such as fridges) left running during the decay period. Additional heat gained during the observation period of 2.00am to 6.00am may provide false results by flattening the decay profile, or void the test by increasing the internal temperature. Further research is required to determine the size of this impact, and what adjustments to the analysis are needed to maintain the integrity of the HTC estimate.

It may be possible to conduct decay method testing on buildings without requiring an active heat source. Such a method would rely on using some other trigger to indicate the 'start' of the decay curve, such as temperature difference. Thermal mass will very likely impact on the analysis here as varying start times will mean the building's thermal mass will be in differing states of discharge. This alternative is in line with the original intention of the decay method as it will decrease the amount of equipment on site, and have a reduced impact on the occupants' lifestyle. Based on the analysis conducted here, it will create additional uncertainties in the decay constant estimate that will need to be addressed.

In the case study, the analysis was carried out on the basis that internal temperature was an average of the central array of sensors. Further study is required to evaluate the impact on HTC estimates if a single temperature sensor is used instead. Analysis as to the overall influence of air mixing in the decay method has not been carried out, and a sensitivity analysis on the effects of stratification will be required to evaluate the potential influence.

The decay method should require similar numbers of temperature sensors to the co-heating test. The versions of the decay method analysed here do in fact require a heater, as it is has

been an important part of determining the decay period's starting parameters. Electricity monitoring does not appear to be essential where there are no other appliances heating the zone; however, it is almost certain that any in field application will require electricity monitoring. It is not plausible to expect no appliances will be on during the decay period. In addition, occupants living in the house during the test will provide heat to the zones, and this will influence the shape of the decay curve. The effects of heat gained from occupants and household appliances should form part of further study into more complex buildings and their impact on the decay method results.

The decay method improves upon the co-heating test experiments. Even though the experiments take a similar number of days, the decay method experiment window is limited to six hours overnight. This allows for the building to be used normally during the day, whereas the co-heating test does not allow for this. The impact of appliances and occupants inside the building during the pre-heat and decay periods of decay method Testing will influence the rate of internal temperature change in some way, and additional research is required to determine the full extent of the impacts. This is required to determine whether a building can truly be lived in during the decay method testing.

6.6.2 Analysis Process

The analysis procedure of the co-heating test is arguably simpler than the decay method analysis. Analysing average readings from the co-heating test through a multiple regression process is straightforward and proven by previous research to account acceptably for the solar and wind variables. The involved process of organising and splitting the data into the relevant pieces and running the Solver function, possibly repeatedly, for the decay method may appear daunting; however, in this study the process was automated using Excel macros. It is likely the decay method in this form requires more expert knowledge to interpret the results, particularly surrounding the test's reliability, as there may be limits on internal/external temperature difference within which the decay method can be used. The reliability of the decay constant when using the Excel Solver can be easily shown as the method is based on minimising the RMSE. The larger this value is, the less the decay constant alone explains the rate of temperature lost during the decay period. This can also be implemented in the calculated average method but is not an intrinsic part of the

calculation. An evaluation of the minimum acceptable NRMSE value for the Excel Solver method should form part of additional research into the limits of the decay method.

Analysis of the uncertainty in the decay method is simplified as there are less data inputs to modify. The co-heating test required separate analysis of the power, temperature, solar and wind inputs, whereas the decay method only uses temperature. Lower values of NRMSE for the initial decay constant analysis did not correspond to lower uncertainties in the final estimates of HTC.

6.6.3 Evaluation of the Building

The decay method shows promising signs for estimating a HTC similar to that of a co-heating test in a way that still evaluates the building system but does not rely on a steady internal temperature to be set up. Both the calculated average and Excel Solver methods for calculating the decay constant were able to show differences between some configurations; however, the uncertainty analysis showed that uncertainties from standard equipment resulted in large uncertainties in final HTC estimates. The Excel Solver method showed a smaller range of uncertainty in field testing, but the function based on simulated data was inaccurate. Using field data means relying on only four data points, but it improved the accuracy of Excel Solver estimates.

Both versions of the experimental decay method suffer from uncertainties in temperature measurements creating large uncertainties in the calculated decay constant. Further research is required to evaluate how to minimise these uncertainties. In the current form, uncertainties in HTC estimates from the decay method are greater than uncertainties from the co-heating test.

6.7 Conclusion

The decay method requires similar equipment and set up as the co-heating test. Where the decay method improves upon the co-heating test is the ability to conduct it while the building is still in use. The test period for the decay method is ultimately limited to a six hour overnight window, allowing for normal operation of the building during the day. It is unclear how much influence occupying the building during the decay test will have on results.

Both the experimental methods showed a significant sensitivity to uncertainty in the temperature measurements which resulted in a comparatively large uncertainty in the decay constant calculations in both sets of analyses. While differences between configurations were shown in the decay constant calculated by both analysis methods, uncertainty in the decay constant means the experimental decay method cannot show definitively that the thermal shell of the configurations are different. By comparison, the co-heating test showed that the thermal shell in Configuration 1 has a lower heat loss than Configurations 2 and 3. Uncertainty in the co-heating test was also unable to discern the difference between Configurations 2 and 3.

Of the two experimental analyses, the Excel Solver method proved more reliable than the calculated average method. Predictions of internal temperature made using Excel Solver figures showed a better match to the observed internal temperature than the calculated average method. The Excel Solver method was also less sensitive to the uncertainty in temperature readings.

The experimental and simulated results aligned exceptionally well when using the calculated average method, but did not align when using the Excel Solver approach. This is due to differences between simulated temperature profiles and observations, and differences in the analysis approaches.

The final HTC figures reported by the experimental decay methods are well within 10% of HTC estimated by the co-heating test. This shows that both approaches have the potential to estimate HTC with the same accuracy as the co-heating test. The largest issue with experimental decay method HTCs is that the uncertainty in the HTC estimate is significantly larger than that of the co-heating test.

While it has been shown that both experimental methods provide good estimates of the HTC, the Excel Solver decay method is recommended as the better approach. This method requires more work in the analysis process to set up the Excel Solver function. However, it is less sensitive to uncertainty in temperature measurements and makes greater use of the field data set. The Calculated Average decay method ultimately uses only two internal temperature data points. This means a large portion of the decay profile is ignored, and any changes in those points is more likely to have a significant influence. The MM model used in the Excel Solver analysis also provides better response to external temperature changes as the predictive model is adjusted at each time step to account for variations in external temperature.

This case study has shown the possibility for using the Experimental decay method to estimate a building's HTC. This represents a step forward in the field of rapid building assessment, adding to the tools available for evaluating a building's thermal performance.

Chapter 7 - RMSE Decay Methods

The RMSE decay methods are based on the same data collection as the experimental decay methods. Both RMSE decay methods use building simulations informed by field data collection to provide the final performance analysis. The 'temperature' RMSE method uses the Root Mean Square Error (RMSE) as a measure of closeness between simulated temperatures and experimental reality. The 'measured heat pulse' method also uses RMSE, but in addition analyses the total energy input during the test's pre-heating phase. Using these analyses, it is then shown what the likely range of HTCs that a building with its particular decay signature may have. This improves upon the experimental decay methods by providing direct links to estimating the building's HTC.

7.1 RMSE Process

As noted previously, the RMSE decay methods use exactly the same data collection as the experimental decay methods. The measured heat pulse method requires heating energy data in addition to temperature and weather data. The following steps form the procedure for assessing a building's heat loss once field data is collected. These steps do not necessarily follow in order; they are at the discretion of the assessor regarding preferred workflow with the building simulation program.

1. A series of buildings similar to the test building are constructed in the simulation program, in this case EnergyPlus.
2. Co-heating tests are simulated on these buildings. The models should represent sensible variations on the base model created from a site assessment. This may be expanded to include the extreme range of HTCs expected from the building should no initial result be settled on. Any noticeable gaps should be filled by creating an additional model with the expected adjustments to the thermal shell to result in that HTC.
3. Field data regarding the internal and external conditions during the monitored period are added to the building model. This data should be continuous for the entire 10 to 14 day period to ensure the building shell's thermal history is accurate and influences of thermal mass will be accounted for as much as possible during the

decay test period. In this study, air temperatures of the ceiling and sub-floor zones are also included.

4. Decay tests are simulated on the building models to obtain predicted internal temperature decay profiles.
5. The 2.00am-6.00am internal temperatures forming the decay profiles are compared with the observed data using the RMSE.

6a. **Temperature RMSE only**: The building model, or models, with the smallest RMSE is identified. The building's HTC is deemed to be in the range of the HTC provided by that building model or models.

6b. **Measured Heat Pulse only**: The total sum of heat energy input observed during the pre-heat phase (midnight to 2.00am) over all days of the test is compared with the simulated data. The estimated building HTC is based on the simulations with nearest matching internal temperature RMSE and energy requirements.

It is not expected there will be a building model that perfectly matches observed temperature decay profiles or energy demands, and it is consequently unlikely to determine exactly what the HTC of the building is. However, it is also expected that such a high level of accuracy is not needed, and the ability to identify the building within 10% of the HTC should be very realistic.

7.1.1 RMSE Simulations

The RMSE simulations are carried out on the model arrays detailed in Section 4.4.5 and used in previous chapters. In this case, the array both provides a wide range of models against which to compare decay curves, and also shows how the method may adjust for incorrect data entry. The assumed thermal mass, or conductivity of other construction elements, is likely to influence both the decay curve's shape and the HTC estimates, and it is important to see how robust the test is if incorrect assumptions are made in the initial stages. By creating a larger array of models with varying initial assumptions we can observe how well the RMSE methods are at identifying erroneous results, and if the analysis can be carried out based only on temperature decay, or if energy data is also required.

For this case study the same simulation is used for both versions of the RMSE decay analysis; the 'temperature' method simply ignores the simulation's energy output.

7.2 Temperature RMSE Method

The basis of the temperature RMSE decay analysis is that the model with the smallest RMSE is the model that best matches the test cell, and as such the HTC estimated from the co-heating test simulated on this model is the best estimate of actual HTC. The NRMSE of the simulated decay tests have been charted against the simulated HTCs in Figure 7.1 below.

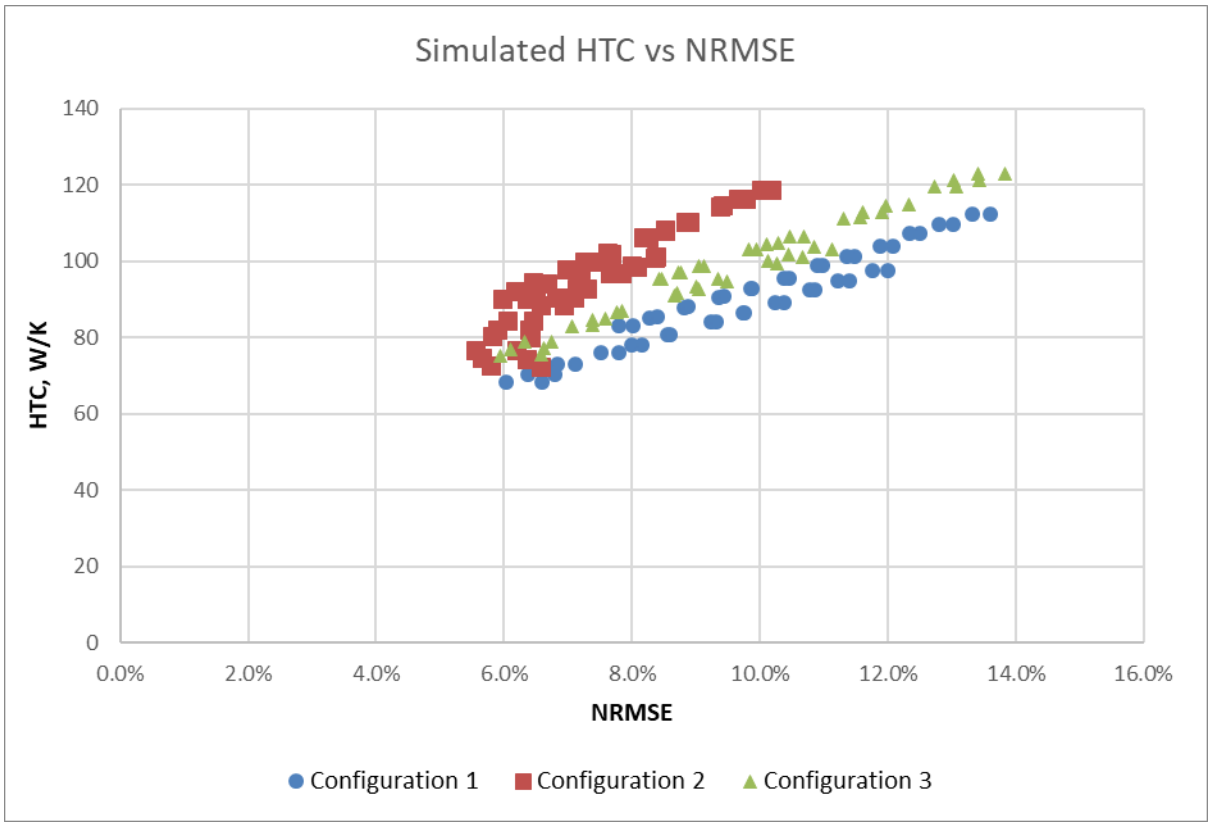

Figure 7.1 NRMSE of decay simulation vs simulated co-heating test HTC

The trend visible in Figure 7.1 is already apparent: as NRMSE reduces, HTC also reduces. As is already known from chapter 5, the HTCs are 81.34 W/K, 93.68 W/K and 97.91 W/K for configurations 1, 2 and 3 respectively: this approach is shown to underestimate building heat loss. Figure 7.1 clearly shows lower NRSMEs for each configuration, predicting a HTC that is below observed HTC.

An alternative view of this data is shown in Figure 7.2, comparing the NRMSE with the difference between simulated HTC and the relevant observed HTC for each configuration.

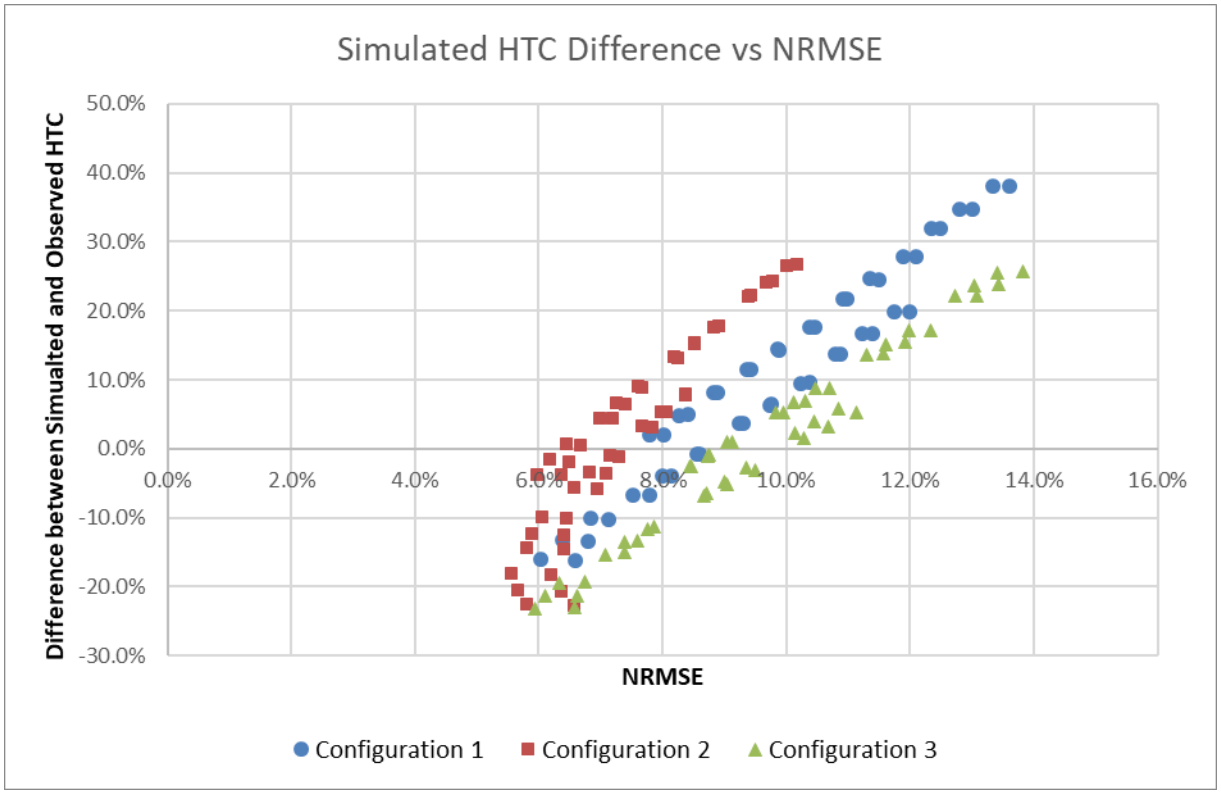

Figure 7.2 NRMSE of simulated decay vs difference between simulated and observed co-heating test HTC

Figure 7.2 shows the higher NRMSE overestimates HTC, and the lowest NRMSE underestimates it. Each of the configurations has a model which predicts a HTC that is very close (within 0.5%) to observed HTC; however, these models have differing NRMSEs. Figure 7.2 also shows there are multiple models that closely predict HTC for each configuration; however, these have differing NRMSEs. There is also no correlation between a particular NRMSE and an accurate HTC across the three configurations. A NRMSE of 10% in Configuration 3 would predict HTC to within 5% of observed HTC, but the same NRMSE in Configuration 2 overestimates HTC by more than 20%.

Figure 7.1 and Figure 7.2 both show that models with different HTCs may have the same NRMSE. If two models were to show the same NRMSE there would be no way to determine which of the related HTCs would be more accurate based only on this value. Table 7.1 shows HTC predicted by the model with the lowest NRMSE for each configuration.

Table 7.1 RMSE prediction of HTC

Configuration	NRMSE	Simulated HTC (W/K)	Observed HTC (W/K)	% difference from observed HTC
1	5.9%	70.39	81.33	-13.4%
2	5.4%	78.98	93.68	-15.7%
3	6.0%	79.02	97.91	-19.3%

As noted from discussion of Figure 7.1, the simulated HTC from the model with the lowest NRMSE for each configuration is much lower than observed HTC from field experiments. The spread of HTCs predicted by the simulations is also much smaller than the spread observed in field. HTCs predicted for Configuration 2 and 3 are much closer to Configuration 1 than was observed.

7.2.1 Summary and Discussion

7.2.1.1 Reliability of the NRMSE in HTC Prediction

Based on the arrays modelled a number of observations can be made. First, it is clear that NRMSE is insufficient as the sole tool for confidently predicting HTC. Simply taking minimum NRMSE of all the building models does not provide a reliable figure for the building's HTC. In fact, the minimum NRMSE only serves to provide an indication of which building model will give the smallest HTC, not the most accurate one. The expectation was that the relationship between the HTC and NRMSE should be parabolic, not linear; that is, having a true minimum, rather than simply showing the lowest value of the simulated set. Overall, the simulations showed a linear correlation, and the NRMSE did not increase as the HTC was underestimated by greater margins. This could mean not enough models were created, and there is some hint that NRMSE is approaching a minimum at 5% for Configuration 2; however, this is occurring when HTC is being underestimated by more than 15% and therefore does not solve the method's inaccuracy. The changing of thermal mass and ceiling R-value did have an impact on the simulations, as differences were shown in NRMSE and HTC when compared with base models. All other things being equal, increases in thermal mass and increases in ceiling R-value reduced NRMSE and reduced HTC. Though these may

not be realistic representations of the test cell, they served to show the method has limitations beyond inaccuracies in the thermal shell, and these are not the root cause of inaccurate HTC predictions. The issue lies in determining a 'close' match, and the differences between the observed decay test temperature profile and the simulated temperature profiles from the EnergyPlus models. The assumption inherent in the method is that the model and the building are truly similar, and temperature profiles are recognisably alike, and while temperature profiles are somewhat similar there are obvious differences.

7.2.1.2 Shape of the Simulated Decay Curves

When observing the raw decay curves, it is immediately clear that the simulated curve behaves in a very different fashion to the observed curve for any given day. This is not surprising due to complexity of thermal simulations, though it highlights the flaws of using only the RMSE calculation and shows why there may be limits on acceptable initial conditions for a valid decay test.

In all simulations across all configurations, the simulation shows a rapid decrease in internal temperature from the point when heating is turned off. Change in observed temperature is much slower by comparison, despite the simulation being subjected to the same initial conditions. Figure 7.3 shows an example from Configuration 1, and Figure 7.4 from Configuration 3.

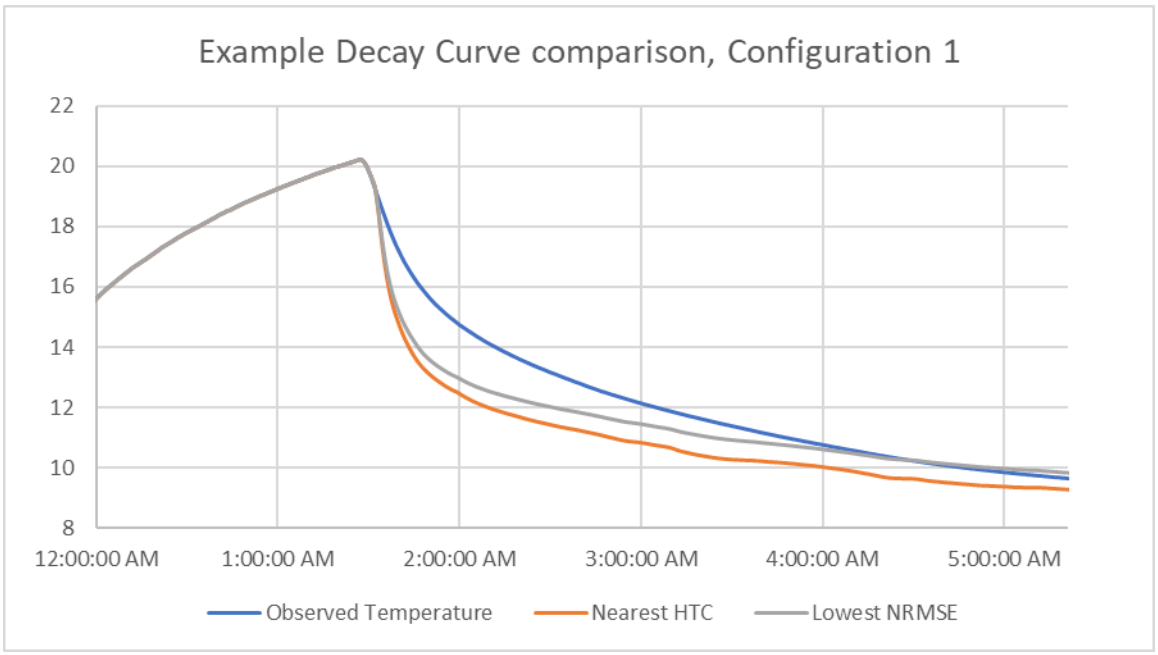

Figure 7.3 Example of simulated and observed temperature decay profiles, Configuration 1

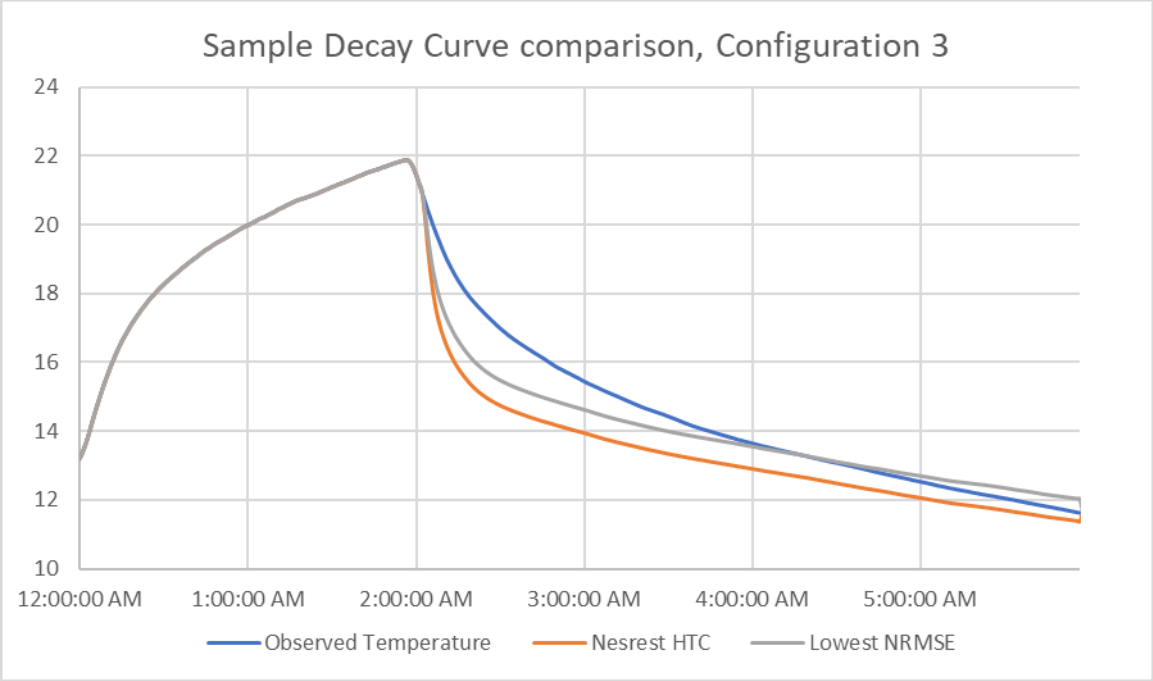

Figure 7.4 Example of simulated and observed temperature decay profiles, Configuration 3

It is not clear why this rapid change exists, and it is still present when the internal temperature set point is lowered. Part of the functionality of the 48 models per configuration was to overcome this, but no combination of insulation or thermal mass reconciled the simulated decay profile with observed decay profiles.

It is this initial rapid drop in temperature that causes the direct relationship between RMSE and HTC. For any given configuration, while it may be lessened by reducing the heat transfer, this drop still exists, and is largely the reason why the RMSE calculation is unable to reliably show a true HTC. This is because as HTC becomes smaller, simulated temperature does eventually rise above observed temperature, but it does not do so by a margin great enough to skew RMSE back away from the minimum for the set.

This sharp drop could be caused by the heat-balance equation used in EnergyPlus and the assumption of a 'well mixed' air volume overestimating the heat transfer between the air volume and surface materials. Dewsbury (2011) also noted that the Chenath engine was underestimating internal air temperatures so this may not be limited to the EnergyPlus thermal calculations. While the experiments were set up to mix air as well as possible, it will not be perfectly mixed and there will be differences in the local air temperature throughout the test cell. This aligns with observations by Hitchin, Delaforce & Martin (1993) that air temperature response is much slower than predicted by models using a well-mixed

assumption. Additional research that accurately monitors surface temperatures in multiple locations is required to validate this hypothesis.

One approach to overcoming this would be to simulate the decay curve from a point where temperature differences are lower. Allowing the simulation model to operate in 'free running' or 'unconditioned' mode from a later point in the decay period could reduce this error. A sub-set of the simulations were re-run with the simulation heating engaged until 2:30am. Figure 7.5 shows results of the original four-hour decay, and the revised 3.5 hour decay, against relevant HTCs.

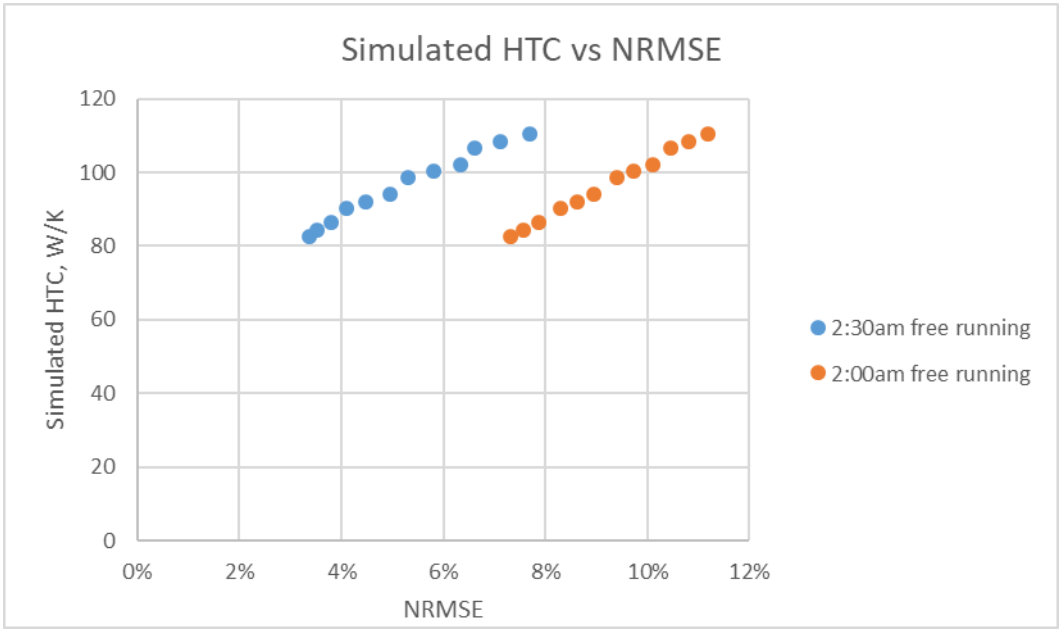

Figure 7.5 Comparison of NRMSE simulations with delayed free running mode start

While this shows an improvement in NRMSE, it has not changed the underlying issue: the ability to predict HTC by using the minimum NRMSE figure. All that has happened is NRMSE is showing the exact same pattern, shifted down the x axis. It is clear that the NRMSE figure in isolation cannot provide a reliable HTC estimate.

7.2.1.3 Additional Parameters

While analysing RMSE in isolation may not be enough, it is possible that other signifiers will indicate more reliable results and increase confidence in the HTC estimate. The influence of wind and temperature signatures on the decay profiles need to be accounted for to assist in removing larger underestimates of HTC from the prediction. Noting there was a complete lack of correlation between RMSE and HTC in configuration 3, these analyses are carried out only on Configurations 1 and 2.

7.2.1.4 Reliability of Individual Decay Curves

In each configuration, there are specific days for which that curve's RMSE is significantly larger than the rest. Being able to identify days when simulation is not responding to conditions in the same way as was observed may assist in improving overall RMSE calculation. The two main factors are expected to be initial temperature difference and wind during the decay period.

7.2.1.4.1 Temperature Difference

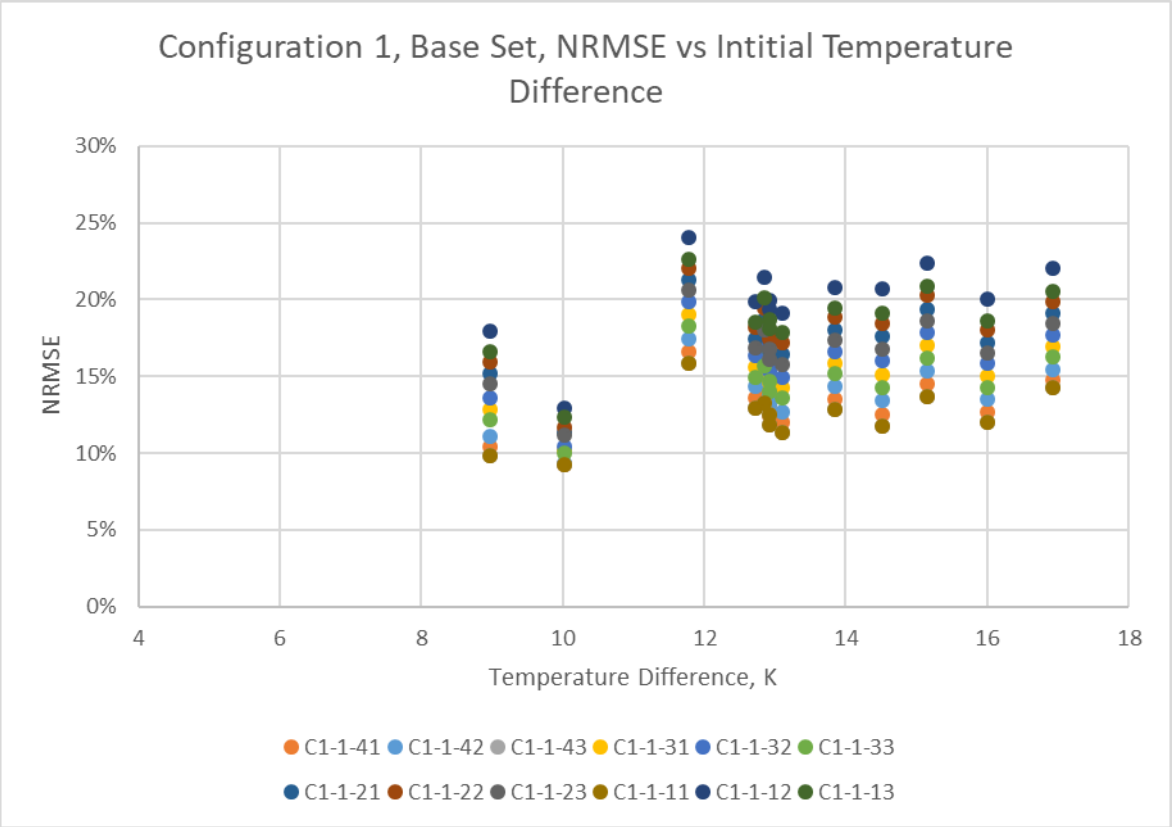

Figure 7.6 Variation of NRMSE result against changes in initial conditions

Figure 7.6 shows the greatest NRMSE occurred on the ninth day of decay simulations, when the temperature difference at the beginning of the decay phase was 11.7 K. This is the second smallest difference in temperature at this time. The two smallest NRMSE figures for each model are on the days with the two smallest initial temperature differences. However, these could be considered outliers as across all other days there is no clear correlation between temperature difference and NRMSE.

7.2.1.4.2 Wind

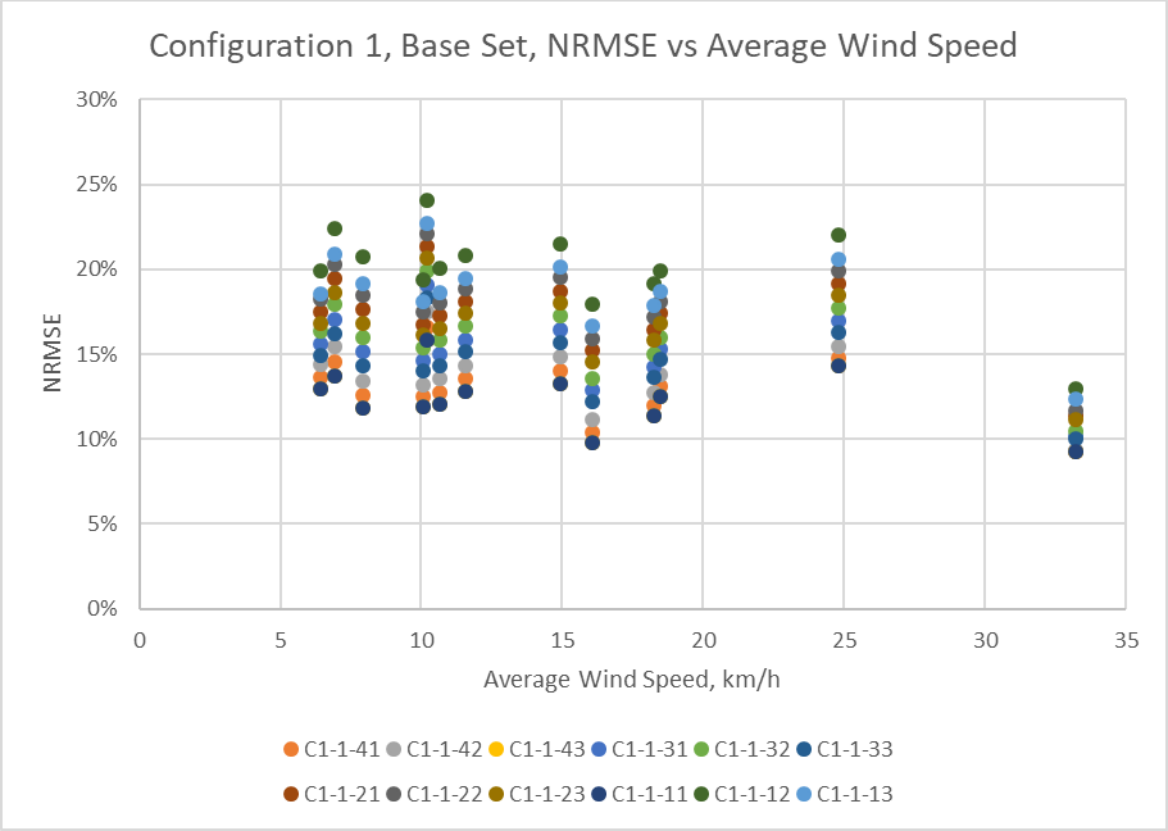

Figure 7.7 Variation in RMSE based on wind speed

As with the temperature, Figure 7.7 does not show a strong correlation between increased wind speeds and increased NRMSE. The day with the highest wind speeds during the decay period coincides with the smallest NRMSE. Including this potential outlier in the dataset, the weak correlation (R^2 <0.5) indicates that as wind speed increases, NRMSE decreases. This goes against all other research into building evaluation as this suggests the RMSE decay method is more reliable in windy conditions than still conditions. A more logical conclusion is the NRMSE calculation is not strongly influenced by wind.

7.2.1.5 Internal Air Temperature Differences

Each simulation shows a large deviation from observed temperatures, and while NRMSE assesses the average difference between the two, some inclusion of the maximum difference may also be important. However, simply assessing maximum variation from observed internal temperature does not provide any new information; it merely shows the average has the smallest absolute deviation. An approach should be developed that accounts for overestimating the internal temperature. Figure 7.8 shows the largest overestimation for each model against the NRMSE.

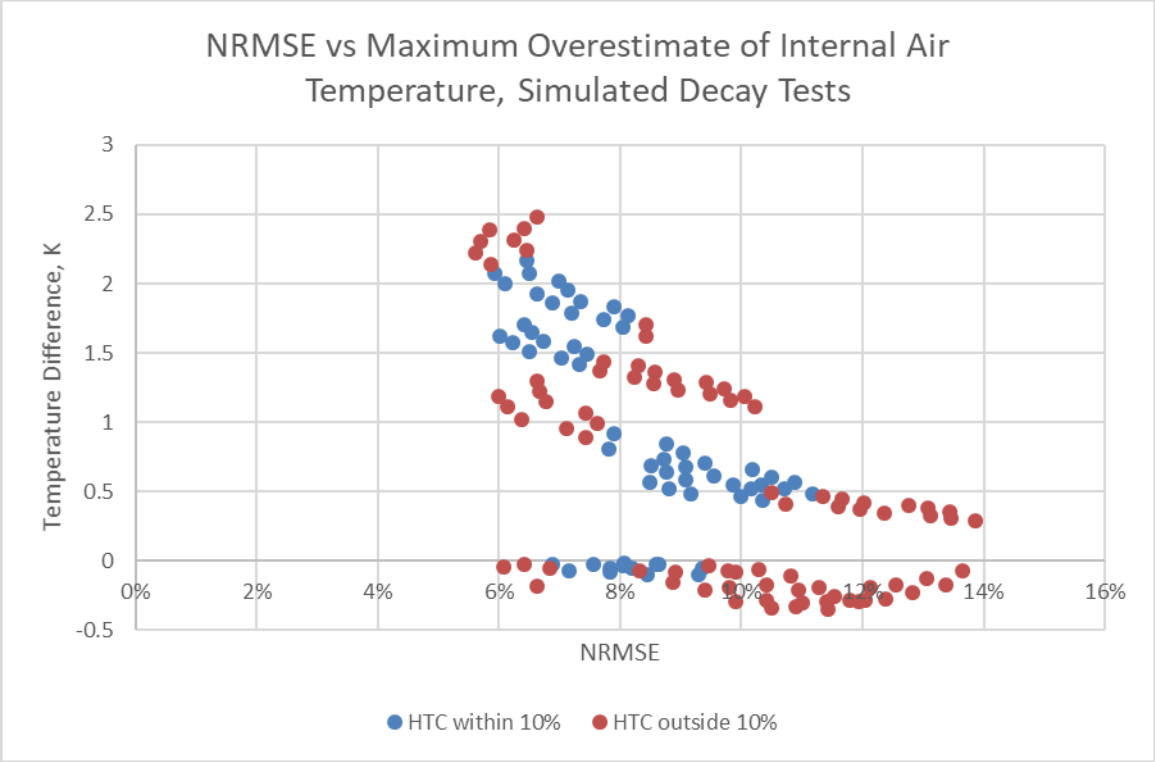

Figure 7.8 NRMSE vs maximum overestimation of internal air temperature during decay test simulation

The results shown in Figure 7.8 are defined by how closely the simulated and observed HTC's match. HTC's within 10% are considered 'accurate' estimations. Negative temperature differences indicate models where the simulated temperature remained below the observed temperature. Each configuration shown in Figure 7.8 forms a separate group, distinguished by temperature difference. Within each configuration there is a section where accurate HTC's are grouped. However, there is no strong pattern across all models that correlates the maximum overestimated temperature with an accurate model. Figure 7.9 shows the same analysis for maximum underestimation of air temperature.

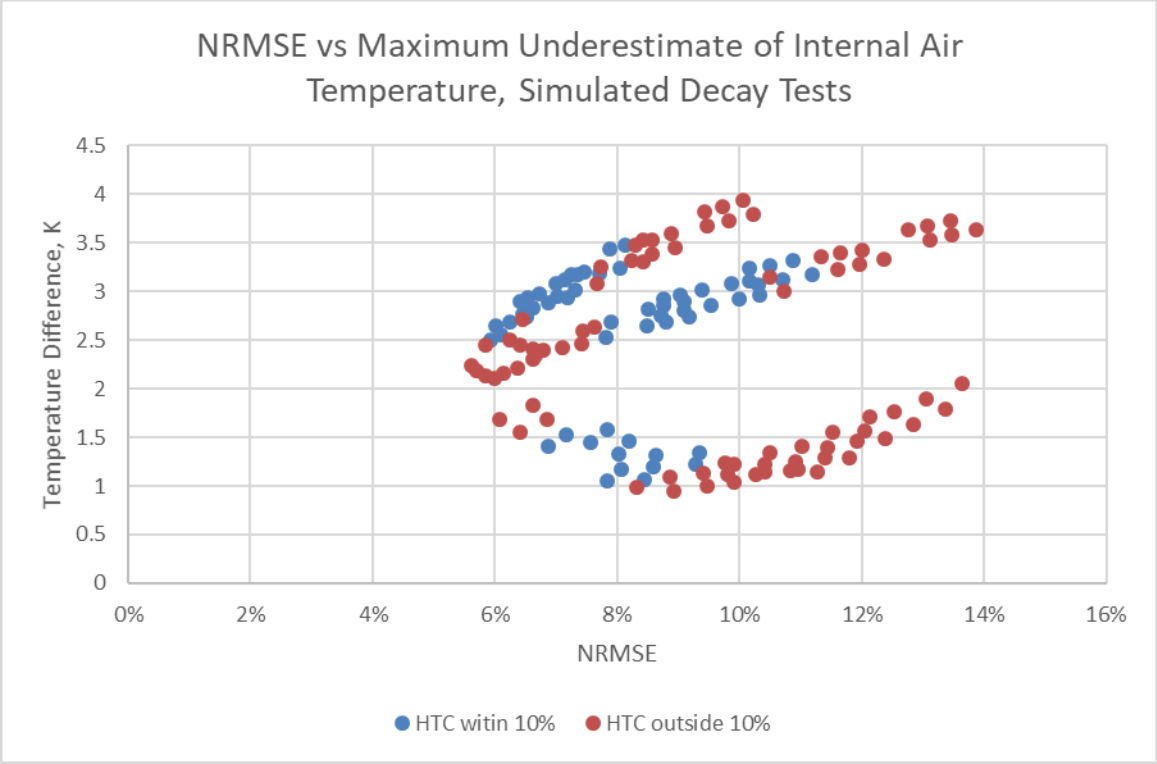

Figure 7.9 NRMSE vs maximum underestimation of internal air temperature during decay test simulation

As in Figure 7.8, Figure 7.9 shows no correlation between underestimation of air temperature during decay test simulations and NRMSE that provide accurate HTC estimates. Similar patterns within configurations are shown, but there is no commonality across the three configurations. Accurate HTC estimates cannot be determined by observing only NRMSE and maximum differences between simulated and observed air temperatures.

7.3 Measured Heat Pulse Method

The measured heat pulse method provides an additional parameter to analyse, namely the energy input, and should allow for greater confidence in smaller datasets. The collection of heat energy data is currently obtained as part of the co-heating test, and the PSTAR tests, though the heating period for both is much longer and more invasive. The main flaw with the RMSE method discussed in Section 7.2 is that there is no way to identify an accurate HTC estimate based on temperature profile alone.

The measured heat pulse method uses the temperature RMSE calculation and total energy input during the heating phase to determine the best computer model representation of the test building. This section shows how these elements combine to assist in eliminating erroneous estimates of HTC from the RMSE-only analysis, and works towards providing a set of minimum standards that indicate the most likely representation of the test building. This is done by identifying commonalities between models that provide a HTC within 10% of the test building.

7.3.1 Measured Heat Pulse Process

The process for the measured heat pulse method is very similar to the original RMSE decay method. Following the steps laid out in Section 7.1, the measured heat pulse method uses step 6b instead of 6a. The measured heat pulse method does require additional field data, namely heat energy added to the building during the pre-heat phase of the decay method. In this case study, this is from midnight to 2.00am, ahead of the 2.00am to 6.00am decay phase. In this research, the 2 kW electric blow heater was used to heat the building during the pre-heating phase of the decay test.

7.3.2 Heat Pulse Simulation Results

The simulations run for the measured heat pulse method are the same simulations described in Section 7.2, except that heat energy output from EnergyPlus is used as well as temperature outputs. Figure 7.10 shows energy used by simulations compared with observed value.

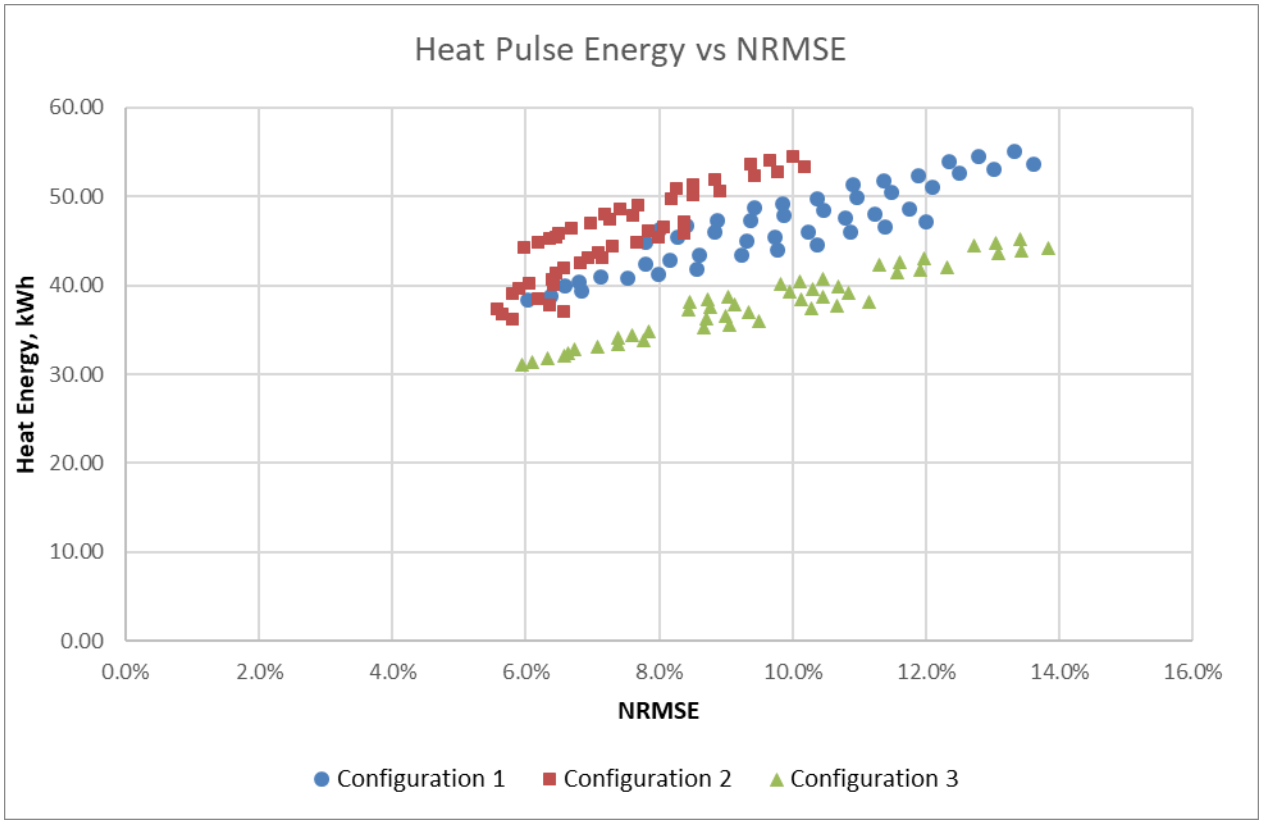

Figure 7.10 Simulated heat pulse energy vs NRMSE

Across all configurations, Figure 7.10 shows that decreases in NRMSE, which correlated with lower HTCs, also correlate generally with lower energy use values. This fits expectation as all models within the same configuration set are heating to the same temperature points. As the heat loss decreases, the heating load also decreases.

It is interesting that simulations for Configuration 3 use less energy for similar NRMSE values compared to Configurations 1 and 2. However, these models have HTCs that are similar to Configuration 1 and 2 models, but internal temperatures during the pre-heating phase in Configuration 3 were not as high. The combination of relatively similar HTCs and lower temperature set points means the heating system in Configuration 3 is not under as much stress and uses less heating energy. Figure 7.11 shows the relative difference in energy use against the NRMSE for each configuration.

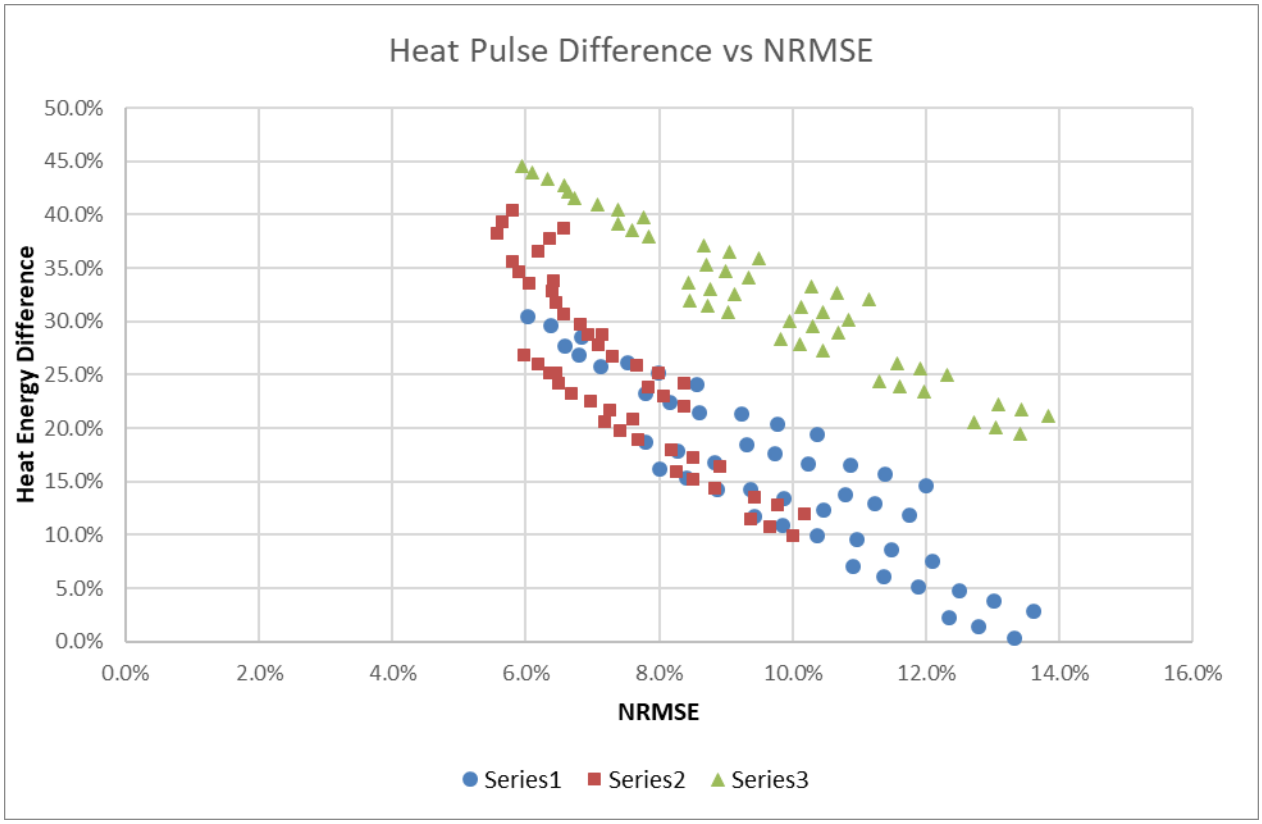

Figure 7.11 Difference between observed and simulated heat pulse energy vs NRMSE

Figure 7.11 shows that an inverse relationship exists for most simulations between NRMSE and the difference in energy use. Configuration 2 shows some change in this trend as the difference in energy use goes beyond 30%. This is in line with observations in Section 7.2 regarding these specific simulations.

Configuration 3 has a much larger difference in energy use for the same range of NRMSE than the other two configurations. Configuration 2 shows an increased difference in energy use at lower values of NRMSE compared with Configuration 1. The models were all adjusted in the same way, so this suggests that Configuration 3 models drastically underestimate the test cell's dynamic heating load compared to observed values.

This shows some of the potential variability in the range of results for the heat pulse method. The three configurations have different patterns when comparing NRMSE with the difference in energy used during the pre-heating phase. Despite this, HTCs that align very closely with the co-heating estimates from field testing were observed from these models in Section 5.6. This means that even though results appear very different from observations for Configuration 3, there are good HTC estimates in this data set.

7.3.3 Heat Pulse Simulation Analysis

From the figures above, the simulations broadly show an inverse relationship between energy use and NRMSE. Altering base assumptions of the model by increasing thermal mass or decreasing conductivity of the ceiling made some difference to the relationship: reduced conductivity improved the NRMSE match, but reduced the heat pulse energy. Increased thermal mass improved the heat pulse energy comparison, and reduced the range of NRMSE figures. The overall set of NRMSE did not shift across the axis, but extremities of the range moved towards the previous mean. These changes, however, did not result in any more or any fewer models falling within the 10% HTC range.

The reason the RMSE method alone does not provide reliable results is that it is unable to discount the models with comparatively low heat loss as it only deals with one building performance indicator. The measured heat pulse method allows for comparison with total heating energy, which may be able to narrow the range of valid options consistently. The challenge presented by the additional data is determining the framework within which we can be confident that models relate closely to the observed building.

7.3.3.1 Zone Analysis

The first round of analysis uses only RMSE and total heating energy. The models are split into two categories: those with a HTC within 10% of the observed building (‘accurate’), and those 10% or greater (‘inaccurate’). The full array of all three configurations is shown in Figure 7.12. Each of the four zones is determined based on the number of ‘accurate’ simulated HTCs lie within it. The zones have been set at a minimum resolution of 0.5% for ease of use. Table 7.2 shows the figures for each zone.

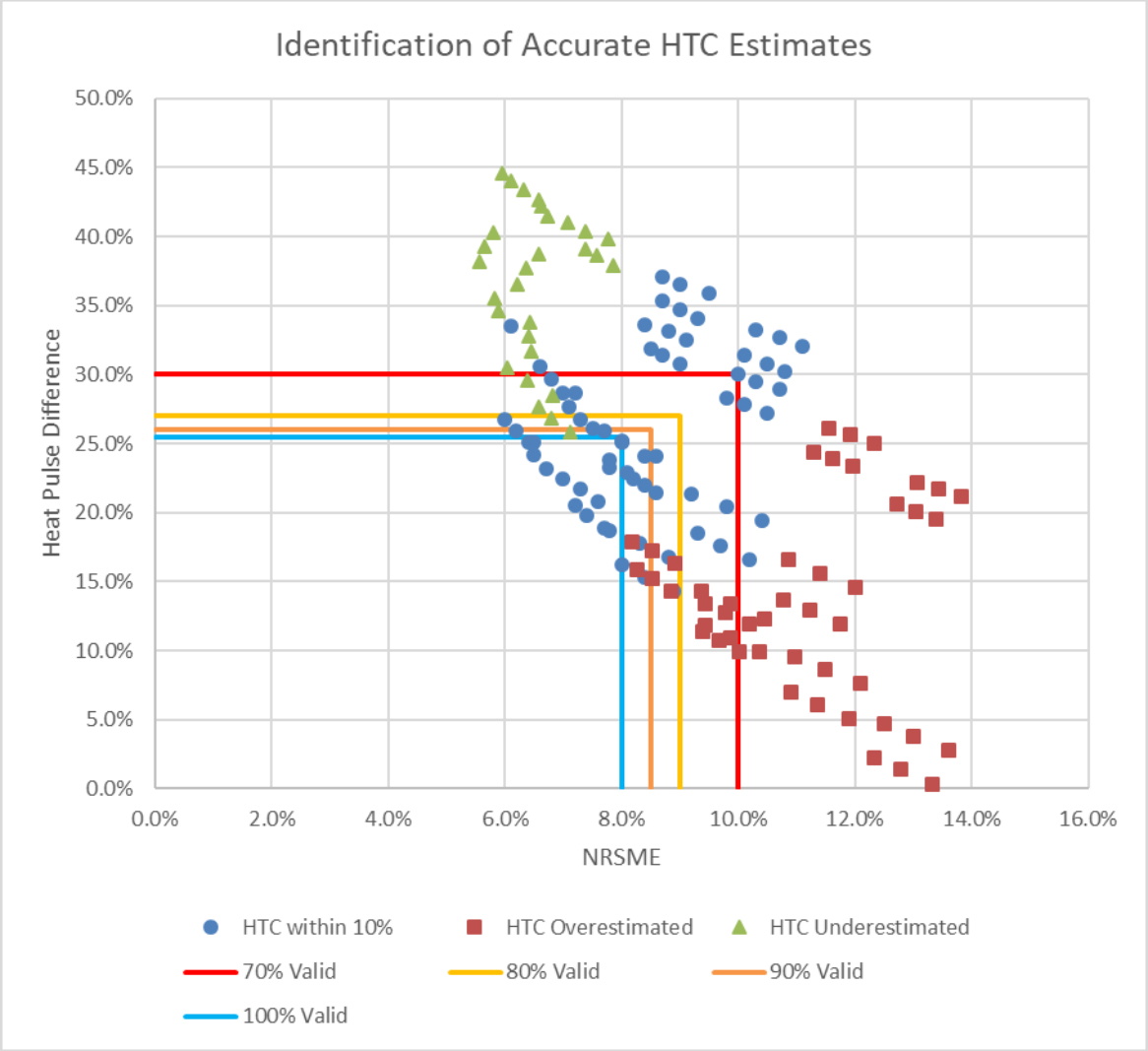

Figure 7.12 Zone analysis of measured heat pulse simulations

In this case study, there are combinations of NRMSE and heat pulse difference (difference between observed and simulated energy used during pre-heat phase) that always result in an accurate HTC estimate. This is shown in Figure 7.12 by the zone inside the blue line. Zones where 90%, 80% and 70% of results are accurate are also identified. Both Configuration 1 and Configuration 2 have models which fall inside the 100% zone, but Configuration 3 only falls inside the 70% zone. Table 7.2 shows the specific criteria setting the zones, and the number of models that fall within them.

Table 7.2 Summary of measured heat pulse simulation zone analysis

Zone	Total heat energy	NRMSE	Number of accurate models	Number of inaccurate models	% accurate
70%	30.0%	10.0%	41	19	68%
80%	27.0%	9.0%	31	8	79%
90%	26.0%	8.5%	24	3	89%
100%	25.5%	8.0%	16	0	100%

The main issue with this technique is highlighted by Configuration 3: half of the models simulated provide an accurate HTC estimate, and yet the combinations of NRMSE and heat pulse difference indicate it could be reported only with 70% confidence. While it has been possible to show a range for which confidence is high in that there are no inaccurate results, a considerable amount of time must be spent in fine tuning and adjusting models to create a set of valid results. This was not achieved for Configuration 3 with any reasonable changes being made. The positive aspect is that if a result is found, it is very likely to be within 10% of the building's experimental HTC. The issue is that there is no guarantee this approach to RMSE decay analysis will converge on a result.

7.3.3.2 Cone Analysis

The major problem with defining the zones as above is that there are no valid results for Configuration 3. Attempts were made to find a model within the 100% zone; however, this was largely trial and error, and unsuccessful. When results are viewed in a different way, there is a central zone where HTC estimate is accurate regardless of the configuration. This is shown in Figure 7.13.

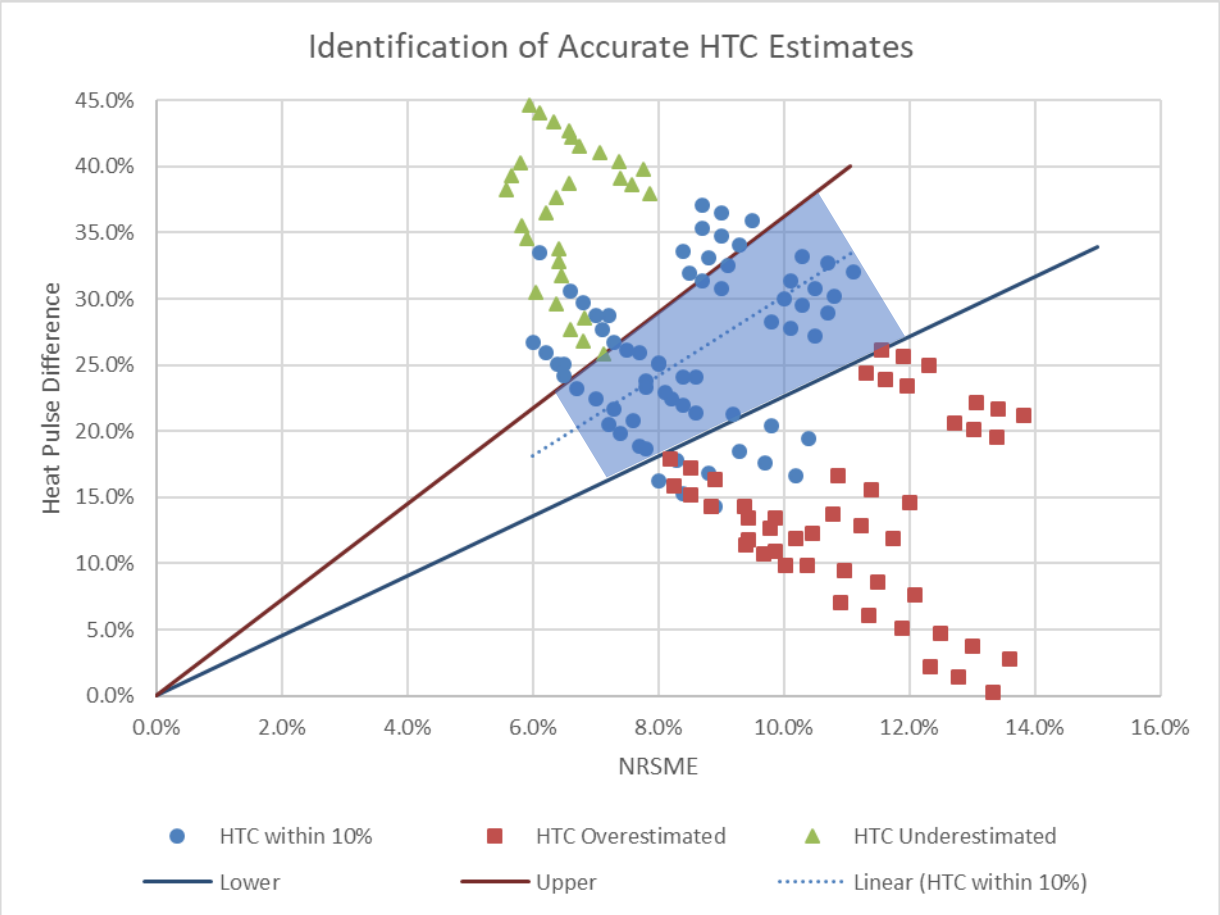

Figure 7.13 'Cone analysis' of measured heat pulse method

Figure 7.13 suggests there is a relationship between NRMSE and heat pulse difference that could be used to identify inaccurate results. Models within the shaded area all estimate the building's HTC within 10% of the observation. Models outside the shaded area may still provide an estimate within 10%, but this cannot be determined solely by the NRMSE and heat pulse analysis. The red and blue lines indicate the wider range that may exist with different models of the same building, however the shaded region indicates the range of results found in this research.

To calculate coefficients that define this range, the ratio of heat pulse difference-to-NRMSE has been calculated. The red 'upper' line is defined by the largest ratio that excludes models that underestimate the building HTC by more than 10%. From the available data this is set at 3.62. The blue 'lower' line is defined as the smallest ratio that excludes models that overestimate building HTC by more than 10%, and is set at 2.26. The result is that anything within these bands must fall within 10% of the building's observed heat loss. The shading shows the limits of the results found in this research. It is not certain that a model that is less accurate on both variables will still provide accurate HTC estimates. This would be, for example, a model that returns an NRMSE of 16% and a heat pulse difference of 45%. This hypothetical model would fall between the bands; however, it may not provide a good HTC estimate.

HTC estimates for each configuration may be calculated by averaging HTCs from these models. Uncertainty in the estimate is taken as the range of estimates from these models. HTC estimates for the RMSE analysis are shown in Table 7.3.

Table 7.3 Measured heat pulse estimates of HTC from cone analysis

Configuration	Co-heating HTC estimate (W/K)	Measured heat pulse HTC estimate (W/K)	Difference
1	81.33	79.62 (+4.62, -3.74)	-2.1%
2	93.68	98.87 (+3.14, -4.68)	5.5%
3	97.91	102.14 (+4.39, -5.21)	4.3%

7.3.4 Summary and Discussion

Using the cone analysis, the HTC estimate from the measured heat pulse method becomes significantly more reliable – by design the individual estimates are all within 10%, and the overall estimates are all within 6% of observed HTC. The aim of this analysis was to identify differences between models providing accurate (within 10%) or inaccurate (outside 10%) HTC estimates. There are accurate estimates outside the range shown in Figure 7.13. However, based on temperature and heat energy there is no way to distinguish between accurate and inaccurate estimates outside the shaded area.

This improves in several ways on the zoning analysis presented in Section 7.3.3.1. The HTC for Configuration 3 can be estimated. The time required to gain accurate results is decreased, as there is only a need to provide the ratio between energy input and RMSE, rather than fine tune a model so that both energy input and RMSE fall inside set maximums. Given the relationship between RMSE and heat pulse difference is roughly linear and inverse, it should always be possible for an assessor to adjust the model's heat loss and converge on a set of valid results.

The common zone identified in Figure 7.13 also removes the influence of incorrect assumptions about the building's basic properties. All but one series of the building models discussed in Section 4.4.5 (Base, Ceiling, Thermal Base and Thermal Ceiling) has a model that estimates HTC to within 10% of the co-heating test estimate, and satisfies the conditions of the cone analysis. The 'Thermal Base' set for Configuration 1 is the only set of models which provides a HTC estimate within 10% but does not satisfy the conditions of the cone analysis.

Following the cone analysis also provides a reduced uncertainty range. This is expected, however, as the analysis was based on models that give close HTC estimates. Figure 7.14 shows how measured heat pulse HTC estimates and uncertainty range from the cone analysis compares with the co-heating test results.

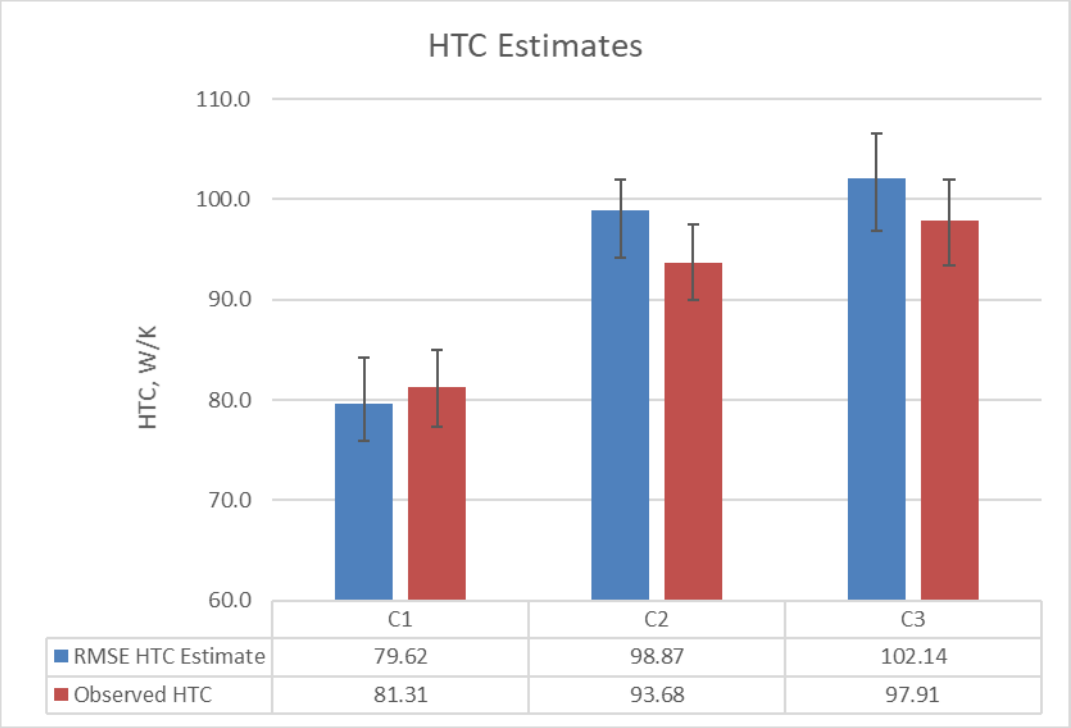

Figure 7.14 Comparison HTC estimates Co-Heating and Measured Heat Pulse tests

As previously shown in Table 7.3, Figure 7.14 shows that the HTC of Configuration 2 and Configuration 3 are overestimated by the decay method; however, the uncertainty analyses show that the range of estimates does overlap in all cases. As with all the experiments, the uncertainty analysis for Configurations 2 and 3 shows that differences in HTC cannot be definitively detected, only implied. Configuration 2 is the only test case where the Co-Heating estimate of HTC does not fall within the range identified by the decay method.

Uncertainty in the HTC estimate from the co-heating test is smaller than the uncertainty in the measured heat pulse decay method, though only by a maximum of 1.1 W/K. This shows the potential for the measured heat pulse decay method to provide HTC estimates to comparable standards of accuracy and precision as the co-heating test.

As it stands, the case study shows very promising signs that the measured heat pulse decay method can provide HTC predictions that are within 10% of the observed figure. Further work is required to expand the case study and identify whether the relationship identified between NRMSE and heat pulse difference is only limited to this building, or is common across a wider range of structures.

7.4 Conclusion

Of the two alternative RMSE decay methods shown in this chapter, undoubtedly the analysis of heating energy in the measured heat pulse variant is critical. The theoretical application of the RMSE decay method is very elegant and straightforward. After experimental examination of the process, however, the reality is that the method is not so simple, and there is difficulty in confidently and reliably estimating the test cell's true HTC. The model with the smallest RMSE identifies the most similar decay profile to the observed building. However, HTC related to this model has in all cases been a significant underestimate of the observed HTC – up to 19.3% lower than the co-heating test estimation. Additionally, the case study found no reliable way to eliminate these models from the analysis. Neither analysis of absolute differences between simulated and observed internal temperatures, nor of weather conditions, was able to refine the selection to give a more accurate HTC estimate. This pattern existed across all variations of the building models, which in practice would be arbitrary trial and error alterations to the thermal shell of the model based on assessor judgements.

The addition of heat pulse energy provides enough additional information to the assessor to enable them to confidently identify misleading results, as a good temperature match was often coupled with a poor heat match, and thus fell outside the cone, as shown in Figure 7.13. Observing this pattern of NRMSE against heat pulse difference from observation to simulation showed that within a certain ratio of NRMSE to heat pulse difference, the HTC predicted by the model was always within 10% of the observed figure. This identifies that the HTC estimate for the building is the average HTC from all models where heat pulse difference divided by NRMSE is greater than 2.26 and less than 3.62. The uncertainty is taken as the range of the HTC estimates from this sub-set of models.

Using the measured heat pulse decay method, this case study shows it is possible to estimate the building's HTC in a way that should provide minimal disruption to the occupant. The limitation in this study is that it cannot be determined from the case study whether the ratio between RMSE and heat pulse difference that forms the basis of the cone analysis is unique to the test cell, or if it is common across a wider range of buildings. It is recommended that further work on the decay method focuses on applying cone analysis to

an array of simple detached homes, allowing for testing of the method under more complex conditions and to identify if the ratio is common across all buildings or unique.

Chapter 8 - Conclusion and Recommendations

8.1 Summary of Research and Results

Improving the energy efficiency of buildings is a critical element in the overall reduction of carbon emissions world-wide. At this stage, increasing the performance requirements of buildings has been implemented by specifying minimum design standards. Unfortunately, these standards are undermined by a significant gap between predicted and actual performance. Identifying the performance gap is a key goal in overall building efficiency improvements. To understand the performance gap, it is necessary to carry out in situ testing for quality assurance and to establish if there is a fundamental reason for the discrepancy.

Current methods of evaluating buildings' performance are very powerful. However, they have limitations in large-scale applications largely due to issues with disruption to the occupant, or inability to evaluate the entire building system. Heat flux tests are very good in determining a building element's thermal resistance, but only evaluate the individual section. Typically heat flux tests do not account for heat lost through, for example, thermal bridging at corners or wall studs. They also require using an air leakage test, either blower door or tracer gas, to determine infiltration heat losses. While not overly disruptive to occupants' daily routines, there are concerns that heat flux tests damage wall surfaces as the sensor must be stuck to it, so reducing the scope for their application.

Air leakage tests that complement the heat flux only evaluate infiltration losses. The most effective technique for evaluating the entire thermal system is the co-heating test. It is quite comprehensive in its ability to evaluate heat loss. However, it requires an empty building for up to three weeks, and does not evaluate cooling loads. Test duration limits widespread application due to disruption of the occupant, or in a new development temporarily removes the house from the sales process. The limitation to heat loss creates a specific period of time during the cooler months of the year when it can be applied, and also limits the effectiveness of the evaluation to cooler climates where heat loss is the main concern.

In response, four methods of analysing overnight temperature decay data were presented. Two of these analyses use only observed data to calculate a decay constant, which is then correlated with the configurations' HTC. These are the 'calculated average' and 'Excel

Solver' decay methods. They are referred to as the 'experimental methods' as they deal only with data gathered from on site experiments. The other two methods combine field data with computer models built in EnergyPlus. These are the 'temperature RMSE and 'measured heat pulse' decay methods, known as the 'RMSE decay methods' as they apply the Root Mean Square Error to test how closely simulations match field data. Both RMSE decay methods use field data to determine which of an array of EnergyPlus models best fits the real building's profile and estimates the building's HTC from co-heating tests simulated on these models.

The approach to evaluating performance of the decay methods is to compare them to the co-heating test applied to a test cell located on the CSIRO site at Highett in Melbourne. Extensive field experimentation and evaluation on the test cell, combined with thousands of EnergyPlus simulations across nearly three years, provides the data for this comparison. The use of heat flux and blower door tests provided additional comparison points, though the uncertainty from these tests could not be estimated in this case study. The HTC estimated in this fashion was significantly higher than that of the co-heating tests. The use of simulations based on the heat flux and blower door testing suggested this is caused by large uncertainty in the conversion from ACH at 50 Pa to the building's natural ventilation rate, and underestimating relative benefits to R-values of floor and ceiling surfaces due to the enclosed sub-floor and attic space.

Co-heating tests and decay method tests were run on the test cell while the insulation in the walls was adjusted to provide three different configurations. This resulted in three different HTCs to be estimated by each version of the decay method.

The co-heating test showed an increase of more than 15% in the HTC between Configuration 1 and Configuration 2, but only a 4.5% increase between Configuration 2 and 3. The uncertainty analysis conducted on the co-heating tests concluded there was a difference between the Configuration 1 heat loss and Configuration 2 and 3 heat losses; however, the analysis showed that the difference between Configuration 2 and Configuration 3 could not be definitively stated as HTC ranges overlapped. Despite this, as it is known that Configuration 3 has less insulation than Configuration 2, it is logical to conclude that the HTC for Configuration 3 is indeed higher.

There is no overall difference in the set up and duration of the co-heating test and the decay method. The decay method experiments required similar amounts of equipment and set up as the co-heating test, with the addition of a timer to control the heater. Co-heating tests conducted for this research ran for 10-14 days, and decay tests ran across 14 days. The largest difference is that the decay method experiment is 6 hours in length, repeated for 14 days, whereas the co-heating test is conducted 24 hours per day for the 10-14 day period. The decay method therefore allows the building to be used normally outside the midnight-6.00am experiment window, whereas the co-heating test requires the building to cease its normal use pattern. The case study was conducted on an empty building. Further analysis is required to determine the additional impacts on heat gains during the decay period due to the presence of occupants and household appliances.

Three of the four decay method analyses predicted the building HTC to within 10% of the HTC estimated by the co-heating test. The comparison of HTCs from the case study experiments is shown in Table 8.1.

Table 8.1 Case study estimates of HTC

	HTC estimates, W/K (% Difference from co-heating estimate)			
	Configuration 1, Test A	Configuration 1, Test B	Configuration 2	Configuration 3
Co-heating	81.34	81.31	93.68	97.91
Heat flux + blower door	116.91 (43.8%)	116.91 (43.8%)	125.94 (34.4%)	133.46 (36.3%)
Calculated average	80.08 (-1.55%)	74.97 (-7.79%)	101.14 (7.96%)	99.16 (1.28%)
Excel Solver	82.32 (1.20%)	80.42 (-1.10%)	95.42 (1.86%)	96.02 (-1.92%)
Temperature RMSE*	70.39 (-13.4%)	70.39 (-13.4%)	78.98 (-15.7%)	79.02 (-19.3%)
Measured heat pulse*	79.62 (-2.1%)	79.62 (-2.1%)	98.87 (5.5%)	102.14 (4.3%)

* Configuration 1 Test A and Test B estimates for the RMSE decay methods are the same as they come from the same building models.

Assuming that the co-heating test calculates the building's 'true' heat loss, the Excel Solver method provides the most accurate estimate. Estimates shown in Table 8.1 are, however, based on a correlation between the co-heating test HTC and the decay constants from the small sample of four decay tests conducted. Further research is required to confirm this correlation exists in a wider data set. The measured heat pulse estimate also relates to observed HTC as the analysis identified commonalities between models that estimated the HTC of the configurations to within 10%. Correlations identified between the temperature profiles and the energy input during the pre-heat phase of the decay test also require further validation to confirm this correlation exists in other building types.

Estimates for the calculated average HTC are based on the correlation observed in the simulated data set, as there was good agreement between the observed results and simulated results. However, this method is shown to be less accurate than the Excel Solver and measured heat pulse decay methods, and predicts a higher heat loss in Configuration 2 than in Configuration 3. This indicates the method is not as sensitive as the co-heating test when attempting to analyse differences between similarly performing buildings.

The temperature RMSE decay method was shown to be unreliable as it drastically underestimated the HTC of each configuration. Without having already conducted the co-heating test to have an estimate of the HTC, there was no way to determine whether these estimates were inaccurate. Using temperature profiles alone does not provide HTC estimates that will address the performance gap.

Based on the uncertainty analysis, only the measured heat pulse decay method provided a good comparison with the precision of the co-heating test. The precision of each estimate is shown in Table 8.2.

Table 8.2 Precision of HTC estimates from case study experiments

	Range of HTC estimates, W/K			
	Configuration 1, Test A	Configuration 1, Test B	Configuration 2	Configuration 3
Co-heating	77.60 – 85.34	77.97 – 84.88	89.99 – 97.41	93.81 – 102.34
Heat flux + blower door*	n/a	n/a	n/a	n/a
Calculated average	67.51 – 98.77	64.40 – 89.84	84.17 – 128.38	82.30 – 132.25
Excel Solver	75.40 – 90.70	73.96 – 88.18	86.96 – 105.83	87.36 – 106.71
Temperature RMSE**	n/a	n/a	n/a	n/a
Measured heat pulse	75.88 - 84.24	75.88 - 84.24	94.19 - 102.01	96.93 - 106.53

*Uncertainty in heat flux calculations could not be estimated

**Temperature RMSE estimates of HTC were so inaccurate that precision was not calculated.

The measured heat pulse analysis provides the most precise estimates. This is expected as the approach identifies building models within 10% of the co-heating test estimate from which to estimate the HTC. The range in Table 8.2 shows the highest and lowest HTC estimates for models that met temperature and energy criteria on which the estimate is based. It is the only estimate in which the range of HTCs predicted is similar to that of the field co-heating test.

The two experimental methods are much less precise than the Heat Pulse method. The uncertainty in the decay constant estimates in both cases are comparatively large, and this corresponds to a larger range of possible HTCs for each configuration. The Excel Solver method was shown to be more robust when analysing the uncertainty in the decay constant. This is because the Excel Solver analysis makes use of the entire temperature decay, where the calculated average method only uses the first and last data points.

There is strong evidence from field experiments and simulations that buildings which lose heat faster under dynamic conditions, also have greater heat losses under steady state conditions than buildings with slower heat losses under dynamic conditions. The case studies undertaken in this research also show that analysis of the dynamic response may allow for the prediction of the steady state heat transfer coefficient as estimated from a co-heating test. Analysis of the case study data concludes that the heat pulse decay method is most likely to provide an accurate prediction of building HTC with a precision similar to the co-heating test. The Excel Solver decay method may also provide accurate estimates, but requires further work to minimise uncertainty in the results.

8.2 Limitations

The conclusion above is based on an extensive research case study undertaken as part of a PhD program. This conclusion must be taken in the context that this case study shows proof of concept only. Additional research on a wider data set must be undertaken to fully explore the decay method.

The main element the case study is unable to address is whether the ratio that forms the basis of the cone analysis is unique to the test cell or common across a wider range of buildings. The presence of a common ratio means it can be used to identify invalid HTC estimates confidently and in an evidence based manner, rather than by trial and error or assessor opinion. The case study is also unable to determine whether the correlation between the HTC and Excel Solver decay constant exists in a wider data set. Confirmation of this would allow the HTC to be directly estimated from the decay constant.

Related to this, the case study was conducted on a simple, single living zone building. It shows the method can be applied to a single airspace, but does not demonstrate whether additional complications arise, or whether increased data detail is required when multiple zones are present to attain a sufficiently accurate temperature profile in more complex configurations.

8.3 Further Research

Two of the four variants of the decay method showed significant merit and warrant further research. The Excel Solver decay method showed accuracy to the co-heating test, but had less precision; the uncertainty in the Excel Solver HTC was more than double that of the co-heating test. The measured heat pulse decay method was able to show common features of models that accurately predict HTC. It is recommended that additional research focus on these two areas as they show the most promise for improving in situ building analysis. The following sections outline the areas that would provide most value to the field.

8.3.1 Influence of Weather

It is not clear how different weather events, such as high wind, influence individual decay profiles. Understanding the influence of such events, and accounting for them in the analysis, should improve the experimental decay methods' effectiveness. Including a wind term in the Excel Solver analysis may provide the means to estimate infiltration losses and reduce the uncertainty in the decay constant.

8.3.2 Multi-Zone Buildings

The case study demonstrates the feasibility of the decay method in a simple building; however, applying the method to a multi-zone building is required to be able to show the true potential for application in field. It is expected that challenges related to combining temperatures in multiple locations into a single figure for analysis would be handled by volume-weighted averages, similar to the co-heating test. However, analysis is needed to determine how increased complexity influences the Excel Solver decay method. There is also potential to calculate decay constants for each building zone, assisting in pinpointing flaws in the building fabric.

For the measured heat pulse method, the most straightforward response would simply be to model all zones. This may prove too time consuming for assessors and result in the method being infeasible in the field. It is necessary to conduct additional analysis of the effects both of simplifying the computer model to a single zone representing the overall thermal shell, and of using a volume weighted average decay profile. There is expected to be minimal influence on the modelling of the co-heating test as the steady state nature relies on the entire building being at very stable temperatures. The dynamic nature of the

decay method may present different challenges if there are significant temperature differences across the zones.

8.3.3 High Thermal Mass Buildings

Analysis of the EnergyPlus simulations indicated that while the co-heating test is not overly influenced by changes in thermal mass, there is a difference in the internal temperature profiles which changes the decay analyses. The test cell is a lightweight building, and the overall correlation between HTC and decay constant may differ when evaluating heavier constructions. The measured heat pulse decay method may already account for thermally massive buildings; however, additional research should be conducted to confirm whether there is still the same relationship between NRMSE and heat pulse differences, as observed in this case study. This will determine whether the model selection cone presented in Section 7.3.3 accurately identifies the HTC of heavier buildings, or if this needs adjustment for building type.

8.3.4 Analysis of Minimum and Maximum Decay Limits

Both promising variants of the decay method have been applied during colder months in a cool climate, and on a building that is neither efficient or inefficient. The current research has not addressed minimum temperature differences required to create a decay profile that creates valid information and avoids misinterpretation. Under more mild conditions with smaller temperature differences, flatter temperature decay profiles are expected with less variation between efficient and inefficient buildings. Under these conditions, the method may be less reliable. Similarly, highly inefficient buildings may have temperature decays that are so steep they may not be able to converge on a stable HTC estimate.

8.3.5 Application of LORD software

As with the application of LORD software to the co-heating test data, it is possible that LORD software could be applied to analyse decay test data. This could provide additional opportunities to identify HTCs directly from the decay data, or provide better estimates of the decay co-efficient.

8.3.6 Application for Evaluating Summer Performance

As with all other tests, the decay method as it currently stands is designed to evaluate heat loss. It has potential, however, to provide information pertaining to a building's rate of heat

gain, and provide information regarding performance in warm climates. It appears this would be unique among in situ evaluation tools.

8.4 Beyond the Co-Heating Test

Demonstrating the decay method's validity, a new way of evaluating buildings, it must make some comparison to current methods. The HTC, as determined by the co-heating test is seen to be the most effective whole-building measure of thermal performance. Yet this way of analysing buildings relies on steady state conditions, and only evaluates heat loss. The P-STAR test is an example of a more dynamic tool, though it has fallen out of favour in the literature. Application of LORD demonstrates dynamic analysis of the co-heating test, though is also not as widely used as the steady state analysis.

A steady state analysis has limitations, particularly when effects of thermal mass are eliminated as part of the evaluation. An improved analysis would include all building fabric elements and observe behaviour under conditions closer to that of day-to-day use. Using temperature gain and temperature loss rates as thermal performance measures may provide a better picture of the building under normal operating circumstances. The decay constant calculated from the Excel Solver decay method demonstrates the possibility for using dynamic responses to compare buildings. The theory behind the method attempts to adjust for external conditions, and simulated results indicate the decay constant changes when thermal mass is increased. While the method may not be perfect in the current format, it represents a possible first step to redefining the way building performance can be analysed and reported for post-construction and post-occupancy evaluation.

References

ABCB, A.B.C.B., 2013. How have Housing Energy Efficiency Requirements made a difference? Available at: http://www.abcb.gov.au/Resources/Publications/Education-Training/How-have-Housing-Energy-Efficiency-Requirements-made-a-difference.

ABCB, A.B.C.B., 2011. National Construction Code series. , p.v. :

ABCB, A.B.C.B., 2016. National Construction Code series. , p.v. :

ABS, A.B. of S., 2013. 2011 Census QuickStats - Dwellings. Available at: http://www.censusdata.abs.gov.au/census_services/getproduct/census/2011/quickstat/0.

ABS, A.B. of S., 2018. 2016 Census QuickStats: Australia. Available at: http://www.censusdata.abs.gov.au/census_services/getproduct/census/2016/quickstat/036?opendocument.

ABS, A.B. of S., 2009. Heating and Cooling. Available at: http://www.abs.gov.au/AUSSTATS/abs@.nsf/Lookup/1345.4Feature%20Article1Aug%202009.

Achenbach, P.R., 1981. Design of a calibrated hot-box for measuring the heat, air, and moisture transfer of composite building walls. *Thermal performance of the exterior envelopes of buildings, Proceedings-1*, pp.308–324.

Aktacir, M.A., Büyükalaca, O. & Yılmaz, T., 2010. A case study for influence of building thermal insulation on cooling load and air-conditioning system in the hot and humid regions. *Applied Energy*, 87(2), pp.599–607.

Alfano, F. d'Ambrosio et al., 2012. Experimental analysis of air tightness in Mediterranean buildings using the fan pressurization method. *Building and environment*, 53, pp.16–25.

Ambrose, M. et al., 2013. *The Evaluation of the 5-Star Energy Efficiency Standard for Residential Buildings*, CSIRO, Australia.

ASBEC, A.S.B.E.C. & ClimateWorks, 2018. *The Bottom Line*, Australian Sustainable Built Environment Council and ClimateWorks.

Asdrubali, F. et al., 2014. Evaluating in situ thermal transmittance of green buildings masonries—A case study. *Case Studies in Construction Materials*, 1, pp.53–59.

Asdrubali, F., Baldinelli, G. & Bianchi, F., 2012. A quantitative methodology to evaluate thermal bridges in buildings. *Applied Energy*, 97, pp.365–373.

Baker, P., 2008. Evaluation of round-robin testing using the PASLINK test facilities. *Building and Environment*, 43(2), pp.181–188.

Baker, P., 2011. U–values and traditional buildings: in situ measurements and their comparisons to calculated values. *Historic Scotland Technical Paper*, 10.

Baker, P. & Van Dijk, H., 2008. PASLINK and dynamic outdoor testing of building components. *Building and Environment*, 43(2), pp.143–151.

Balaras, C. & Argiriou, A., 2002. Infrared thermography for building diagnostics. *Energy and buildings*, 34(2), pp.171–183.

Balaras, C.A. et al., 2005. Heating energy consumption and resulting environmental impact of European apartment buildings. *Energy and Buildings*, 37(5), pp.429–442.

Ballarini, I. & Corrado, V., 2012. Analysis of the building energy balance to investigate the effect of thermal insulation in summer conditions. *Energy and Buildings*, 52, pp.168–180.

Barreira, E. et al., 2013. Infrared Thermography Application in Buildings Diagnosis: A Proposal for Test Procedures. In *Industrial and Technological Applications of Transport in Porous Materials*. Springer, pp. 91–117.

Barreira, E. & Freitas, V.P. de, 2007. Evaluation of building materials using infrared thermography. *Construction and Building Materials*, 21(1), pp.218–224.

Bassett, M., 1983. Preliminary survey of air tightness levels in New Zealand houses. In *Building Services Group: Proceedings of the Technical Sessions of the Group Held at the Annual Conference of the Institution, University of Waikato, Hamilton, 14-18 February, 1983*. Institution of Professional Engineers New Zealand, p. 475.

Bauer, E. et al., 2015. Infrared thermography–evaluation of the results reproducibility. *Structural Survey*, 33(1), pp.20–35.

Bauwens, G. & Roels, S., 2014. Co-heating test: A state-of-the-art. *Energy and Buildings*, 82, pp.163–172.

Beerepoot, M. & Beerepoot, N., 2007. Government regulation as an impetus for innovation: Evidence from energy performance regulation in the Dutch residential building sector. *Energy Policy*, 35(10), pp.4812–4825.

Bell, M. et al., 2010. Low carbon housing: lessons from Elm Tree Mews.

Belleri, A., Lollini, R. & Dutton, S.M., 2014. Natural ventilation design: An analysis of predicted and measured performance. *Building and Environment*, 81, pp.123–138.

Bernstein, L. et al., 2007. *Climate Change 2007: Synthesis Report*, Intergovernmental Panel on Climate Change.

Bloem, J., 2010. Dynamic methods for building performance assessment. In *5th European Conference on Energy Performance & Indoor Climate in Buildings, PALENC, Rhodes, September*.

Blomsterberg, Å. et al., 1999. Air flows in dwellings—simulations and measurements. *Energy and buildings*, 30(1), pp.87–95.

Branco, G. et al., 2004. Predicted versus observed heat consumption of a low energy multifamily complex in Switzerland based on long-term experimental data. *Energy and Buildings*, 36(6), pp.543–555.

Brounen, D., Kok, N. & Quigley, J.M., 2012. Residential energy use and conservation: Economics and demographics. *European Economic Review*, 56(5), pp.931–945.

Buchberg, H., 1969. Sensitivity of the thermal response of buildings to perturbations in the climate. *Building Science*, 4(1), pp.43–61.

Budadin, O. et al., 2003. Thermal nondestructive testing of buildings and builded constructions. *Russian journal of nondestructive testing*, 39(5), pp.395–409.

Butler, D. & Dengle, A., 2013. Review of co-heating test methodologies. *Report F54. Milton Keynes, NHBC Foundation*.

Byrne, A. et al., 2013. Transient and quasi-steady thermal behaviour of a building envelope due to retrofitted cavity wall and ceiling insulation. *Energy and Buildings*, 61, pp.356–365.

Carrillo, A., Dominguez, F. & Cejudo, J.M., 2009. Calibration of an EnergyPlus simulation model by the STEM-PSTAR method. In *Eleventh International IBPSA Conference, Glasgow, Scotland*. pp. 2043–2050.

Cattarin, G. et al., 2016. Outdoor test cells for building envelope experimental characterisation–A literature review. *Renewable and Sustainable Energy Reviews*, 54, pp.606–625.

Cesaratto, P.G., De Carli, M. & Marinetti, S., 2011. Effect of different parameters on the in situ thermal conductance evaluation. *Energy and Buildings*, 43(7), pp.1792–1801.

Chan, W.R. et al., 2005. Analyzing a database of residential air leakage in the United States. *Atmospheric Environment*, 39(19), pp.3445–3455.

Chan, W.R., Joh, J. & Sherman, M.H., 2013. Analysis of air leakage measurements of US houses. *Energy and Buildings*, 66, pp.616–625.

COAG, C. of A.G., 2015. National Energy Productivity Plan 2015-2030. Available at: http://www.coagenergycouncil.gov.au/publications/national-energy-productivity-plan-2015-2030.

Cucumo, M. et al., 2006. A method for the experimental evaluation in situ of the wall conductance. *Energy and buildings*, 38(3), pp.238–244.

Depecker, P. et al., 2001. Design of buildings shape and energetic consumption. *Building and Environment*, 36(5), pp.627–635.

Desogus, G., Mura, S. & Ricciu, R., 2011. Comparing different approaches to in situ measurement of building components thermal resistance. *Energy and Buildings*, 43(10), pp.2613–2620.

DEWHA, H.& the A. Department of the Environment Water, 2008. *Energy Use in the Australian Residential Sector 1986-2020*, Commonwealth of Australia.

Dewsbury, M., 2011. The empirical validation of house energy rating (HER) software for lightweight housing in cool temperate climates. School of Architecture & Design. Launceston, University of Tasmania. *Doctor of Philosophy*.

Dewsbury, M., Fay, R. & Nolan, G., 2008. Thermal performance of light-weight timber test buildings. *World Congress of Timber Engineering, Miyazaki*.

Dewsbury, M., Nolan, G. & Fay, R., 2007a. Comparison of test cell thermal performance: August to December 2006. *Project Report. Centre for Sustainable Architecture with Wood, School of Architecture & Design, University of Tasmania*.

Dewsbury, M., Nolan, G. & Fay, R., 2007b. The design of three thermal performance test cells in Launceston. *The 41st Annual Conference of the Architectural Association ANZAScA, Geelong, Deakin University*.

Doran, S., 2008. *Thermal transmittance of walls of dwellings before and after application of insulation*, Energy Saving Trust.

Elasfouri, A., Maraqa, R. & Tabbalat, R., 1991. Shading control by neighbouring buildings: application to buildings in Amman, Jordan. *International journal of refrigeration*, 14(2), pp.112–116.

Elster, 2014. A100C Specification Sheet. Available at: http://www.elstersolutions.com/en/product-details-emea/32/en/A100C___A102C?fid=A6D29F0D893A460F9F004AB0CDFBD870#sbox0=field1,downloads;

European Union, E.P.& the Council of the, 2010. *Directive 2010/31/EU of the European Parliament and of the council* E. Parliament & the Council of the European Union, eds.,

Everett, R., Horton, A. & Doggart, J., 1985. Linford low energy houses.

Fabi, V. et al., 2012. Occupants' window opening behaviour: A literature review of factors influencing occupant behaviour and models. *Building and Environment*, 58, pp.188–198.

Fels, M.F., 1986. PRISM: an introduction. *Energy and Buildings*, 9(1), pp.5–18.

Ficco, G. et al., 2015. U-value in situ measurement for energy diagnosis of existing buildings. *Energy and Buildings*, 104, pp.108–121.

Frontline, 2018. EXCEL SOLVER - ALGORITHMS AND METHODS USED. Available at: https://www.solver.com/excel-solver-algorithms-and-methods-used.

Garcıa-Gáfaro, C. et al., 2012. Experience gained in the Thermal Characterization of Building Components by using PASLINK Test Cells. In *5th International Building Physics Conference (IBPC), Kyoto*.

Gasparella, A. et al., 2011. Analysis and modelling of window and glazing systems energy performance for a well insulated residential building. *Energy and Buildings*, 43(4), pp.1030–1037.

Geros, V. et al., 1999. Experimental evaluation of night ventilation phenomena. *Energy and Buildings*, 29(2), pp.141–154.

Givoni, B., 2011. Indoor temperature reduction by passive cooling systems. *Solar Energy*, 85(8), pp.1692–1726.

Greening, L.A., Greene, D.L. & Difiglio, C., 2000. Energy efficiency and consumption—the rebound effect—a survey. *Energy policy*, 28(6), pp.389–401.

Gregory, K. et al., 2008. Effect of thermal mass on the thermal performance of various Australian residential constructions systems. *Energy and Buildings*, 40(4), pp.459–465.

Grinzato, E., Vavilov, V. & Kauppinen, T., 1998. Quantitative infrared thermography in buildings. *Energy and Buildings*, 29(1), pp.1–9.

Guerra-Santin, O. et al., 2013. Monitoring the performance of low energy dwellings: Two UK case studies. *Energy and Buildings*, 64, pp.32–40.

Guerra-Santin, O. & Itard, L., 2010. Occupants' behaviour: determinants and effects on residential heating consumption. *Building Research & Information*, 38(3), pp.318–338.

Guerra-Santin, O. & Itard, L., 2012. The effect of energy performance regulations on energy consumption. *Energy Efficiency*, 5(3), pp.269–282.

Guerra-Santin, O., Itard, L. & Visscher, H., 2009. The effect of occupancy and building characteristics on energy use for space and water heating in Dutch residential stock. *Energy and buildings*, 41(11), pp.1223–1232.

Gupta, R. & Dantsiou, D., 2013. Understanding the Gap between "as Designed"and "as Built"Performance of a New Low Carbon Housing Development in UK. In *Sustainability in Energy and Buildings*. Springer, pp. 567–580.

Gutschker, O., 2004. *LORD – Modelling and identification software for thermal systems, User Manual*, Brandenburg Technical University of Cottbus.

Haralambopoulos, D. & Paparsenos, G., 1998. Assessing the thermal insulation of old buildings—The need for in situ spot measurements of thermal resistance and planar infrared thermography. *Energy conversion and management*, 39(1), pp.65–79.

Heard, C. & Ward, I., 1982. The design and use of low-cost heat flux plates for the measurement of building heat transfer rates. *Building and Environment*, 17(3), pp.229–233.

Henninger, R.H., Witte, M.J. & Crawley, D.B., 2004. Analytical and comparative testing of EnergyPlus using IEA HVAC BESTEST E100–E200 test suite. *Energy and Buildings*, 36(8), pp.855–863.

Hens, H., 2010. Energy efficient retrofit of an end of the row house: confronting predictions with long-term measurements. *Energy and Buildings*, 42(10), pp.1939–1947.

Hitchin, E., Delaforce, S. & Martin, C., 1993. A comparison of the measured and simulated thermal response of a simple enclosure. *Building and Environment*, 28(2), pp.189–199.

Hitchin, E. & Wilson, C., 1967. A review of experimental techniques for the investigation of natural ventilation in buildings. *Building Science*, 2(1), pp.59–82.

Hsueh, L.M. & Gerner, J.L., 1993. Effect of thermal improvements in housing on residential energy demand. *Journal of Consumer Affairs*, 27(1), pp.87–105.

Hukseflux, 2014. HPF01 - Heat Flux Plate. Available at: http://www.hukseflux.com/product/hfp01?referrer=/product_group/heat-flux-sensors.

ISO, B., 2014. 9869-1: 2014 Thermal insulation–Building elements–In-situ measurement of thermal resistance and thermal transmittance–Part 1: Heat flow meter method. *London: BSI*.

Jack, R. et al., 2017. First evidence for the reliability of building co-heating tests. *Building Research and Information*, 46:4, pp.383–401.

Johnston, D. et al., 2014. Bridging the domestic building fabric performance gap. *Building Research and Information*, 44.

Johnston, D. et al., 2013. Whole house heat loss test method (Coheating). *Leeds Beckett University, Leeds*.

Johnston, D., Miles-Shenton, D. & Farmer, D., 2015. Quantifying the domestic building fabric 'performance gap. *Building Services Engineering Research and Technology*, p.0143624415570344.

Jokisalo, J. et al., 2009. Building leakage, infiltration, and energy performance analyses for Finnish detached houses. *Building and Environment*, 44(2), pp.377–387.

Judkoff, R. et al., 2000. *Side-by-side thermal tests of modular offices: A validation study of the STEM method*, National Renewable Energy Laboratory.

Kalamees, T., 2007. Air tightness and air leakages of new lightweight single-family detached houses in Estonia. *Building and environment*, 42(6), pp.2369–2377.

Karlsson, J., Karlsson, B. & Roos, A., 2001. A simple model for assessing the energy performance of windows. *Energy and Buildings*, 33(7), pp.641–651.

Kim, J.-J. & Moon, J.W., 2009. Impact of insulation on building energy consumption. In *Eleventh International IBPSA Conference, Building Simulation*. Citeseer.

Kim, M.-H., Jo, J.-H. & Jeong, J.-W., 2013. Feasibility of building envelope air leakage measurement using combination of air-handler and blower door. *Energy and Buildings*, 62, pp.436–441.

Knauff, 2014. Earthwool Insulation Product Flyer. Available at: http://www.knaufinsulation.com.au/media/1051927/earthwool_top_web.pdf.

Kronvall, J., 1978. Testing of houses for air leakage using a pressure method. *ASHRAE Transactions*, 84.1, pp.72–79.

Krüger, E. & Givoni, B., 2004. Predicting thermal performance in occupied dwellings. *Energy and Buildings*, 36(3), pp.301–307.

Krüger, E. & Givoni, B., 2008. Thermal monitoring and indoor temperature predictions in a passive solar building in an arid environment. *building and environment*, 43(11), pp.1792–1804.

Law, A., Wong, J. & Ridley, I., 2016. Calibration of a building model using the co-heating test. In *PLEA 2016: Cities, Buildings People: Toward Regenerative Environments*. PLEA 2016 Los Angeles, pp. 901–906.

Letherman, K. & Palin, C., 1982. Experiments on the dynamic thermal response of rooms. *Building and Environment*, 17(3), pp.235–241.

Leth-Petersen, S. & Togeby, M., 2001. Demand for space heating in apartment blocks: measuring effects of policy measures aiming at reducing energy consumption. *Energy Economics*, 23(4), pp.387–403.

Liao, H.-C. & Chang, T.-F., 2002. Space-heating and water-heating energy demands of the aged in the US. *Energy Economics*, 24(3), pp.267–284.

Liddament, M. & Orme, M., 1998. Energy and ventilation. *Applied Thermal Engineering*, 18(11), pp.1101–1109.

Liley, J.B., 2017. *Creation of NatHERS 2016 Reference Meterological Years*, Department of Environment and Energy.

Lo, T.Y. & Choi, K., 2004. Building defects diagnosis by infrared thermography. *Structural Survey*, 22(5), pp.259–263.

Lomas, K. et al., 1997. Empirical validation of building energy simulation programs. *Energy and buildings*, 26(3), pp.253–275.

Lomas, K.J. & Eppel, H., 1992. Sensitivity analysis techniques for building thermal simulation programs. *Energy and Buildings*, 19(1), pp.21–44. Available at: http://www.sciencedirect.com/science/article/pii/037877889290033D.

Loutzenhiser, P.G. et al., 2009. An empirical validation of window solar gain models and the associated interactions. *International Journal of Thermal Sciences*, 48(1), pp.85–95.

Lowe, R. et al., 2007. Evidence for heat losses via party wall cavities in masonry construction. *Building Services Engineering Research and Technology*, 28(2), pp.161–181.

Lundin, M., Andersson, S. & Östin, R., 2004. Development and validation of a method aimed at estimating building performance parameters. *Energy and Buildings*, 36(9), pp.905–914.

Makaka, G., Meyer, E.L. & McPherson, M., 2008. Thermal behaviour and ventilation efficiency of a low-cost passive solar energy efficient house. *Renewable energy*, 33(9), pp.1959–1973.

Maladague, X.P.V., 2001. *Theory and practice of infrared technology for nondestructive testing*, John Wiley & Sons.

Malik, N., 1978. Field studies of dependence of air infiltration on outside temperature and wind. *Energy and Buildings*, 1(3), pp.281–292.

Mangematin, E., Pandraud, G. & Roux, D., 2012. Quick measurements of energy efficiency of buildings. *Comptes Rendus Physique*, 13(4), pp.383–390.

McLeod, P. & Fay, R., 2010. Costs of improving the thermal performance of houses in a cool-temperate climate. *Architectural Science Review*, 53(3), pp.307–314.

Miller, W.F., 1990. *Short-term hourly temperature interpolation*, AIR FORCE ENVIRONMENTAL TECHNICAL APPLICATIONS CENTER SCOTT AFB IL.

Mlecnik, E., Visscher, H. & Van Hal, A., 2010. Barriers and opportunities for labels for highly energy-efficient houses. *Energy Policy*, 38(8), pp.4592–4603.

Moody, D., 2002. Empirical Research Methods. Available at: http://folk.uio.no/patrickr/refdoc/methods.pdf.

Morrissey, J., Moore, T. & Horne, R., 2011. Affordable passive solar design in a temperate climate: An experiment in residential building orientation. *Renewable Energy*, 36(2), pp.568–577.

Al-Mumin, A., Khattab, O. & Sridhar, G., 2003. Occupants' behavior and activity patterns influencing the energy consumption in the Kuwaiti residences. *Energy and Buildings*, 35, pp.549–559.

Nabinger, S. & Persily, A., 2011. Impacts of airtightening retrofits on ventilation rates and energy consumption in a manufactured home. *Energy and Buildings*, 43(11), pp.3059–3067.

NREL, Nb.R.E.L., 2015. *Engineering Reference: The Reference to EnergyPlus calculations*, U.S. Department of Energy (DOE). Available at: https://energyplus.net/sites/default/files/pdfs_v8.3.0/EngineeringReference.pdf.

O'Connell, J., 1999. Heating water: Rate correction due to Newtonian cooling. *The Physics Teacher*, 37, pp.551–552.

Onset, 2014. HOBO Temperature/Relative Humidity/2 External Channel Data Logger. Available at: http://www.onsetcomp.com/products/data-loggers/u12-013.

Ortega, J.K. et al., 1981. *Electric coheating experiment to determine the heat-loss coefficient of a double-envelope house*, Solar Energy Research Inst., Golden, CO (USA).

Ouyang, J. & Hokao, K., 2009. Energy-saving potential by improving occupants' behavior in urban residential sector in Hangzhou City, China. *Energy and Buildings*, 41(7), pp.711–720.

Pacheco, R., Ordóñez, J. & Martınez, G., 2012. Energy efficient design of building: a review. *Renewable and Sustainable Energy Reviews*, 16(6), pp.3559–3573.

Page, A. et al., 2011. A study of the thermal performance of Australian housing.

Pan, D. et al., 2012. The effects of external wall insulation thickness on annual cooling and heating energy uses under different climates. *Applied Energy*, 97, pp.313–318.

Pan, W., 2010. Relationships between air-tightness and its influencing factors of post-2006 new-build dwellings in the UK. *Building and Environment*, 45(11), pp.2387–2399.

Parkinson, M. et al., 2010. *Report of the Prime Minster's Task Group on Energy Efficiency*, Department of Climate Change and Energy Efficiency.

Peng, C. & Wu, Z., 2008. In situ measuring and evaluating the thermal resistance of building construction. *Energy and Buildings*, 40(11), pp.2076–2082.

Pérez-Lombard, L., Ortiz, J. & Pout, C., 2008. A review on buildings energy consumption information. *Energy and buildings*, 40(3), pp.394–398.

Persson, M.-L., Roos, A. & Wall, M., 2006. Influence of window size on the energy balance of low energy houses. *Energy and Buildings*, 38(3), pp.181–188.

Rachlin, J., Fels, M.F. & Socolow, R.H., 1986. The stability of PRISM estimates. *Energy and buildings*, 9(1), pp.149–157.

Raftery, P., Keane, M. & O'Donnell, J., 2011. Calibrating whole building energy models: An evidence-based methodology. *Energy and Buildings*, 43(9), pp.2356–2364.

Reardon, C. et al., 2007. *YourHome Technical Manual* P. Downton, ed., DoE, Department of the Environment, Water, Heritage and the Arts.

Rehdanz, K., 2007. Determinants of residential space heating expenditures in Germany. *Energy Economics*, 29(2), pp.167–182.

Retrotec, 2014. 6101 Hi-Power. Available at: https://retrotec.com/products/6101-hi-power.

Rezaie, B., Dincer, I. & Esmailzadeh, E., 2013. Energy options for residential buildings assessment. *Energy Conversion and Management*, 65, pp.637–646.

Rhee-Duverne, S. & Baker, D.P., 2015. *A Retrofit of a Victorian Terrace House in New Bolsover: A Whole House Thermal Performance Assessment*, Historic England.

Ridley, I. et al., 2013. The monitored performance of the first new London dwelling certified to the Passive House standard. *Energy and Buildings*, 63, pp.67–78.

Ridley, I. et al., 2014. The side by side in use monitored performance of two passive and low carbon Welsh houses. *Energy and Buildings*, 82, pp.13–26.

Roetzel, A. et al., 2010. A review of occupant control on natural ventilation. *Renewable and Sustainable Energy Reviews*, 14(3), pp.1001–1013.

Ryan, E.M. & Sanquist, T.F., 2012. Validation of building energy modeling tools under idealized and realistic conditions. *Energy and Buildings*, 47, pp.375–382.

Rye, C. & Scott, C., 2010. THE SPAB RESEARCH REPORT 1. U-VALUE REPORT. *The Society for the Protection of Ancient Buildings, London*.

Sadineni, S.B., Madala, S. & Boehm, R.F., 2011. Passive building energy savings: A review of building envelope components. *Renewable and Sustainable Energy Reviews*, 15(8), pp.3617–3631.

SAP, 2012. *The Government's Standard Assessment Procedure for Energy Rating of Dwellings*, BRE.

Schweiker, M. & Shukuya, M., 2010. Comparative effects of building envelope improvements and occupant behavioural changes on the exergy consumption for heating and cooling. *Energy Policy*, 38(6), pp.2976–2986.

Sfakianaki, A. et al., 2008. Air tightness measurements of residential houses in Athens, Greece. *Building and Environment*, 43(4), pp.398–405.

Shaviv, E., Yezioro, A. & Capeluto, I.G., 2001. Thermal mass and night ventilation as passive cooling design strategy. *Renewable energy*, 24(3), pp.445–452.

Sherman, M.H., 1987. Estimation of infiltration from leakage and climate indicators. *Energy and Buildings*, 10(1), pp.81–86.

Sherman, M.H., 1990. Tracer-gas techniques for measuring ventilation in a single zone. *Building and Environment*, 25(4), pp.365–374.

Sinnott, D. & Dyer, M., 2012. Air-tightness field data for dwellings in Ireland. *Building and environment*, 51, pp.269–275.

Siviour, J., 1981. Experimental thermal calibration of houses. *Rapid Thermal Calibration of Houses; Everett, R., Ed.; Technical Report ERG*, 55.

Sonderegger, R., 1979. Electric co-heating: a method for evaluating seasonal heating efficiencies and heat loss rates in dwellings. In *Proceedings of the Second International CIB Symposium, Energy Conservation in the Built Environment, Copenhagen*.

Spanos, I., Simons, M. & Holmes, K.L., 2005. Cost savings by application of passive solar heating. *Structural Survey*, 23(2), pp.111–130.

Stamp, S., 2013. *Coheating Test of Camden Passivhaus*, UCL Energy Institute.

Stamp, S., 2011. *The Error and Uncertainty in Coheating Tests*. University College London.

Stazi, F., Mastrucci, A. & Perna, C. di, 2012. The behaviour of solar walls in residential buildings with different insulation levels: an experimental and numerical study. *Energy and Buildings*, 47, pp.217–229.

Stecher, D. & Allison, K., 2012. Maximum Residential Energy Efficiency: Performance Results from Long-Term Monitoring of a Passive House. *ASHRAE Transactions*, 118(1).

Strachan, P. & Vandaele, L., 2008. Case studies of outdoor testing and analysis of building components. *Building and Environment*, 43(2), pp.129–142.

Stram, D.O. & Fels, M.F., 1986. The applicability of PRISM to electric heating and cooling. *Energy and Buildings*, 9(1), pp.101–110.

Stymne, H., Boman, C.A. & Kronvall, J., 1994. Measuring ventilation rates in the Swedish housing stock. *Building and environment*, 29(3), pp.373–379.

Su, B., 2008. Building passive design and housing energy efficiency. *Architectural Science Review*, 51(3), pp.277–286.

Subbarao, K. et al., 1988. *Short-Term Energy Monitoring (STEM): Application of the PSTAR method to a residence in Fredericksburg, Virginia*, Solar Energy Research Inst., Golden, CO (USA).

Sugo, H. et al., 2004. A comparative study of the thermal performance of cavity and brick veneer construction. In *13th International Brick and Block Masonary Conference*. University of Newcastle Eindhoven, pp. 767–776.

Sugo, H. et al., 2005. The study of heat flows in masonry walls in a thermal test building incorporating a window.

Taylor, T. et al., 2012. In-construction testing of the thermal performance of dwellings using thermography. In *Sustainability in Energy and Buildings*. Springer, pp. 307–318.

Thompson, P. & Bootland, J., 2011. *Good Homes Alliance: Monitoring Programme 2009-11: Technical Report*, Good Homes Alliance.

Titman, D., 2001. Applications of thermography in non-destructive testing of structures. *NDT & E International*, 34(2), pp.149–154.

Tommerup, H., Rose, J. & Svendsen, S., 2007. Energy-efficient houses built according to the energy performance requirements introduced in Denmark in 2006. *Energy and Buildings*, 39(10), pp.1123–1130.

Trethowen, H., 1986. Measurement errors with surface-mounted heat flux sensors. *Building and Environment*, 21(1), pp.41–56.

Vollmer, M., 2009. Newton's law of cooling revisited. *European Journal of Physics*, 30(5), p.1063. Available at: http://stacks.iop.org/0143-0807/30/i=5/a=014.

Wang, S. & Chen, Y., 2002. A simple procedure for calculating thermal response factors and conduction transfer functions of multilayer walls. *Applied thermal engineering*, 22(3), pp.333–338.

Wang, X., Chen, D. & Ren, Z., 2010. Assessment of climate change impact on residential building heating and cooling energy requirement in Australia. *Building and Environment*, 45(7), pp.1663–1682.

Wang, X., Chen, D. & Ren, Z., 2011. Global warming and its implication to emission reduction strategies for residential buildings. *Building and Environment*, 46(4), pp.871–883.

De Wilde, P., 2014. The gap between predicted and measured energy performance of buildings: A framework for investigation. *Automation in Construction*, 41, pp.40–49.

Wingfield, J. et al., 2008. Lessons from Stamford Brook: understanding the gap between designed and real performance.

Yu, Z. et al., 2011. A systematic procedure to study the influence of occupant behavior on building energy consumption. *Energy and Buildings*, 43(6), pp.1409–1417.

ZCH, Z.C.H., 2014. *Closing the gap between design and as-built performance - End of Term Report*, Zero Carbon Hub.

Zhou, J. et al., 2008. Coupling of thermal mass and natural ventilation in buildings. *Energy and Buildings*, 40(6), pp.979–986.

Zhu, L. et al., 2009. Detailed energy saving performance analyses on thermal mass walls demonstrated in a zero energy house. *Energy and Buildings*, 41(3), pp.303–310.

Appendix A - Energy Plus Model of Base Test Cell

The following pages show the text output of the IDF file representing the building model from EnergyPlus. The schedules that define the HVAC control have been removed as they are 1100 pages in length.

```
!-Generator IDFEditor 1.44
!-Option SortedOrder

!-NOTE: All comments with '!-' are ignored by the IDFEditor and are
generated automatically.
!-      Use '!' comments if they need to be retained when using the
IDFEditor.


!-   ===========  ALL OBJECTS IN CLASS: VERSION ===========

Version,
    8.3;                    !- Version Identifier


!-   ===========  ALL OBJECTS IN CLASS: SIMULATIONCONTROL ===========

! Generator UCLIDF 1
! Biddulph October 2008
SimulationControl,
    No,                     !- Do Zone Sizing Calculation
    No,                     !- Do System Sizing Calculation
    No,                     !- Do Plant Sizing Calculation
    No,                     !- Run Simulation for Sizing Periods
    Yes;                    !- Run Simulation for Weather File Run
Periods


!-   ===========  ALL OBJECTS IN CLASS: BUILDING ===========

Building,
    Test Cell,              !- Name
    0.0,                    !- North Axis {deg}
    Country,                !- Terrain
    0.0000004,              !- Loads Convergence Tolerance Value
    0.0000004,              !- Temperature Convergence Tolerance Value
{deltaC}
    FullExterior,           !- Solar Distribution
    ,                       !- Maximum Number of Warmup Days
    6;                      !- Minimum Number of Warmup Days


!-   ===========  ALL OBJECTS IN CLASS: SHADOWCALCULATION ===========

ShadowCalculation,
    AverageOverDaysInFrequency,  !- Calculation Method
    20;                     !- Calculation Frequency
```

```
!-   ===========  ALL OBJECTS IN CLASS:
SURFACECONVECTIONALGORITHM:INSIDE ===========

SurfaceConvectionAlgorithm:Inside,
    TARP;                    !- Algorithm


!-   ===========  ALL OBJECTS IN CLASS:
SURFACECONVECTIONALGORITHM:OUTSIDE ===========

SurfaceConvectionAlgorithm:Outside,
    AdaptiveConvectionAlgorithm;  !- Algorithm


!-   ===========  ALL OBJECTS IN CLASS: TIMESTEP ===========

Timestep,
    60;                      !- Number of Timesteps per Hour


!-   ===========  ALL OBJECTS IN CLASS: RUNPERIOD ===========

RunPeriod,
    a,                       !- Name
    6,                       !- Begin Month
    18,                      !- Begin Day of Month
    7,                       !- End Month
    1,                       !- End Day of Month
    Thursday,                !- Day of Week for Start Day
    No,                      !- Use Weather File Holidays and Special
Days
    Yes,                     !- Use Weather File Daylight Saving Period
    No,                      !- Apply Weekend Holiday Rule
    Yes,                     !- Use Weather File Rain Indicators
    Yes,                     !- Use Weather File Snow Indicators
    1;                       !- Number of Times Runperiod to be
Repeated

!-   ===========  ALL OBJECTS IN CLASS: MATERIAL ===========

Material,
    Cemintel 7mm board,      !- Name
    MediumSmooth,            !- Roughness
    0.0075,                  !- Thickness {m}
    0.2776,                  !- Conductivity {W/m-K}
    1350,                    !- Density {kg/m3}
    1000;                    !- Specific Heat {J/kg-K}

Material,
    Door,                    !- Name
    MediumSmooth,            !- Roughness
    0.05,                    !- Thickness {m}
    0.227273,                !- Conductivity {W/m-K}
    200,                     !- Density {kg/m3}
    1630;                    !- Specific Heat {J/kg-K}

Material,
    Subfloor to Earth layer, !- Name
```

```
    MediumRough,              !- Roughness
    0.01,                     !- Thickness {m}
    100,                      !- Conductivity {W/m-K}
    1.2,                      !- Density {kg/m3}
    1005,                     !- Specific Heat {J/kg-K}
    0.9,                      !- Thermal Absorptance
    0.7,                      !- Solar Absorptance
    0.7;                      !- Visible Absorptance

Material,
    Hem-Fir - Spruce-Pine-Fir - 25mm,  !- Name
    MediumSmooth,             !- Roughness
    0.019,                    !- Thickness {m}
    0.19,                     !- Conductivity {W/m-K}
    447,                      !- Density {kg/m3}
    1630;                     !- Specific Heat {J/kg-K}

Material,
    Particleboard High density,  !- Name
    MediumSmooth,             !- Roughness
    0.019,                    !- Thickness {m}
    0.052778,                 !- Conductivity {W/m-K}
    1000,                     !- Density {kg/m3}
    1300;                     !- Specific Heat {J/kg-K}

Material,
    I04 89mm batt insulation,!- Name
    VeryRough,                !- Roughness
    0.0894,                   !- Thickness {m}
    0.046597,                 !- Conductivity {W/m-K}
    19,                       !- Density {kg/m3}
    960;                      !- Specific Heat {J/kg-K}

Material,
    M11 100mm lightweight concrete,  !- Name
    MediumRough,              !- Roughness
    0.1016,                   !- Thickness {m}
    0.53,                     !- Conductivity {W/m-K}
    1280,                     !- Density {kg/m3}
    840;                      !- Specific Heat {J/kg-K}

Material,
    Gyprock Plasterboard,     !- Name
    MediumSmooth,             !- Roughness
    0.01,                     !- Thickness {m}
    0.0625,                   !- Conductivity {W/m-K}
    800,                      !- Density {kg/m3}
    1090;                     !- Specific Heat {J/kg-K}

Material,
    RoofTile - Concrete,      !- Name
    MediumRough,              !- Roughness
    0.02,                     !- Thickness {m}
    0.53,                     !- Conductivity {W/m-K}
    1280,                     !- Density {kg/m3}
    840;                      !- Specific Heat {J/kg-K}
```

```
!-   ===========  ALL OBJECTS IN CLASS: MATERIAL:NOMASS ===========

Material:NoMass,
    SW_Wall,                 !- Name
    MediumSmooth,            !- Roughness
    0.24,                    !- Thermal Resistance {m2-K/W}
    0.01,                    !- Thermal Absorptance
    0.7,                     !- Solar Absorptance
    0.7;                     !- Visible Absorptance

Material:NoMass,
    OtherWalls,              !- Name
    Smooth,                  !- Roughness
    0.24,                    !- Thermal Resistance {m2-K/W}
    0.01,                    !- Thermal Absorptance
    0.7,                     !- Solar Absorptance
    0.7;                     !- Visible Absorptance

Material:NoMass,
    Roof_and_Floor,          !- Name
    MediumSmooth,            !- Roughness
    0.24,                    !- Thermal Resistance {m2-K/W}
    0.01,                    !- Thermal Absorptance
    0.7,                     !- Solar Absorptance
    0.7;                     !- Visible Absorptance


!-   ===========  ALL OBJECTS IN CLASS: MATERIAL:AIRGAP ===========

Material:AirGap,
    F05 Ceiling air space resistance,  !- Name
    0.18;                    !- Thermal Resistance {m2-K/W}

Material:AirGap,
    WallAirGap,              !- Name
    0.15;                    !- Thermal Resistance {m2-K/W}


!-   ===========  ALL OBJECTS IN CLASS:
WINDOWMATERIAL:SIMPLEGLAZINGSYSTEM ===========

WindowMaterial:SimpleGlazingSystem,
    Window,                  !- Name
    6.7,                     !- U-Factor {W/m2-K}
    0.57;                    !- Solar Heat Gain Coefficient


!-   ===========  ALL OBJECTS IN CLASS: WINDOWMATERIAL:SHADE
===========

WindowMaterial:Shade,
    MEDIUM REFLECT - LOW TRANS SHADE,  !- Name
    0.1,                     !- Solar Transmittance {dimensionless}
    0.5,                     !- Solar Reflectance {dimensionless}
    0.1,                     !- Visible Transmittance {dimensionless}
    0.5,                     !- Visible Reflectance {dimensionless}
    0.9,                     !- Infrared Hemispherical Emissivity
{dimensionless}
```

```
    0.0,                     !- Infrared Transmittance {dimensionless}
    0.005,                   !- Thickness {m}
    0.1,                     !- Conductivity {W/m-K}
    0.05,                    !- Shade to Glass Distance {m}
    0.5,                     !- Top Opening Multiplier
    0.5,                     !- Bottom Opening Multiplier
    0.5,                     !- Left-Side Opening Multiplier
    0.5,                     !- Right-Side Opening Multiplier
    0.0;                     !- Airflow Permeability {dimensionless}


!-   ===========  ALL OBJECTS IN CLASS: CONSTRUCTION ===========

Construction,
    Door,                    !- Name
    Door;                    !- Outside Layer

Construction,
    Window,                  !- Name
    Window;                  !- Outside Layer

Construction,
    SE_Wall,                 !- Name
    Cemintel 7mm board,      !- Outside Layer
    I04 89mm batt insulation,!- Layer 2
    Gyprock Plasterboard;    !- Layer 3

Construction,
    NE_Walls,                !- Name
    Cemintel 7mm board,      !- Outside Layer
    I04 89mm batt insulation,!- Layer 2
    Gyprock Plasterboard;    !- Layer 3

Construction,
    subfloor,                !- Name
    Subfloor to Earth layer; !- Outside Layer

Construction,
    subfloorwalls,           !- Name
    Cemintel 7mm board;      !- Outside Layer

Construction,
    Roof,                    !- Name
    RoofTile - Concrete;     !- Outside Layer

Construction,
    RoofSides,               !- Name
    Cemintel 7mm board;      !- Outside Layer

Construction,
    SW_Wall,                 !- Name
    Cemintel 7mm board,      !- Outside Layer
    I04 89mm batt insulation,!- Layer 2
    Hem-Fir - Spruce-Pine-Fir - 25mm;  !- Layer 3

Construction,
    NW_Walls,                !- Name
    Cemintel 7mm board,      !- Outside Layer
```

```
    I04 89mm batt insulation,!- Layer 2
    Gyprock Plasterboard;    !- Layer 3

Construction,
    Ceiling,                 !- Name
    Hem-Fir - Spruce-Pine-Fir - 25mm;  !- Outside Layer

Construction,
    Floor,                   !- Name
    Particleboard High density;  !- Outside Layer


!-   ===========  ALL OBJECTS IN CLASS: GLOBALGEOMETRYRULES ===========

GlobalGeometryRules,
    UpperLeftCorner,         !- Starting Vertex Position
    Counterclockwise,        !- Vertex Entry Direction
    Relative;                !- Coordinate System


!-   ===========  ALL OBJECTS IN CLASS: ZONE ===========

Zone,
    TestCell,                !- Name
    0,                       !- Direction of Relative North {deg}
    0,                       !- X Origin {m}
    0,                       !- Y Origin {m}
    0.5,                     !- Z Origin {m}
    1,                       !- Type
    1,                       !- Multiplier
    autocalculate,           !- Ceiling Height {m}
    autocalculate;           !- Volume {m3}

Zone,
    RoofSpace,               !- Name
    0,                       !- Direction of Relative North {deg}
    0,                       !- X Origin {m}
    0,                       !- Y Origin {m}
    2.87,                    !- Z Origin {m}
    1,                       !- Type
    1,                       !- Multiplier
    autocalculate,           !- Ceiling Height {m}
    autocalculate;           !- Volume {m3}

Zone,
    SubFloor,                !- Name
    0,                       !- Direction of Relative North {deg}
    0,                       !- X Origin {m}
    0,                       !- Y Origin {m}
    0,                       !- Z Origin {m}
    1,                       !- Type
    1,                       !- Multiplier
    autocalculate,           !- Ceiling Height {m}
    autocalculate;           !- Volume {m3}


!-   ===========  ALL OBJECTS IN CLASS: BUILDINGSURFACE:DETAILED
===========
```

```
BuildingSurface:Detailed,
    Subfloor SURFACE NORTH,  !- Name
    Wall,                    !- Surface Type
    subfloorwalls,           !- Construction Name
    SubFloor,                !- Zone Name
    Outdoors,                !- Outside Boundary Condition
    ,                        !- Outside Boundary Condition Object
    SunExposed,              !- Sun Exposure
    WindExposed,             !- Wind Exposure
    0,                       !- View Factor to Ground
    4,                       !- Number of Vertices
    4.51,                    !- Vertex 1 X-coordinate {m}
    4.515,                   !- Vertex 1 Y-coordinate {m}
    0.5,                     !- Vertex 1 Z-coordinate {m}
    4.51,                    !- Vertex 2 X-coordinate {m}
    4.515,                   !- Vertex 2 Y-coordinate {m}
    0,                       !- Vertex 2 Z-coordinate {m}
    0,                       !- Vertex 3 X-coordinate {m}
    4.515,                   !- Vertex 3 Y-coordinate {m}
    0,                       !- Vertex 3 Z-coordinate {m}
    0,                       !- Vertex 4 X-coordinate {m}
    4.515,                   !- Vertex 4 Y-coordinate {m}
    0.5;                     !- Vertex 4 Z-coordinate {m}

BuildingSurface:Detailed,
    Subfloor SURFACE EAST,   !- Name
    Wall,                    !- Surface Type
    subfloorwalls,           !- Construction Name
    SubFloor,                !- Zone Name
    Outdoors,                !- Outside Boundary Condition
    ,                        !- Outside Boundary Condition Object
    SunExposed,              !- Sun Exposure
    WindExposed,             !- Wind Exposure
    0,                       !- View Factor to Ground
    4,                       !- Number of Vertices
    4.51,                    !- Vertex 1 X-coordinate {m}
    0,                       !- Vertex 1 Y-coordinate {m}
    0.5,                     !- Vertex 1 Z-coordinate {m}
    4.51,                    !- Vertex 2 X-coordinate {m}
    0,                       !- Vertex 2 Y-coordinate {m}
    0,                       !- Vertex 2 Z-coordinate {m}
    4.51,                    !- Vertex 3 X-coordinate {m}
    4.515,                   !- Vertex 3 Y-coordinate {m}
    0,                       !- Vertex 3 Z-coordinate {m}
    4.51,                    !- Vertex 4 X-coordinate {m}
    4.515,                   !- Vertex 4 Y-coordinate {m}
    0.5;                     !- Vertex 4 Z-coordinate {m}

BuildingSurface:Detailed,
    Subfloor SURFACE SOUTH,  !- Name
    Wall,                    !- Surface Type
    subfloorwalls,           !- Construction Name
    SubFloor,                !- Zone Name
    Outdoors,                !- Outside Boundary Condition
    ,                        !- Outside Boundary Condition Object
    SunExposed,              !- Sun Exposure
    WindExposed,             !- Wind Exposure
```

```
    0,                        !- View Factor to Ground
    4,                        !- Number of Vertices
    0,                        !- Vertex 1 X-coordinate {m}
    0,                        !- Vertex 1 Y-coordinate {m}
    0.5,                      !- Vertex 1 Z-coordinate {m}
    0,                        !- Vertex 2 X-coordinate {m}
    0,                        !- Vertex 2 Y-coordinate {m}
    0,                        !- Vertex 2 Z-coordinate {m}
    4.51,                     !- Vertex 3 X-coordinate {m}
    0,                        !- Vertex 3 Y-coordinate {m}
    0,                        !- Vertex 3 Z-coordinate {m}
    4.51,                     !- Vertex 4 X-coordinate {m}
    0,                        !- Vertex 4 Y-coordinate {m}
    0.5;                      !- Vertex 4 Z-coordinate {m}

BuildingSurface:Detailed,
    Subfloor SURFACE WEST,    !- Name
    Wall,                     !- Surface Type
    subfloorwalls,            !- Construction Name
    SubFloor,                 !- Zone Name
    Outdoors,                 !- Outside Boundary Condition
    ,                         !- Outside Boundary Condition Object
    SunExposed,               !- Sun Exposure
    WindExposed,              !- Wind Exposure
    0,                        !- View Factor to Ground
    4,                        !- Number of Vertices
    0,                        !- Vertex 1 X-coordinate {m}
    4.515,                    !- Vertex 1 Y-coordinate {m}
    0.5,                      !- Vertex 1 Z-coordinate {m}
    0,                        !- Vertex 2 X-coordinate {m}
    4.515,                    !- Vertex 2 Y-coordinate {m}
    0,                        !- Vertex 2 Z-coordinate {m}
    0,                        !- Vertex 3 X-coordinate {m}
    0,                        !- Vertex 3 Y-coordinate {m}
    0,                        !- Vertex 3 Z-coordinate {m}
    0,                        !- Vertex 4 X-coordinate {m}
    0,                        !- Vertex 4 Y-coordinate {m}
    0.5;                      !- Vertex 4 Z-coordinate {m}

BuildingSurface:Detailed,
    Subfloor SURFACE FLOOR,   !- Name
    Floor,                    !- Surface Type
    subfloor,                 !- Construction Name
    SubFloor,                 !- Zone Name
    Ground,                   !- Outside Boundary Condition
    ,                         !- Outside Boundary Condition Object
    NoSun,                    !- Sun Exposure
    NoWind,                   !- Wind Exposure
    0,                        !- View Factor to Ground
    4,                        !- Number of Vertices
    0,                        !- Vertex 1 X-coordinate {m}
    0,                        !- Vertex 1 Y-coordinate {m}
    0,                        !- Vertex 1 Z-coordinate {m}
    0,                        !- Vertex 2 X-coordinate {m}
    4.515,                    !- Vertex 2 Y-coordinate {m}
    0,                        !- Vertex 2 Z-coordinate {m}
    4.51,                     !- Vertex 3 X-coordinate {m}
    4.515,                    !- Vertex 3 Y-coordinate {m}
```

```
    0,                       !- Vertex 3 Z-coordinate {m}
    4.51,                    !- Vertex 4 X-coordinate {m}
    0,                       !- Vertex 4 Y-coordinate {m}
    0;                       !- Vertex 4 Z-coordinate {m}

BuildingSurface:Detailed,
    Subfloor SURFACE ROOF,   !- Name
    Ceiling,                 !- Surface Type
    Floor,                   !- Construction Name
    SubFloor,                !- Zone Name
    Zone,                    !- Outside Boundary Condition
    TestCell,                !- Outside Boundary Condition Object
    NoSun,                   !- Sun Exposure
    NoWind,                  !- Wind Exposure
    0,                       !- View Factor to Ground
    4,                       !- Number of Vertices
    0,                       !- Vertex 1 X-coordinate {m}
    4.515,                   !- Vertex 1 Y-coordinate {m}
    0.5,                     !- Vertex 1 Z-coordinate {m}
    0,                       !- Vertex 2 X-coordinate {m}
    0,                       !- Vertex 2 Y-coordinate {m}
    0.5,                     !- Vertex 2 Z-coordinate {m}
    4.51,                    !- Vertex 3 X-coordinate {m}
    0,                       !- Vertex 3 Y-coordinate {m}
    0.5,                     !- Vertex 3 Z-coordinate {m}
    4.51,                    !- Vertex 4 X-coordinate {m}
    4.515,                   !- Vertex 4 Y-coordinate {m}
    0.5;                     !- Vertex 4 Z-coordinate {m}

BuildingSurface:Detailed,
    Roofspace SURFACE EAST,  !- Name
    Roof,                    !- Surface Type
    Roof,                    !- Construction Name
    RoofSpace,               !- Zone Name
    Outdoors,                !- Outside Boundary Condition
    ,                        !- Outside Boundary Condition Object
    SunExposed,              !- Sun Exposure
    WindExposed,             !- Wind Exposure
    0,                       !- View Factor to Ground
    4,                       !- Number of Vertices
    2.505,                   !- Vertex 1 X-coordinate {m}
    0,                       !- Vertex 1 Y-coordinate {m}
    1,                       !- Vertex 1 Z-coordinate {m}
    4.51,                    !- Vertex 2 X-coordinate {m}
    0,                       !- Vertex 2 Y-coordinate {m}
    0,                       !- Vertex 2 Z-coordinate {m}
    4.51,                    !- Vertex 3 X-coordinate {m}
    4.515,                   !- Vertex 3 Y-coordinate {m}
    0,                       !- Vertex 3 Z-coordinate {m}
    2.505,                   !- Vertex 4 X-coordinate {m}
    4.515,                   !- Vertex 4 Y-coordinate {m}
    1;                       !- Vertex 4 Z-coordinate {m}

BuildingSurface:Detailed,
    Roofspace SURFACE SOUTH, !- Name
    Wall,                    !- Surface Type
    RoofSides,               !- Construction Name
    RoofSpace,               !- Zone Name
```

```
    Outdoors,                !- Outside Boundary Condition
    ,                        !- Outside Boundary Condition Object
    SunExposed,              !- Sun Exposure
    WindExposed,             !- Wind Exposure
    0,                       !- View Factor to Ground
    3,                       !- Number of Vertices
    2.505,                   !- Vertex 1 X-coordinate {m}
    0,                       !- Vertex 1 Y-coordinate {m}
    1,                       !- Vertex 1 Z-coordinate {m}
    4.51,                    !- Vertex 2 X-coordinate {m}
    0,                       !- Vertex 2 Y-coordinate {m}
    0,                       !- Vertex 2 Z-coordinate {m}
    0,                       !- Vertex 3 X-coordinate {m}
    0,                       !- Vertex 3 Y-coordinate {m}
    0;                       !- Vertex 3 Z-coordinate {m}

BuildingSurface:Detailed,
    Roofspace SURFACE WEST,  !- Name
    Roof,                    !- Surface Type
    Roof,                    !- Construction Name
    RoofSpace,               !- Zone Name
    Outdoors,                !- Outside Boundary Condition
    ,                        !- Outside Boundary Condition Object
    SunExposed,              !- Sun Exposure
    WindExposed,             !- Wind Exposure
    0,                       !- View Factor to Ground
    4,                       !- Number of Vertices
    2.505,                   !- Vertex 1 X-coordinate {m}
    4.515,                   !- Vertex 1 Y-coordinate {m}
    1,                       !- Vertex 1 Z-coordinate {m}
    0,                       !- Vertex 2 X-coordinate {m}
    4.515,                   !- Vertex 2 Y-coordinate {m}
    0,                       !- Vertex 2 Z-coordinate {m}
    0,                       !- Vertex 3 X-coordinate {m}
    0,                       !- Vertex 3 Y-coordinate {m}
    0,                       !- Vertex 3 Z-coordinate {m}
    2.505,                   !- Vertex 4 X-coordinate {m}
    0,                       !- Vertex 4 Y-coordinate {m}
    1;                       !- Vertex 4 Z-coordinate {m}

BuildingSurface:Detailed,
    Roofspace SURFACE NORTH, !- Name
    Wall,                    !- Surface Type
    RoofSides,               !- Construction Name
    RoofSpace,               !- Zone Name
    Outdoors,                !- Outside Boundary Condition
    ,                        !- Outside Boundary Condition Object
    SunExposed,              !- Sun Exposure
    WindExposed,             !- Wind Exposure
    0,                       !- View Factor to Ground
    3,                       !- Number of Vertices
    2.505,                   !- Vertex 1 X-coordinate {m}
    4.515,                   !- Vertex 1 Y-coordinate {m}
    1,                       !- Vertex 1 Z-coordinate {m}
    4.51,                    !- Vertex 2 X-coordinate {m}
    4.515,                   !- Vertex 2 Y-coordinate {m}
    0,                       !- Vertex 2 Z-coordinate {m}
    0,                       !- Vertex 3 X-coordinate {m}
```

```
    4.515,                   !- Vertex 3 Y-coordinate {m}
    0;                       !- Vertex 3 Z-coordinate {m}

BuildingSurface:Detailed,
    Roofspace SURFACE FLOOR, !- Name
    Floor,                   !- Surface Type
    Ceiling,                 !- Construction Name
    RoofSpace,               !- Zone Name
    Zone,                    !- Outside Boundary Condition
    TestCell,                !- Outside Boundary Condition Object
    NoSun,                   !- Sun Exposure
    NoWind,                  !- Wind Exposure
    0,                       !- View Factor to Ground
    4,                       !- Number of Vertices
    0,                       !- Vertex 1 X-coordinate {m}
    0,                       !- Vertex 1 Y-coordinate {m}
    0,                       !- Vertex 1 Z-coordinate {m}
    0,                       !- Vertex 2 X-coordinate {m}
    4.515,                   !- Vertex 2 Y-coordinate {m}
    0,                       !- Vertex 2 Z-coordinate {m}
    4.51,                    !- Vertex 3 X-coordinate {m}
    4.515,                   !- Vertex 3 Y-coordinate {m}
    0,                       !- Vertex 3 Z-coordinate {m}
    4.51,                    !- Vertex 4 X-coordinate {m}
    0,                       !- Vertex 4 Y-coordinate {m}
    0;                       !- Vertex 4 Z-coordinate {m}

BuildingSurface:Detailed,
    Testcell SURFACE NORTH,  !- Name
    Wall,                    !- Surface Type
    NE_Walls,                !- Construction Name
    TestCell,                !- Zone Name
    Outdoors,                !- Outside Boundary Condition
    ,                        !- Outside Boundary Condition Object
    SunExposed,              !- Sun Exposure
    WindExposed,             !- Wind Exposure
    0,                       !- View Factor to Ground
    4,                       !- Number of Vertices
    4.51,                    !- Vertex 1 X-coordinate {m}
    4.515,                   !- Vertex 1 Y-coordinate {m}
    2.37,                    !- Vertex 1 Z-coordinate {m}
    4.51,                    !- Vertex 2 X-coordinate {m}
    4.515,                   !- Vertex 2 Y-coordinate {m}
    0,                       !- Vertex 2 Z-coordinate {m}
    0,                       !- Vertex 3 X-coordinate {m}
    4.515,                   !- Vertex 3 Y-coordinate {m}
    0,                       !- Vertex 3 Z-coordinate {m}
    0,                       !- Vertex 4 X-coordinate {m}
    4.515,                   !- Vertex 4 Y-coordinate {m}
    2.37;                    !- Vertex 4 Z-coordinate {m}

BuildingSurface:Detailed,
    Testcell SURFACE EAST,   !- Name
    Wall,                    !- Surface Type
    SE_Wall,                 !- Construction Name
    TestCell,                !- Zone Name
    Outdoors,                !- Outside Boundary Condition
    ,                        !- Outside Boundary Condition Object
```

```
    SunExposed,               !- Sun Exposure
    WindExposed,              !- Wind Exposure
    0,                        !- View Factor to Ground
    4,                        !- Number of Vertices
    4.51,                     !- Vertex 1 X-coordinate {m}
    0,                        !- Vertex 1 Y-coordinate {m}
    2.37,                     !- Vertex 1 Z-coordinate {m}
    4.51,                     !- Vertex 2 X-coordinate {m}
    0,                        !- Vertex 2 Y-coordinate {m}
    0,                        !- Vertex 2 Z-coordinate {m}
    4.51,                     !- Vertex 3 X-coordinate {m}
    4.515,                    !- Vertex 3 Y-coordinate {m}
    0,                        !- Vertex 3 Z-coordinate {m}
    4.51,                     !- Vertex 4 X-coordinate {m}
    4.515,                    !- Vertex 4 Y-coordinate {m}
    2.37;                     !- Vertex 4 Z-coordinate {m}

BuildingSurface:Detailed,
    Testcell SURFACE SOUTH,   !- Name
    Wall,                     !- Surface Type
    SW_Wall,                  !- Construction Name
    TestCell,                 !- Zone Name
    Outdoors,                 !- Outside Boundary Condition
    ,                         !- Outside Boundary Condition Object
    SunExposed,               !- Sun Exposure
    WindExposed,              !- Wind Exposure
    0,                        !- View Factor to Ground
    4,                        !- Number of Vertices
    0,                        !- Vertex 1 X-coordinate {m}
    0,                        !- Vertex 1 Y-coordinate {m}
    2.37,                     !- Vertex 1 Z-coordinate {m}
    0,                        !- Vertex 2 X-coordinate {m}
    0,                        !- Vertex 2 Y-coordinate {m}
    0,                        !- Vertex 2 Z-coordinate {m}
    4.51,                     !- Vertex 3 X-coordinate {m}
    0,                        !- Vertex 3 Y-coordinate {m}
    0,                        !- Vertex 3 Z-coordinate {m}
    4.51,                     !- Vertex 4 X-coordinate {m}
    0,                        !- Vertex 4 Y-coordinate {m}
    2.37;                     !- Vertex 4 Z-coordinate {m}

BuildingSurface:Detailed,
    Testcell SURFACE WEST,    !- Name
    Wall,                     !- Surface Type
    NW_Walls,                 !- Construction Name
    TestCell,                 !- Zone Name
    Outdoors,                 !- Outside Boundary Condition
    ,                         !- Outside Boundary Condition Object
    SunExposed,               !- Sun Exposure
    WindExposed,              !- Wind Exposure
    0,                        !- View Factor to Ground
    4,                        !- Number of Vertices
    0,                        !- Vertex 1 X-coordinate {m}
    4.515,                    !- Vertex 1 Y-coordinate {m}
    2.37,                     !- Vertex 1 Z-coordinate {m}
    0,                        !- Vertex 2 X-coordinate {m}
    4.515,                    !- Vertex 2 Y-coordinate {m}
    0,                        !- Vertex 2 Z-coordinate {m}
```

```
    0,                        !- Vertex 3 X-coordinate {m}
    0,                        !- Vertex 3 Y-coordinate {m}
    0,                        !- Vertex 3 Z-coordinate {m}
    0,                        !- Vertex 4 X-coordinate {m}
    0,                        !- Vertex 4 Y-coordinate {m}
    2.37;                     !- Vertex 4 Z-coordinate {m}

BuildingSurface:Detailed,
    Testcell SURFACE FLOOR,   !- Name
    Floor,                    !- Surface Type
    Floor,                    !- Construction Name
    TestCell,                 !- Zone Name
    Zone,                     !- Outside Boundary Condition
    SubFloor,                 !- Outside Boundary Condition Object
    NoSun,                    !- Sun Exposure
    NoWind,                   !- Wind Exposure
    0,                        !- View Factor to Ground
    4,                        !- Number of Vertices
    0,                        !- Vertex 1 X-coordinate {m}
    0,                        !- Vertex 1 Y-coordinate {m}
    0,                        !- Vertex 1 Z-coordinate {m}
    0,                        !- Vertex 2 X-coordinate {m}
    4.515,                    !- Vertex 2 Y-coordinate {m}
    0,                        !- Vertex 2 Z-coordinate {m}
    4.51,                     !- Vertex 3 X-coordinate {m}
    4.515,                    !- Vertex 3 Y-coordinate {m}
    0,                        !- Vertex 3 Z-coordinate {m}
    4.51,                     !- Vertex 4 X-coordinate {m}
    0,                        !- Vertex 4 Y-coordinate {m}
    0;                        !- Vertex 4 Z-coordinate {m}

BuildingSurface:Detailed,
    Testcell SURFACE ROOF,    !- Name
    Ceiling,                  !- Surface Type
    Ceiling,                  !- Construction Name
    TestCell,                 !- Zone Name
    Zone,                     !- Outside Boundary Condition
    RoofSpace,                !- Outside Boundary Condition Object
    NoSun,                    !- Sun Exposure
    NoWind,                   !- Wind Exposure
    0,                        !- View Factor to Ground
    4,                        !- Number of Vertices
    0,                        !- Vertex 1 X-coordinate {m}
    4.515,                    !- Vertex 1 Y-coordinate {m}
    2.37,                     !- Vertex 1 Z-coordinate {m}
    0,                        !- Vertex 2 X-coordinate {m}
    0,                        !- Vertex 2 Y-coordinate {m}
    2.37,                     !- Vertex 2 Z-coordinate {m}
    4.51,                     !- Vertex 3 X-coordinate {m}
    0,                        !- Vertex 3 Y-coordinate {m}
    2.37,                     !- Vertex 3 Z-coordinate {m}
    4.51,                     !- Vertex 4 X-coordinate {m}
    4.515,                    !- Vertex 4 Y-coordinate {m}
    2.37;                     !- Vertex 4 Z-coordinate {m}


!-   ===========  ALL OBJECTS IN CLASS: WINDOW ===========
```

```
Window,
    Window1,                  !- Name
    Window,                   !- Construction Name
    Testcell SURFACE WEST,    !- Building Surface Name
    Shade1,                   !- Shading Control Name
    ,                         !- Frame and Divider Name
    1,                        !- Multiplier
    1.5,                      !- Starting X Coordinate {m}
    1.5,                      !- Starting Z Coordinate {m}
    0.6,                      !- Length {m}
    0.6;                      !- Height {m}


!-   ===========  ALL OBJECTS IN CLASS: DOOR ===========

Door,
    Door1,                    !- Name
    Door,                     !- Construction Name
    Testcell SURFACE EAST,    !- Building Surface Name
    1,                        !- Multiplier
    1.5,                      !- Starting X Coordinate {m}
    0,                        !- Starting Z Coordinate {m}
    0.84,                     !- Length {m}
    2.04;                     !- Height {m}


!-   ===========  ALL OBJECTS IN CLASS: WINDOWPROPERTY:SHADINGCONTROL
===========

WindowProperty:ShadingControl,
    Shade1,                   !- Name
    InteriorShade,            !- Shading Type
    ,                         !- Construction with Shading Name
    AlwaysOn,                 !- Shading Control Type
    ,                         !- Schedule Name
    ,                         !- Setpoint {W/m2, W or deg C}
    No,                       !- Shading Control Is Scheduled
    No,                       !- Glare Control Is Active
    MEDIUM REFLECT - LOW TRANS SHADE,  !- Shading Device Material Name
    FixedSlatAngle,           !- Type of Slat Angle Control for Blinds
    ;                         !- Slat Angle Schedule Name


!-   ===========  ALL OBJECTS IN CLASS: ROOMAIRMODELTYPE ===========

RoomAirModelType,
    Airmix,                   !- Name
    TestCell,                 !- Zone Name
    UserDefined,              !- Room-Air Modeling Type
    Direct;                   !- Air Temperature Coupling Strategy


!-   ===========  ALL OBJECTS IN CLASS:
ROOMAIR:TEMPERATUREPATTERN:USERDEFINED ===========

RoomAir:TemperaturePattern:UserDefined,
    AirMix,                   !- Name
    TestCell,                 !- Zone Name
```

```
    ON,                      !- Availability Schedule Name
    AirMixing;               !- Pattern Control Schedule Name


!-   ===========  ALL OBJECTS IN CLASS:
ROOMAIR:TEMPERATUREPATTERN:NONDIMENSIONALHEIGHT ===========

RoomAir:TemperaturePattern:NondimensionalHeight,
    Air1,                    !- Name
    1,                       !- Control Integer for Pattern Control
Schedule Name
    0.13,                    !- Thermostat Offset {deltaC}
    1,                       !- Return Air Offset {deltaC}
    1,                       !- Exhaust Air Offset {deltaC}
    0.05,                    !- Pair 1 Zeta Nondimensional Height
    -1.27,                   !- Pair 1 Delta Adjacent Air Temperature
{deltaC}
    0.25,                    !- Pair 2 Zeta Nondimensional Height
    0.06,                    !- Pair 2 Delta Adjacent Air Temperature
{deltaC}
    0.5,                     !- Pair 3 Zeta Nondimensional Height
    0.12,                    !- Pair 3 Delta Adjacent Air Temperature
{deltaC}
    0.75,                    !- Pair 4 Zeta Nondimensional Height
    0.22,                    !- Pair 4 Delta Adjacent Air Temperature
{deltaC}
    0.95,                    !- Pair 5 Zeta Nondimensional Height
    0.47;                    !- Pair 5 Delta Adjacent Air Temperature
{deltaC}

RoomAir:TemperaturePattern:NondimensionalHeight,
    Air2,                    !- Name
    2,                       !- Control Integer for Pattern Control
Schedule Name
    0.08,                    !- Thermostat Offset {deltaC}
    1,                       !- Return Air Offset {deltaC}
    1,                       !- Exhaust Air Offset {deltaC}
    0.05,                    !- Pair 1 Zeta Nondimensional Height
    -.86,                    !- Pair 1 Delta Adjacent Air Temperature
{deltaC}
    0.25,                    !- Pair 2 Zeta Nondimensional Height
    -.05,                    !- Pair 2 Delta Adjacent Air Temperature
{deltaC}
    0.5,                     !- Pair 3 Zeta Nondimensional Height
    0.1,                     !- Pair 3 Delta Adjacent Air Temperature
{deltaC}
    0.75,                    !- Pair 4 Zeta Nondimensional Height
    0.2,                     !- Pair 4 Delta Adjacent Air Temperature
{deltaC}
    0.95,                    !- Pair 5 Zeta Nondimensional Height
    0.36;                    !- Pair 5 Delta Adjacent Air Temperature
{deltaC}

RoomAir:TemperaturePattern:NondimensionalHeight,
    Air3,                    !- Name
    3,                       !- Control Integer for Pattern Control
Schedule Name
    -.01,                    !- Thermostat Offset {deltaC}
```

```
    1,                        !- Return Air Offset {deltaC}
    1,                        !- Exhaust Air Offset {deltaC}
    0.05,                     !- Pair 1 Zeta Nondimensional Height
    0.01,                     !- Pair 1 Delta Adjacent Air Temperature
{deltaC}
    0.25,                     !- Pair 2 Zeta Nondimensional Height
    -.06,                     !- Pair 2 Delta Adjacent Air Temperature
{deltaC}
    0.5,                      !- Pair 3 Zeta Nondimensional Height
    0,                        !- Pair 3 Delta Adjacent Air Temperature
{deltaC}
    0.75,                     !- Pair 4 Zeta Nondimensional Height
    0.02,                     !- Pair 4 Delta Adjacent Air Temperature
{deltaC}
    0.95,                     !- Pair 5 Zeta Nondimensional Height
    0.06;                     !- Pair 5 Delta Adjacent Air Temperature
{deltaC}

RoomAir:TemperaturePattern:NondimensionalHeight,
    Air4,                     !- Name
    4,                        !- Control Integer for Pattern Control
Schedule Name
    -.02,                     !- Thermostat Offset {deltaC}
    1,                        !- Return Air Offset {deltaC}
    1,                        !- Exhaust Air Offset {deltaC}
    0.05,                     !- Pair 1 Zeta Nondimensional Height
    0.07,                     !- Pair 1 Delta Adjacent Air Temperature
{deltaC}
    0.25,                     !- Pair 2 Zeta Nondimensional Height
    -.04,                     !- Pair 2 Delta Adjacent Air Temperature
{deltaC}
    0.5,                      !- Pair 3 Zeta Nondimensional Height
    -.01,                     !- Pair 3 Delta Adjacent Air Temperature
{deltaC}
    0.75,                     !- Pair 4 Zeta Nondimensional Height
    -.01,                     !- Pair 4 Delta Adjacent Air Temperature
{deltaC}
    0.95,                     !- Pair 5 Zeta Nondimensional Height
    0.04;                     !- Pair 5 Delta Adjacent Air Temperature
{deltaC}

RoomAir:TemperaturePattern:NondimensionalHeight,
    Air5,                     !- Name
    5,                        !- Control Integer for Pattern Control
Schedule Name
    -.02,                     !- Thermostat Offset {deltaC}
    1,                        !- Return Air Offset {deltaC}
    1,                        !- Exhaust Air Offset {deltaC}
    0.05,                     !- Pair 1 Zeta Nondimensional Height
    0.09,                     !- Pair 1 Delta Adjacent Air Temperature
{deltaC}
    0.25,                     !- Pair 2 Zeta Nondimensional Height
    -.03,                     !- Pair 2 Delta Adjacent Air Temperature
{deltaC}
    0.5,                      !- Pair 3 Zeta Nondimensional Height
    -.01,                     !- Pair 3 Delta Adjacent Air Temperature
{deltaC}
    0.75,                     !- Pair 4 Zeta Nondimensional Height
```

```
    -.02,                    !- Pair 4 Delta Adjacent Air Temperature
{deltaC}
    0.95,                    !- Pair 5 Zeta Nondimensional Height
    0.03;                    !- Pair 5 Delta Adjacent Air Temperature
{deltaC}

RoomAir:TemperaturePattern:NondimensionalHeight,
    Air6,                    !- Name
    6,                       !- Control Integer for Pattern Control
Schedule Name
    -.02,                    !- Thermostat Offset {deltaC}
    1,                       !- Return Air Offset {deltaC}
    1,                       !- Exhaust Air Offset {deltaC}
    0.05,                    !- Pair 1 Zeta Nondimensional Height
    0.11,                    !- Pair 1 Delta Adjacent Air Temperature
{deltaC}
    0.25,                    !- Pair 2 Zeta Nondimensional Height
    -.02,                    !- Pair 2 Delta Adjacent Air Temperature
{deltaC}
    0.5,                     !- Pair 3 Zeta Nondimensional Height
    -.02,                    !- Pair 3 Delta Adjacent Air Temperature
{deltaC}
    0.75,                    !- Pair 4 Zeta Nondimensional Height
    -.03,                    !- Pair 4 Delta Adjacent Air Temperature
{deltaC}
    0.95,                    !- Pair 5 Zeta Nondimensional Height
    0.02;                    !- Pair 5 Delta Adjacent Air Temperature
{deltaC}

RoomAir:TemperaturePattern:NondimensionalHeight,
    Air7,                    !- Name
    7,                       !- Control Integer for Pattern Control
Schedule Name
    -.02,                    !- Thermostat Offset {deltaC}
    1,                       !- Return Air Offset {deltaC}
    1,                       !- Exhaust Air Offset {deltaC}
    0.05,                    !- Pair 1 Zeta Nondimensional Height
    0.12,                    !- Pair 1 Delta Adjacent Air Temperature
{deltaC}
    0.25,                    !- Pair 2 Zeta Nondimensional Height
    -.02,                    !- Pair 2 Delta Adjacent Air Temperature
{deltaC}
    0.5,                     !- Pair 3 Zeta Nondimensional Height
    -.02,                    !- Pair 3 Delta Adjacent Air Temperature
{deltaC}
    0.75,                    !- Pair 4 Zeta Nondimensional Height
    -.03,                    !- Pair 4 Delta Adjacent Air Temperature
{deltaC}
    0.95,                    !- Pair 5 Zeta Nondimensional Height
    0.02;                    !- Pair 5 Delta Adjacent Air Temperature
{deltaC}

RoomAir:TemperaturePattern:NondimensionalHeight,
    Air8,                    !- Name
    8,                       !- Control Integer for Pattern Control
Schedule Name
    -.02,                    !- Thermostat Offset {deltaC}
    1,                       !- Return Air Offset {deltaC}
```

```
    1,                        !- Exhaust Air Offset {deltaC}
    0.05,                     !- Pair 1 Zeta Nondimensional Height
    0.13,                     !- Pair 1 Delta Adjacent Air Temperature
{deltaC}
    0.25,                     !- Pair 2 Zeta Nondimensional Height
    -.02,                     !- Pair 2 Delta Adjacent Air Temperature
{deltaC}
    0.5,                      !- Pair 3 Zeta Nondimensional Height
    -.02,                     !- Pair 3 Delta Adjacent Air Temperature
{deltaC}
    0.75,                     !- Pair 4 Zeta Nondimensional Height
    -.03,                     !- Pair 4 Delta Adjacent Air Temperature
{deltaC}
    0.95,                     !- Pair 5 Zeta Nondimensional Height
    0.01;                     !- Pair 5 Delta Adjacent Air Temperature
{deltaC}

RoomAir:TemperaturePattern:NondimensionalHeight,
    Air9,                     !- Name
    9,                        !- Control Integer for Pattern Control
Schedule Name
    -.02,                     !- Thermostat Offset {deltaC}
    1,                        !- Return Air Offset {deltaC}
    1,                        !- Exhaust Air Offset {deltaC}
    0.05,                     !- Pair 1 Zeta Nondimensional Height
    0.13,                     !- Pair 1 Delta Adjacent Air Temperature
{deltaC}
    0.25,                     !- Pair 2 Zeta Nondimensional Height
    -.01,                     !- Pair 2 Delta Adjacent Air Temperature
{deltaC}
    0.5,                      !- Pair 3 Zeta Nondimensional Height
    -.02,                     !- Pair 3 Delta Adjacent Air Temperature
{deltaC}
    0.75,                     !- Pair 4 Zeta Nondimensional Height
    -.04,                     !- Pair 4 Delta Adjacent Air Temperature
{deltaC}
    0.95,                     !- Pair 5 Zeta Nondimensional Height
    0;                        !- Pair 5 Delta Adjacent Air Temperature
{deltaC}

RoomAir:TemperaturePattern:NondimensionalHeight,
    Air10,                    !- Name
    10,                       !- Control Integer for Pattern Control
Schedule Name
    -.02,                     !- Thermostat Offset {deltaC}
    1,                        !- Return Air Offset {deltaC}
    1,                        !- Exhaust Air Offset {deltaC}
    0.05,                     !- Pair 1 Zeta Nondimensional Height
    0.12,                     !- Pair 1 Delta Adjacent Air Temperature
{deltaC}
    0.25,                     !- Pair 2 Zeta Nondimensional Height
    -.01,                     !- Pair 2 Delta Adjacent Air Temperature
{deltaC}
    0.5,                      !- Pair 3 Zeta Nondimensional Height
    -.02,                     !- Pair 3 Delta Adjacent Air Temperature
{deltaC}
    0.75,                     !- Pair 4 Zeta Nondimensional Height
```

```
    -.03,                    !- Pair 4 Delta Adjacent Air Temperature
{deltaC}
    0.95,                    !- Pair 5 Zeta Nondimensional Height
    0;                       !- Pair 5 Delta Adjacent Air Temperature
{deltaC}

RoomAir:TemperaturePattern:NondimensionalHeight,
    Air11,                   !- Name
    11,                      !- Control Integer for Pattern Control
Schedule Name
    -.02,                    !- Thermostat Offset {deltaC}
    1,                       !- Return Air Offset {deltaC}
    1,                       !- Exhaust Air Offset {deltaC}
    0.05,                    !- Pair 1 Zeta Nondimensional Height
    0.1,                     !- Pair 1 Delta Adjacent Air Temperature
{deltaC}
    0.25,                    !- Pair 2 Zeta Nondimensional Height
    -.01,                    !- Pair 2 Delta Adjacent Air Temperature
{deltaC}
    0.5,                     !- Pair 3 Zeta Nondimensional Height
    -.01,                    !- Pair 3 Delta Adjacent Air Temperature
{deltaC}
    0.75,                    !- Pair 4 Zeta Nondimensional Height
    -.03,                    !- Pair 4 Delta Adjacent Air Temperature
{deltaC}
    0.95,                    !- Pair 5 Zeta Nondimensional Height
    0;                       !- Pair 5 Delta Adjacent Air Temperature
{deltaC}

RoomAir:TemperaturePattern:NondimensionalHeight,
    Air12,                   !- Name
    12,                      !- Control Integer for Pattern Control
Schedule Name
    -.01,                    !- Thermostat Offset {deltaC}
    1,                       !- Return Air Offset {deltaC}
    1,                       !- Exhaust Air Offset {deltaC}
    0.05,                    !- Pair 1 Zeta Nondimensional Height
    0.06,                    !- Pair 1 Delta Adjacent Air Temperature
{deltaC}
    0.25,                    !- Pair 2 Zeta Nondimensional Height
    -.02,                    !- Pair 2 Delta Adjacent Air Temperature
{deltaC}
    0.5,                     !- Pair 3 Zeta Nondimensional Height
    -.01,                    !- Pair 3 Delta Adjacent Air Temperature
{deltaC}
    0.75,                    !- Pair 4 Zeta Nondimensional Height
    -.02,                    !- Pair 4 Delta Adjacent Air Temperature
{deltaC}
    0.95,                    !- Pair 5 Zeta Nondimensional Height
    0.02;                    !- Pair 5 Delta Adjacent Air Temperature
{deltaC}

RoomAir:TemperaturePattern:NondimensionalHeight,
    Air13,                   !- Name
    13,                      !- Control Integer for Pattern Control
Schedule Name
    -.01,                    !- Thermostat Offset {deltaC}
    1,                       !- Return Air Offset {deltaC}
```

```
    1,                        !- Exhaust Air Offset {deltaC}
    0.05,                     !- Pair 1 Zeta Nondimensional Height
    0.03,                     !- Pair 1 Delta Adjacent Air Temperature
{deltaC}
    0.25,                     !- Pair 2 Zeta Nondimensional Height
    -.03,                     !- Pair 2 Delta Adjacent Air Temperature
{deltaC}
    0.5,                      !- Pair 3 Zeta Nondimensional Height
    -.01,                     !- Pair 3 Delta Adjacent Air Temperature
{deltaC}
    0.75,                     !- Pair 4 Zeta Nondimensional Height
    0,                        !- Pair 4 Delta Adjacent Air Temperature
{deltaC}
    0.95,                     !- Pair 5 Zeta Nondimensional Height
    0.06;                     !- Pair 5 Delta Adjacent Air Temperature
{deltaC}

RoomAir:TemperaturePattern:NondimensionalHeight,
    Air14,                    !- Name
    14,                       !- Control Integer for Pattern Control
Schedule Name
    -.02,                     !- Thermostat Offset {deltaC}
    1,                        !- Return Air Offset {deltaC}
    1,                        !- Exhaust Air Offset {deltaC}
    0.05,                     !- Pair 1 Zeta Nondimensional Height
    -.01,                     !- Pair 1 Delta Adjacent Air Temperature
{deltaC}
    0.25,                     !- Pair 2 Zeta Nondimensional Height
    -.04,                     !- Pair 2 Delta Adjacent Air Temperature
{deltaC}
    0.5,                      !- Pair 3 Zeta Nondimensional Height
    -.01,                     !- Pair 3 Delta Adjacent Air Temperature
{deltaC}
    0.75,                     !- Pair 4 Zeta Nondimensional Height
    0.01,                     !- Pair 4 Delta Adjacent Air Temperature
{deltaC}
    0.95,                     !- Pair 5 Zeta Nondimensional Height
    0.1;                      !- Pair 5 Delta Adjacent Air Temperature
{deltaC}

RoomAir:TemperaturePattern:NondimensionalHeight,
    Air15,                    !- Name
    15,                       !- Control Integer for Pattern Control
Schedule Name
    -.01,                     !- Thermostat Offset {deltaC}
    1,                        !- Return Air Offset {deltaC}
    1,                        !- Exhaust Air Offset {deltaC}
    0.05,                     !- Pair 1 Zeta Nondimensional Height
    -.04,                     !- Pair 1 Delta Adjacent Air Temperature
{deltaC}
    0.25,                     !- Pair 2 Zeta Nondimensional Height
    -.05,                     !- Pair 2 Delta Adjacent Air Temperature
{deltaC}
    0.5,                      !- Pair 3 Zeta Nondimensional Height
    -.01,                     !- Pair 3 Delta Adjacent Air Temperature
{deltaC}
    0.75,                     !- Pair 4 Zeta Nondimensional Height
```

```
    0.02,                    !- Pair 4 Delta Adjacent Air Temperature
{deltaC}
    0.95,                    !- Pair 5 Zeta Nondimensional Height
    0.12;                    !- Pair 5 Delta Adjacent Air Temperature
{deltaC}

RoomAir:TemperaturePattern:NondimensionalHeight,
    Air16,                   !- Name
    16,                      !- Control Integer for Pattern Control
Schedule Name
    -.01,                    !- Thermostat Offset {deltaC}
    1,                       !- Return Air Offset {deltaC}
    1,                       !- Exhaust Air Offset {deltaC}
    0.05,                    !- Pair 1 Zeta Nondimensional Height
    -.03,                    !- Pair 1 Delta Adjacent Air Temperature
{deltaC}
    0.25,                    !- Pair 2 Zeta Nondimensional Height
    -.05,                    !- Pair 2 Delta Adjacent Air Temperature
{deltaC}
    0.5,                     !- Pair 3 Zeta Nondimensional Height
    -.01,                    !- Pair 3 Delta Adjacent Air Temperature
{deltaC}
    0.75,                    !- Pair 4 Zeta Nondimensional Height
    0.02,                    !- Pair 4 Delta Adjacent Air Temperature
{deltaC}
    0.95,                    !- Pair 5 Zeta Nondimensional Height
    0.12;                    !- Pair 5 Delta Adjacent Air Temperature
{deltaC}

RoomAir:TemperaturePattern:NondimensionalHeight,
    Air17,                   !- Name
    17,                      !- Control Integer for Pattern Control
Schedule Name
    -.02,                    !- Thermostat Offset {deltaC}
    1,                       !- Return Air Offset {deltaC}
    1,                       !- Exhaust Air Offset {deltaC}
    0.05,                    !- Pair 1 Zeta Nondimensional Height
    -.01,                    !- Pair 1 Delta Adjacent Air Temperature
{deltaC}
    0.25,                    !- Pair 2 Zeta Nondimensional Height
    -.05,                    !- Pair 2 Delta Adjacent Air Temperature
{deltaC}
    0.5,                     !- Pair 3 Zeta Nondimensional Height
    -.01,                    !- Pair 3 Delta Adjacent Air Temperature
{deltaC}
    0.75,                    !- Pair 4 Zeta Nondimensional Height
    0.02,                    !- Pair 4 Delta Adjacent Air Temperature
{deltaC}
    0.95,                    !- Pair 5 Zeta Nondimensional Height
    0.11;                    !- Pair 5 Delta Adjacent Air Temperature
{deltaC}

RoomAir:TemperaturePattern:NondimensionalHeight,
    Air18,                   !- Name
    18,                      !- Control Integer for Pattern Control
Schedule Name
    -.02,                    !- Thermostat Offset {deltaC}
    1,                       !- Return Air Offset {deltaC}
```

```
    1,                        !- Exhaust Air Offset {deltaC}
    0.05,                     !- Pair 1 Zeta Nondimensional Height
    0.01,                     !- Pair 1 Delta Adjacent Air Temperature
{deltaC}
    0.25,                     !- Pair 2 Zeta Nondimensional Height
    -.05,                     !- Pair 2 Delta Adjacent Air Temperature
{deltaC}
    0.5,                      !- Pair 3 Zeta Nondimensional Height
    -.02,                     !- Pair 3 Delta Adjacent Air Temperature
{deltaC}
    0.75,                     !- Pair 4 Zeta Nondimensional Height
    0.01,                     !- Pair 4 Delta Adjacent Air Temperature
{deltaC}
    0.95,                     !- Pair 5 Zeta Nondimensional Height
    0.1;                      !- Pair 5 Delta Adjacent Air Temperature
{deltaC}

RoomAir:TemperaturePattern:NondimensionalHeight,
    Air19,                    !- Name
    19,                       !- Control Integer for Pattern Control
Schedule Name
    -.02,                     !- Thermostat Offset {deltaC}
    1,                        !- Return Air Offset {deltaC}
    1,                        !- Exhaust Air Offset {deltaC}
    0.05,                     !- Pair 1 Zeta Nondimensional Height
    0.04,                     !- Pair 1 Delta Adjacent Air Temperature
{deltaC}
    0.25,                     !- Pair 2 Zeta Nondimensional Height
    -.04,                     !- Pair 2 Delta Adjacent Air Temperature
{deltaC}
    0.5,                      !- Pair 3 Zeta Nondimensional Height
    -.02,                     !- Pair 3 Delta Adjacent Air Temperature
{deltaC}
    0.75,                     !- Pair 4 Zeta Nondimensional Height
    0,                        !- Pair 4 Delta Adjacent Air Temperature
{deltaC}
    0.95,                     !- Pair 5 Zeta Nondimensional Height
    0.08;                     !- Pair 5 Delta Adjacent Air Temperature
{deltaC}

RoomAir:TemperaturePattern:NondimensionalHeight,
    Air20,                    !- Name
    20,                       !- Control Integer for Pattern Control
Schedule Name
    -.02,                     !- Thermostat Offset {deltaC}
    1,                        !- Return Air Offset {deltaC}
    1,                        !- Exhaust Air Offset {deltaC}
    0.05,                     !- Pair 1 Zeta Nondimensional Height
    0.07,                     !- Pair 1 Delta Adjacent Air Temperature
{deltaC}
    0.25,                     !- Pair 2 Zeta Nondimensional Height
    -.04,                     !- Pair 2 Delta Adjacent Air Temperature
{deltaC}
    0.5,                      !- Pair 3 Zeta Nondimensional Height
    -.02,                     !- Pair 3 Delta Adjacent Air Temperature
{deltaC}
    0.75,                     !- Pair 4 Zeta Nondimensional Height
```

```
    -.01,                    !- Pair 4 Delta Adjacent Air Temperature
{deltaC}
    0.95,                    !- Pair 5 Zeta Nondimensional Height
    0.06;                    !- Pair 5 Delta Adjacent Air Temperature
{deltaC}

RoomAir:TemperaturePattern:NondimensionalHeight,
    Air21,                   !- Name
    21,                      !- Control Integer for Pattern Control
Schedule Name
    -.02,                    !- Thermostat Offset {deltaC}
    1,                       !- Return Air Offset {deltaC}
    1,                       !- Exhaust Air Offset {deltaC}
    0.05,                    !- Pair 1 Zeta Nondimensional Height
    0.09,                    !- Pair 1 Delta Adjacent Air Temperature
{deltaC}
    0.25,                    !- Pair 2 Zeta Nondimensional Height
    -.03,                    !- Pair 2 Delta Adjacent Air Temperature
{deltaC}
    0.5,                     !- Pair 3 Zeta Nondimensional Height
    -.02,                    !- Pair 3 Delta Adjacent Air Temperature
{deltaC}
    0.75,                    !- Pair 4 Zeta Nondimensional Height
    -.02,                    !- Pair 4 Delta Adjacent Air Temperature
{deltaC}
    0.95,                    !- Pair 5 Zeta Nondimensional Height
    0.04;                    !- Pair 5 Delta Adjacent Air Temperature
{deltaC}

RoomAir:TemperaturePattern:NondimensionalHeight,
    Air22,                   !- Name
    22,                      !- Control Integer for Pattern Control
Schedule Name
    -.02,                    !- Thermostat Offset {deltaC}
    1,                       !- Return Air Offset {deltaC}
    1,                       !- Exhaust Air Offset {deltaC}
    0.05,                    !- Pair 1 Zeta Nondimensional Height
    0.1,                     !- Pair 1 Delta Adjacent Air Temperature
{deltaC}
    0.25,                    !- Pair 2 Zeta Nondimensional Height
    -.03,                    !- Pair 2 Delta Adjacent Air Temperature
{deltaC}
    0.5,                     !- Pair 3 Zeta Nondimensional Height
    -.02,                    !- Pair 3 Delta Adjacent Air Temperature
{deltaC}
    0.75,                    !- Pair 4 Zeta Nondimensional Height
    -.02,                    !- Pair 4 Delta Adjacent Air Temperature
{deltaC}
    0.95,                    !- Pair 5 Zeta Nondimensional Height
    0.03;                    !- Pair 5 Delta Adjacent Air Temperature
{deltaC}

RoomAir:TemperaturePattern:NondimensionalHeight,
    Air23,                   !- Name
    23,                      !- Control Integer for Pattern Control
Schedule Name
    -.02,                    !- Thermostat Offset {deltaC}
    1,                       !- Return Air Offset {deltaC}
```

```
    1,                        !- Exhaust Air Offset {deltaC}
    0.05,                     !- Pair 1 Zeta Nondimensional Height
    0.12,                     !- Pair 1 Delta Adjacent Air Temperature
{deltaC}
    0.25,                     !- Pair 2 Zeta Nondimensional Height
    -.02,                     !- Pair 2 Delta Adjacent Air Temperature
{deltaC}
    0.5,                      !- Pair 3 Zeta Nondimensional Height
    -.02,                     !- Pair 3 Delta Adjacent Air Temperature
{deltaC}
    0.75,                     !- Pair 4 Zeta Nondimensional Height
    -.03,                     !- Pair 4 Delta Adjacent Air Temperature
{deltaC}
    0.95,                     !- Pair 5 Zeta Nondimensional Height
    0.02;                     !- Pair 5 Delta Adjacent Air Temperature
{deltaC}

RoomAir:TemperaturePattern:NondimensionalHeight,
    Air24,                    !- Name
    24,                       !- Control Integer for Pattern Control
Schedule Name
    0.03,                     !- Thermostat Offset {deltaC}
    1,                        !- Return Air Offset {deltaC}
    1,                        !- Exhaust Air Offset {deltaC}
    0.05,                     !- Pair 1 Zeta Nondimensional Height
    -.34,                     !- Pair 1 Delta Adjacent Air Temperature
{deltaC}
    0.25,                     !- Pair 2 Zeta Nondimensional Height
    0.07,                     !- Pair 2 Delta Adjacent Air Temperature
{deltaC}
    0.5,                      !- Pair 3 Zeta Nondimensional Height
    0.01,                     !- Pair 3 Delta Adjacent Air Temperature
{deltaC}
    0.75,                     !- Pair 4 Zeta Nondimensional Height
    0.01,                     !- Pair 4 Delta Adjacent Air Temperature
{deltaC}
    0.95,                     !- Pair 5 Zeta Nondimensional Height
    0.17;                     !- Pair 5 Delta Adjacent Air Temperature
{deltaC}


!-   ===========  ALL OBJECTS IN CLASS: OTHEREQUIPMENT ===========

OtherEquipment,
    fan,                      !- Name
    TestCell,                 !- Zone or ZoneList Name
    ON,                       !- Schedule Name
    EquipmentLevel,           !- Design Level Calculation Method
    33;                       !- Design Level {W}


!-   ===========  ALL OBJECTS IN CLASS: ZONEINFILTRATION:DESIGNFLOWRATE
===========

ZoneInfiltration:DesignFlowRate,
    Floorleak,                !- Name
    SubFloor,                 !- Zone or ZoneList Name
    ON,                       !- Schedule Name
```

```
    AirChanges/Hour,          !- Design Flow Rate Calculation Method
    ,                         !- Design Flow Rate {m3/s}
    ,                         !- Flow per Zone Floor Area {m3/s-m2}
    ,                         !- Flow per Exterior Surface Area {m3/s-
m2}
    0,                        !- Air Changes per Hour {1/hr}
    1,                        !- Constant Term Coefficient
    ,                         !- Temperature Term Coefficient
    ,                         !- Velocity Term Coefficient
    ;                         !- Velocity Squared Term Coefficient

ZoneInfiltration:DesignFlowRate,
    Leakage,                  !- Name
    TestCell,                 !- Zone or ZoneList Name
    ON,                       !- Schedule Name
    AirChanges/Hour,          !- Design Flow Rate Calculation Method
    ,                         !- Design Flow Rate {m3/s}
    ,                         !- Flow per Zone Floor Area {m3/s-m2}
    ,                         !- Flow per Exterior Surface Area {m3/s-
m2}
    1.2375,                   !- Air Changes per Hour {1/hr}
    1,                        !- Constant Term Coefficient
    ,                         !- Temperature Term Coefficient
    ,                         !- Velocity Term Coefficient
    ;                         !- Velocity Squared Term Coefficient

ZoneInfiltration:DesignFlowRate,
    Roofleak,                 !- Name
    RoofSpace,                !- Zone or ZoneList Name
    ON,                       !- Schedule Name
    AirChanges/Hour,          !- Design Flow Rate Calculation Method
    ,                         !- Design Flow Rate {m3/s}
    ,                         !- Flow per Zone Floor Area {m3/s-m2}
    ,                         !- Flow per Exterior Surface Area {m3/s-
m2}
    0,                        !- Air Changes per Hour {1/hr}
    1,                        !- Constant Term Coefficient
    ,                         !- Temperature Term Coefficient
    ,                         !- Velocity Term Coefficient
    ;                         !- Velocity Squared Term Coefficient


!-   ===========  ALL OBJECTS IN CLASS: ZONECONTROL:THERMOSTAT
===========

ZoneControl:Thermostat,
    TestCell Thermostat,      !- Name
    TestCell,                 !- Zone or ZoneList Name
    TestCellThermostatYear,   !- Control Type Schedule Name
    ThermostatSetpoint:DualSetpoint,  !- Control 1 Object Type
    Therm Dual SP Control;    !- Control 1 Name

ZoneControl:Thermostat,
    RoofSpace Thermostat,     !- Name
    RoofSpace,                !- Zone or ZoneList Name
    HVACTemplate-Always 4,    !- Control Type Schedule Name
    ThermostatSetpoint:DualSetpoint,  !- Control 1 Object Type
    roof Dual SP Control;     !- Control 1 Name
```

```
ZoneControl:Thermostat,
    SubFloor Thermostat,     !- Name
    SubFloor,                !- Zone or ZoneList Name
    HVACTemplate-Always 4,   !- Control Type Schedule Name
    ThermostatSetpoint:DualSetpoint,  !- Control 1 Object Type
    subfloor Dual SP Control;!- Control 1 Name


!-   ===========  ALL OBJECTS IN CLASS: THERMOSTATSETPOINT:DUALSETPOINT
===========

ThermostatSetpoint:DualSetpoint,
    Therm Dual SP Control,   !- Name
    Heat,                    !- Heating Setpoint Temperature Schedule
Name
    Heat;                    !- Cooling Setpoint Temperature Schedule
Name

ThermostatSetpoint:DualSetpoint,
    roof Dual SP Control,    !- Name
    RoofTemp,                !- Heating Setpoint Temperature Schedule
Name
    RoofTemp;                !- Cooling Setpoint Temperature Schedule
Name

ThermostatSetpoint:DualSetpoint,
    subfloor Dual SP Control,!- Name
    SubfloorTemp,            !- Heating Setpoint Temperature Schedule
Name
    SubfloorTemp;            !- Cooling Setpoint Temperature Schedule
Name


!-   ===========  ALL OBJECTS IN CLASS: ZONEHVAC:IDEALLOADSAIRSYSTEM
===========

ZoneHVAC:IdealLoadsAirSystem,
    TestCell Ideal Loads Air System,  !- Name
    ,                        !- Availability Schedule Name
    TestCell Ideal Loads Supply Inlet,  !- Zone Supply Air Node Name
    ,                        !- Zone Exhaust Air Node Name
    50,                      !- Maximum Heating Supply Air Temperature
{C}
    5,                       !- Minimum Cooling Supply Air Temperature
{C}
    0.0156,                  !- Maximum Heating Supply Air Humidity
Ratio {kgWater/kgDryAir}
    0.0077,                  !- Minimum Cooling Supply Air Humidity
Ratio {kgWater/kgDryAir}
    NoLimit,                 !- Heating Limit
    ,                        !- Maximum Heating Air Flow Rate {m3/s}
    ,                        !- Maximum Sensible Heating Capacity {W}
    NoLimit,                 !- Cooling Limit
    ,                        !- Maximum Cooling Air Flow Rate {m3/s}
    ,                        !- Maximum Total Cooling Capacity {W}
    ,                        !- Heating Availability Schedule Name
    ,                        !- Cooling Availability Schedule Name
```

```
    ConstantSensibleHeatRatio,  !- Dehumidification Control Type
    0.7,                        !- Cooling Sensible Heat Ratio
{dimensionless}
    None,                       !- Humidification Control Type
    ,                           !- Design Specification Outdoor Air Object
Name
    ,                           !- Outdoor Air Inlet Node Name
    None,                       !- Demand Controlled Ventilation Type
    NoEconomizer,               !- Outdoor Air Economizer Type
    None,                       !- Heat Recovery Type
    0.7,                        !- Sensible Heat Recovery Effectiveness
{dimensionless}
    0.65;                       !- Latent Heat Recovery Effectiveness
{dimensionless}

ZoneHVAC:IdealLoadsAirSystem,
    RoofSpace Ideal Loads Air System,  !- Name
    ,                           !- Availability Schedule Name
    RoofSpace Ideal Loads Supply Inlet,  !- Zone Supply Air Node Name
    ,                           !- Zone Exhaust Air Node Name
    50,                         !- Maximum Heating Supply Air Temperature
{C}
    5,                          !- Minimum Cooling Supply Air Temperature
{C}
    0.0156,                     !- Maximum Heating Supply Air Humidity
Ratio {kgWater/kgDryAir}
    0.0077,                     !- Minimum Cooling Supply Air Humidity
Ratio {kgWater/kgDryAir}
    NoLimit,                    !- Heating Limit
    ,                           !- Maximum Heating Air Flow Rate {m3/s}
    ,                           !- Maximum Sensible Heating Capacity {W}
    NoLimit,                    !- Cooling Limit
    ,                           !- Maximum Cooling Air Flow Rate {m3/s}
    ,                           !- Maximum Total Cooling Capacity {W}
    ,                           !- Heating Availability Schedule Name
    ,                           !- Cooling Availability Schedule Name
    ConstantSensibleHeatRatio,  !- Dehumidification Control Type
    0.7,                        !- Cooling Sensible Heat Ratio
{dimensionless}
    None,                       !- Humidification Control Type
    ,                           !- Design Specification Outdoor Air Object
Name
    ,                           !- Outdoor Air Inlet Node Name
    None,                       !- Demand Controlled Ventilation Type
    NoEconomizer,               !- Outdoor Air Economizer Type
    None,                       !- Heat Recovery Type
    0.7,                        !- Sensible Heat Recovery Effectiveness
{dimensionless}
    0.65;                       !- Latent Heat Recovery Effectiveness
{dimensionless}

ZoneHVAC:IdealLoadsAirSystem,
    SubFloor Ideal Loads Air System,  !- Name
    ,                           !- Availability Schedule Name
    SubFloor Ideal Loads Supply Inlet,  !- Zone Supply Air Node Name
    ,                           !- Zone Exhaust Air Node Name
    50,                         !- Maximum Heating Supply Air Temperature
{C}
```

```
    5,                        !- Minimum Cooling Supply Air Temperature
{C}
    0.0156,                   !- Maximum Heating Supply Air Humidity
Ratio {kgWater/kgDryAir}
    0.0077,                   !- Minimum Cooling Supply Air Humidity
Ratio {kgWater/kgDryAir}
    NoLimit,                  !- Heating Limit
    ,                         !- Maximum Heating Air Flow Rate {m3/s}
    ,                         !- Maximum Sensible Heating Capacity {W}
    NoLimit,                  !- Cooling Limit
    ,                         !- Maximum Cooling Air Flow Rate {m3/s}
    ,                         !- Maximum Total Cooling Capacity {W}
    ,                         !- Heating Availability Schedule Name
    ,                         !- Cooling Availability Schedule Name
    ConstantSensibleHeatRatio,  !- Dehumidification Control Type
    0.7,                      !- Cooling Sensible Heat Ratio
{dimensionless}
    None,                     !- Humidification Control Type
    ,                         !- Design Specification Outdoor Air Object
Name
    ,                         !- Outdoor Air Inlet Node Name
    None,                     !- Demand Controlled Ventilation Type
    NoEconomizer,             !- Outdoor Air Economizer Type
    None,                     !- Heat Recovery Type
    0.7,                      !- Sensible Heat Recovery Effectiveness
{dimensionless}
    0.65;                     !- Latent Heat Recovery Effectiveness
{dimensionless}


!-   ===========  ALL OBJECTS IN CLASS: ZONEHVAC:EQUIPMENTLIST
===========

ZoneHVAC:EquipmentList,
    TestCell Equipment,       !- Name
    ZoneHVAC:IdealLoadsAirSystem,  !- Zone Equipment 1 Object Type
    TestCell Ideal Loads Air System,  !- Zone Equipment 1 Name
    1,                        !- Zone Equipment 1 Cooling Sequence
    1;                        !- Zone Equipment 1 Heating or No-Load
Sequence

ZoneHVAC:EquipmentList,
    RoofSpace Equipment,      !- Name
    ZoneHVAC:IdealLoadsAirSystem,  !- Zone Equipment 1 Object Type
    RoofSpace Ideal Loads Air System,  !- Zone Equipment 1 Name
    1,                        !- Zone Equipment 1 Cooling Sequence
    1;                        !- Zone Equipment 1 Heating or No-Load
Sequence

ZoneHVAC:EquipmentList,
    SubFloor Equipment,       !- Name
    ZoneHVAC:IdealLoadsAirSystem,  !- Zone Equipment 1 Object Type
    SubFloor Ideal Loads Air System,  !- Zone Equipment 1 Name
    1,                        !- Zone Equipment 1 Cooling Sequence
    1;                        !- Zone Equipment 1 Heating or No-Load
Sequence
```

```
!-   ===========  ALL OBJECTS IN CLASS: ZONEHVAC:EQUIPMENTCONNECTIONS
===========

ZoneHVAC:EquipmentConnections,
    TestCell,                !- Zone Name
    TestCell Equipment,      !- Zone Conditioning Equipment List Name
    TestCell Ideal Loads Supply Inlet,  !- Zone Air Inlet Node or
NodeList Name
    ,                        !- Zone Air Exhaust Node or NodeList Name
    TestCell Zone Air Node,  !- Zone Air Node Name
    TestCell Return Outlet;  !- Zone Return Air Node Name

ZoneHVAC:EquipmentConnections,
    RoofSpace,               !- Zone Name
    RoofSpace Equipment,     !- Zone Conditioning Equipment List Name
    RoofSpace Ideal Loads Supply Inlet,  !- Zone Air Inlet Node or
NodeList Name
    ,                        !- Zone Air Exhaust Node or NodeList Name
    RoofSpace Zone Air Node, !- Zone Air Node Name
    RoofSpace Return Outlet; !- Zone Return Air Node Name

ZoneHVAC:EquipmentConnections,
    SubFloor,                !- Zone Name
    SubFloor Equipment,      !- Zone Conditioning Equipment List Name
    SubFloor Ideal Loads Supply Inlet,  !- Zone Air Inlet Node or
NodeList Name
    ,                        !- Zone Air Exhaust Node or NodeList Name
    SubFloor Zone Air Node,  !- Zone Air Node Name
    SubFloor Return Outlet;  !- Zone Return Air Node Name


!-   ===========  ALL OBJECTS IN CLASS: OUTPUT:VARIABLEDICTIONARY
===========

Output:VariableDictionary,
    regular;                 !- Key Field


!-   ===========  ALL OBJECTS IN CLASS: OUTPUT:VARIABLE ===========

Output:Variable,
    *,                       !- Key Value
    Site Outdoor Air Drybulb Temperature ,  !- Variable Name
    Timestep;                !- Reporting Frequency

Output:Variable,
    *,                       !- Key Value
    Zone Ideal Loads Zone Total Heating Rate ,  !- Variable Name
    Timestep;                !- Reporting Frequency

Output:Variable,
    *,                       !- Key Value
    Zone Air Temperature ,   !- Variable Name
    Timestep;                !- Reporting Frequency

Output:Variable,
    *,                       !- Key Value
    Site Direct Solar Radiation Rate per Area ,  !- Variable Name
```

```
    Timestep;                !- Reporting Frequency

Output:Variable,
    *,                       !- Key Value
    Site Diffuse Solar Radiation Rate per Area ,  !- Variable Name
    Timestep;                !- Reporting Frequency

Output:Variable,
    *,                       !- Key Value
    Zone Ideal Loads Zone Total Cooling Rate ,  !- Variable Name
    Timestep;                !- Reporting Frequency
```

Appendix B - Estimated Heat Losses from Heat Flux and blower door testing

Table B.1 Estimated heat loss, Configuration 1

Building Element	R-Value, m^2K/W	Rsi	Rse	Total Effective R-Value	U-value, W/m^2K	Area, m^2	**Heat Loss, W/K**
North-East Wall	2.06	0.13	0.04	2.23	0.45	10.69	**4.79**
North-West Wall	2.06	0.13	0.04	2.23	0.45	10.16	**4.56**
South-East Wall	2.06	0.13	0.04	2.23	0.45	9.02	**4.04**
South-West Wall	2.04	0.13	0.04	2.21	0.45	10.70	**4.84**
Thermal Bridging (Walls)						40.57	**6.09**
Ceiling	0.1	0.1	0.24	0.44	2.27	20.36	**46.27**
Floor	0.36	0.17	0.57	1.1	0.91	20.36	**18.51**
Window*					6.70	0.54	**3.62**
Door	0.22	0.13	0.04	0.39	2.56	1.67	**4.28**
Ventilation							**19.91**
Total							**116.91**

*U-value for window taken from the Single Glazed, Aluminium Window in the AccuRate 'Default Windows' Library

Table B.2 Estimated heat loss, Configuration 2

Building Element	R-Value, m^2K/W	Rsi	Rse	Total Effective R-Value	U-value, W/m^2K	Area, m^2	**Heat Loss, W/K**
North-East Wall	2.06	0.13	0.04	2.23	0.45	10.69	**4.79**
North-West Wall	2.06	0.13	0.04	2.23	0.45	10.16	**4.56**
South-East Wall	2.06	0.13	0.04	2.23	0.45	9.02	**4.04**
South-West Wall, Insulated	2.04	0.13	0.04	2.21	0.45	5.35	**2.41**
South-West Wall, Uninsulated	0.38	0.13	0.04	0.55	1.82	5.35	**9.73**
Thermal Bridging (Walls)						40.57	**6.09**
Ceiling	0.1	0.1	0.24	0.44	2.27	20.36	**46.27**
Floor	0.36	0.17	0.57	1.1	0.91	20.36	**18.51**
Window*					6.70	0.54	**3.62**
Door	0.22	0.13	0.04	0.39	2.56	1.67	**4.28**
Ventilation							**21.64**
Total							**125.94**

Table B.3 Estimated heat loss, Configuration 3

Building Element	R-Value, m^2K/W	Rsi	Rse	Total Effective R-Value	U-value, W/m^2K	Area, m^2	**Heat Loss, W/K**
North-East Wall	2.06	0.13	0.04	2.23	0.45	10.69	**4.79**
North-West Wall	2.06	0.13	0.04	2.23	0.45	10.16	**4.56**
South-East Wall	2.06	0.13	0.04	2.23	0.45	9.02	**4.04**
South-West Wall (uninsulated)	0.38	0.13	0.04	0.55	1.82	10.70	**19.46**
Thermal Bridging (Walls)						40.57	**6.09**
Ceiling	0.1	0.1	0.24	0.44	2.27	20.36	**46.27**
Floor	0.36	0.17	0.57	1.1	0.91	20.36	**18.51**
Window*					6.70	0.54	**3.62**
Door	0.22	0.13	0.04	0.39	2.56	1.67	**4.28**
Ventilation							**21.84**
Total							**133.46**

Appendix C - Cooling Models for calculating the Decay Coefficient

It was found that across all models and all simulations that the RMSE on the IA model was the smallest, though across all models there was a variation in NRMSE of 8% or smaller. Figure C.1 and Figure C.2 show the decay constant and NRMSE values for each of the models across the configurations. Observing these figures indicates which of the models is likely to be the most reliable in determining an accurate decay constant.

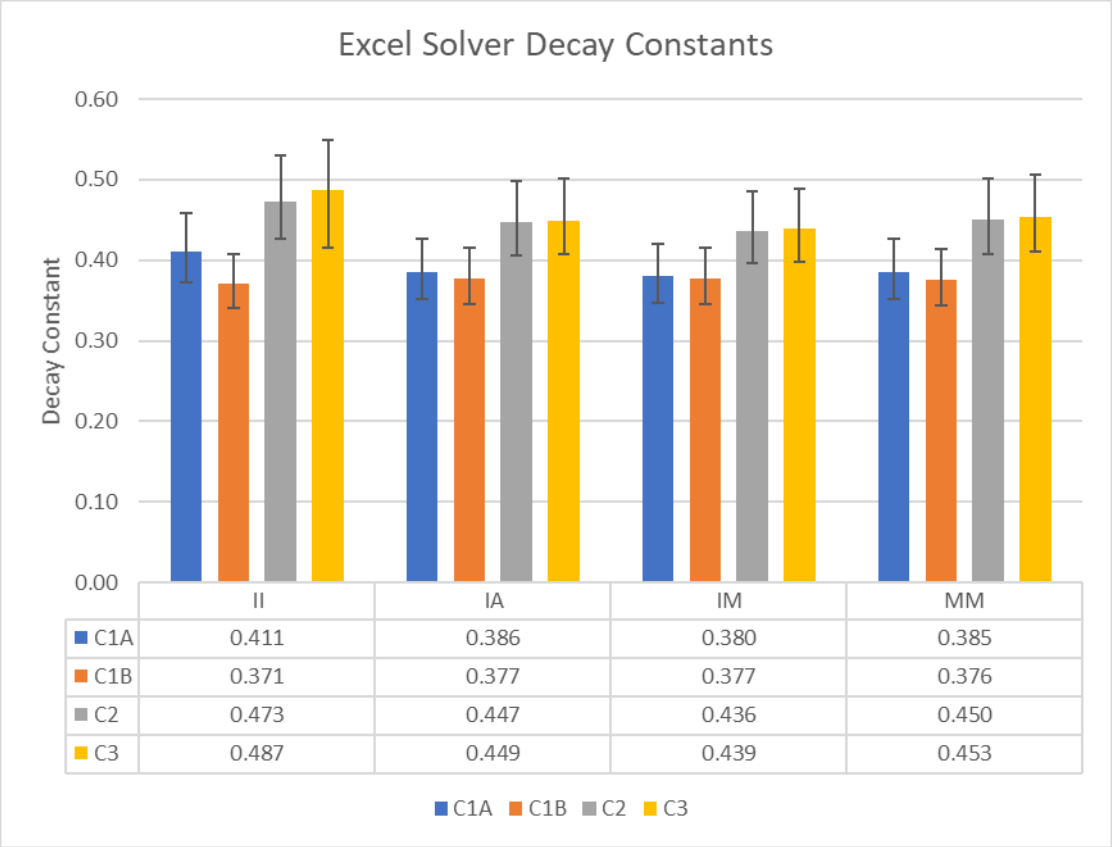

	II	IA	IM	MM
C1A	0.411	0.386	0.380	0.385
C1B	0.371	0.377	0.377	0.376
C2	0.473	0.447	0.436	0.450
C3	0.487	0.449	0.439	0.453

Figure C.1 Decay constant from Excel solver, by cooling model

Figure C.1 does not immediately indicate which model is the most accurate, however it shows that the decay constants in the II model appears to be less reliable that the other three. It is expected that Configuration 1 Test A and Test B will be similar, as these are the same configuration tested at different times. This is not the case for model II, where there is the largest difference between the Configuration 1 Test A and Test B of any model. Model IM shows the best match between Configuration 1 Test A and Test B. Across all of the models there is not much difference between the constants for configurations 2 and 3. There was not a significant difference between the HTCs for configurations 2 and 3 (93.34 W/K and 97.91 W/K), so this may represent a limitation on the sensitivity of the test.

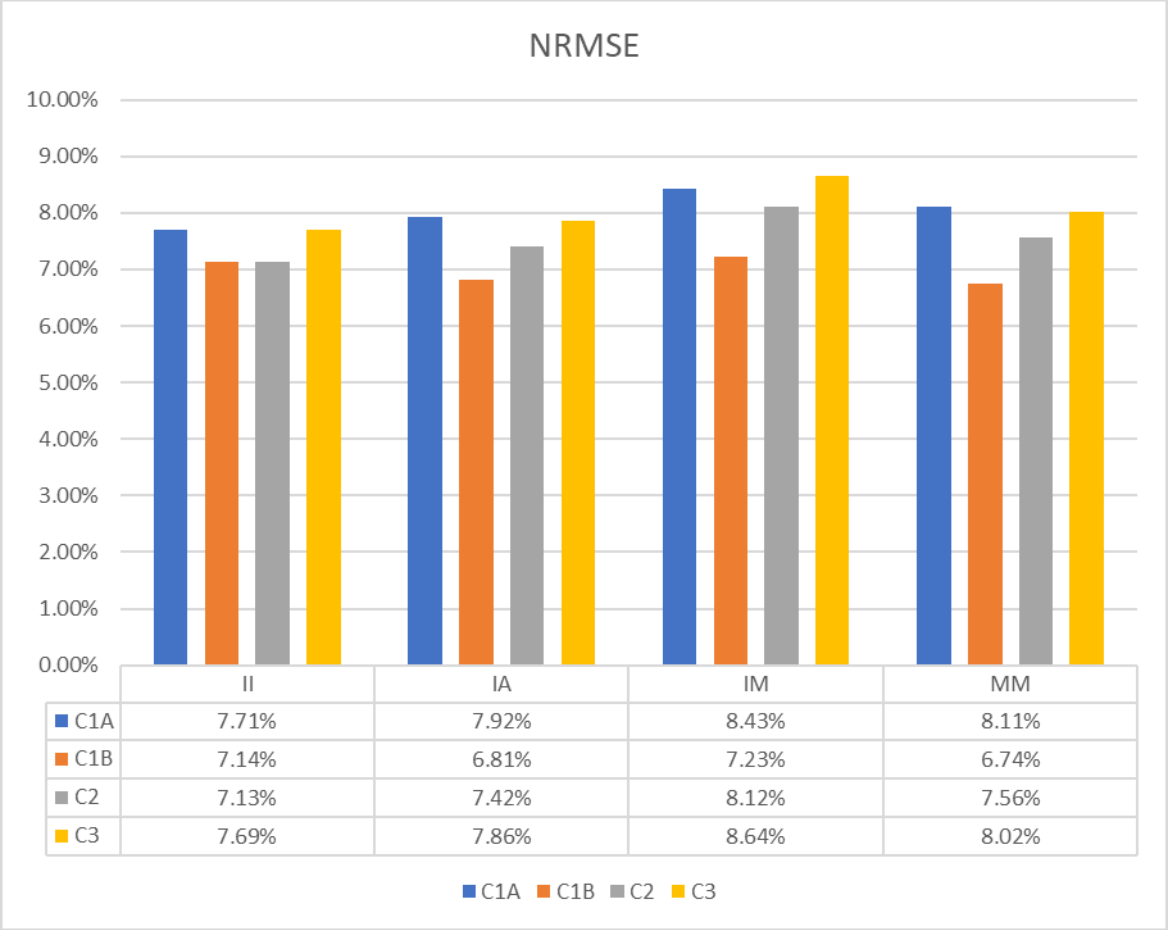

	II	IA	IM	MM
C1A	7.71%	7.92%	8.43%	8.11%
C1B	7.14%	6.81%	7.23%	6.74%
C2	7.13%	7.42%	8.12%	7.56%
C3	7.69%	7.86%	8.64%	8.02%

Figure C.2 NRMSE for Cooling models under Excel Solver

Figure C.2 shows that all models predict the internal temperature to within 9%, the best being model II which predicts the internal temperature to within 7.42 % on average. This is well within a 10% accuracy target, indicating that any of these could be used and still

Each of the cooling models provides a good estimate of the behaviour of the internal temperature; all the NRMSE values are less than 9%. Given the goal to keep estimates within 10% of observations any of these models could be considered a satisfactory way to estimate the decay constant. The II model consistently provides a good estimate of the internal temperature, however the variation between the results for Configuration 1 Test A and Test B indicate that caution should be used when applying this model. The IA and MM models show the next best estimates of internal temperature based on NRMSE, and showed very similar decay constants. Either of these models should be able to be used confidently in estimating the decay constant of the test cell.

Decay Constant and HTC

The adjusted HTC for each of the four test cases was calculated via the co-heating test in Chapter 5.3. A non-linear regression analysis has been done to determine whether any of the cooling models shows a greater correlation with the co-heating test HTC estimates. The anlaysis uses a power function to regress the decay constant against the HTC as this naturally passes through the origin. This is done on the basis that a building with a decay constant of 0 would not lose heat over time, and therefore have a HTC of zero. The Power Function allows for this to be expressed mathematically without artificially supressing the curve through the origin as is done in the co-heating test analysis. The analysis is shown in Figure C.3.

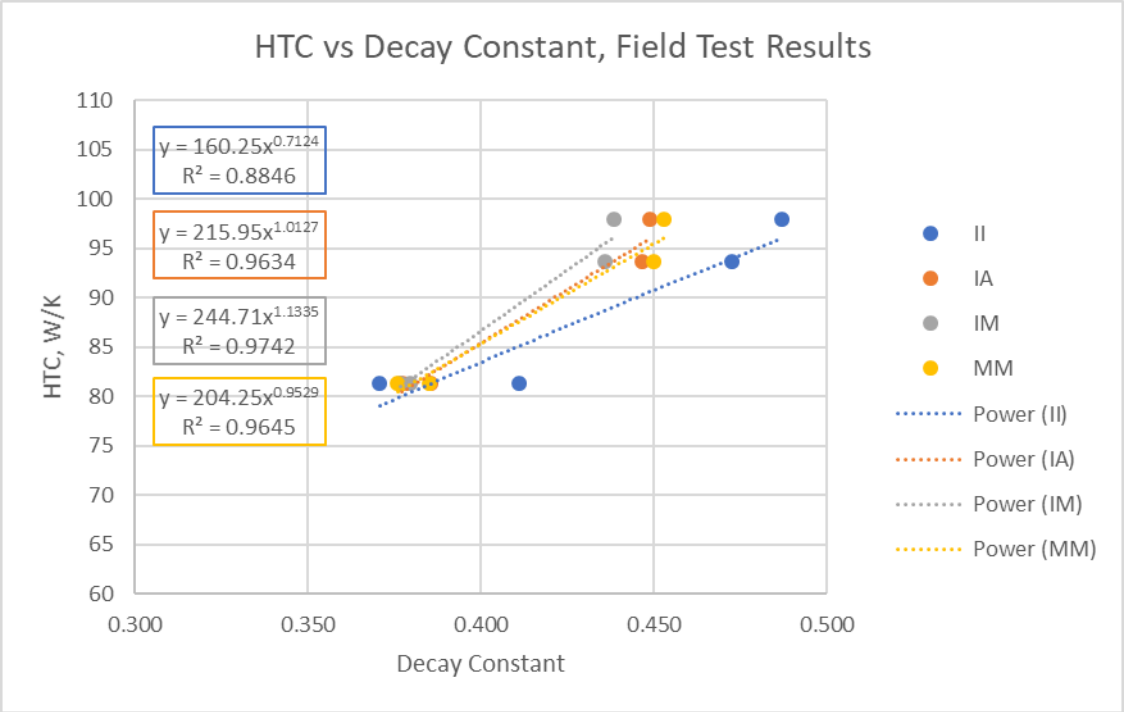

Figure C.3 HTC vs decay constant, Excel Solver analysis on field experiment data

Determining a true relationship from these test cases is difficult given the small number of data points. With this in mind however, there is some evidence in all models that as the decay constant increases, so does the HTC. Noting that Model IM was previously noted to be less accurate at determining the internal temperature than models IA and MM, there is a slightly better correlation between the HTC and the decay constant for Model IM. Model IM does have a steeper curve than Models IA and MM and so small variations in decay constant

will result in larger variations in HTC than the other two models. This may result in a larger uncertainty in the HTC estimate when using the IM model.

In order to further examine the relationship between the decay constant and the HTC, a number of simulations were conducted. As described in Section 4.4.5, 48 models per configuration were created. These models were run through co-heating test and decay test simulations. Each configuration was matched with the observed weather conditions for both tests. For the co-heating test, all internal conditions were matched and the simulation directed to adjust the heat input accordingly. The HTC was adjusted for wind and solar gains using the same multiple regression technique specified in Section 5.3.3.

For the decay test, the internal temperature was set until the start of the decay period, where the thermostat was switched off and the internal temperature decay was simulated. The internal temperature during the decay periods was matched for the other 20 hours of the day to match all conditions as closely as possible. Figure C.4 shows the adjusted HTC against the decay constant for each of the cooling models discussed earlier in this chapter.

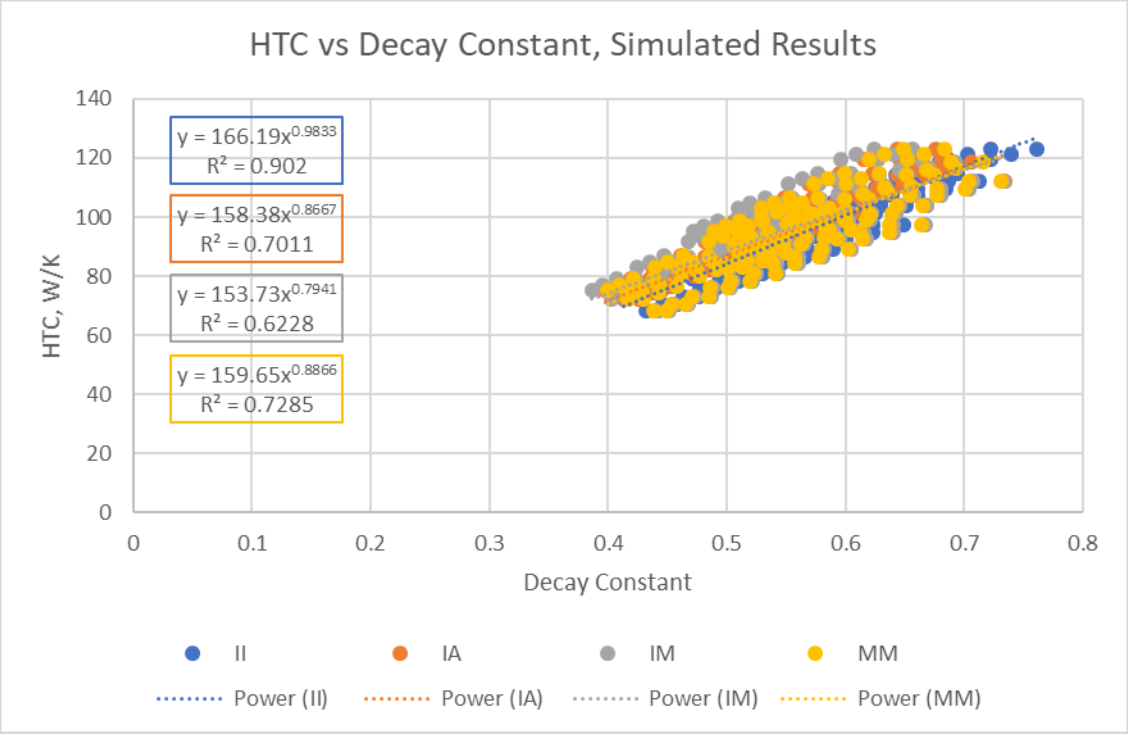

Figure C.4 HTC vs decay constant, Excel Solver analysis for simulated data

Figure C.4 shows that when conducted on the simulated data there is minimal difference between the models. Model II is the most compact, and as a result has the highest R^2 value.

There is again very little difference between the IA and MM models, though the MM model does have a slightly higher R^2. Based on the simulations the IM model shows the least correlation between HTC and decay constant.

Based on the analysis of the cooling models presented here, Model II and Model IM have some flaws that are not present in the IA and MM models. Model II showed a large difference between Configuration 1 Test A and Test B where no difference was detected in the other three models. Model IM is less reliable at determining the internal temperature than the other three models, and the simulated results indicate that there is a much lower correlation between the decay constant and the HTC when using this cooling model. Models IA and MM are shown to provide very similar results at each stage of the analysis, and either could be confidently used. The MM model is theoretically more dynamic than model IA, as the model is a series of smaller cooling curves, each informing the next, and the external temperature is adjusted at each stage. This is a more unique approach than using the initial internal air temperature and the average external air temperature and has the potential to be more reliable in changing conditions. On the basis that the underlying approach to modelling the temperature decay is more in line with the dynamic assessment of the building, the MM model will therefore be used.